

Dissertation
submitted to the
Combined Faculties for the Natural Sciences and for Mathematics
of the Ruperto-Carola University of Heidelberg, Germany
for the degree of
Doctor of Natural Sciences

presented by
Diana Helling
born in: Bielefeld, Germany
Oral-examination: December 7th, 2005

**Functional Analysis of Nt-Hypo1 and NtPLC3,
Two Novel Pollen-Specific Proteins
From *Nicotiana tabacum***

Referees: Prof. Dr. Thomas Rausch
Prof. Dr. David G. Robinson

CONTENTS

Contents	I
Summary	VII
Zusammenfassung	IX
1 Introduction	1
1.1 Pollen tube growth: a model system for polarized plant cell growth	1
1.1.1 Ion gradients and fluxes involved in polarized pollen tube growth	3
1.1.1.1 Calcium.....	3
1.1.1.2 Protons.....	4
1.1.1.3 Potassium and chloride.....	4
1.1.2 Cytoskeleton and polarized pollen tube growth	4
1.1.2.1 Microfilaments.....	4
1.1.2.2 Microtubules.....	5
1.2 The role of small GTPases in the control of pollen tube tip growth	6
1.2.1 The small GTPase superfamily Ras.....	6
1.2.2 The regulation of Rho GTPases.....	7
1.2.2.1 Rho GTPases and their regulation in plants	8
1.2.2.2 The role of Rho GTPases in the regulation of pollen tube growth.....	9
1.2.3 Guanine nucleotide exchange factors.....	11
1.2.3.1 Guanine nucleotide exchange factors in plants	13
1.2.3.1.1 Plant-specific Rho GEFs do exist in plants	15
1.2.4 Aims of the dissertation (1 st project)	16
1.3 Phospholipid signaling in pollen tubes.....	17
1.3.1 Phosphoinositides	17
1.3.2 Phosphatidylinositol 4,5-bisphosphate synthesis and functions.....	18
1.3.3 Phosphoinositide-specific phospholipases C.....	20
1.3.3.1 General overview.....	20
1.3.3.2 Molecular domain structure.....	21
1.3.3.3 Membrane binding.....	22
1.3.3.4 Phosphoinositide hydrolysis	22
1.3.3.5 Cloning and cellular functions of PI-PLCs in plants.....	23
1.3.3.5.1 PI-PLCs and their role in pollen tube growth.....	25
1.3.4 Aims of the dissertation (2 nd project)	27
2 Results	28

2.1	Identification and functional characterization of a new interactor of pollen tube Nt-Rac5	28
2.1.1	Sequence analysis of Nt-Hypo1 and comparison with <i>Arabidopsis thaliana</i> and <i>Oryza sativa</i> proteins of unknown function	31
2.1.2	Analysis of Nt-Hypo1 expression by Northern blotting.....	32
2.1.3	Effects of transient expression of Nt-Hypo1 in pollen tubes of <i>Nicotiana tabacum</i>	33
2.1.3.1	Transient over-expression of YFP and Nt-Hypo1	33
2.1.3.2	Subcellular localization of Nt-Hypo1	34
2.1.3.3	<i>In vivo</i> interaction of Nt-Hypo1 and Nt-Rac5	35
2.1.4	Over-expression of recombinant Nt-Hypo1 and purification from <i>E. coli</i> ..	36
2.1.4.1	<i>In vitro</i> interaction of Nt-Hypo1 with wild-type and mutant Nt-Rac5....	36
2.1.4.2	Nt-Hypo1 – antibody production.....	39
2.1.5	Nt-Hypo1 gene-knockout by antisense oligodeoxynucleotides, T-DNA insertions and RNA interference.....	39
2.1.5.1	Antisense oligodeoxynucleotides	39
2.1.5.2	T-DNA insertion.....	40
2.1.5.3	RNA interference.....	40
2.1.6	Identification of novel Nt-Hypo1 interactors by yeast two-hybrid screening.	43
2.2	Identification of novel phosphoinositide-specific phospholipase C isoforms from <i>Nicotiana tabacum</i>	47
2.2.1	Identification and sequence analysis of NtPLC3 and NtPLC4.....	47
2.2.1.1	Phylogenetic analysis of NtPLC3 and NtPLC4.....	50
2.2.2	Analysis of NtPLC3 expression by Northern blotting.....	51
2.2.3	Determination of the enzymatic activity of wild-type and mutant NtPLC3	52
2.2.3.1	Purification of recombinant NtPLC3 over-expressed in <i>E. coli</i>	52
2.2.3.2	<i>In vitro</i> enzyme activity assay using [³ H] phosphatidylinositol 4,5-bisphosphate	54
2.2.4	Effects of transient expression of NtPLC3 in pollen tubes of <i>Nicotiana tabacum</i>	56
2.2.4.1	Transient expression of wild-type and mutant NtPLC3	56
2.2.4.2	Subcellular localization of NtPLC3.....	58
2.2.4.3	Subcellular localization of NtPLC3 domain-deletion mutants.....	59

2.2.4.4	Determination of the specific function of NtPLC3's catalytic core in membrane association.....	61
2.2.5	Inhibition of PI-PLC activity by U-73122 treatment <i>in vivo</i>	63
2.2.5.1	Complementation of PI-PLC inhibition by NtPLC3 over-expression <i>in vivo</i>	64
2.2.6	Visualization of PI-4,5-P ₂ and its implication in pollen tube polarity.....	65
2.2.7	Visualization of diacylglycerol and its dependence on PI-PLC activity.....	67
3	Discussion	72
3.1	Identification of a novel pollen-specific protein that interacts with Nt-Rac5	72
3.1.1	Transient over-expression of Nt-Hypo1 does not affect tobacco pollen tube growth or morphology	73
3.1.2	Nt-Hypo1 accumulates in the cytosol of growing pollen tubes.....	73
3.1.3	Interaction of Nt-Hypo1 with Nt-Rac5 cannot be visualized <i>in vivo</i>	73
3.1.4	Nt-Hypo1 interacts with Nt-Rac5 <i>in vitro</i>	74
3.1.5	Effects of Nt-Hypo1 gene-knockdown.....	74
3.1.6	Nt-Hypo1 interacts with several pollen tube proteins	76
3.1.7	Note added in proof.....	79
3.2	Identification of two novel phosphoinositide-specific phospholipases C from <i>Nicotiana tabacum</i>	81
3.2.1	NtPLC3 and NtPLC4 are plant-specific PI-PLC isoforms from <i>N. tabacum</i>	82
3.2.2	NtPLC3 is a pollen-specific PI-PLC isoform.....	82
3.2.3	NtPLC3 hydrolyzes PI-4,5-P ₂ <i>in vitro</i>	83
3.2.4	Transient expression of NtPLC3 in pollen tubes of <i>Nicotiana tabacum</i>	88
3.2.4.1	Transient over-expression of NtPLC3 wild-type and mutant versions does not affect pollen tube growth.....	88
3.2.4.2	NtPLC3 is a plasma membrane-associated enzyme	90
3.2.4.3	EF hand-like domain and C2 domain are essential for membrane association	90
3.2.4.4	The catalytic core is responsible for the absence of NtPLC3 from the pollen tube tip	92
3.2.5	PI-PLCs maintain pollen tube polarity and restrict PI-4,5-P ₂ to the tip	93
3.2.6	Diacylglycerol, a product of PI-PLC activity, accumulates at the plasma membrane in the pollen tube tip.....	97

4	Materials and Methods	101
4.1	Chemicals, kits, enzymes.....	101
4.2	Apparatus.....	104
4.3	Bacteria Strains.....	105
4.4	Yeast Strain.....	105
4.5	Plant cultivation.....	106
4.5.1	<i>Nicotiana tabacum</i>	106
4.5.2	<i>Arabidopsis thaliana</i>	106
4.5.2.1	Sterile cultures	106
4.5.2.2	Growth on Soil.....	106
4.6	Methods related to the treatment of <i>Escherichia coli</i>	106
4.6.1	<i>E. coli</i> cultivation.....	106
4.6.2	Chemical transformation of competent <i>E. coli</i> cells (after Inoue <i>et al.</i> , 1990)	107
4.6.3	Transformation of <i>E. coli</i> via electroporation	107
4.6.4	Colony lift for cDNA library screen.....	108
4.7	Methods related to the treatment of <i>Agrobacterium tumefaciens</i>	109
4.7.1	Transformation of competent <i>A. tumefaciens</i>	109
4.8	Methods related to the treatment of <i>Saccharomyces cerevisiae</i>	109
4.8.1	<i>S. cerevisiae</i> cultivation.....	109
4.8.2	Transformation of <i>S. cerevisiae</i> HF7c cells.....	110
4.8.2.1	Library scale	110
4.8.2.2	Plasmid scale (re-transformation described for 24 probes).....	111
4.9	DNA-related techniques	112
4.9.1	Vectors.....	112
4.9.2	Plasmids.....	114
4.9.3	Oligonucleotides.....	119
4.9.4	Isolation of plasmid DNA.....	121
4.9.4.1	Plasmid DNA isolation from <i>E. coli</i>	121
4.9.4.1.1	TELT mini-preparation.....	121
4.9.4.1.2	Mini- and maxi-preparations	121
4.9.4.2	<i>S. cerevisiae</i> HF7c glycerol stocks and plasmid preparation	121
4.9.5	Isolation of genomic DNA from plants	122
4.9.6	Determination of DNA concentration	122

4.9.7	DNA restriction endonuclease analysis.....	122
4.9.8	DNA dephosphorylation.....	123
4.9.9	Ligation.....	123
4.9.10	cDNA synthesis.....	123
4.9.11	PCR techniques.....	123
4.9.11.1	Site-directed mutagenesis PCR.....	124
4.9.12	Purification of PCR products.....	124
4.9.13	Sequencing.....	124
4.9.14	DNA agarose gel-electrophoresis.....	124
4.9.15	Purification of DNA fragments from agarose gels.....	125
4.10	RNA-related techniques.....	125
4.10.1	Isolation of total RNA.....	125
4.10.2	Determination of RNA concentration.....	125
4.10.3	Northern Blot analysis.....	125
4.11	Methods related to protein treatment.....	126
4.11.1	Discontinuous SDS polyacrylamide gel-electrophoresis (SDS PAGE; Laemmli 1970).....	126
4.11.2	Western Blot analysis.....	127
4.11.3	Protein over-expression and purification of GST fusion proteins from <i>E. coli</i>	128
4.11.4	Antibody preparation.....	129
4.11.5	<i>In vitro</i> interaction studies.....	129
4.12	Transient ballistic transformation of <i>Nicotiana tabacum</i> pollen grains.....	130
4.12.1	Particle preparation.....	130
4.12.2	Pollen bombardment.....	130
4.13	Stable transformation of <i>Nicotiana tabacum</i> plants.....	131
4.13.1	Preparation of <i>A. tumefaciens</i> for transformation.....	131
4.13.2	Leaf-disc transformation.....	131
4.13.3	Shoot induction.....	131
4.13.4	From root induction to the flowering plant.....	131
4.13.5	β -galactosidase assay.....	131
4.13.6	Tobacco transformation media.....	132
4.14	[³ H] PI-4,5-P ₂ activity assay.....	133
4.14.1	Preparation of lipid stock solutions.....	133

4.14.2	Enzyme activity assay	133
4.15	Microscopy	134
4.15.1	Light microscopy	134
4.15.2	Epifluorescence microscopy	134
4.15.3	Confocal laser scanning microscopy	134
4.16	Bioinformatic methods	135
5	Abbreviations and list of figures and tables.....	136
6	References.....	142
7	Appendix.....	156
8	Curriculum vitae.....	170
9	List of publications	172
10	General Statement	173
	Danksagung.....	174

SUMMARY

Pollen tubes are an excellent model system to investigate molecular mechanisms controlling polar plant cell growth, a process that is essential for cellular and organ morphogenesis throughout plant development. Pollen tubes are large cells that grow rapidly in a strictly polar manner through female flower tissue and transport sperm cells enclosed in their cytoplasm to egg cells. Thus, in only a short time period they grow up to several centimeters to reach the embryo sac and to ensure fertilization. To guarantee the highly complex process of polarized growth, several cellular signal transduction cascades have to be initiated or enhanced in order to guide the pollen tube's way through the style and to deliver cell wall and plasma membrane material to the site of maximum growth, the tip. Although to date only little is known about the mechanisms involved in tip growth, it is known that plant homologues of the Rho family of small GTPases act in a common pathway with PI-4,5-P₂ and represent key regulators of polarized cell growth.

The present dissertation focused on two independent subjects. The first and minor project represents the attempt to identify a plant-specific guanine nucleotide exchange factor (GEF). When the work presented here was initiated, it was unclear how plant Rac/Rop GTPases are activated and no Rho GEF had been identified in the plant kingdom. In a yeast two-hybrid screen using a dominant negative mutant of the tobacco small GTPase Nt-Rac5 as bait, we identified a novel protein of 76 amino acids. This hypothetical protein interacted with Nt-Rac5 in yeast cells and in *in vitro* pull-down assays. It was shown to be a pollen-specific, soluble protein that accumulated in the cytosol of growing pollen tubes. Loss-of-function mutant plants have been generated by RNA interference and are still under investigation. Further experiments are in progress to finally solve the question whether Nt-Hyp1 is a plant-specific GEF or not.

The second and major project of this dissertation represents the identification and functional characterization of a phosphoinositide-specific phospholipase C from tobacco. PI-PLCs are Ca²⁺-dependent enzymes that hydrolyze PI-4,5-P₂ and generate two second messengers: Diacylglycerol remains associated with the plasma membrane, whereas inositol 1,4,5-trisphosphate diffuses to the cytosol where it opens Ca²⁺ channels and thereby increases the intracellular Ca²⁺ concentration. PI-4,5-P₂ is known to play an important role in the regulation of polarized pollen tube growth acting together with Rac/Rop GTPases. In this dissertation we intended to solve the question if PI-PLCs

represent a link between Rac/Rop GTPases, PI-4,5-P₂ and the establishment of a tip-focused Ca²⁺ gradient, which all have key functions in the regulation of pollen tube tip growth.

We identified a novel pollen-specific PI-PLC isoform, NtPLC3, from tobacco by cDNA library colony hybridization and determined its localization in living pollen tubes by YFP-tagging. Furthermore, through the generation of single- or multiple-domain deletion mutants, we showed that two domains, the EF hand and the C2 domain, are both essential for membrane association of this enzyme. The generation of chimeric constructs, combining plant and mammalian PI-PLC domains, showed that regions within the catalytic core of NtPLC3 kept PI-PLCs from associating with the plasma membrane in the pollen tube tip, whether the enzyme was active or not. We moreover demonstrated that NtPLC3 hydrolyzed PI-4,5-P₂ in a Ca²⁺-dependent manner *in vitro*. This activity could be significantly reduced by introducing single amino acid exchanges into the catalytic core of the enzyme or by treatment with the aminosteroid U-73122. Using the PH domain of the mammalian PI-PLC δ_1 as a biosensor for PI-4,5-P₂, we visualized the complementary distribution of this lipid, which is a PI-PLC substrate, and of NtPLC3 *in vivo*. Based on the experiments and on the observation that PI-4,5-P₂ spreads to a larger area of the plasma membrane at the pollen tube tip after U-73122 treatment, we concluded that PI-PLCs restrict PI-4,5-P₂ to the pollen tube apex.

Our data demonstrate that PI-PLC activity is essential for pollen tube growth. We propose that a key function of PI-PLCs in pollen tubes is to limit PI-4,5-P₂ distribution to the tip and thereby ensure spatially restricted binding of *e.g.* actin-binding proteins or proteins that mediate vesicle fusion with the plasma membrane. Based on this mechanism, pollen tube PI-PLC activity plays a key role in maintaining polarization of cell expansion.

ZUSAMMENFASSUNG

Pollenschläuche stellen ein ideales Modellsystem zur Erforschung der Prozesse dar, die pflanzliches Spitzenwachstum steuern oder regulieren. Dieser Prozess ist essentiell für die zelluläre Entwicklung sowie die Organmorphogenese in der gesamten Pflanzenentwicklung. Pollenschläuche sind longitudinale Zellen, die äußerst schnell und zielgerichtet durch das weibliche Blütengewebe wachsen und der Übertragung männlicher Geschlechtszellen in die Samenanlage und somit der Befruchtung der Eizelle dienen. Um den hochkomplizierten Prozess des polaren Wachstums gewährleisten zu können, müssen in der Zelle zahlreiche Signalübertragungsprozesse in Gang gesetzt oder beschleunigt werden, um dem Pollenschlauch seinen Weg zu weisen und ausreichend Zellwand- bzw. Plasmamembranmaterial zur Verfügung zu stellen. Man geht heute davon aus, dass pflanzliche Homologe der Rho-Familie kleiner GTPasen im Zusammenspiel mit PI-4,5-P₂ eine wichtige Aufgabe der Signaltransduktion übernehmen und somit eine ganz entscheidende Rolle in der Regulation des Spitzenwachstums einnehmen.

Die vorliegende Dissertation befasst sich mit zwei voneinander unabhängigen Projekten. Das zu Anfang beschriebene Projekt repräsentiert das Nebenprojekt. Die Intention des Projektes war es, einen pflanzen-spezifischen Guanine-Nukleotid-Exchange-Faktor (GEF) zu identifizieren. Zu Beginn der Dissertation war die Aktivierung der Rac/Rop GTPasen im Pflanzenreich noch nicht geklärt und pflanzen-spezifische Rho GEFs waren bislang nicht identifiziert. In einem zwei-Hybrid-Interaktionsversuch, in dem eine dominant negative Mutante der kleinen GTPase Nt-Rac5 aus Tabak als "bait" eingesetzt wurde, haben wir ein Protein identifiziert, das 76 Aminosäuren umfasst. Dieses hypothetische Protein interagiert mit Nt-Rac5 in Hefezellen sowie in *in vitro* pull-down Experimenten. Nt-Hypol ist ein pollenspezifisches, lösliches Protein, das im Zytoplasma der Pollenschläuche akkumuliert. Durch RNA-Interferenz wurden transgene Tabak-Pflanzen erzeugt, in denen die Expression des hypothetischen Proteins ausgeschaltet wurde. Diese Pflanzen werden weiterhin in bezug auf Defekte im Pollenschlauchwachstum und der Fertilisation untersucht. Weitere Experimente werden durchgeführt, um die Frage nach der Funktion des hypothetischen Proteins bzw. seine Beteiligung in einem Multi-proteinkomplex mit potentieller GEF-Aktivität zu beantworten.

Das Hauptprojekt dieser Dissertation befasst sich mit der Identifizierung und funktionellen Charakterisierung einer Phosphoinositid-spezifischen Phospholipase C aus Tabak. PI-PLCs

sind Ca^{2+} -abhängige Enzyme, die PI-4,5- P_2 hydrolysieren und dabei die Botenstoffe Diacylglycerol und Inositol 1,4,5-trisphosphat bilden. DAG verbleibt mit der Membran assoziiert, InsP_3 hingegen diffundiert ins Zytoplasma, öffnet möglicherweise Ca^{2+} -Kanäle und erhöht somit die intrazelluläre Ca^{2+} -Konzentration. PI-4,5- P_2 spielt eine bedeutende Rolle in der Regulation des polaren Pollenschlauchwachstums und arbeitet dabei zusammen mit Rac/Rop GTPasen. Die Intention dieses Projektes war es, eine Verbindung der PI-PLCs mit Rac/Rop GTPasen, PI-4,5- P_2 und der Etablierung eines spitzenfokussierten Ca^{2+} -Gradienten herstellen, die alle nachweislich an der Regulation des pflanzlichen Spitzenwachstums beteiligt sind.

Wir haben eine neue pollenspezifische PI-PLC Isoform, NtPLC3, aus Tabak durch Kolonie-Hybridisierung isoliert sowie ihre Lokalisierung in Pollenschläuchen durch YFP-Markierung *in vivo* bestimmt. Überdies haben wir durch die Herstellung einzelner Deletionsmutanten gezeigt, dass zwei Domänen, die EF-Hand, sowie die C2 Domäne, essentiell für die Membranbindung der PI-PLC sind. Die Herstellung von Chimären aus pflanzlichen und tierischen PI-PLC Domänen hat weiterhin gezeigt, dass Regionen im katalytischen Zentrum dafür verantwortlich sind, NtPLC3 von der Membran an der Pollenschlauchspitze fernzuhalten, unabhängig davon, ob das Enzym aktiv ist oder nicht. Weiterhin haben wir gezeigt, dass NtPLC3 Ca^{2+} -abhängig PI-4,5- P_2 *in vitro* hydrolysiert und die Hydrolyse entweder durch einfache Punktmutationen im katalytischen Zentrum oder durch das Aminosteroid U-73122 gehemmt werden kann. Durch den Einsatz der PH-Domäne der tierischen PI-PLC δ_1 , der als Bioindikator für PI-4,5- P_2 dient, haben wir die komplementäre Anordnung von PI-4,5- P_2 und NtPLC3 *in vivo* gezeigt.

Basierend auf den beschriebenen Experimenten und der Beobachtung, dass sich PI-4,5- P_2 an der Plasmamembran in der Pollenschlauchspitze nach Inhibitor-Zugabe ausbreitet, schließen wir, dass PI-PLCs die lokal begrenzte Verteilung von PI-4,5- P_2 kontrollieren. Unsere Daten zeigen, dass PI-PLCs essentiell am pflanzlichen Spitzenwachstum beteiligt sind. Wir schlagen daher vor, dass eine Schlüsselfunktion der PI-PLCs in Pollenschläuchen die räumliche Begrenzung der PI-4,5- P_2 -Verteilung in der Spitze der Pollenschläuche ist und sie somit gewährleisten, dass Aktin-bindende Proteine sowie Proteine, die Vesikelfusionen mit der Plasmamembran begünstigen, lokal an PI-4,5- P_2 in der Spitze binden können und auf diese Weise das polare Wachstum gewährleistet wird.

1 INTRODUCTION

1.1 Pollen tube growth: a model system for polarized plant cell growth

Reproduction in flowering plants is achieved by pollination, followed by fertilization. Pollination initiates when the male gametes, *i.e.* the pollen grains, from the male reproductive organs, the anthers, land on the stigma of the female reproductive organ, the pistil. If the pollen is deposited on a compatible stigma, it hydrates, germinates and the pollen tube emerges from a pore in the exine surface (Bedinger, 1992). Thus, germination transforms the non-polar pollen grains into highly polarized cells. The vegetative pollen tube is a longitudinally expanding single cell that carries all cellular contents, including generative cells, ensuring double fertilization. In maize, *e.g.*, within 5 minutes after deposition on the silk, pollen tubes germinate and expand approximately 1 cm/h, migrating through up to 50 cm of the style in only 24 to 36 h (Mascarenhas, 1993). Pollen tubes invade the pistil and migrate through different cell types. They are first growing between the wall of the stigmatic cells, then continuing through a dense extracellular matrix in the transmitting tissue of the style and finally arriving at the ovary, where they reach the ovule that contains an egg. One single pollen tube is usually guided towards each ovule micropyle where the pollen tube bursts and delivers the sperm cells. One sperm cell fuses with the egg cell, the other with the central cell, giving rise to the embryo and endosperm, respectively (Bedinger *et al.*, 1994; Palanivelu and Preuss, 2000).

Pollen tubes are used in laboratories all over the world as a model system because of their extraordinary rapid cell elongation and their characteristic tip growth to understand the mechanism and regulation of polarized cell growth.

Plant cells generally show diffuse growth, *i.e.* in every direction through cell expansion, whereas pollen tube growth is restricted to a small area at the tube apex. This specialized tip growth is, apart from pollen tubes, also found in root hairs, in fern/moss protonemata, in algal rhizoids, in fungal hyphae or in axon growth to neural synapses. The mechanism of cell expansion by rapid tip growth involves several processes such as the incorporation of Golgi-derived secretory vesicles containing new cell wall and plasma membrane material at a defined area at the tip, endocytic membrane recycling and polarized actin-mediated organelle movements (Hepler *et al.*, 2001). Pharmacological experiments with the actin-depolymerizing drug Latrunculin B have demonstrated that an intact actin cytoskeleton is

essential for pollen tube elongation (Vidali *et al.*, 2001).

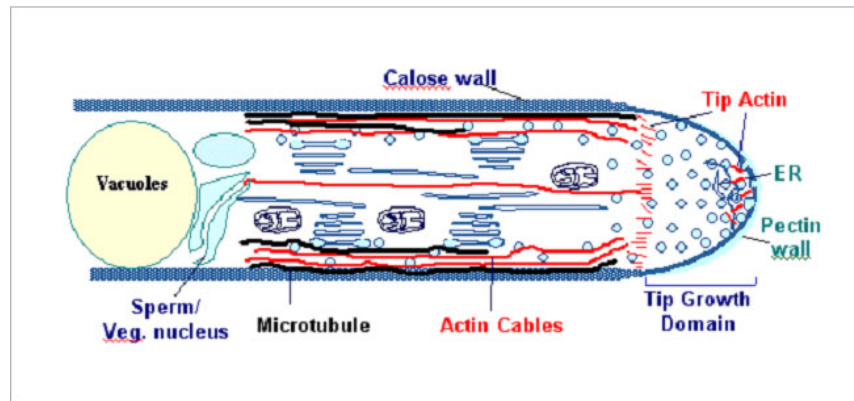


Figure 1: Pollen tube model showing the two nuclei, the vacuole, the cytoskeleton, organelles and the clear zone at the tip. Modified from: http://cepceb.ucr.edu/images/members/yang/figure_2.gif.

The pollen tube itself is highly polarized and is characterized by distinct zones. One of them comprises the vesicle-rich apical region, the so-called clear-zone at the apex a few micrometers from the tip, and is characteristic for the absence of other organelles (Hepler *et al.*, 2001). The next zone is rich in endoplasmic reticulum and mitochondria, followed by a region, which contains all organelle types, including the nuclei. Most of the cytoplasm is accumulated in the apex, less is localized to the cell cortex of the pollen tube flanks, whereas the vacuole fills a large area in the centre of the basal part of the pollen tube. Older and more distant parts of the tube are blocked by callose plugs, thereby keeping the concentration and the volume of the pollen tube cytoplasm constant during pollen tube extension (Mascarenhas, 1993; Franklin-Tong *et al.*, 1996).

Pollen tube growth to the target embryo sac is known to be guided by extracellular and intracellular signaling networks. Extracellular pollen tube attraction controls each growth step by complex interactions with the female reproductive system and is supposed to be dependent on lipids on the stigma, on arabinogalactan proteins in the style, on the two synergid cells and on γ -aminobutyric acid (GABA; Lennon *et al.*, 1998; Higashiyama *et al.*, 2001; Palanivelu *et al.*, 2003). A long list of intracellular guidance cues through signaling networks has been established, including cyclic AMP, Ca^{2+} , phosphatidylinositol monophosphate kinase or plant-specific Rho-type GTPases (Feijó *et al.*, 2001; Hepler *et al.*, 2001; Kost *et al.*, 1999; Moutinho *et al.*, 2001).

1.1.1 Ion gradients and fluxes involved in polarized pollen tube growth

Pollen tube tip growth is dependent on markedly polarized intracellular ion gradients and localized ion fluxes. The role of the two major ions, calcium and protons, as well as two minor ions, potassium and chloride, involved in polarized cell growth, is described in the following paragraphs.

1.1.1.1 Calcium

Calcium plays a central role in ensuring correct pollen tube growth. Pollen tubes actively take up Ca^{2+} and the inhibition of this uptake results in growth arrest. Ca^{2+} levels in growing pollen tubes may be influenced by influx from the extracellular space through Ca^{2+} channels and/or Ca^{2+} influx from intracellular stores such as the vacuole or the endoplasmic reticulum (Hepler *et al.*, 2001). Pollen tubes exhibit a tip-focused Ca^{2+} gradient, which is essential for polarized cell growth (Taylor and Hepler, 1997) and in which the peak concentration at the tip was measured with $10 \mu\text{M}$ Ca^{2+} (Messerli *et al.*, 2000). Interestingly, the Ca^{2+} concentration falls off rapidly from this high level close to the inner surface of the plasma membrane to basal levels of approximately 150 to 200 nM at a distance of 20 μm from the apex. Apart from the intracellular tip-focused gradient, another gradient exists in pollen tube cells. Thus, Ca^{2+} influx is highest at the pollen tube apex and decreases with increasing distance from the tip (Holdaway-Clark *et al.*, 1997). Intriguingly, the intracellular Ca^{2+} levels are not static, but oscillate alternating with periodic cycles of pollen tube growth. This finding prompted to the proposal that growth oscillations provoke Ca^{2+} oscillations followed by secretion, which in turn is essential for the subsequent growth oscillations (Messerli *et al.*, 2000). Additionally, it has been observed that there is a positive correlation between Ca^{2+} levels and the direction of pollen tube elongation. Also a positive correlation between high Ca^{2+} levels and the stimulation of targeted secretion was described, thereby contributing towards polarized cell expansion (Hepler *et al.*, 2001).

Zheng and Yang (2000) stated that the small GTPase from *Arabidopsis thaliana*, At-Rop1, which is spatially localized to the pollen tube tip, is involved in the maintenance of the tip-focused Ca^{2+} gradient. Inhibition of the GTPase by injection of antibodies against At-Rop1 or by the expression of a dominant negative mutant of At-Rop1, altered the tip-localized Ca^{2+} gradient and growth arrested (Zheng and Yang, 2000).

1.1.1.2 Protons

Feijó *et al.* (1999) observed that apart from the Ca^{2+} gradient, also a gradient in pH exists in growing pollen tubes. The extreme apex is considered to be slightly acidic, with the pH increasing almost one pH unit, to a distinct alkaline band towards the base of the clear zone. Additionally to the measured internal pH, proton fluxes have also been observed. In short pollen tubes, proton influxes are directed towards the tube apex, effluxes occur from a region near the pollen grain. A continued proton influx at the apex was observed when pollen tubes expanded, efflux could be measured at the base of the clear zone (Feijó, 1999). These proton fluxes form a current loop, which is supposed to be driven by an H^+ -ATPase located in the plasma membrane towards the base of the clear zone. The importance of protons for the regulation of polarized cell growth has emerged only recently. The regulation through protons might be even more fundamental than the regulation via Ca^{2+} . Even when pollen tube growth is inhibited, the alkaline band remains. Indicating that H^+ -ATPases are still active even when growth is inhibited.

1.1.1.3 Potassium and chloride

Potassium and chloride ions have been associated with pollen tube growth (Messerli *et al.*, 1999), although the involvement of potassium is not clear to date. Chloride efflux was reported from the tube apex, influx from the flanks, in a distance of approximately 20 to 25 μm from the tip. Chloride effluxes are supposed to control water movement and turgor pressure and might even be involved in the deposition of the granular cytoplasm and in size reduction of the clear zone during ion effluxes (Zonia *et al.*, 2002).

1.1.2 Cytoskeleton and polarized pollen tube growth

1.1.2.1 Microfilaments

The actin cytoskeleton is fundamental for pollen tube growth (Geitmann and Emons, 2000; Vidali and Hepler, 2001). The actomyosin force-generating system might have two major functions in the pollen tube. First, it is thought to be responsible for the transport of Golgi-derived vesicles containing cell wall and plasma membrane material to a defined area at the apex, second, it may be the driving force for cytoplasmic streaming (Hepler *et al.*, 2001). Indeed, pollen tubes show an interesting streaming pattern, referred to as inverse fountain streaming. The acropetal lanes of the cytoplasm move forward along the outer borders of the pollen tube, whereas the centripetal lanes move backward along the central

longitudinal axis of the tube, excluding the clear zone (Taylor and Hepler, 1997).

Filamentous actin is mostly organized as longitudinally, or slightly helically, cables in cortical and endoplasmic regions (Kost *et al.*, 1998; Geitmann and Emons, 2000; Vidali and Hepler, 2001). The actin arrangement in the apical zone is still controversial, although recent investigations on live or well-preserved pollen tubes after rapid-freeze fixation, support the observation that actin filaments are disorganized and in fewer numbers found in the apex and in a subapical cortical ring of microfilament bundles (Kost *et al.*, 1998; Lovy-Wheeler *et al.*, 2005). These fine structures in the apex are thought to have functions in vesicle trafficking (Hepler, 2001). The subapical ring region overlaps with the alkaline band (Feijó *et al.*, 1999) and also with the site, where the cytoplasmic streaming reverses direction, so it might also be a zone of microfilament turnover and growth (Hepler *et al.*, 2001). However, the role of actin in polarization is still not clear. Several models have been suggested, but to date they are neither proved nor rejected. It was suggested that actin microfilaments should complement the cell wall as a structure that can oppose turgor pressure and by a Ca^{2+} -dependent mechanism promote growth. Another proposal was that apical actin microfilaments form a sieve to sort out secretory vesicles from the bulk endoplasm. A third, but nevertheless not convincing model was, that actin polymerization should generate enough force to promote cell growth, similar to filopodial and lamellipodial protrusion (Hepler *et al.*, 2001).

Nevertheless, two hierarchical levels for the participation of actin in tip growth have been postulated: First, actin may contribute to polarized pollen tube growth by the polarized elongation of microfilament bundles, second, actin microfilaments may provoke a bidirectional cytoplasmic streaming and thereby might establish cell polarity.

1.1.2.2 Microtubules

The microtubules in pollen tubes are oriented longitudinally and adopt sometimes a slightly helical distribution (Geitmann and Emons, 2000), but are absent from the pollen tube tip (Lancelle and Hepler, 1992). Pharmacological treatments with microtubule inhibitors did not have an effect on germination or growth in angiosperm pollen (Heslop-Harrison *et al.*, 1988). Although oryzalin or colchicine do not affect pollen tube growth, they do affect the cytoplasmic organization. Oryzalin retards the movement of the vegetative nucleus and the generative cell from the pollen grain to the pollen tube and causes their absence from the tip. Colchicine, in contrast, promotes the movement of large vacuoles to the tip and a random distribution of cytoplasmic components along the tip

(Joos *et al.*, 1994). Interestingly, microtubules co-align and co-localize with microfilaments in pollen tubes (Geitmann and Emons, 2000) and form also complexes with the endoplasmic reticulum and the plasma membrane (Lancelle and Hepler, 1992). Nevertheless, microtubules do not seem to be essential for polarized pollen tube growth.

1.2 The role of small GTPases in the control of pollen tube tip growth

1.2.1 The small GTPase superfamily Ras

Low molecular weight GTPases are of special interest for cell biologist because they are supposed to be key regulators of many aspects of cell behaviour. They are monomeric guanine nucleotide binding proteins of 21 to 30 kDa and they are related to the α subunit of heterotrimeric G proteins (Yang, 2002). Although they exhibit a remarkable similarity in structure and employ the same basic mechanism, they regulate diverse signaling cascades such as vesicle trafficking or hormone signaling.

All small GTPases belong to one superfamily, the Ras superfamily of small GTPases. Ras GTPases are further divided into five major groups: Ras, Rho, Rab, Arf and Ran. Arf GTPases, *e.g.*, are required for vesicle budding in the secretory system, Rabs control membrane transport processes and the docking mechanism of specific vesicles and Ran GTPases regulate the trafficking of RNA and proteins through the nuclear pores. In summary, although Arf, Rab and Ran GTPases have essential functions in fundamental cellular processes, these small GTPases are not considered to comprise signaling proteins that transduce extracellular signals (Yang, 2002).

The plant genome only consists of a very limited number of heterotrimeric G proteins compared to the number in animal cells and this might be the reason for the increasing importance of small GTPases in signaling events in plants. In the *Arabidopsis* genome, 93 genes have been identified that might encode for small GTPases (Yang, 2002; Vernoud *et al.*, 2003).

This introduction focuses in the following specifically on Rho GTPases, because they are supposed to form the most important subgroup related to polarized cell growth. Although Rho GTPases were first solely shown to regulate the organization of the actin cytoskeleton and the development of cell polarity in eukaryotes, now they are shown to be also involved in gene transcription, cell wall synthesis, vesicular transport, H₂O₂ production, in endo- and exocytosis, in cytokinesis, in microtubule dynamics, in G1 cell cycle progression and

cell differentiation (Etienne-Manneville and Hall, 2002; Yang, 2002).

1.2.2 The regulation of Rho GTPases

Rho GTPases are known to act as molecular switches that transmit extracellular signals and activate multiple intracellular signal transduction cascades. Animal and yeast Rho GTPases cycle between two conformational stages: an active GTP-bound and an inactive GDP-bound state (see Figure 2). In the GTP-bound state, they are able to interact with effector or target proteins and initiate a downstream response to an extracellular signal. The GTPases are inactive in the GDP-bound conformation after GTP hydrolysis. Their intrinsic GTPase activity is low, but can be dramatically stimulated by regulatory proteins of the GAP family (*i.e.* GTPase activating proteins). Another class of regulatory proteins is the GEF family (*i.e.* guanine nucleotide exchange factors). GEFs promote the dissociation of the GDP from the inactivated Rho GTPase, which in turn results in GTP binding and activation of the protein. GEFs will be discussed more in detail in the following paragraphs (see chapter 1.2.3).

Rho GTPases are only active when bound to membranes. They are post-translationally prenylated at their COOH-terminus by a prenyl cysteine carboxy methylation transferase. The COOH-terminal CAAX domain of Rho GTPases is isoprenylated at the cysteine residue and responsible for the partial membrane association of these proteins.

A third group of regulatory proteins, the GDIs (*i.e.* guanine nucleotide dissociation inhibitors), are thought to inactivate Rho GTPases by removing them from the plasma membrane, preferentially in the GDP-bound conformation, and transferring them to the cytosol.

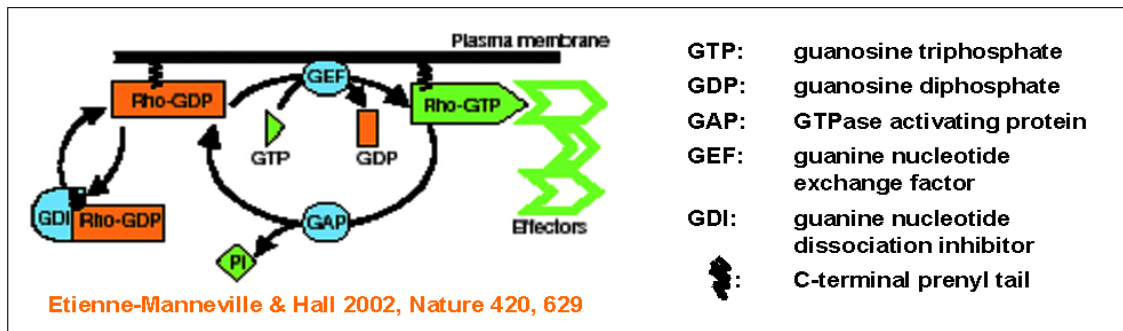


Figure 2: The Rho GTPase cycle. Rho GTPases are highly regulated by three classes of proteins: Guanine nucleotide exchange factors (GEFs) catalyse nucleotide exchange and mediate activation. GTPase-activating proteins (GAPs) stimulate GTP hydrolysis, leading to inactivation. Guanine nucleotide dissociation inhibitors (GDIs) extract the inactive GTPase from membranes. All Rho GTPases are post-translationally prenylated at their COOH-terminus, which is required for function. (Modified from Etienne-Manneville and Hall, 2002.)

Point mutations have been introduced into the highly conserved guanine nucleotide binding site of Rho family small GTPases in order to generate constitutively active (CA; $G^{15}V$; Chardin, 1993) or dominant negative (DN; $T^{20}N$; Feig, 1999) mutant forms of these proteins. Constitutively active GTPases show dramatically reduced GTPase activity, which cannot be activated by GAPs. Dominant negative Rho GTPases, in contrast, show reduced binding to guanine nucleotides, do not interact with effectors anymore and have a high affinity to GEFs. The over-expression of dominant negative mutants in living cells results in the inhibition of the endogenous Rho GTPases by sequestering the GEFs essential for their activation (Feig, 1999). Activated Rac/Rop GTPases interact with downstream effector proteins and thereby transduce external stimuli, for example, to the actin cytoskeleton.

1.2.2.1 Rho GTPases and their regulation in plants

Plant cells, however, lack Ras family GTPases and contain only a subgroup of Rho-like GTPases, the Rop GTPases, *i.e.* Rho of plants (Valster *et al.*, 2000). Plant Rac/Rop GTPases appear to be distinctively regulated and to employ a unique set of regulators and effectors. Sequences showing significant homology to genes encoding key regulators (Dbl family GEFs) and effectors of animal Rho GTPases are absent from the *Arabidopsis* or rice genomes (Valster *et al.*, 2000). Although plant Rac/Rop GTPases were demonstrated to be important factors in the control of cell behaviour (Gu *et al.*, 2004), the signaling networks into which they are integrated have remained poorly characterized to date. Plant proteins

with sequence homology to Rho GAPs or GDIs were identified (Bischoff *et al.*, 2000; Vernoud *et al.*, 2003; Wu *et al.*, 2000). Indeed, a novel class of plant Rho GAPs was identified in a yeast two-hybrid screen, the Rop GAP (Wu *et al.*, 2000). Some Rop GAPs contain a CRIB (Cdc42/Rac interactive binding) motif upstream of their GAP domain. Interestingly, CRIB motifs are in animal cells exclusively found in downstream effectors of small GTPases. The CRIB domain in plant Rop GAPs is thought to facilitate the formation of the transitional state of the Rop GTPase (Wu *et al.*, 2000). On the other hand, three Rho GDI homologues are present in the *Arabidopsis* genome. The AtROP GDI1 is shown to interact with AtROP GTPases (Bischoff *et al.*, 2000) and plays a role in the regulation of AtROP1 localization (Fu *et al.*, 2001). Nevertheless, the expression patterns and functions of these proteins have only begun to be explored.

1.2.2.2 The role of Rho GTPases in the regulation of pollen tube growth

A detailed functional characterization of upstream regulators of pollen tube Rac/Rop GTPases is required to understand the molecular mechanisms responsible for the polarized accumulation of activated forms of these proteins at the plasma membrane in the tip, which determines the direction of pollen tube expansion. In addition to cell-autonomously controlling polarized cell growth in the absence of guidance cues, these mechanisms are likely to be responsive to extra-cellular signals that direct pollen tube growth within the pistil.

On the other hand, a number of signaling molecules were demonstrated or proposed to act downstream of activated Rac/Rop GTPases in pollen tubes. Among these effectors a phosphatidylinositol monophosphate kinase (PIP-K) was identified. PIP-K is a known effector of animal Rho GTPases (Bishop and Hall, 2000) and was shown to physically associate with a Rac/Rop GTPase expressed in pollen tubes and to be responsible for the accumulation of the signaling lipid phosphatidylinositol 4,5-bisphosphate (PI-4,5-P₂) in the plasma membrane specifically at the tip of these cells (Kost *et al.*, 1999). PI-4,5-P₂ itself is known as a key regulator of the actin organization and as a recruitment signal for secretory vesicles (Martin, 1998). Thus, PI-4,5-P₂ may control tip growth by the regulation of the activity of actin-binding proteins, such as profilin, gelsolin or vinculin (Drøbak *et al.*, 1994; Martin, 1998; Kovar *et al.*, 2000). In addition, PI-4,5-P₂ is also a substrate for hydrolysis by phosphoinositide-specific phospholipases C (PI-PLCs), which in turn produces the membrane-bound diacylglycerol and the soluble inositol 1,4,5-trisphosphate (InsP₃), a signaling molecule known to open Ca²⁺-channels. Through this pathway, Rac

GTPases might control the establishment of the tip-focused Ca^{2+} gradient known to be essential for polarized pollen tube growth (Hepler *et al.*, 2001). Based on these observations, Rac GTPases might coordinate actin organization, targeted secretion and membrane recycling during pollen tube tip growth via the interaction with various effector proteins.

CRIB (Cdc42/Rac-interactive binding) domains are known to mediate the binding of effectors specifically to activated forms of animal or yeast Rho GTPases (Pirone *et al.*, 2001). Based on database searches, a number of *Arabidopsis* pollen tube proteins containing putative CRIB domains have been identified, which were demonstrated to interact with activated Rac *in vitro* and to be localized to the plasma membrane at the pollen tube tip (Wu *et al.*, 2001). At least some of these proteins are likely to act as effectors of pollen tube Rac/Rop GTPases, although their expression patterns and cellular functions have not been clarified to date.

In addition, evidence has been generated suggesting that pollen tube Rac/Rop GTPases control the activity of the actin regulatory protein actin depolymerization factor (ADF; Chen *et al.*, 2003) and may thereby be responsible for the establishment of a tip-focused cytoplasmic Ca^{2+} gradient (Li *et al.*, 1999). However, the molecular mechanisms linking Rac/Rop GTPases to ADF or Ca^{2+} signaling have not been determined to date.

PI-4,5- P_2 , ADF and Ca^{2+} play important roles in the regulation of actin organization and/or membrane traffic, *e.g.* secretion or endocytosis in non-plant cells (Martin, 1997) and were proposed to have similar functions in pollen tubes.

Recently, a novel effector of AtROP1 was identified in a yeast two-hybrid screen, which contains a CRIB motif and was named RIC (ROP-interacting CRIB domain containing protein). In the *Arabidopsis* genome, 10 homologues of the identified RIC have been found by database searches, which may control various ROP-dependent pathways (Wu *et al.*, 2001), although their exact functions remain to be investigated.

Initially, a pea Rop GTPase, Rop1, was shown to be localized to the pollen tube tip and pollen tube growth was inhibited by the injection of an anti-Rop1 antibody (Lin and Yang, 1997). Injection of the same Rop1 antibody against the pea ROP1 additionally disrupted the tip-focused Ca^{2+} gradient in *Arabidopsis* pollen tubes (Li *et al.*, 1999).

A Rac/Rop GTPase from *Arabidopsis thaliana*, At-Rac2, has been shown to be associated with the plasma membrane specifically in the apex and to act as a key regulator of pollen tube tip growth (see Figure 3b). Over-expression of the constitutively active (CA) mutant

of At-Rac2 depolarized pollen tube growth, whereas the expression of the dominant negative (DN) mutant of At-Rac2 inhibited this process (Kost *et al.*, 1999; Li *et al.*, 1999 and compare Figure 3d and e).

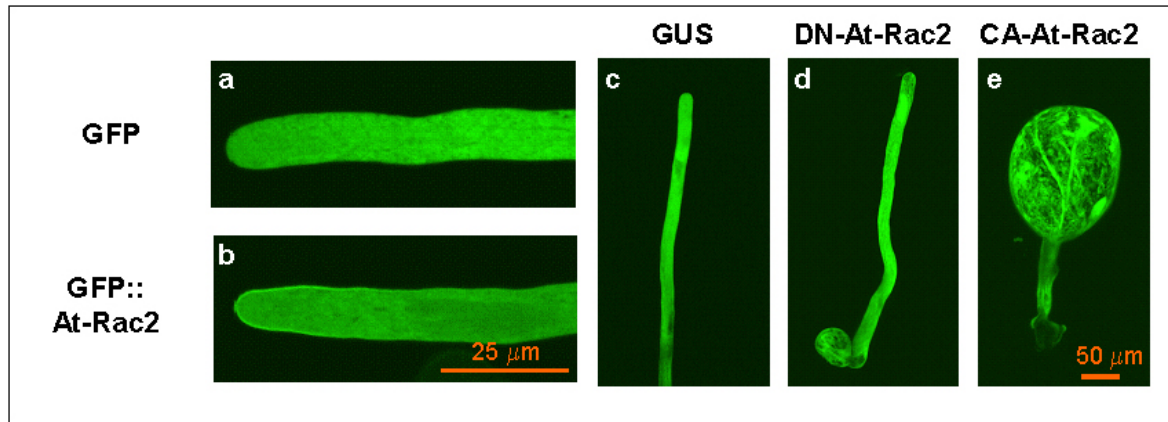


Figure 3: Transient over-expression of the *Arabidopsis thaliana* pollen tube Rac/Rop GTPase At-Rac2. (a) + (c) Control pollen tubes of *Nicotiana tabacum* expressing green fluorescent protein (GFP) and β -glucuronidase (GUS), respectively. (b) GFP fused to At-Rac2. (d) Over-expression of DN-At-Rac2 plus GFP. (e) Over-expression of CA-At-Rac2 + GFP. Pollen tube length (grain to tip) at the time of imaging: 4 mm (c), 400 μ m (d). (Modified from Kost *et al.*, 1999.)

In conclusion, research during the past few years has established that the specific activation of Rho GTPases in plants at the plasma membrane in the tip controls the extremely polarized growth of pollen tubes. Upstream regulators and mechanisms restricting Rac/Rop activation to this location remain to be characterized. Activated pollen tube Rac/Rop GTPases are likely to stimulate multiple downstream signaling pathways thereby controlling and co-ordinating cellular processes essential for tip growth. Although a number of potential regulators and effectors of plant Rho GTPases have been identified, neither the signaling network into which they are integrated, nor how this network influences cellular processes is currently understood.

1.2.3 Guanine nucleotide exchange factors

Three classes of upstream regulators were described above (Chapter 1.2.2). The guanine nucleotide exchange factors (GEFs) constitute the critical mediators of the Rho GTPase activation in mammalian and yeast cells and will be highlighted in more detail in the following paragraphs.

Extracellular signals seem to act predominantly on GEFs, which stimulate the exchange of

the tightly bound GDP by GTP and generate the activated form of the GTPase. It has been shown that GEFs bind to small GTPases in the GDP-bound conformation and comprise a dual biochemical activity by first destabilizing the low-affinity GEF-GTPase-GDP-Mg²⁺ complex while, secondly, stabilizing the high-affinity nucleotide-free reaction intermediate GEF-GTPase concomitant with the expulsion of GDP and Mg²⁺ (Cherfils and Chardin, 1999; Rossman *et al.*, 2002). Subsequently, the reaction proceeds with the binding of GTP and Mg²⁺ to form the unstable GEF-GTPase-GTP-Mg²⁺ complex, which is followed by the dissociation of the GEF.

GEF proteins are unrelated to other proteins that interact with small G-proteins and are thought to have evolved independently of small GTP-binding proteins (Cherfils and Chardin, 1999), a fact that complicates the identification of new GEFs. Therefore, approximately 50 % of the mammalian GEFs have either been identified based on their ability to stimulate the nucleotide exchange on Rho GTPases *in vitro* or by analyzing their effects after over-expression *in vivo*. Little is known about the regulation of GEFs. It is thought that they might be tightly regulated and that different types of GEFs might be controlled by distinct mechanisms. Apart from other models of GEF activation, which will not be discussed here, an interesting hypothesis predicts that GEFs are regulated by protein-protein interactions (Cherfils and Chardin, 1999; Zheng, 2001). Homo- and hetero-oligomerization has been reported to be essential for GEF activity and is important within the cell to form larger signaling complexes involved in GTPase activation (Schmidt and Hall, 2002).

The first mammalian RhoGEF, Dbl, was originally isolated in the 1980s as an oncogene from a diffuse B-cell lymphoma. Dbl was shown to catalyze nucleotide exchange on the human GTPase Cdc42 *in vitro*. Dbl and Cdc24, a yeast cell-division cycle protein, both contain a conserved domain known as the Dbl-homology (DH) domain, which is necessary for catalytic activity. Both proteins were shown to act as GEFs (Zheng, 2001). Many additional DH-containing Rho GEFs have been identified in several organisms, such as *Saccharomyces cerevisiae*, *Caenorhabditis elegans*, *Drosophila melanogaster* and humans, but not in plants. DH domain proteins are mostly multidomain proteins and contain three conserved regions, CR1, CR2 and CR3. These proteins, nevertheless, share only little homology outside of the DH domain. Even if they utilize the same substrate, DH-GEFs often do not share more than 20 % sequence identity.

In addition to the DH domain, most Rho GEFs contain a pleckstrin homology (PH) domain

adjacent and COOH-terminal to the DH domain. It was found that the tandem DH-PH module is the minimal structural unit that can promote nucleotide exchange *in vitro* (Zheng, 2001). The PH domain is known to bind to phosphorylated phosphoinositides (PIPs) and may target the GEF to the appropriate intracellular location or directly affect the catalytic activity of the DH domain (Schmidt and Hall, 2002).

In contrast to the described DH domain containing GEFs, an unconventional GEF has been described. DOCK180 was identified as an interactor of nucleotide-free mammalian Rac, which is in fact a characteristic feature of exchange factors. In a complex with ELMO1, DOCK180 contains Rac GEF activity *in vivo* and *in vitro* (Raftopoulou and Hall, 2004). DOCK180 and ELMO1 both do not contain a conserved Dbl-homology domain. Orthologues of DOCK180 and ELMO1 were also identified in *C. elegans* (CED-5) and *Drosophila* (MYOBLAST CITY, MBC; Brugnera *et al.*, 2002; Côté and Vuori, 2002). A specific domain within the DOCK180 protein, the DOCKER or DHR-2 (Dock Homology Region 2) domain, was shown to specifically bind to nucleotide-free Rac and to promote Rac-GTP loading *in vitro* (Côté and Vuori, 2002), but does not resemble the DH domain and has a different tertiary structure (Brugnera *et al.*, 2002). ELMO1, instead, lacks any obvious catalytic domains and fails to have a notable effect on Rac GTP-loading *in vivo*, when expressed alone (Côté and Vuori, 2002). Although the results for DOCK180/ELMO1 are partially controversial in respect to the requirement of ELMO1 in GTP-loading of the GTPase (Brugnera *et al.*, 2002; Côté and Vuori, 2002), the presence of DOCK180/ELMO1 complexes in several organisms suggests the common existence of independent two-part exchange factors if not multi-protein GEF complexes in addition to Dbl family GEFs.

1.2.3.1 Guanine nucleotide exchange factors in plants

Although it has been stated that the plant genome lacks DH-containing GEFs for Rho GTPase activation, an Arf GEF has been identified, suggesting that plants do regulate their GTPase cycle by the involvement of GEFs. Arf GTPases are of course different from Rho GTPases, as they are predominantly involved in secretory and vacuolar trafficking pathways (Vernoud *et al.*, 2003). The Arf specific exchange factor, GNOM, has been identified in a mutant screen for *A. thaliana* with defective body organization in embryos. GNOM is localized to endosomes and controls the polarized trafficking of the auxin efflux carrier PIN1 to the basal plasma membrane (Geldner *et al.*, 2003). All Arf GEFs contain a Sec7 domain and eight Sec7 domain-containing proteins have been identified in *A.*

thaliana, constituting only two subfamilies of Arf GEFs, in contrast to five encoded in the mammalian genome. Only GNOM was characterized further. Nevertheless, GNOM mutants are shown to be neither affected in pollen tube growth, nor in cytokinesis (Geldner *et al.*, 2003). In conclusion, GNOM activity is not essential for polarized pollen tube growth.

Apart from Arf GEFs, also plant proteins with homology to yeast and mammalian Rab GEFs and Ran GEFs have been identified (Vernoud *et al.*, 2003).

Rho GTPases are the only low molecular weight GTP-binding proteins shown to be directly involved in the regulation of polarized pollen tube growth. The fact that the plant genome lacks conventional DH-containing proteins is even more surprising considering the existence of plant proteins with significant homologies to exchange factors of Arf, Rab and Ran GTPases. These observations insinuate that the Rho GTPase cycle might be differentially regulated or that plants may employ plant-specific Rho GEFs. The human, worm or yeast DOCK180 and ELMO1 proteins acting as Rho GEFs in addition to the DH-containing proteins were identified in the same year as a plant-specific protein, called SPIKE1, which resembles homology to DOCK180 (Qiu *et al.*, 2002). SPIKE1 was identified in a screen for *A. thaliana* trichome-morphogenesis mutants and knock-out of the gene encoding this protein causes trichome, cotyledon and leaf-shape defects. The COOH-terminal region of SPIKE1 showed homology to *C. elegans* CED-5, to human DOCK180, to *Drosophila* MYOBLAST CITY, which constitute the CDM family of proteins. CDM proteins are adapter proteins thought to transduce extracellular signals and to mediate the cytoskeletal reorganization. The homologous region in SPIKE1 was subsequently called the CDMS domain, but the protein also contained two additional conserved regions, which are only found in multicellular organisms, named MOD1 and MOD2. These domains are thought to either recruit additional proteins or to autoregulate the activity of other proteins (Qiu *et al.*, 2002). Only a single copy of the gene was found in *Arabidopsis*, although eleven AtRop GTPase genes were identified.

The identification of SPIKE1 leads to the conclusion that plants contain proteins that share sequence similarities to characterized Rho GEFs. However, it seems unlikely that a single copy gene, like SPIKE1, might encode a GEF protein that unspecifically regulates all eleven AtRop GTPases. Therefore, other exchange factors are likely to exist in plants.

1.2.3.1.1 Plant-specific Rho GEFs do exist in plants

Very recently Berken *et al.* (2005) described the identification, cloning and functional analysis of plant-specific Rho GEFs. They screened an *A. thaliana* cDNA library using a dominant inhibitory mutant of AtRop4 (D¹²¹N), as bait in a yeast two-hybrid screen. The identified proteins do not show sequence homologies to known mammalian or yeast Rho GEFs, but belong to a family of highly related proteins in plants with approximately fourteen members in *A. thaliana*, eleven in rice, one in tomato and one in *Medicago truncatula*. These proteins of 500 to 550 amino acid residues contain three individual domains, one of them being a plant-specific domain of unknown function, DUF 315. The identified Rop GEFs were shown to specifically stimulate nucleotide dissociation from AtRop4 a thousand times and were shown to form a tight complex with nucleotide-free AtRop4 (Berken *et al.*, 2005).

1.2.4 Aims of the dissertation (1st project)

We intended to screen a tobacco pollen tube-specific cDNA library in order to identify novel plant-specific Rho GEFs. Therefore, a DN mutant for the tobacco Nt-Rac5 was generated by the amino acid exchange at position 20, resulting in the mutant Nt-Rac5 T²⁰N.

Dominant negative (DN) mutants cannot interact with downstream target proteins, but bind strongly to their specific GEFs in “dead-end” complexes, thereby preventing the activation of the endogenous GTPase (Feig, 1999; Debreceni *et al.*, 2004). The specific and strong binding to GEFs is a characteristic feature for DN mutants of GTPases and provides the basis for the experiments described in the first part of the thesis.

Goals:

- Identification of plant-specific Rho GEFs as interactors of DN-Nt-Rac5 in a yeast two-hybrid screen
- Elucidation of the subcellular localization of Nt-Hypo1
- Determination of the role of Nt-Hypo1 in the regulation of polarized pollen tube growth through *in vivo* over-expression experiments and through the generation of loss-of-function RNAi plants
- Verification of the identified interaction between DN-Nt-Rac5 and Nt-Hypo1 *in vivo* and *in vitro*
- Determination of the intrinsic GTPase activity of Nt-Rac5 and characterization of enzymatic activities of the potential Rho GEF *in vitro*
- Antibody production against Nt-Hypo1 to perform *in vitro* pull-down assays and immunolabelings
- Identification of proteins other than Nt-Rac5 that interact with Nt-Hypo1 and characterization of regulatory complexes formed by these proteins

1.3 Phospholipid signaling in pollen tubes

1.3.1 Phosphoinositides

Phosphoinositides are mainly involved in various membrane-trafficking events (Wang, 2001), as will be elucidated in the following paragraphs. The membrane-associated phospholipid phosphatidylinositol serves as a precursor of lipid second messengers, known as phosphoinositides. Phosphoinositides differ from each other in the phosphorylation status of their inositol groups (Figure 4). They function as spatially restricted membrane-associated second messengers, because their synthesis and turnover from the relatively abundant phosphatidylinositol membrane precursor can be fast and highly concentrated within discrete membrane micro-domains. In order to ensure sufficient binding of interacting proteins, specific phosphoinositides are typically more abundant than their binding partners, so that a saturation of the binding sites does generally not occur (Cullen *et al.*, 2001). Structurally distinct phosphoinositides can activate different downstream effectors and thereby mediate multiple signal transduction pathways in one cell.

The identification of highly conserved modular protein domains that specifically bind various phosphoinositides represented a major advance in the understanding of phosphoinositide signaling. Identified domains are, *e.g.*, the epsin amino-terminal homology (ENTH) domain, the Fab1, YOTB, Vac1 and EEA1 (FYVE) domain, the band 4.1 ezrin, radixin and moesin (FERM) domain, the phox homology (PX) domain or the pleckstrin homology (PH) domain. The listed modules are found in multiple cellular proteins and recruit their host protein to specific regions inside the cell via their interactions with phosphoinositides (Cullen *et al.*, 2001; Lemmon, 2003). Subsequently, any increase in the concentration of the partner lipid, results in a local enrichment or translocation of the signaling protein. These interactions can last from some seconds to several minutes. Phosphoinositide-binding proteins usually diffuse through the cytosol, ready to interact with their specific phosphoinositide, activated by only a single extra- or intracellular signal.

This introduction focuses exclusively on the identified pleckstrin-homology (PH) domain in the following paragraph, because the PH domain is frequently found in proteins involved in membrane trafficking pathways. The PH domain is described to be the eleventh most common domain in humans, it comprises a small β -sandwich protein module of 100 to 120 amino acid residues (Essen *et al.*, 1996; Martin, 1998; Lemmon 2003). PH domains can be observed once or several times in a protein sequence. Soluble proteins, containing a PH domain, usually require membrane association to be fully

functional. Most PH domain-containing proteins, if not all, bind to phosphoinositides, but their degree of specificity or affinity differs (Cullen *et al.*, 2001; Lemmon 2003).

The PH domain of the mammalian PI-PLC δ_1 specifically binds to PI-4,5-P₂ and is thereby responsible to target this protein to the plasma membrane (Stauffer *et al.*, 1998). Fusions of that specific PH domain to the green fluorescent protein (GFP) have shown that phosphoinositide binding by PH domains is sufficient for their independent, signal regulated targeting to cell membranes (Hurley and Meyer, 2001). In fact, this fusion is widely used as a biosensor to visualize PI-4,5-P₂ *in vivo* and has been used to show that PI-4,5-P₂ is mainly concentrated in the plasma membrane. These observations showed that PI-4,5-P₂ is present in the cell in a discontinuous, raft-like clustering and not uniformly distributed over all membranes (Stauffer *et al.*, 1998; Kost *et al.*, 1999). Furthermore, PI-4,5-P₂ is present in gradients and spatially restricted. The dynamic and highly localized distribution may result from selective recruitment factors or from the activation of specific phosphoinositide kinases, increasing the synthesis of PI-4,5-P₂ in restricted areas of the cell (Martin, 1998).

1.3.2 Phosphatidylinositol 4,5-bisphosphate synthesis and functions

Animal cells use two distinct pathways to generate PI-4,5-P₂ (Figure 4). First, the classical phosphoinositide cycle, involves the sequential phosphorylation of phosphatidylinositol to phosphatidylinositol-4-monophosphate [PI(4)P] and PI-4,5-P₂. Second, a recently revealed pathway, synthesizes PI-4,5-P₂ from PI via the novel lipid phosphatidylinositol-5-monophosphate [PI(5)P]. The second step in the synthesis, then, in each pathway is catalyzed by homologous type I and type II PIP kinases. Type I kinases phosphorylate PI(4)P to PI-4,5-P₂ and are called PI(4)P-5-kinases, whereas type II kinases generate PI-4,5-P₂ by phosphorylation of PI(5)P and are consequently called PI(5)P-4-kinases (Martin, 1998; Cullen *et al.*, 2001).

Considering, that PI-4,5-P₂ levels in plants are ten times lower than in mammalian cells, its synthesis during PI-PLC activity must increase enormously to reach an InsP₃ concentration comparable to those in animal cells (Meijer and Munnik, 2003).

PI-4,5-P₂ is known to play fundamental roles in the regulation of the actin cytoskeleton, thus, its restricted localization during endocytic uptake might affect the cytoskeleton. It is also known to bind several actin-binding proteins, such as profilin, gelsolin, cofilin or α -actinin. These proteins are binding to the actin cytoskeleton thereby regulating its assembly

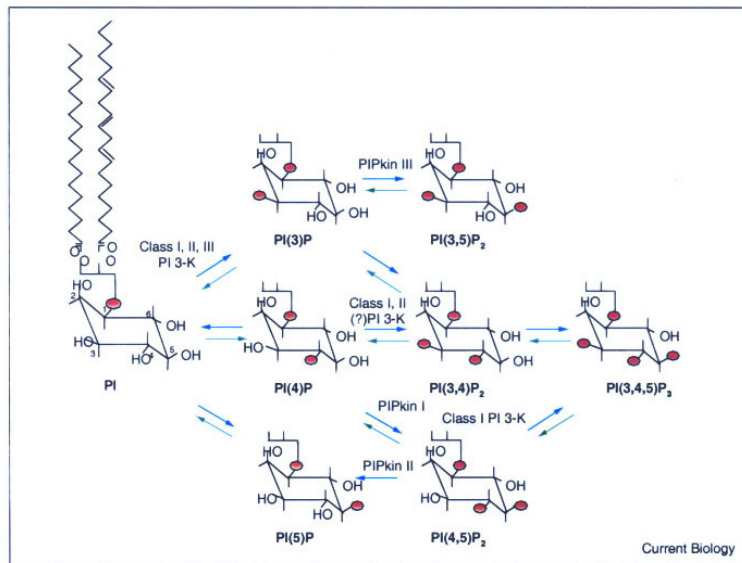


Figure 4: Phosphoinositide metabolism. Phosphatidylinositol (PI) consists of D-myo-inositol-1-phosphate linked via its phosphate group to 1-stearoyl, 2-arachidonyl diacylglycerol. The inositol ring at the PI can reversibly be phosphorylated at one or a combination of the 3', 4' or 5' positions. Phosphatidylinositol and its phosphorylated derivatives are collectively referred to as phosphoinositides. The two distinct pathways of PI-4,5-P₂ synthesis are shown at the lower mid position in the graphic. (Modified from Cullen *et al.*, 2001.)

(Drøbak *et al.*, 1994; Kovar *et al.*, 2000; Lemmon, 2003). Therefore, PI-4,5-P₂ is supposed to be directly involved in cell functions, which involve the cytoskeleton and these are cytokinesis or cell motility (Homma and Emori, 1995).

By the use of the biosensor GFP-PI-PLC- δ_1 -PH in transient expression experiments in tobacco pollen tubes, it was shown that PI-4,5-P₂ accumulated at the plasma membrane in the pollen tube apex (Kost *et al.*, 1999). PI-4,5-P₂ was further shown to act in a common pathway with Rac GTPase homologues and thereby regulates polarized pollen tube growth. It has been shown that its compartmentalization at the tip is controlled by Rac homologues. PI-4,5-P₂ in the pollen tube tip may induce capping and uncapping of actin filaments by causing the translocation of actin-binding proteins, which may subsequently stimulate elongation of longitudinally oriented actin cables and may control the formation of actin structures in the pollen tube apex (Kost *et al.*, 1999). Apart from its role in actin organization, PI-4,5-P₂ may directly contribute to exocytosis at the pollen tube tip, either by recruiting proteins that regulate membrane fusions or by locally altering the membrane lipid composition (Martin, 1998; Kost *et al.*, 1999). Additionally to act as an effector itself, PI-4,5-P₂ serves as the substrate for PI-PLC hydrolysis, which in turn generates the two second messengers diacylglycerol and inositol 1,4,5-trisphosphate.

1.3.3 Phosphoinositide-specific phospholipases C

1.3.3.1 General overview

Phosphoinositide-specific phospholipases C (PI-PLCs) are best characterized in mammalian cells and are known to act as a cellular response to stimulation of cell surface receptors by extracellular signals and represent one of the key enzymes involved in signal transduction processes. As Ca^{2+} -dependent enzymes, they catalyze the hydrolysis of the formerly described phosphatidylinositol 4,5-bisphosphate (PI-4,5- P_2) into the second messengers diacylglycerol (DAG) and inositol 1,4,5-trisphosphate (Ins P_3). Ins P_3 is water-soluble and diffuses into the cytosol. It is known to trigger Ca^{2+} -influx from intracellular stores, *e.g.* the vacuole or the endoplasmic reticulum. Diacylglycerol, on the other hand, remains associated with the membrane, is not supposed to accumulate in plant cells, where it seems to be phosphorylated to phosphatidic acid (PA) by a DAG kinase, instead (Meijer and Munnik, 2003). In mammalian cells DAG is known to activate certain members of the protein kinase C family. In plants, these enzymes have not been identified to date, as they are not encoded in the *Arabidopsis* or rice genome.

PI-PLCs are divided into different subfamilies in animal cells. Five subfamilies have been identified based on protein isolation, immunological characterization or on sequence analyses: β , γ , δ , ϵ and ζ (Figure 5). Their enzymatic activities are all regulated by different mechanisms. The β isozymes, for example, are known to be activated by heterotrimeric G-

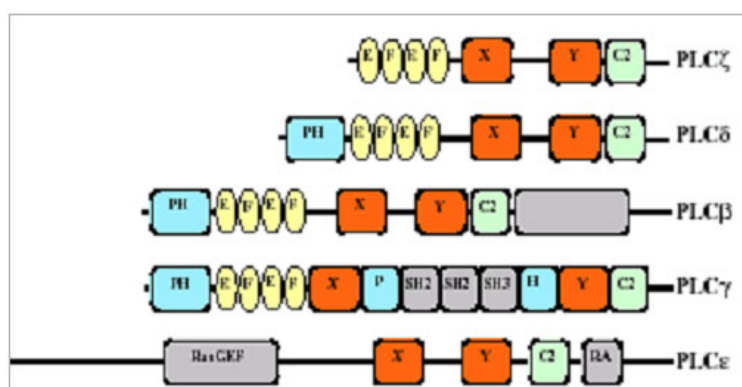


Figure 5: Schematic illustration of the predicted domains from mouse PLC ζ and mammalian PLC isoforms β , γ , δ and ϵ . (Modified from Saunders *et al.*, 2002.)

proteins that include the $G_{\alpha q}$ subfamily of G_{α} proteins. PI-PLCs β contain an additional regulatory COOH-terminal region that is responsible for the specific binding and activation by G-protein αq subunits. PI-PLCs γ , instead, are regulated by tyrosine kinase-linked receptors and comprise an internal major regulatory element consisting of a split PH

domain and SH2 and SH3 domains (Essen *et al.*, 1996; Rebecchi and Pentylala, 2000). PI-PLC δ activity might be regulated on its interaction with a Gh-type G-protein (transglutaminase II). PI-PLCs ϵ are thought to be activated by small monomeric GTPases of the Ras and Rho families and by herterotrimeric G-proteins and PI-PLC ζ 's regulatory mechanism is still unknown (Swann *et al.*, 2004).

Two types of PI-PLCs are known to date. One is membrane associated and prefers PI-4,5-P₂ and PIP over PI as substrate at physiological Ca²⁺ concentrations, in the μ M range, the other is predominantly present in the cytosol and prefers PI as substrate and requires millimolar Ca²⁺ concentrations (Wang, 2001; Mueller-Roeber and Pical, 2002). In contrast to eukaryotic PI-PLCs, prokaryotic PI-PLCs are metal-independent enzymes and hydrolyze solely PI and its analogues, but not PIP or PI-4,5-P₂ (Essen *et al.*, 1996).

Additionally, no evidence for direct activation of PI-PLCs by G protein activators, nucleotides or non-hydrolyzable GTP γ S in plasma membranes from different species of higher plants was gained (Cho *et al.*, 1995, references therein and Ortega *et al.*, 2005).

1.3.3.2 Molecular domain structure

The revelation of the crystallographic structure of the mammalian PI-PLC δ_1 allowed insights into the involvement of specific residues in possible membrane binding or catalysis mechanisms. PI-PLCs usually comprise five distinct domains. At the NH₂-terminus a pleckstrin homology (PH) domain is situated, followed by the EF-hand motif. Mammalian PI-PLCs contain four consecutive EF hands, which are characteristic for their helix-loop-helix topology. They are pairwise distributed into two lobes (Essen *et al.*, 1996; Rebecchi and Pentylala, 2000). The function of the EF hand is still unresolved. The centre of the protein is build by the catalytic domain, which consists of the X and the Y domains. This represents the region of highest sequence homology, not only among mammalian PI-PLCs and contains two conserved histidine residues, His₃₁₁ and His₃₅₆. The topology resembles that of a distorted, but closed triose phosphate isomerase (TIM) barrel. The X region forms half of the TIM barrel-like architecture with an alternating $\beta\alpha$ motif. The other half of the barrel is formed by the Y region and this half in fact lacks a helix region to form a typical TIM barrel. The missing helix is accomplished by an extensive loop region, instead. The rest of the Y region folds up in $\beta\alpha$ -repeat units. The spanning region or Z-region, between the X and the Y domains, consists of a stretch of charged residues that is obviously not required for catalysis (Essen *et al.*, 1996; Rebecchi and Pentylala, 2000). The C2 domain at the COOH-terminus of the protein, is also called CalB domain due to its

involvement in calcium and lipid binding. This motif consists of approximately 120 residues and is arranged as an eight-stranded anti-parallel β -sandwich.

1.3.3.3 Membrane binding

Membrane binding of the PI-PLC δ_1 and probably also of almost all other identified mammalian PI-PLCs is mediated by two domains, the NH₂-terminally PH domain and the COOH-terminally C2 domain, which are also known from other proteins to be involved in membrane association. Membrane binding is actually a three-step process, consisting of tethering and fixing of the protein plus the penetration of the membrane by the active site of the enzyme. First, the PH domain tethers the enzyme to the membrane by specific binding to PI-4,5-P₂ and then, the C2 domain fixes the catalytic core in a productive orientation relative to the membrane (Essen *et al.*, 1996; Rebecchi and Pentylala, 2000). This binding mechanism provides two sites of possible regulation, either by altering the intracellular Ca²⁺ concentration or by modifying the phospholipid composition of the membrane. If one factor required for binding is missing, *e.g.* by deletion of the C2 domain, the protein loses its enzymatic activity (Otterhag *et al.*, 2001). PI-PLCs are mostly membrane-associated enzymes and their activity requires that the catalytic core adsorbs to the membrane so that its active site gains access to the scissible phosphodiester bond. The active site does not exhibit hydrophobic surface features, which might accommodate the lipid portion of phosphoinositides. However, the hydrophobic rim might penetrate the hydrophobic portion of the membrane during the catalysis reaction, in order to facilitate entry of the phospholipid substrate into the active site. Further structural investigations lead to the idea, that approximately 1 nm² of the protein surface penetrates the membrane, which roughly comprises the size of the hydrophobic ridge (Essen *et al.*, 1996).

1.3.3.4 Phosphoinositide hydrolysis

The hydrolysis of PI-4,5-P₂ is then a two-step reaction. In the first step, a cyclic phosphodiester intermediate is formed by nucleophilic attack of the axial 2-hydroxyl group of PI-4,5-P₂. In a second step, the 1,2-cyclic-inositolphosphate intermediate undergoes hydrolysis to yield cyclic InsP₃. The central role for Ca²⁺ in this reaction is to act together with one of the conserved histidine residues, His₃₁₁, in order to stabilize the highly negatively charged pentavalent phosphoryl transition state.

1.3.3.5 Cloning and cellular functions of PI-PLCs in plants

A number of PI-PLC genes have been cloned from plants to date, including *Arabidopsis thaliana* (Hirayama *et al.*, 1995, 1997), *Glycine max* (Shi *et al.*, 1995), *Solanum tuberosum* (Kopka *et al.*, 1998a), *Nicotiana rustica* (Ståxen *et al.*, 1999), *Pisum sativum* (Venkataraman *et al.*, 2003), *Physcomitrella patens* (Repp *et al.*, 2004), *Vigna radiata* (Kim *et al.*, 2004), *Brassica napus* (Das *et al.*, 2005), *Lilium daviddi* (Pan *et al.*, 2005) and *Zea mays* (Zhai *et al.*, 2005). Plant PI-PLCs have always been grouped with mammalian PI-PLCs of the δ -subgroup, based on comparisons of domain structure, size or sequence similarities (Wang, 2001 and references therein). The identification of δ -type PI-PLCs also in yeast and filamentous fungi leads to the conclusion that PI-PLCs of the δ -subgroup must be an archetypal enzyme class, which has evolved rather early in eukaryotes (Essen *et al.*, 1996; Rebecchi and Pentylala, 2000). PI-PLCs of the β - and γ -subgroup might have arisen later after the split between plant, fungi or animals. But, a recently identified novel subgroup of PI-PLCs, the PI-PLC ζ (Saunders *et al.*, 2002 and 2004), in fact resembles more closely the plant PI-PLC-type, so that the classification of plant PI-PLCs belonging to the δ -type of PI-PLCs, has to be reassessed.

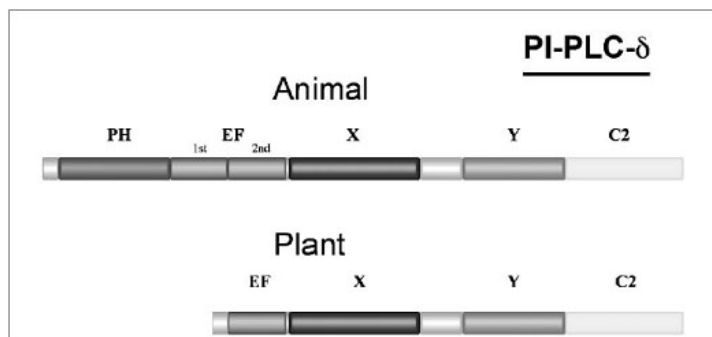


Figure 6: Representation of the modular domain structures of PI-PLC δ from animals and plant PI-PLC isoforms. Conserved domains are represented by blocks of different colours. The EF-hand domain of plant PI-PLCs corresponds to the second loop of the EF-hand domain of animal PI-PLCs. The X and Y domains constitute together the catalytic domain of PI-PLCs. (From Mueller-Roeber and Pical, 2002.)

It is striking that plant PI-PLCs show two important sequence variations compared to mammalian PI-PLCs. They lack the NH₂-terminal PH domain and the Ca²⁺-binding EF hands are incomplete or even missing in some isozymes (Figure 6; Rebecchi and Pentylala, 2000; Meijer and Munnik, 2003). But, nevertheless, all identified plant PI-PLCs to date, are predominantly membrane-associated enzymes (Shi *et al.*, 1995; Otterhag *et al.*, 2001; Hunt *et al.*, 2003; Kim *et al.*, 2004). This observation raises the question of how plant PI-PLCs interact in the first step with membranes and their substrate? Although this question is not solved to date, it is obvious that plants must differ from their mammalian counterparts, as they are missing the PH domain, which is essential for membrane binding in mammals. It has been suggested that the C2 domain might be sufficient to target the

enzyme to the membrane or that other regions of PI-PLC proteins, such as hydrophobic moieties with or without post-translational modifications, might be required in addition (Mueller-Roeber and Pical, 2002). Nevertheless, the conservation of the C2 domain and the two histidine residues in the catalytic core, indicate that the catalytic mechanism of plant PI-PLCs might be the same as in mammalian ones (Wang, 2001).

Although nothing is known about the regulation of plant PI-PLCs, these proteins have been reported to be involved in a number of cellular processes in plants, including stomatal closure (Staxén *et al.*, 1999), cytoskeleton organization (Kovar *et al.*, 2000) and pollen tube growth (Kost *et al.*, 1999). They have also been implicated in other signaling pathways, such as those mediated by (blue) light, ABA, gravity, pathogen attack, drought or cold (Hirayama *et al.*, 1995; Pical *et al.*, 1999; Kopka *et al.*, 1998a; Perera *et al.*, 2001; Coursol *et al.*, 2002; Harada *et al.*, 2003; Repp *et al.*, 2004; Zhai *et al.*, 2005), mostly because the activation of these pathways was shown to result in an increase of phosphoinositide concentrations. For example, PI-PLC activity increases after treatment with the wasp venom peptide mastoparan or its active analogue Mas7, two peptides that have stimulating effects on most heterotrimeric G proteins in animal systems (Legendre *et al.*, 1993; Cho *et al.*, 1995; Drøbak and Watkins, 1994; Munnik 1998), but it is not clear whether this is a direct or indirect effect mediated by Ca^{2+} .

Additionally, increasing PI-4,5-P₂ concentrations have been measured in *Arabidopsis thaliana*, which caused subsequently an increase in InsP₃ production within 15 min after salt-stress treatment and also a further increase in the intracellular Ca^{2+} concentration has been reported (de Wald *et al.*, 2001), which all might be the result of an elevated PI-4,5-P₂ hydrolysis by PI-PLCs. But this observation raises another question. InsP₃ is one of the products of PI-4,5-P₂ hydrolysis by PI-PLCs in animal systems, but no sequence similarities to InsP₃-receptor-mediated Ca^{2+} -channels have been reported from the *Arabidopsis* genome. Only functional InsP₃-binding sites have been identified on ER membranes in plant cells (Munnik *et al.*, 1998 and references therein). A comparison to yeast cells has also been drawn, in which InsP₃ is further phosphorylated to InsP₆, which in turn affects gene transcription and RNA transport (Laxalt and Munnik, 2002). This might also be a suitable explanation for the absence of InsP₃ receptor genes in the plant kingdom. In addition to the doubts mentioned above, concerning InsP₃-mediated Ca^{2+} release in plants, the signaling pathway concerning the second product of the PI-4,5-P₂ hydrolysis, the DAG functioning as a Protein Kinase C activator, is still in question (Meijer and

Munnik, 2003). *In planta*, the DAG is thought to be immediately phosphorylated to phosphatidic acid (PA) by a diacylglycerol kinase (DGK; Munnik, 2001). And, also PA is not supposed to accumulate in plant cells, but might be further phosphorylated to diacylglycerol pyrophosphate by a phosphatidic acid kinase (PAK). Although PA is emerging as another second messenger in plants, its signaling mechanism is still unclear (Munnik, 2001).

In order to gain further insights into the regulation or function of plant PI-PLCs, loss-of-function mutants have been investigated. Ellis *et al.* (1998) down-regulated or completely abolished the activity of the mammalian PI-PLC δ_1 by various mutations in the active site of the enzyme. Apart from antisense-mediated downregulations of the PI-PLC gene in *A. thaliana* (Sánchez and Chua, 2001), another frequently used method to inhibit PI-PLC activity is by pharmacological treatment with the aminosteroid U-73122. Although the mechanism of action of this inhibitor remains unclear, it was shown to reduce the accumulation of intracellular InsP₃ in both animal and plant systems (Bleasdale *et al.*, 1990; Shigaki *et al.*, 2000) and blocked the activity of purified recombinant PI-PLC *in vitro* (Staxén *et al.*, 1999; Feißt *et al.*, 2005). It was supposed that the reduction of InsP₃ content after inhibitor treatment was due to the inhibition of PI-4,5-P₂ hydrolysis by PI-PLCs. Subsequently, an increase of PI-4,5-P₂ would be expected, which in turn might trigger effects by regulating various enzymes for cellular functions, *e.g.* actin-binding proteins or recruiting proteins that mediate vesicle fusion (Martin, 1998).

1.3.3.5.1 PI-PLCs and their role in pollen tube growth

To date, a strong Ca²⁺ dependency of PI-PLC activity has been reported for all characterized plant PI-PLCs (Melin *et al.*, 1992; Drøbak *et al.*, 1994; Hirayama *et al.*, 1995; Stáxén *et al.*, 1999). Not only that Ca²⁺ is the most important second messenger in plant cells, it has also been reported that the intracellular Ca²⁺ concentration is one of the major regulators of polar pollen tube growth (chapter 1.2.1). A tip-focused Ca²⁺-gradient is proved to be essential for polarized growth (Hepler *et al.*, 2001). This spatially restricted high Ca²⁺ concentration may either contribute to PI-PLC activity in pollen tubes by facilitating membrane association and enzymatic activity or on the other hand may be established itself by PI-PLC activity and the subsequent increase in the intracellular Ca²⁺ concentration caused by the generation of InsP₃.

An *A. thaliana* PI-PLC isoform, AtPLC4, was shown to be highly expressed in pollen and is thought to allow an immediate release of Ca^{2+} and activation of signaling cascades upon contact with the stigma. Thereby, it may play an important role in fertilization or may be translocated from the grain to the pollen tube tip during pollen tube expansion, suggesting a later function in the interaction between the pollen tube with the ovule (Hunt *et al.*, 2004).

InsP₃ and phosphoinositides have also been reported to be strongly involved in pollen tube growth and in the organization of its cytoskeleton. The photolysis of caged InsP₃, *e.g.*, resulted in an increase of the intracellular Ca^{2+} concentration. Treatment with the G-protein activator mastoparan or the InsP₃-receptor inhibitor heparin, instead, resulted in a pollen tube growth stop (Franklin-Tong *et al.*, 1996). Pollen-pistil interactions are also accompanied by a transient increase in cytosolic-free Ca^{2+} levels during the self-incompatibility (SI) response of *Papaver rhoeas*, which results in the inhibition of pollen tube expansion and lead to the death of the incompatible pollen. They have additionally provided pharmacological evidence for the presence of a Ca^{2+} -dependent PI-PLC activity in *P. rhoeas* pollen and their results indicate the involvement of PI-PLCs in pollen tube growth during the SI response, but direct evidence of the existence of PI-PLC transcripts are still missing (Franklin-Tong *et al.*, 1993, 1996, 2003).

A comparison of the role of PI-PLCs in pollen tubes and the role of the recently identified PI-PLC ζ involved in sperm-egg interactions in mammals has been drawn by Hunt *et al.* (2004). The release of sperm-specific PI-PLC ζ on fertilization, results in oscillations of the free Ca^{2+} concentration in mouse eggs and triggers activation of embryo development (Saunders *et al.*, 2002; Swann *et al.*, 2004). The injection of plant sperm cell extracts from *Brassica* anthers, triggered also Ca^{2+} oscillations in mouse eggs (Li *et al.*, 2001). Therefore, Hunt *et al.* speculate that the function of pollen-specific PI-PLCs may be analogous to that of PI-PLC ζ in sperm-egg interactions in mammals. Pollen-specific PI-PLCs may be important in the recognition of pollen by the stigma or in subsequent pollen germination and tube growth.

1.3.4 Aims of the dissertation (2nd project)

Kost *et al.* (1999) showed that Rac homologues of the family of small Rac/Rop GTPases physically associate with a lipid kinase which specifically generates PI-4,5-P₂. Thus, Rac/Rop GTPases and PI-4,5-P₂ act in a common pathway in order to regulate polarized pollen tube growth and are both spatially restricted to the plasma membrane in the pollen tube apex. It was of major interest for the present work to investigate if a link between Rac/Rop GTPases and PI-PLCs exists, considering that PI-PLCs use PI-4,5-P₂ as their substrate. A further point of interest was, if PI-PLCs are mainly involved in the establishment and maintenance of the tip-focused Ca²⁺-gradient by hydrolyzing PI-4,5-P₂, and thereby also representing key regulators of polar pollen tube growth.

Goals:

- Identification and cloning of novel PI-PLC isoforms from tobacco
- Characterization of the enzymatic activity of NtPLC3 *in vitro*
- Visualization of the intracellular localization of NtPLC3 and determination of domains essential for the targeting of the protein to the plasma membrane
- Characterization of effects of altered activity of NtPLC3 on pollen tube growth or morphology. NtPLC3's activity was modulated using:
 - a) Over-expression of WT, truncated and mutated NtPLC3 and
 - b) Inhibition of PI-PLCs using the PI-PLC specific inhibitor U-73122 and
 - c) Gene knock-out by RNA interference (in progress)
- Visualization of the localization of PI-PLC substrates or products in pollen tubes and analysis of effects on their intracellular distribution resulting from the modulation of PI-PLC activity

2 RESULTS

2.1 Identification and functional characterization of a new interactor of pollen tube Nt-Rac5

With the intention of identifying regulators and effectors of the tobacco pollen tube Rac/Rop GTPase Nt-Rac5 (Kieffer *et al.*, 2000), yeast two-hybrid screens were performed. The yeast two-hybrid system is a powerful genetic technique designed to identify novel protein-protein interactions, which was previously limited exclusively to biochemical assays. The advantage of the two-hybrid system is that it allows in only a single step, the identification of potential interacting proteins and at the same time the isolation of the encoding genes. In the first step, the cDNA of a protein of interest is fused to the DNA binding domain of a transcription factor and serves as the “bait” in the hybrid assay. In a second step, a cDNA library is fused to the transcriptional activation domain and functions as the “prey” (Fields and Song, 1989).

The yeast two-hybrid screen was employed in a slightly different way in our laboratory and will briefly be explained here. The transformation of *Saccharomyces cerevisiae* HF7c cells in library scale assays served to identify yeast two-hybrid protein-protein interactions of an already known protein, the bait, and its putative interactors encoded in the cDNA library. The plasmid scale assays, instead, or re-transformations, served as a tool to verify yeast two-hybrid protein-protein interactions of already known proteins and/or as a control to exclude false positive interactors identified in the library scale experiment. Bait and prey constructs were simultaneously co-transformed into HF7c cells using a small scale lithium acetate method (see MATERIALS AND METHODS). As negative controls, to exclude the interaction of the protein of interest with *e.g.* the DNA activating or binding region, served co-transformed bait and prey constructs with empty pGBKT7 and pGAD-GH, respectively.

In the following paragraphs, the Y2H screen will be described using a dominant negative mutant of Nt-Rac5 as the bait. The yeast two-hybrid system employed in this work was the Matchmaker™ Gal4 Two-Hybrid System from Clontech™. The protein of interest, DN-Nt-Rac5, was cloned into the bait vector pGBKT7. A translational fusion was thereby generated between the DN-Nt-Rac5 and the DNA-binding domain of the Gal4 transcription factor. Second, a tobacco pollen tube cDNA library was cloned into the prey vector, pGAD-GH, creating translational fusions between pollen tube proteins and the activating domain of the same Gal4 transcription factor. The cDNA library used in this assay was

highly complex (5.5 million clones, 95 % with insert, 30 % of the inserts \geq 1 kb; data not shown) and represented genes expressed in tobacco pollen tubes three hours after germination. As two-hybrid interactions take place in the nucleus of yeast cells, the sequence of DN-Nt-Rac5 was modified by an additional point mutation. Like most Rho GTPases, Nt-Rac5 contains a CAAX domain at the COOH-terminus, which is post-translationally prenylated and targets the protein to the plasma membrane. To ensure effective import of DN-Nt-Rac5 into the nucleus of the yeast cells, the cysteine in the CAAX domain was mutated to serine by site-directed mutagenesis (C¹⁹⁴S).

HF7c cells are incapable of synthesizing histidine, because they are missing a functional copy of the *his3* gene. If two proteins are interacting in Y2H assays, the Gal4 DNA binding domain and the Gal4 activating domain are physically brought into contact, building a transcriptional activator that binds to the Gal4 upstream activating sequence (UAS) situated upstream of the reporter gene *his3* and thus allowing the transcription of this gene. The HIS3 protein is required for histidine synthesis in these cells and its expression allows the HF7c cells to grow on histidine-free medium. Yeast cells growing on histidine-free medium indicate therefore an interaction of two proteins. HF7c cells are known to be slightly leaky as far as the inhibition of the histidine synthesis is concerned. Growth medium was therefore supplemented with 3-amino-1,2,4-triazole (3-AT), a competitive inhibitor of the HIS3 protein, to suppress residual histidine synthesis and to increase the stringency of two hybrid assays.

Two-hybrid screening for proteins interacting with DN-Nt-Rac5 were performed as described (Chapter 4.8.2.1). Plating of approximately 3×10^5 yeast transformants on medium containing 5 mM 3-AT resulted in the identification of one full-length cDNA clone encoding a polypeptide that showed specific interaction with DN-Nt-Rac5. This polypeptide was similar to hypothetical proteins expressed in *Arabidopsis thaliana* and rice and the clone 2-N was renamed to *Nicotiana tabacum* hypothetical protein number 1 (Nt-Hypo1), hereafter. The correctness of the sequence and NH₂- and COOH-termini were confirmed by several sequencing reactions. The identified interactor comprises an open reading frame of 76 amino acids, which does not show sequence homology to any characterized protein. Figure 7 (upper panel) shows the yeast two-hybrid interactions five days after transformation into HF7c cells between the coding region of Nt-Hypo1 and wild-type and mutant versions of Nt-Rac5, harbouring the SAAX domain. Yeast growth on SD –L –T –H plates lacking 3-AT was due to leakiness of the hybrid system, *i.e.* residual *his3* activity. On the other hand, Nt-Hypo1 was shown to even promote growth of HF7c

cells without histidine, either in the presence or absence of Gal4-DB. A phenomenon, only observed for Nt-Hypo1. Rac GTPases, instead, are commonly known to inhibit yeast growth. However, a clear and specific interaction of Nt-Hypo1 with DN-Nt-Rac5 was detected on plates containing 1 mM and 2 mM 3-AT. A yeast two-hybrid assay using Nt-Hypo1 and the DN-Nt-Rac5 version with intact CAAX domain as a bait is much less sensitive (Figure 7, lower panel), because of the reduced presence of the GTPase in the yeast nucleus. Indeed, growth of yeast cells transformed with Nt-Hypo1 and with the Gal4 DNA binding domain is stronger than the interaction of the two proteins Nt-Hypo1 and DN-Nt-Rac5 on medium lacking 3-AT (compare above). Even after five days no interaction of Nt-Hypo1 with DN-Nt-Rac5 could be detected on 3-AT-containing plates. In conclusion, Nt-Hypo1 was the only interactor of DN-Nt-Rac5 identified in the yeast two-hybrid screen and it is a specific interactor of DN-Nt-Rac5.

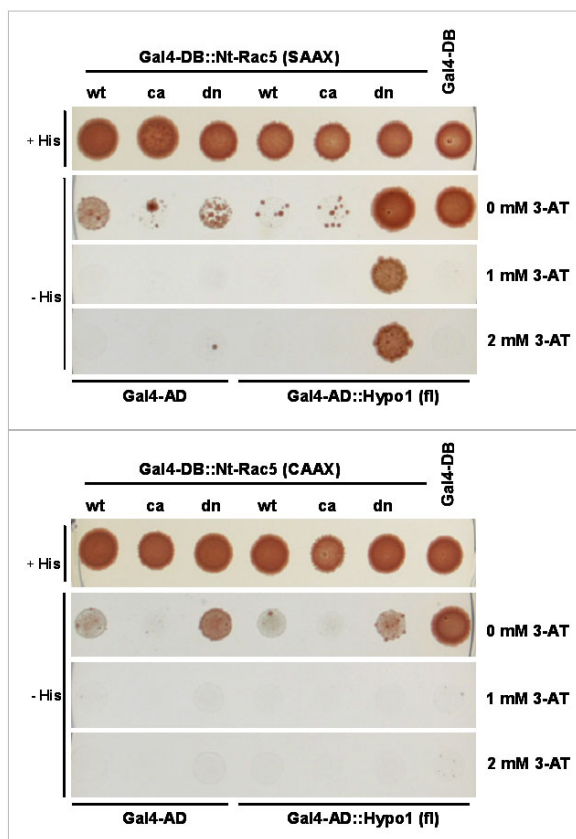


Figure 7: Yeast two-hybrid interaction of Nt-Hypo1 and Nt-Rac5 wild-type and mutant proteins. 10 ml of liquid culture of respective yeast colonies grown in SD-L-T distributed on SD-L-T+H (growth control) and on SD-L-T-H agar plates and grown for five days. pGBKT7 (Gal4-DB) and pGAD-GH (Gal4-AD) represent empty bait and prey vectors, respectively. These transformants serve as controls for specific interactions. **A:** Nt-Rac5 wild-type, constitutive active or dominant negative with mutated SAAX domain functioning as baits in the Y2H assay with Nt-Hypo1. Nt-Hypo1 strongly and specifically interacts with DN-Nt-Rac5. Transformed yeast cells with Nt-Hypo1 and empty pGBKT7 usually grow on SD-L-T-H plates. Interaction can therefore only be concluded from plates containing additionally 1 mM 3-AT or more, inhibiting histidine synthesis. **B:** Y2H assay as described in (A) with intact CAAX domain of the GTPase Nt-Rac5. Interaction of Nt-Hypo1 and Nt-Rac5 is significantly weaker as with the SAAX domain, shown in (A).

2.1.1 Sequence analysis of Nt-Hypo1 and comparison with *Arabidopsis thaliana* and *Oryza sativa* proteins of unknown function

BLAST searches (Altschul *et al.*, 1997) with the nucleotide or peptide sequences of Nt-Hypo1 have shown that homologies exist to other uncharacterized plant proteins. Nt-Hypo1 is 40 % identical to an *Arabidopsis thaliana* expressed protein with the GenBank accession AAM61592 (locus At3g57450) and 38 % identical to an *Oryza sativa* protein with the accession XP_476911. Figure 8 shows a CLUSTALW alignment (Thompson *et al.*, 1994) of the deduced amino acid sequences of the three unknown proteins. Nt-Hypo1 is a protein of 76 amino acids, whereas the *Arabidopsis* and rice proteins consist of 96 aa and 80 aa, respectively. Obviously, the three proteins are highly homologous in their NH₂- and COOH-termini, more divergent in the centre of the protein.

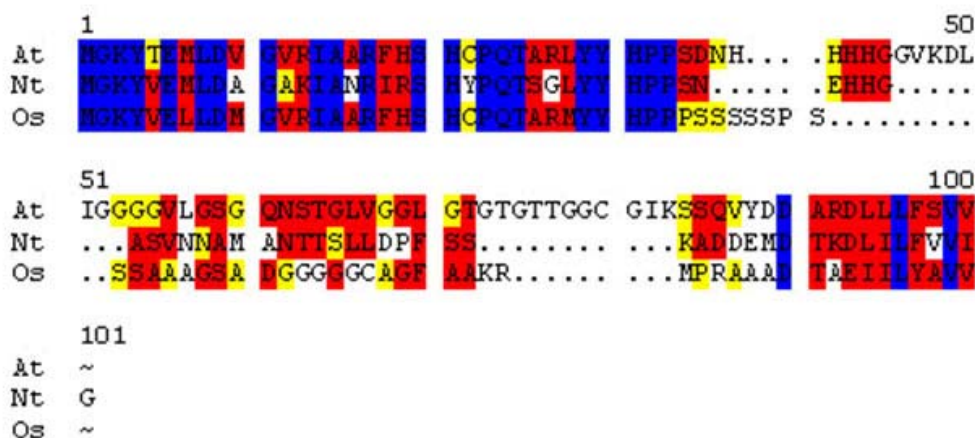


Figure 8: CLUSTALW alignment of deduced amino acid sequences of three unknown plant proteins. At, *Arabidopsis thaliana* (AAM61592), Os, *Oryza sativa* (XP_476911) and Nt, *Nicotiana tabacum* (Nt-Hypo1), the newly identified tobacco protein, which has not been deposited in the GenBank so far.

2.1.2 Analysis of Nt-Hypo1 expression by Northern blotting

Nt-Hypo1 was identified in a tobacco pollen tube cDNA library representing genes expressed three hours after germination. It interacts with Nt-Rac5, which was shown to be

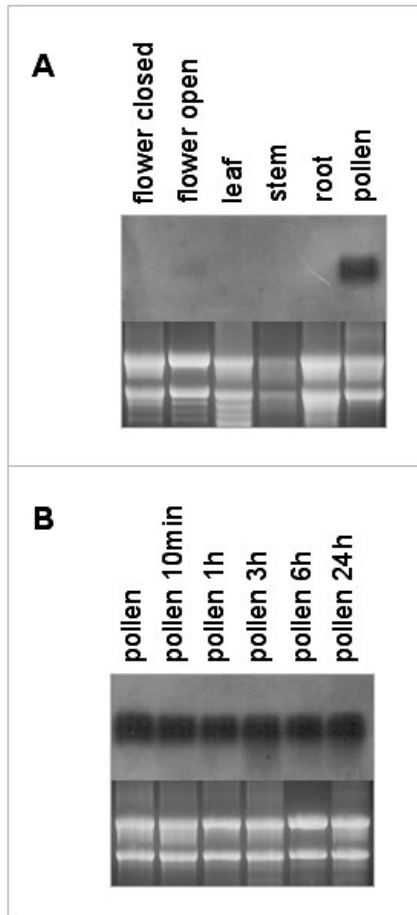


Figure 9: RNA expression analysis. Nt-Hypo1 is very weakly expressed in mature flower tissue, but strongly expressed in pollen (A) and pollen tubes at different developmental stages (B). 5 μ g of total RNA were loaded per lane. Gel images are shown to ensure equal loading of gels before blotting.

specifically expressed at high levels in pollen grains and pollen tubes of *Nicotiana tabacum* (U. Klahre and B. Kost, unpublished). Northern blot analysis was performed to investigate, if Nt-Hypo1 is also specifically expressed in pollen and pollen tubes of *Nicotiana tabacum*.

A 373 bps-long PCR fragment comprising the coding region of Nt-Hypo1 as well as the 3'- and 5'- untranslated regions, was used as a hybridization probe. The PCR product was amplified using the original Y2H clone 2-N as template and the gene-specific primer pair bot 42 – bot 43. Figure 9A shows that Nt-Hypo1 is weakly expressed in mature tobacco flowers, but strongly expressed in pollen grains. Figure 9B proves that Nt-Hypo1 is strongly expressed and accumulates to a similar degree in pollen and pollen tubes at

different stages after germination. Considering the high amount of mature pollen in the open flowers collected for the Northern blot analysis and the very weak band detected on the blot, we conclude that Nt-Hypo1 is a pollen-specific protein of *Nicotiana tabacum*.

2.1.3 Effects of transient expression of Nt-Hypo1 in pollen tubes of *Nicotiana tabacum*

2.1.3.1 Transient over-expression of YFP and Nt-Hypo1

Particle bombardment is a suitable and widely used method of gene transfer into eukaryotic cells and used frequently in our laboratory for tobacco pollen tube

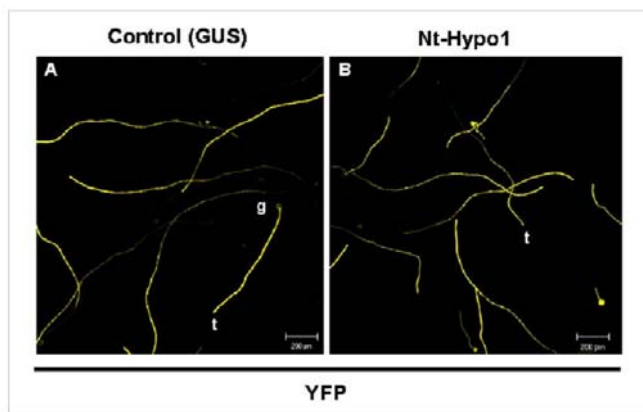


Figure 10: Low magnification images (5x) of transfected tobacco pollen tubes. Pollen tubes over-expressing YFP + GUS (A) 6 h after particle bombardment. (B) Tobacco pollen tubes over-expressing Nt-Hypo1 + YFP. All plasmids are under the control of the pollen-specific lat52 promoter. (g = pollen grain; t = pollen tube tip)

transformation. To functionally characterize Nt-Hypo1, the full-length cDNA, coding for the entire protein, was cloned into an over-expression vector under the control of the strong pollen-specific lat52 promoter. The lat52 promoter, from the late anther tomato 52 protein, is known to be active in late stages of pollen development and specifically in pollen and anther tissue (Twell *et al.*, 1989). In order to visualize transfected pollen tubes, the yellow fluorescent protein (YFP) was simultaneously co-expressed with the full-length Nt-Hypo1. To ensure equal amounts of protein synthesized in all probes, a construct expressing the non-invasive marker protein β -glucuronidase (GUS) was co-expressed with YFP in control experiments. Figure 10A shows tobacco pollen tubes transiently over-expressing YFP plus GUS 6 h after particle bombardment. These pollen tubes served as a control to compare normal pollen tube length and morphology with Figure 10B showing tobacco pollen tubes over-expressing Nt-Hypo1 and YFP. Nt-Hypo1 over-expression did not alter growth or morphology of tobacco pollen tubes *in vivo*.

2.1.3.2 Subcellular localization of Nt-Hypo1

Rac/Rop GTPases were shown to be membrane associated proteins. GFP fusions to the *Arabidopsis thaliana* At-Rac2 localized to the plasma membrane of tobacco pollen tubes *in*

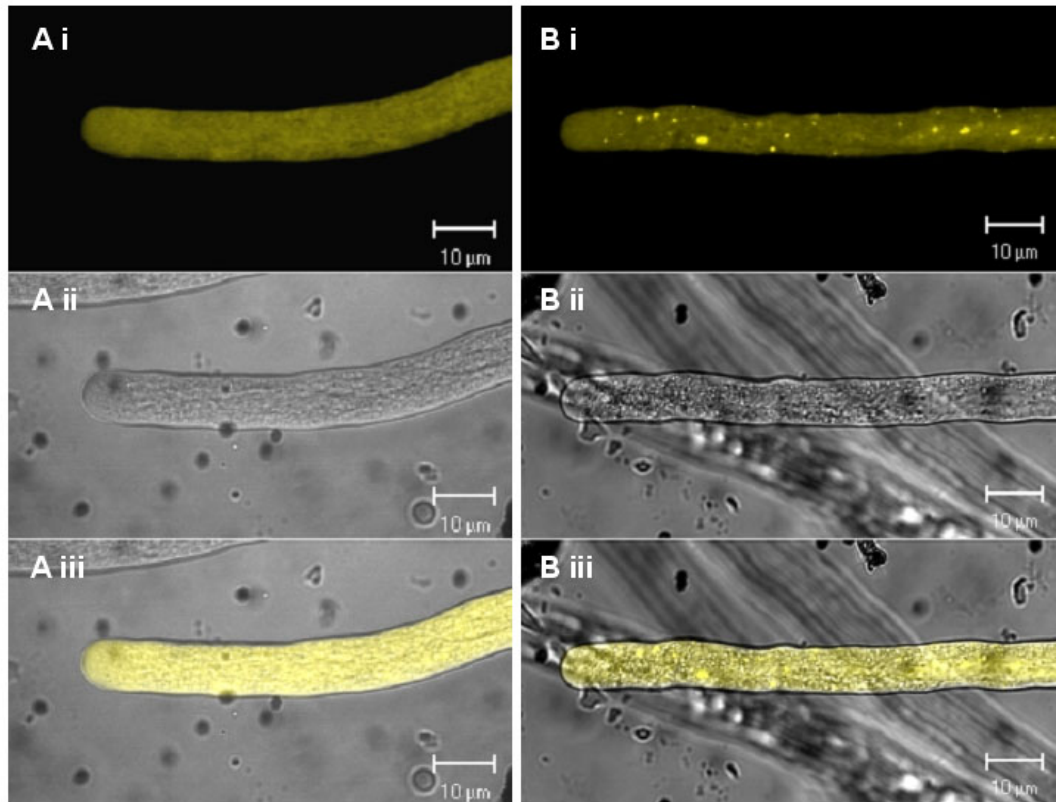


Figure 11: Medial optical confocal sections. (A_i) shows tobacco pollen tubes 6 h after particle bombardment expressing YFP-Nt-Hypo1. (A_{ii}) is a DIC image of the same pollen tube and (A_{iii}) is a merge of both. Nt-Hypo1 is evenly distributed in the cytoplasm of the cell. (B_i) shows a tobacco pollen tube 12 h after particle bombardment expressing the same construct as in (A). Nt-Hypo1 accumulates also in the cytosol, but is additionally found in aggregates in the cell, which cannot be identified by DIC imaging (B_{ii}). (B_{iii}) is a merge of both.

in vivo (Kost *et al.*, 1999; see Figure 3b). Because Nt-Hypo1 was identified as an interactor of such a Rac/Rop GTPase, we tested whether Nt-Hypo1 was also a membrane-associated protein. YFP fusions to the NH₂- or COOH-terminus of full-length Nt-Hypo1 were generated and transiently expressed in tobacco pollen tubes. Confocal imaging was performed to observe the subcellular localization of the protein. Figure 11A_i shows a tobacco pollen tube expressing YFP-Nt-Hypo1 6 h after particle bombardment. Nt-Hypo1 was found to accumulate in the cytoplasm of the cell. Pollen tubes showing higher expression levels of Nt-Hypo1 and pollen tubes after a longer period after transfection, *i.e.* 10 to 12 h, (Figure 11B_i) showed a different labeling pattern. Nt-Hypo1 was not only detected in the cytosol, but also in small aggregates in the cytoplasm of the cell, which could not be identified by DIC imaging (Figure B_{ii}). These aggregates were even enlarged

after longer time periods. Summarizing the observations gained by transient expression of YFP fusions to Nt-Hypo1, we know that Nt-Hypo1 is evenly distributed throughout the cytoplasm 6 h after transfection and in low-expressing tubes even longer after transfection. At higher expression levels Nt-Hypo1 forms unidentified aggregates that do not interfere with cytoplasmic streaming or pollen tube growth. Another YFP fusion to the COOH-terminus of Nt-Hypo1, Nt-Hypo1-YFP, showed the same results.

2.1.3.3 *In vivo* interaction of Nt-Hypo1 and Nt-Rac5

In an attempt to confirm the yeast two-hybrid interaction between Nt-Hypo1 and DN-Nt-Rac5, DN-Nt-Rac5 and YFP fused to Nt-Hypo1 were transiently co-over-expressed in pollen tubes, both under the control of the *lat52* promoter. It has been shown before, that the over-expression of a dominant negative mutant of Rho GTPases results in short and slightly swollen tubes (Kost *et al.*, 1999 and Figure 3). YFP fusions to DN-At-Rac2 showed a strong membrane labeling not only at the pollen tube tip, but also at the flanks of the tubes after particle bombardment (Kost *et al.*, 1999), confirming its plasma membrane association. The idea of the experiment described here was to visualize the interaction of YFP-Nt-Hypo1 with DN-Nt-Rac5 *in vivo*. If the two proteins interact in the growing pollen tube, DN-Nt-Rac5 over-expression should tether YFP-Nt-Hypo1 to the plasma membrane, resulting in membrane labeling. Figure 12A shows membrane association of transiently expressed YFP-DN-Nt-Rac5. Figure 12B shows the over-expression of YFP-Nt-Hypo1 and DN-Nt-Rac5. The pollen tubes show the typical phenotype caused by dominant negative Nt-Rac5. The pollen tubes are short, slightly swollen. However, YFP fluorescence was only detected in the cytosol and never at the plasma membrane. Thus, *in vivo* interaction of Nt-Hypo1 and DN-Nt-Rac5 could not be demonstrated in these experiments.

Further control experiments have been performed in which the DN version of Nt-Rac5 was substituted by wild-type and CA-Nt-Rac5. However, also in these experiments, an interaction of Nt-Hypo1 with wild-type or CA Nt-Rac5 could not be demonstrated *in vivo*.

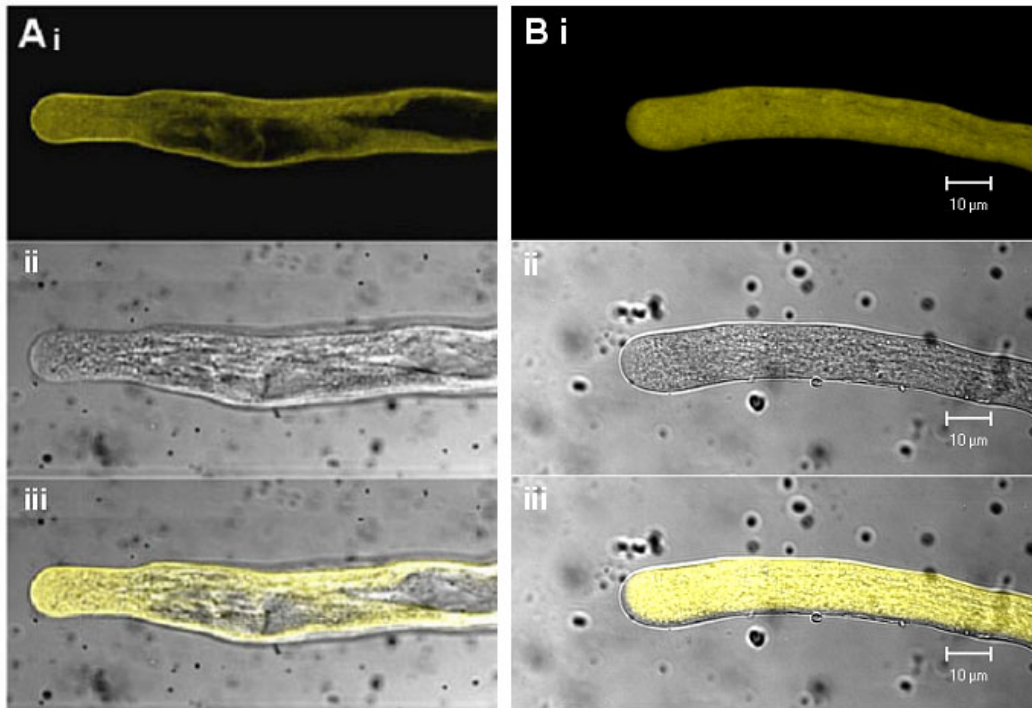


Figure 12: Medial optical confocal sections 6 to 8 h after particle bombardment. (A_i) Transient expression of YFP-DN-Nt-Rac5. YFP-DN-Nt-Rac5 is localized to the plasma membrane of the pollen tube tip and to the flanks. (A_{ii}) DIC image of (A_i). (A_{iii}) Merge of both. (B_i) *In vivo*-interaction experiment: YFP-Nt-Hypo1 and co-over-expression of DN-Nt-Rac5. YFP-Nt-Hypo1 accumulates only in the cytosol. (B_{ii}) shows a DIC image of (B_i) and (B_{iii}) is a merge of both.

2.1.4 Over-expression of recombinant Nt-Hypo1 and purification from *E. coli*

2.1.4.1 *In vitro* interaction of Nt-Hypo1 with wild-type and mutant Nt-Rac5

Because we failed to show *in vivo* interactions, we tried to biochemically demonstrate interactions between the two proteins *in vitro*. The intention now was to over-express the proteins of interest and test them in a biochemical *in vitro* pull-down assay. The coding sequences of Nt-Hypo1 (231 bps) as well as of wild-type, CA- and DN-Nt-Rac5 (594 bps) were cloned in frame with a sequence encoding glutathione-S-transferase (GST) into the pGEX-4T-2 expression vector, resulting in the plasmids pHD67, pHD115, pHD116 and pHD117. The different proteins were expressed in *E. coli* BL21 (DE3) as glutathione-S-transferase (GST) fusion proteins and purified as described (compare MATERIALS AND METHODS). Purified proteins were separated on 12 % SDS PAGEs and Coomassie-stained. GST-Nt-Hypo1 was a 35.23 kDa protein, whereas the GST-Nt-Rac5 versions were proteins of 48.11 kDa, detected on a Coomassie-stained SDS PAGE (Figure 13A and B). GST-Nt-Hypo1 was a very unstable protein, showing several degradation products on the gel. A

strong band at 27 kDa was always detected, which comprises exactly the size of the unfused GST protein (A). BSA was additionally loaded on the SDS PAGE and used as a standard to estimate the amount of protein.

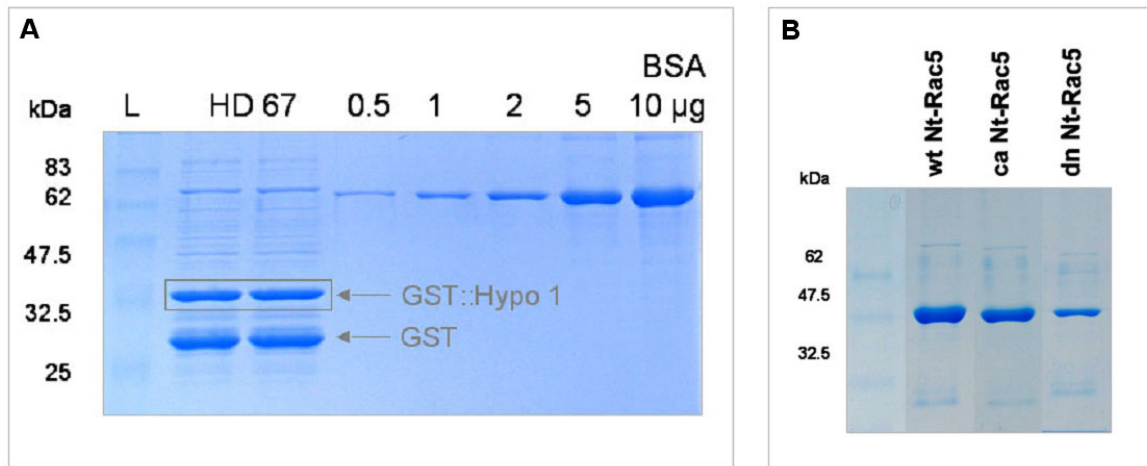


Figure 13: Purified recombinant Nt-Hypo1 and Nt-Rac5. Coomassie stained 12% SDS PAGEs showing the expressed GST-Nt-Hypo1 protein (HD67; A) and GST fusion proteins of WT-, CA- and DN-Nt-Rac5 (B). (A) shows also a dilution series of BSA, used as a standard to estimate the amount of protein loaded.

Figure 13B shows recombinant purified wild-type, constitutively active or dominant negative Nt-Rac5 fused to GST. All Nt-Rac5 GST fusions were stable and gave discrete bands at 48.11 kDa. Interestingly, the dominant negative version of Nt-Rac5 always accumulated to slightly lower levels in BL21 cells. For the *in vitro* interaction assay it was necessary to cleave-off the GST-tag from one of the two proteins. Because Nt-Rac5 was the more stable protein, it was chosen for thrombin treatment. After the cleavage, Nt-Rac5, either WT, CA or DN, accumulated in a single band at 21.11 kDa (data not shown).

For the interaction assay, 500 ng of Nt-Rac5 (WT, CA or DN) were pre-incubated for 10 min in a proteinase inhibitor cocktail, before an excess of GST-Nt-Hypo1, approximately 2.5 µg, was added and the volume was adjusted to 500 µl with 1 x PBS. The whole reaction mixture was loaded on a GST sepharose mini-column. After an incubation on ice for one hour, and several washing steps, proteins were eluted with glutathione and immediately loaded on a 12 % SDS PAGE. In control experiments, the GST protein was incubated with different versions of GST-Nt-Rac5 and treated in the same way as described above.

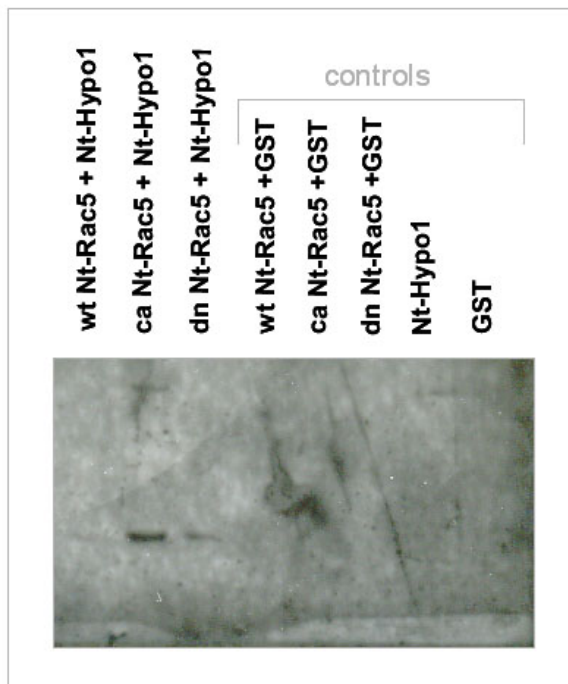


Figure 14: Western blot analysis of the *in vitro* interaction between Nt-Hypo1 and different versions of Nt-Rac5. Lanes 1 to 3 show interaction of GST-Nt-Hypo1 with WT-, CA- or DN-Nt-Rac5. Lanes 4 to 6 show controls of GST alone plus WT-, CA- or DN-Nt-Rac5. GST-Nt-Hypo1 and GST were loaded as controls in lanes 7 and 8. Interaction was detected using an antibody raised against Nt-Rac1.

Western blot analysis and immuno-detection were used to visualize protein-protein interactions. The primary antiserum was an antibody raised against the *Nicotiana tabacum* Rac1 (accession: AY029330). Nt-Rac1 and Nt-Rac5 are closely related, they share 98 % identical amino acids. α -Nt-Rac1 was diluted 1:25. It was a kind gift of Dr. Alice Cheung (University of Massachusetts, Amherst, USA). Alkaline phosphatase-conjugated secondary antibodies raised against rabbit IgG, were diluted 1:2000. Proteins were detected by chemiluminescence and three bands were detected at about 21 kDa. Interaction of Nt-Hypo1 with different versions of Nt-Rac5 is shown in Figure 14. Whereas the interaction of Nt-Hypo1 with Nt-Rac5 in yeast is specific for the dominant negative mutant, the *in vitro* interaction gave different results. We detected weak interactions of Nt-Hypo1 with WT- and DN-Nt-Rac5, but a strong interaction with the CA mutant of the GTPase (lane 1 to 3). In the control experiments (lanes 4 to 6), no bands were detected, showing that Nt-Rac5 did not interact with GST. Additionally, the primary antibody against Nt-Rac1 was tested for unspecific binding. Lanes 7 and 8 show that α -Nt-Rac1 did not unspecifically detect Nt-Hypo1 or GST. Repetition of this experiment showed that these results were reproducible.

2.1.4.2 Nt-Hypo1 – antibody production

The intention of generating an antibody against Nt-Hypo1 was to determine the intracellular localization of this protein based on immuno-gold labeling and electron microscopy in non-transformed tobacco pollen grains and tubes fixed by rapid freeze-freeze substitution (Lancelle *et al.*, 1987). The antibody should also serve to identify protein-protein interactions of Nt-Hypo1 biochemically in pull-down experiments. In order to send GST-Nt-Hypo1 as an antigen, large amounts of protein were over-expressed as described above. Nt-Hypo1 was a very unstable protein. Several degradation products were detected on Coomassie-stained gels (see Figure 13A) and a strong band corresponding to the GST protein was detected. Therefore, we decided to send a gel slice containing intact GST-Nt-Hypo1 to Eurogentec (Seraing, Belgium) for the antibody production and one rabbit was immunized. The pre-immune-serum, the first and the final bleed were tested by Western blotting using different antiserum concentrations. We could not detect a specific band for Nt-Hypo1 in several independent experiments (data not shown) using an alkaline phosphatase-conjugated secondary antibody against rabbit IgG. A second attempt was made to raise a Nt-Hypo1 specific antibody by sending another gel slice, with the same negative result. In conclusion, we were not able to obtain an antibody against Nt-Hypo1.

2.1.5 Nt-Hypo1 gene-knockout by antisense oligodeoxynucleotides, T-DNA insertions and RNA interference

2.1.5.1 Antisense oligodeoxynucleotides

Gene-knockout experiments in mammalian cells are frequently performed by the use of antisense oligodeoxynucleotides (Estruch *et al.*, 1994; Lewis *et al.*, 1996; Bertrand *et al.*, 2002) designed against mRNA sequences of the protein of interest. In plants, this technique appears to have been successfully employed in knocking-out the expression of specific genes in pollen tubes by the groups of Rui Malhó in Lissabon, Portugal (2001) and of Victor Žárský in Prague, Czech Republic (personal communication). We designed antisense oligodeoxynucleotides against Nt-Hypo1 (listed in MATERIALS AND METHODS) and followed a slightly modified protocol described by (Estruch *et al.*, 1994; Malhó *et al.*, 2001). However, we did not detect effects on growing pollen tubes treated with these oligonucleotides.

2.1.5.2 T-DNA insertion

Another suitable method to analyze effects of gene-knockout in plants is the investigation of T-DNA insertion lines of *Arabidopsis thaliana*, which are made available in publicly accessible collections. We searched for T-DNA insertions in promoters or coding regions of the *A. thaliana* gene At3g57450 that encodes a protein with high homology to Nt-Hypo1. Considering that Nt-Hypo1 is a very small protein, chances of finding a suitable insertion line were low. A single line was obtained from ABRC (Columbus, Ohio, USA) with an insertion in the homologous gene and was tested for reduced T-DNA transmission during sexual reproduction. Normal T-DNA segregation ratios were determined based on PCR. In populations of seedlings derived from self-fertilization, we observed also that T-DNA insertion plants showed normal pollen tube growth and morphology. These results indicate that either the At-Hypo1 homologue is not essential for pollen tube growth or a functional redundant protein exists in the cells. Alternatively, the insertion might not have disrupted expression of At-Hypo1. Additional work would be required to distinguish between these possibilities.

2.1.5.3 RNA interference

RNA interference has only emerged as a topic of general interest in the past seven years, but is now a common way of post-transcriptional gene silencing. We employed RNAi to investigate effects of reduced Nt-Hypo1 expression on pollen tube growth and generated transgenic plants of *Nicotiana tabacum*. A vector for efficient gene-silencing in plants, pHANNIBAL, has been generated by Wesley *et al.* (2001). Based on this plasmid, which we obtained from Dr. Waterhouse (CSIRO, Canberra, Australia), a vector has been constructed that allows the expression of double-stranded self-complementary hairpin RNA in pollen tubes corresponding to the cDNA encoding Nt-Hypo1. We modified pHANNIBAL by replacing the 35S promoter with the pollen-specific lat52 promoter. In a single PCR using primers which introduced two restriction sites (bot245 – bot246; see MATERIALS AND METHODS) a fragment of 444 bps was amplified. This PCR fragment was cloned in sense and antisense orientation into the modified pHANNIBAL vector behind the lat52 promoter. The newly generated construct was designed to produce an intron-spliced hairpin RNA with a loop of approximately 30 to 50 bases. The intron was later spliced in the plant (Wesley *et al.*, 2001). A further cloning step was performed to transfer the Nt-Hypo1 RNAi expression cassette into a binary vector, which contained a sequence encoding a YFP-GUS fusion protein under the control of the pollen specific At-profilin4

promoter from *Arabidopsis thaliana* (Christensen *et al.*, 1996). Expression of this fusion protein can be used to identify transgenic pollen tubes in segregating populations, either in culture by YFP fluorescence or *in situ* by histochemical GUS assays.

The transformation of *Nicotiana tabacum* with the binary vector described above was performed by *Agrobacterium*-mediated leaf-disc transformation (Horsch *et al.*, 1988). Leaf discs, calli and resulting tobacco plants were treated as outlined in MATERIALS AND METHODS. Nine independent transgenic lines carrying the Nt-Hypo1 RNAi construct were obtained. In order to identify transgenic pollen tubes, anthers were harvested and the pollen grains were cultivated on solid medium. Pollen produced by six independent transgenic lines was analyzed under the microscope for growth behaviour and morphology. Three hours after germination, pollen tubes were stained for two hours with the GUS substrate X-Gluc before images were taken. The studied primary transformants were heterozygous as expected. Only 50 % of the pollen tubes contained the RNAi construct and were expressing GUS as indicated by blue staining. Figure 15 shows low magnification images of six independent transgenic pollen tubes from tobacco. Three lines, 249-2-2, 249-2-4 and 249-4-1, did not show significant morphological effects or a reduction in pollen tube growth. Statistical analysis showed, that pollen tubes of these three lines were almost as long as the wild-type pollen tubes. Pollen tubes from other three transgenic lines, 249-11-2, 249-14-2 and 249-15-2, showed reduced growth and in the cases of 249-14-2 and 249-15-2 morphological defects including slightly swollen tubes. Different results obtained with the independent transgenic lines do not have to be surprising. Wesley *et al.* (2001) reported variations in the degree of silencing in the plants transformed with intron-spliced hairpin RNA.

Three additional lines remain to be tested, 249-2-3, 249-5-1 and 249-7-1, whereas 249-2-3 derives from the same callus as 249-2-2 and 249-2-4 and might not be affected in its growth behaviour comparable to the two lines, which have already been tested.

The fact that transgenic pollen grains germinated and pollen tubes expanded in most cases normally, shows that the Nt-Hypo1 gene-knockout might not have a lethal effect on pollen development. At the same time no sporophytic defects were observed, which alter the vegetative development of the transgenic tobacco plants. But, they were not expected to be caused by lat52/RNA duplex expression cassettes, because the lat52 promoter activity is restricted to anthers and pollen (Twell *et al.*, 1991).

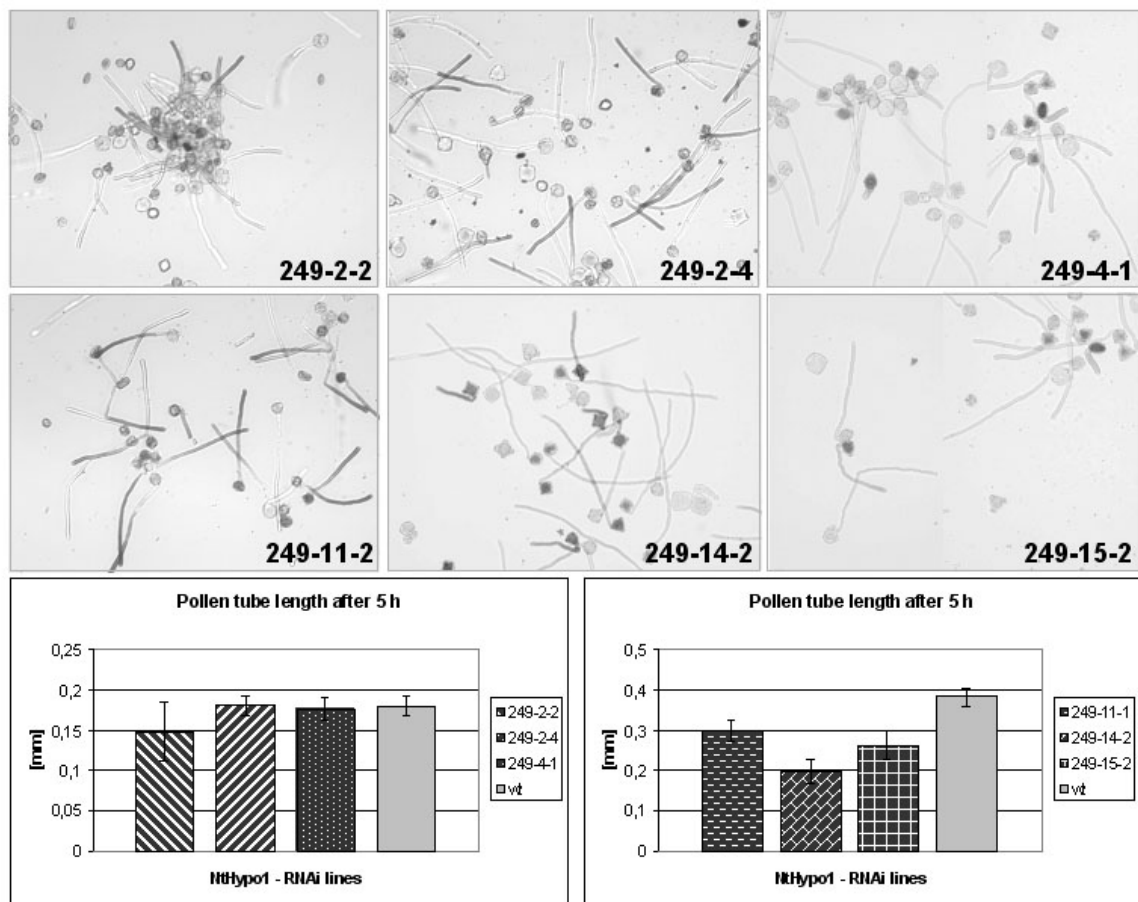


Figure 15: Nt-Hypo1 RNAi knock-down in pollen tubes of *Nicotiana tabacum*. Stably transformed tobacco pollen tubes containing a Nt-Hypo1 RNAi construct and expressing at the same time a YFP::GUS fusion protein driven by the Prof4 promoter from *Arabidopsis thaliana*. Here, GUS expression was employed to detect transformed pollen tubes. Pollen tubes were stained with X-Gluc 3 h after germination and grown for further 2 h. Low magnification images taken with a 5 x objective show transgenic pollen tubes (blue) and wild-type pollen tubes (clear). When primary generations were analyzed, 50 % of the pollen tubes were transgenic. Pollen tube morphology and length was not altered in three lines: 249-2-2, 249-2-4 and 249-4-1. Lines 249-11-2, 249-14-2 and 249-15-2 showed a significant reduction in pollen tube length. The two diagrams show a statistical analysis of pollen tube length 5 h after germination. Error bars indicate a confidence range of 95 %.

The Nt-Hypo1 RNAi data presented are of course only preliminary. Only the primary transformed plants and F₂ generations were available for analysis. For further investigations, T₁ seeds were collected and plated on selective medium. Primary regenerants were additionally back-crossed as male parents to determine T-DNA transmission through the male gametophyte. If pollen tube growth is affected by Nt-Hypo1 gene-knockdown, reduced T-DNA transmission should be observed in these experiments resulting in a reduced proportion of BASTA resistant seedlings in the next generation. Molecular analysis (*e.g.* Northern blotting) is required to demonstrate reduced Nt-Hypo1 expression in these RNAi lines.

The segregation ratio for the daughter population after self-progeny was determined based on the linked BASTA-resistance transgene, which allowed only transgenic seedlings to grow on antibiotic-containing culture plates. Results are shown in table 1. The segregation ratio was determined to be 3:1 (mutant:wild-type) for most transgenic lines or even higher on the transgenic site. A 3:1 ratio is expected, if pollen tube growth and fertilization was not affected. A single line, 249-15-2, showed a segregation of 1:2, which might indicate a defect in pollen tube growth, but the segregation ratio must be reassessed, as it is the only line out of nine transgenic lines, which shows a defect in pollen tube growth and fertilization.

Table 1: Segregation ratios for Nt-Hypo1 RNAi plants in the F₂ generation

transgenic line	segregation		ratio
	resistant	non-resistant	
249-2-2	38	0	38:0
249-2-3	40	12	3:1
249-2-4	35	2	17:1
249-4-1	51	18	3:1
249-5-1	62	14	4:1
249-7-1	49	14	3:1
249-11-1	42	13	3:1
249-14-2	31	11	3:1
249-15-2	16	35	1:2

So far only one back-crossing has been performed, using a wild-type mother plant and the heterozygous pollen of the line 249-14-2. The segregation ratio was determined to be 1:1, again observed based on BASTA resistance. This result is in accordance with the data of the self-progeny, as the ratio for 249-14-2 was shown to be 3:1. Neither in the self-progeny, nor in the back-crossing with a wild-type mother plant, 249-14-2 showed defects in sperm delivery and fertilization.

2.1.6 Identification of novel Nt-Hypo1 interactors by yeast two-hybrid screening

Nt-Hypo1 itself was identified as an interactor of DN mutant of the small GTPase Nt-Rac5 in a yeast two-hybrid screen. It is a small protein, comprising only 76 aa. Because of its specific interaction with the DN-Nt-Rac5 it is thought to function as a plant-specific GEF or, due to its size, it may constitute a part of a whole GEF-complex as it is possible that plants employ a multi-protein complex to promote the nucleotide exchange of their

Rac/Rop GTPases. A yeast two-hybrid screen was performed to identify proteins that interact with Nt-Hypo1 and play a role in Nt-Rac5 signaling, possibly by forming a complex with Nt-Hypo1 that has GEF activity.

The screen was performed using the same protocol as described above (Chapter 2.1). Nt-Hypo1 served as a bait to screen the same cDNA library as described above, which represents genes expressed in pollen tubes 3 h after germination. Approximately 1.2×10^5 yeast transformants were plated on medium, containing either 0 mM 3-AT (50 % of the transformants) or 1 mM 3-AT. 133 clones were identified growing on selective medium. These clones were replated on SD –L –T –H medium containing various concentrations of 3-AT (1 to 5 mM 3-AT). The prey construct was only extracted from clones growing on 5 mM 3-AT. In order to confirm the interaction of the polypeptide encoded by this construct with Nt-Hypo1, re-transformations were performed. To this end, plasmid DNA extracted from yeast cells was transformed into *E. coli* and selected through the ampicillin resistance gene (= prey vector).

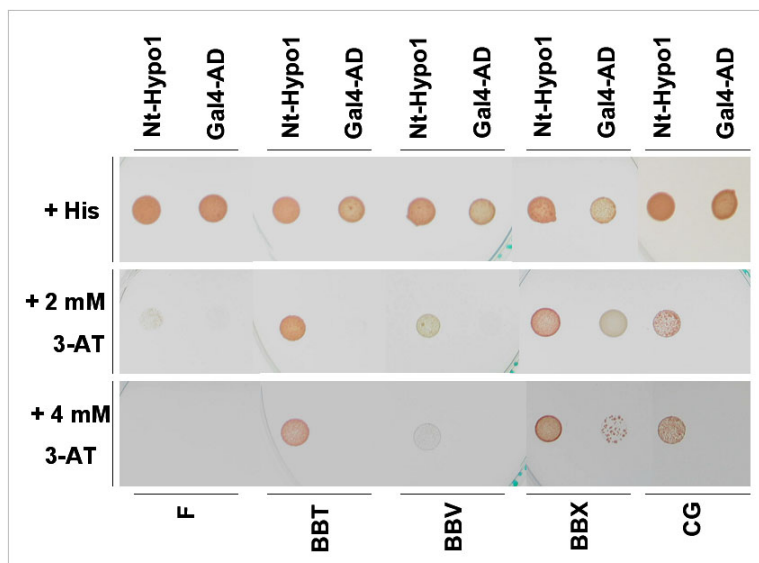


Figure 16: Yeast two-hybrid interaction of Nt-Hypo1 with five newly identified interactors. 10 μ l of liquid culture of respective yeast colonies grown in SD-L-T and distributed to solid medium containing SD-L-T+H (growth control) and SD-L-T-H with or without 3-AT. Gal4-AD represents the empty prey vector. This transformation served as a control for specific interactions.

Plasmid DNA of the prey constructs then was co-transformed with the bait Nt-Hypo1 and re-tested for interaction on medium containing various 3-AT concentrations. Re-transformations showed that five polypeptides identified in the screen in turn specifically interacted with Nt-Hypo1 (Figure 16). Neither bait nor prey constructs alone stimulated growth of yeast cells on histidine-free medium. Furthermore, the corresponding prey constructs were restricted with EcoR I and Xho I to determine the insert size. Both restriction endonucleases cut inside the prey vector, *i.e.* before and after the insert. Five cDNAs encoding the interactors were partially sequenced using vector-specific

oligonucleotides. The resulting partial sequences were further used for various BLAST searches (Altschul *et al.*, 1997; for sequence information and CLUSTAW alignments with putative homologous proteins see APPENDIX), which gave information about their homology to known proteins. The identified polypeptides were similar to a pollen-specific protein (*Nicotiana tabacum*), to a pectin esterase family protein (*Arabidopsis thaliana*), to a C2 domain-containing protein (*Arabidopsis thaliana*), a phosphate translocator-related protein (*Arabidopsis thaliana*), another hypothetical protein (*Arabidopsis thaliana*) and two times Nt-Hypo1 was identified as an interactor with itself. The five most promising interactors are listed in table 2.

Table 2: Identified yeast two-hybrid interactors of Nt-Hypo1

Y2H interactor	BLAST search result	GenBank accession	insert size	interaction with Nt-Hypo1
12-F	Pectin esterase family protein, <i>Arabidopsis thaliana</i>	NP_182226	1800 bps	weak
12-BBT	phosphate translocator-related protein <i>Arabidopsis thaliana</i>	NP_187640	1200 bps	strong
12-BBV	unknown/hypothetical protein <i>Arabidopsis thaliana</i>	CAB80709	800 bps	weak
12-BBX	C2 domain-containing protein <i>Arabidopsis thaliana</i>	AAM67146 or AAB80650	800 bps	strong
12-CG	Pollen-specific protein <i>Nicotiana tabacum</i>	CAA43454	1500 bps	strong

Time was too limited to clone full-length cDNAs of the interactors, but preliminary experiments were performed to investigate, which clones were the most interesting ones. Fragments identified in the yeast two-hybrid screen were fused to YFP and transient expression analyses were performed in tobacco pollen tubes.

Co-over-expression of Nt-Hypo1 with one of its interactors, respectively, was performed to determine morphological effects after over-expression. If Nt-Hypo1 and the identified interactors act in a GEF-complex in the cell, bulging of the pollen tube apex was expected. Nevertheless, co-over-expression of these proteins did not alter growth or morphology of the pollen tubes (data not shown).

On the other hand, the intracellular localization of these five identified interactors was determined after particle bombardment of YFP fusions and imaged 6 h after transfection (Figure 17). Transient transformation with the interactors 12-BBV and 12-CG resulted only in cytoplasmic labeling (Figure 17C and E). The interactors 12-F, 12-BBT and 12-BBX, instead, localized to unidentified intracellular structures (Figure 17A, B and D).

These aggregates showed a fast movement, comparable to the cytoplasmic streaming of the pollen tubes. Only in the case of 12-BBX, which shares homology to a C2 domain-containing protein, a localization at the plasma membrane in the pollen tube flanks in a distance of approximately 20 μm or even more from the tip was observed (Figure 17D, arrows).

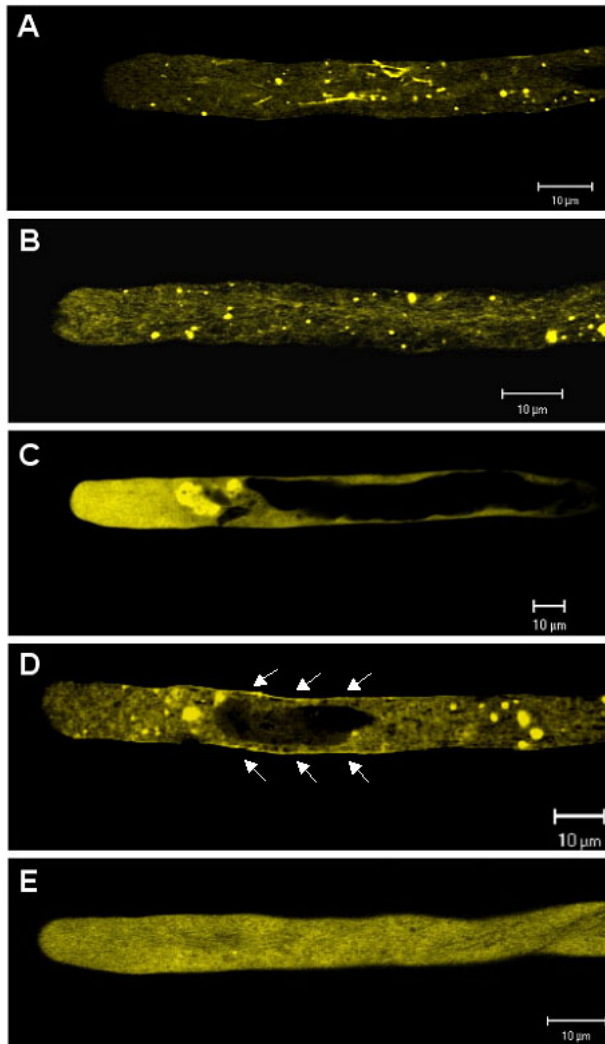


Figure 17: Medial optical confocal sections of identified interactors with Nt-Hypo1. Tobacco pollen tubes 6 h after transient transfection. (A) YFP-12-F, (B) YFP-12-BBT, (C) YFP-12-BBV, (D) YFP-12-BBX or (E) YFP-12-CG.

Neither the co-over-expression of Nt-Hypo1 with its interactors, nor the intracellular localization observed after transient transfection with YFP fusions, facilitated the decision which interactor was particularly interesting for further experiments investigating the function of Nt-Hypo1 in pollen tube growth or guidance.

2.2 Identification of novel phosphoinositide-specific phospholipase C isoforms from *Nicotiana tabacum*

2.2.1 Identification and sequence analysis of NtPLC3 and NtPLC4

Although the sequences of two *N. tabacum* PI-PLC isoforms, NtPLC1 (586 aa; accession: AF223351) and NtPLC2 (605 aa; accession: AF223573.1), were deposited in the GenBank by the laboratory of Prof. Goswami (New Delhi, India) in the year 2000, no functional characterization of the corresponding proteins has been reported to date. Based on these two sequences, we designed primers in order to amplify homologous sequences using RT PCR for pollen tube RNA or by performing regular PCRs on a pollen tube cDNA library. A number of PCR fragments were sequenced and showed very high sequence homology to NtPLC1 and 2. However, the sequences of all PCR fragments were slightly divergent from each other and from NtPLC1 and 2, indicating that pollen tubes may express several closely related PI-PLCs. Because we could not exclude that some or all of the amplification products were chimeric, with different regions corresponding to distinct PI-PLC isoforms, we decided to employ a cDNA library colony hybridization based on a protocol by Roche (“DIG Application Manual for Filter Hybridization”, compare MATERIALS AND METHODS) to clone pollen tube PI-PLC cDNAs, using as a template one of the PI-PLC fragments from *N. tabacum* amplified by PCR (pWEN 238-1; lat52::NtPLC3-1::NOS). A DIG-labeled 745 bps-long fragment was amplified as hybridization probe. Using this probe, four clones were identified. These four clones were further cultivated, plasmid DNA extracted and sent for sequencing. One of them did not show any homologies to known proteins based on a BLAST search (Altschul *et al.*, 1997), another showed highest homology to an α -tubulin and the two other clones were identified as novel full-length PI-PLCs. These two PI-PLCs were named NtPLC3 and NtPLC4. The sequences of the NtPLC 3 and 4 cDNAs, including 5'- and 3'-UTR regions, were confirmed and are ready to be deposited in the GenBank before publishing (for sequence information see APPENDIX). NtPLC3 and 4 consist of 588 amino acids and have a size of 66.78 and 66.96 kDa, respectively. NtPLC3 and 4 differ from each other in only 14 amino acid residues and show 97 % sequence identity. Based on sequence comparisons with other published plant PI-PLCs and on a domain search employing Scan Prosite (<http://www.expasy.ch>) it was concluded that both proteins consist of four distinct domains, a NH₂-terminal EF hand-like domain, the catalytic X and Y domains and the COOH-terminal C2 domain or CalB domain, known to be responsible for Ca²⁺-dependent

protein-lipid interactions (Essen *et al.*, 1996; Kopka *et al.*, 1998b). Obviously both proteins, like all plant PI-PLCs identified to date, are missing the pleckstrin homology (PH) domain, which is essential for membrane association of most mammalian PI-PLCs. In conclusion, plant PI-PLCs must associate with the plasma membrane in a manner that is completely different from their mammalian homologues.

Figure 18 shows a sequence alignment (CLUSTALW; Thompson *et al.*, 1994) of the deduced amino acid sequences of four plant PI-PLC isoforms and two mammalian PI-PLCs. Mammalian PI-PLCs δ and ζ are significantly longer than the plant isoforms, because of their NH₂-terminal PH domain. However, plant PI-PLCs share the other domains with the mammalian PI-PLCs and contain invariant amino acids, especially in the catalytic core. The residues required for catalysis (His₃₁₁ and His₃₅₆ of RnPLC δ_1), for the coordination of Ca²⁺ at the active site (Asn₃₁₂, Glu₃₄₁, Asp₃₄₃ and Glu₃₉₀), for van der Waals interactions with the inositol ring (Tyr₅₅₁), for the recognition of the 4- and 5-phosphate groups (Ser₅₂₂ and Arg₅₄₉; Essen *et al.*, 1996) are unchanged in the newly identified tobacco PI-PLCs. Differences, nevertheless, are observed in the amino acid residue Lys₄₃₈, which is involved in substrate recognition in the mammalian PI-PLCs, and which is substituted by serine in the tobacco sequences. Major differences are found in the C2 domain of the proteins. Residues required for Ca²⁺ coordination in the mammalian C2 domain are not conserved in the tobacco PI-PLCs. Asn₆₄₅ is substituted by histidine, Ser₆₅₀ by alanine, Asp₆₅₃ by proline and Asp₇₀₆ by glutamate. The only conserved residue in the C2 domain of the tobacco PI-PLCs compared to the mammalian PI-PLC δ_1 is the Asp₇₀₈. Further sequence comparisons indicate that the EF hand-like domain preceding the X domain in plant PI-PLCs and the linker between the X and Y domains are less conserved than the rest of the protein. Sequence comparison of NtPLC3 with PsPLC resulted in 80.4 % similarity, of NtPLC3 with AtPLC1 in 67.6 %, with MnPLC ζ in 43 % and with RnPLC δ_1 in 41.9 % similarity.

Based on the extremely high homology of the two identified PI-PLC isoforms from *Nicotiana tabacum* we decided to concentrate on the PI-PLC isoform NtPLC3 in the present work. All expression data, enzyme activity measurements and *in vivo* studies were performed with this isoform.

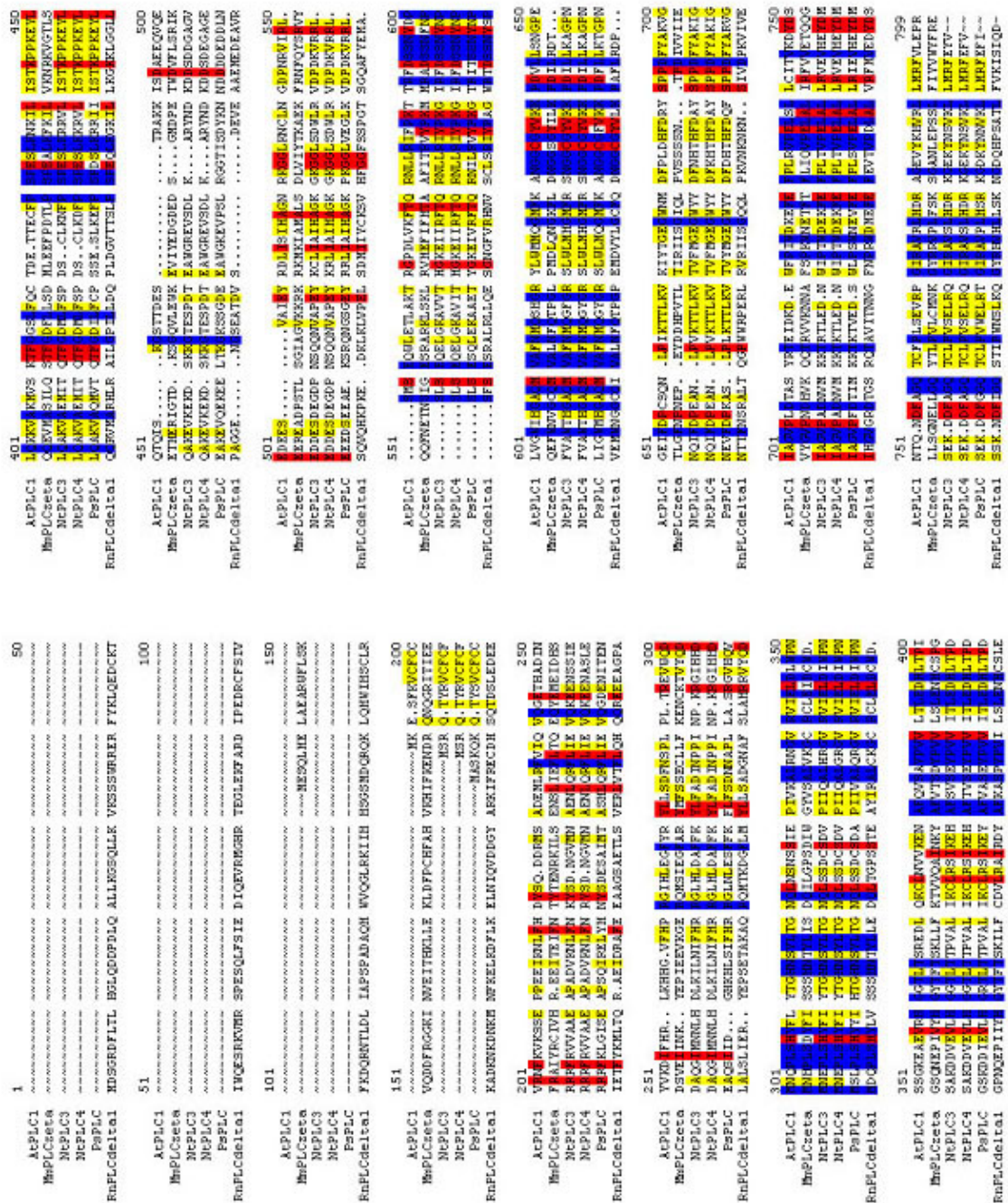


Figure 18: Sequence alignment of deduced amino acids of four plant PI-PLCs and two mammalian PI-PLCs. At, *Arabidopsis thaliana* (BAA07547), Ps, *Pisum sativum* (CAA75546), Mm, *Mus musculus* (AAM95914), Rn, *Rattus norvegicus* (P10688). Nt, *Nicotiana tabacum* (NtPLC3 and 4 are newly identified PI-PLCs, which have not been deposited in the GenBank so far).

2.2.1.1 Phylogenetic analysis of NtPLC3 and NtPLC4

Phylogenetic and molecular evolutionary analyses were conducted using MEGA version 3.0 (Kumar *et al.*, 2004). An alignment of 13 plant PI-PLC isoforms and two mammalian isoforms δ and ζ formed the basis for constructing the unrooted neighbour joining tree (Figure 19). The plant PI-PLCs group into five different clades, separate from the mammalian PI-PLCs, which group together. Recent gene duplications might be the reason for high similarity of NtPLC1 and 4 and NtPLC2 and 3.

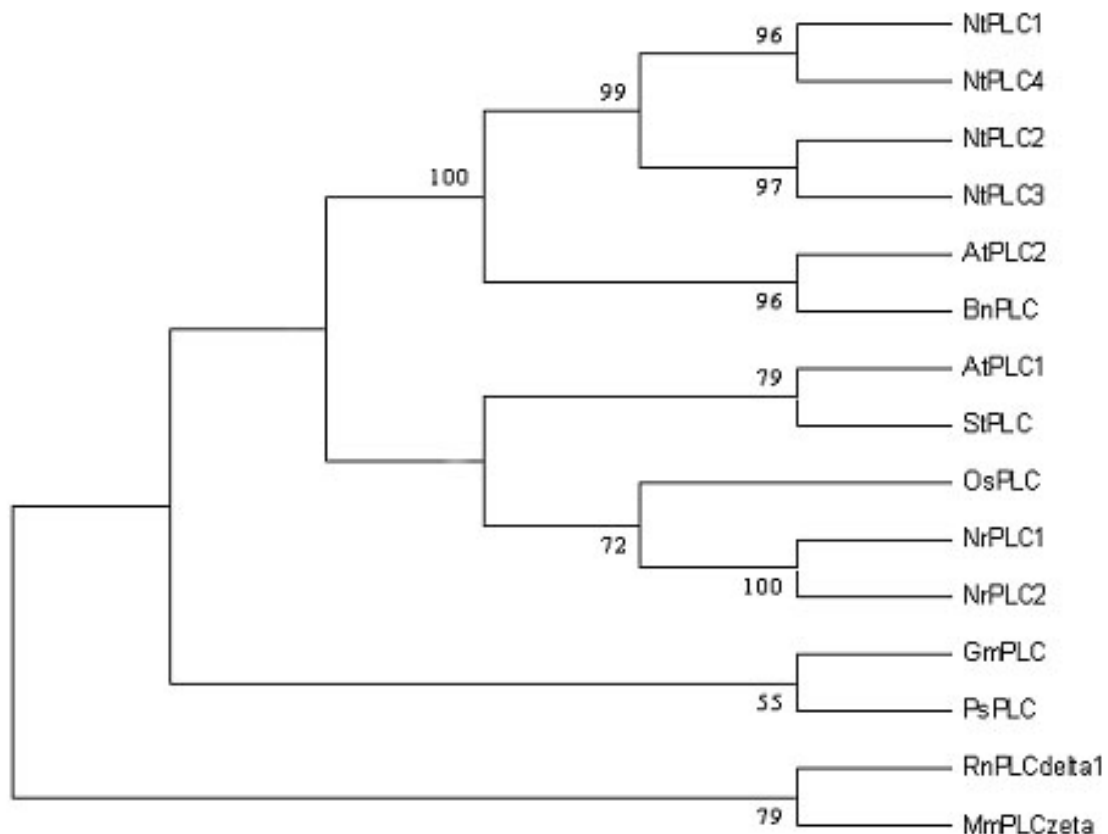


Figure 19: Unrooted neighbour joining tree showing the relationship between 13 plant PI-PLC isoforms and two mammalian PI-PLCs. The phylogenetic tree was constructed based on the amino acid sequences deduced from phospholipase C gene sequences reported from different plants and mammals. Bootstrap values are shown for nodes having more than 50 % support in a bootstrap analysis of 1000 replicates. Accession numbers: At, *Arabidopsis thaliana* PLC1 and 2 (BAA07547 and BAA09432), Bn, *Brassica napus* PLC (AAD26119); Gm, *Glycine max* PLC (AAA74441); Mm, *Mus musculus* PLC ζ (AAM95914); Nr, *Nicotiana rustica* PLC1 and 2 (CAA65127 and CAA72681); Nt, *Nicotiana tabacum* PLC1 and 2 (AAF33823 and AAF33824); Os, *Oryza sativa* PLC (AAK01711); Ps, *Pisum sativum* PLC (CAA75546); Rn, *Rattus norvegicus* PLC δ_1 (P10688) and St, *Solanum tuberosum* PLC (CAA63777).

2.2.2 Analysis of NtPLC3 expression by Northern blotting

The amplification of PI-PLCs from *N. tabacum* by PCR (Chapter 2.2.1) indicated that several PI-PLC isoforms may be expressed in pollen tubes. In order to determine the expression pattern of NtPLC3, Northern Blot analyses were performed. The same DNA fragment that was employed for the library screen was used in these experiments. The results showed that NtPLC3 is not expressed in leaf and root tissue, weakly expressed in flower and stem tissues and much stronger expressed in pollen grains and pollen tubes (Figure 20A). The lower part of Figure 20A shows equal loading of the RNA gel used for blotting.

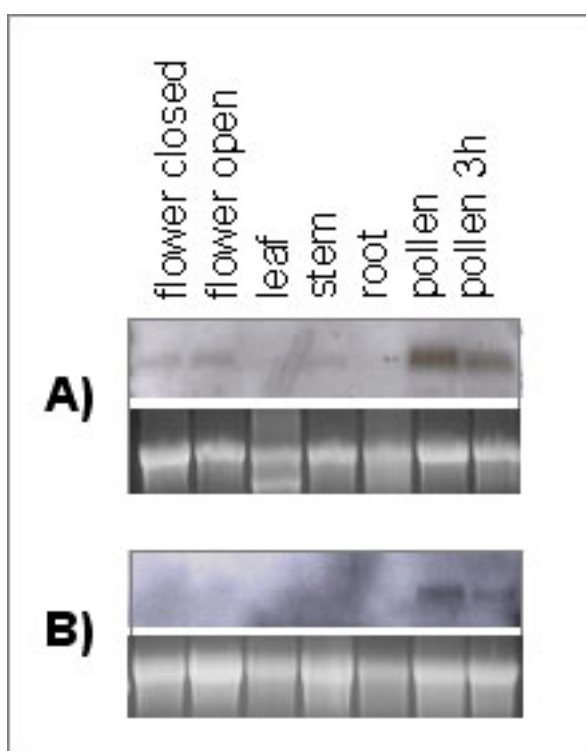


Figure 20: Northern blot analysis of NtPLC3. NtPLC3 expression in different tissues of mature *Nicotiana tabacum* plants. (A) Expression in flowers, leaves, stems, roots and pollen. 5 μ g total RNA loaded per lane. (B) Expression pattern of the 3' UTR region.

The hybridization probe described above is likely to hybridize with multiple PI-PLC isoforms. Therefore, a gene-specific DNA probe corresponding to the untranslated region at the 3' end of NtPLC3 was amplified by PCR and used as a hybridization probe in a second Northern Blot. This probe should not hybridize to the known PI-PLC sequences of NtPLC1, 2 or 4. The probe had a size of 183 bps. Northern blotting with this probe showed that NtPLC3 is specifically expressed in pollen grains and pollen tubes of *Nicotiana tabacum* (Figure 20B).

2.2.3 Determination of the enzymatic activity of wild-type and mutant NtPLC3

2.2.3.1 Purification of recombinant NtPLC3 over-expressed in *E. coli*

Although NtPLC3 is highly homologous to already characterized mammalian and plant PI-PLCs it was necessary to confirm that this protein has PI-PLC activity. Especially, considering the recently identified inactive PI-PLC isoform from pea (Venkataraman *et al.*, 2003) and the two *A. thaliana* isoforms, AtPLC8 and AtPLC9, which are believed to be inactive enzymes because of amino acid substitutions in their Y domains (Hunt *et al.*, 2004). The coding sequence of wild-type NtPLC3 (1764 bps) was cloned in frame with a sequence encoding GST into the pGEX-4T-2 expression vector and expressed in *E. coli* BL21 (DE3) as a glutathione-S-transferase fusion protein. Methods employed for protein over-expression, french press treatment and affinity-purification over GST-sepharose mini columns are described in chapter 4.11.3 and were employed for all protein purifications mentioned in the following paragraphs.

Full-length GST-NtPLC3 ran as a discrete band at 94.35 kDa in the Coomassie-stained SDS PAGE (Figure 21A, lane 2). Thrombin cleavage of the GST-tag was not performed in order to prevent loss of protein. In all experiments, independent of the over-expression protocol used, GST-NtPLC3 was always expressed at low levels only.

Ellis *et al.* (1998) demonstrated that single amino acid exchanges in the catalytic domain of the mammalian phosphoinositide-specific phospholipase C δ_1 reduced the catalytic activity of the enzyme significantly. By crystal structural analysis and comparison of 23 sequences of catalytic PI-PLC domains from mammals, slime molds, yeast and plants, they identified amino acids which are invariant in all PI-PLCs and generated 20 different mutants of PI-PLC δ_1 . Wild-type and mutants were tested for activity in a sodium cholate/PI-4,5-P₂ mixed micelle assay. Mutation of His³¹¹ in PI-PLC δ_1 , which corresponds to His¹²⁴ in NtPLC3, resulted in a 20.000 fold reduction in activity, suggesting a key function of this residue in catalysis. Substitution of Asp³⁴³ in PI-PLC δ_1 , the amino acid corresponding to Asp¹⁵⁶ in NtPLC3, resulted in higher Ca²⁺ concentrations required for PI-4,5-P₂ hydrolysis, suggesting that Asp³⁴³ contributes to Ca²⁺ binding.

NtPLC3 mutants were generated based on this information by site-directed mutagenesis. The positively charged His¹²⁴ was replaced by the small hydrophobic amino acid alanine (H¹²⁴A). The negatively charged Asp¹⁵⁶ was replaced by the positively charged amino acid arginine (D¹⁵⁶R). Furthermore, NtPLC3 H¹²⁴A D¹⁵⁶R was generated, which contained both

point mutations described above. All three NtPLC3 mutants were expressed as GST fusion proteins and were detected as discrete bands at 94.35 kDa on the Coomassie-stained SDS PAGE (Figure 21A, lanes 3, 4 and 5).

PI-PLCs consist of distinct domains as described above (Chapter 1.3.3.2). Plant PI-PLCs contain four domains, the NH₂-terminal EF hand-like domain, the X and Y domains, constituting the catalytic core and the COOH-terminal C2 domain. Single- or multiple domains were purified from *E. coli* as GST fusions with the aim to examine the importance of EF hand and C2 domains with respect to NtPLC3 enzymatic activity *in vitro* and to investigate if the X and Y domains may be sufficient for PI-4,5-P₂ hydrolysis. Domain-deletion constructs were generated comparable to the recently published truncations of mammalian PI-PLC ζ by Nomikos *et al.* (2005). They indeed showed that the single XY catalytic domain displays PI-4,5-P₂ hydrolysis of PI-PLC ζ , but 100 % activity were only achieved by the full-length enzyme. Interestingly, the EF hand and the C2 domain were not essential for enzymatic activity *in vitro*, but they were both necessary to trigger the characteristic Ca²⁺ oscillations in mouse eggs, observed upon fertilization by sperm.

With the same intention as Nomikos *et al.* (2005), of probing NtPLC3 domain-deletion constructs, we generated the following truncated proteins: GST-EF hand (40.14 kDa), GST-EF hand-X-Y (76.48 kDa), GST-X-Y (63.55 kDa), GST-X-Y-C2 (81.63 kDa) and GST-C2 (45.37 kDa). All fusion proteins were separated by discontinuous SDS PAGE (Figure 21). Bands corresponding to the expected size of the different fusion proteins are marked by arrow heads. Significant amounts of intact GST-EF hand-X-Y, GST-X-Y-C2 and GST-C2 were detected on the SDS PAGE along with some degradation products. Because the GST-EF hand and GST-X-Y were mostly degraded, intein fusions to these domains were generated by cloning sequences encoding the EF hand and X-Y domains into the vector pTYB2 (New England Biolabs). Because of lack of time, no attempts were made to purify the intein fusion proteins from *E. coli* and Ca²⁺-binding or enzyme activity assays remain to be performed.

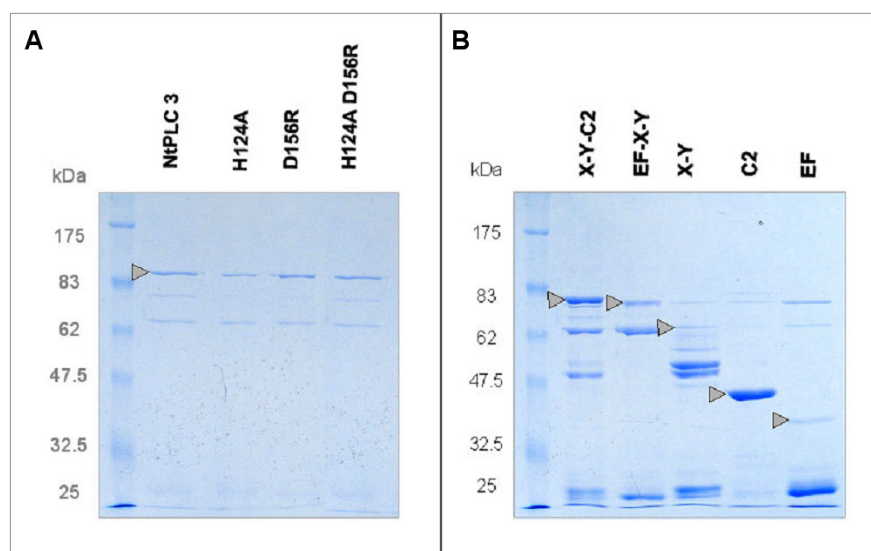


Figure 21: Recombinant GST-NtPLC3 fusion proteins analyzed on a 10 % SDS PAGE. (A) Lane 1, molecular mass marker of 175, 83, 62, 47.5, 32.5 and 25 kDa. Lane 2, NtPLC3 full-length GST fusion protein; lane 3, 4 and 5, GST-NtPLC3 mutants. (B) Lane 1, molecular mass marker, lane 2, NtPLC3 truncation GST-X-Y-C2; lane 3, GST-EF hand-X-Y; lane 4, GST-X-Y; lane 5, GST-C2; lane 6, GST-EF hand. Arrowheads indicate correct size of bands.

2.2.3.2 *In vitro* enzyme activity assay using [³H] phosphatidylinositol 4,5-bisphosphate

The catalytic activity of wild-type and mutant NtPLC3 was determined *in vitro* using radio-labeled PI-4,5-P₂ as the substrate. Assays were performed according to the protocol by Melin *et al.* (1992) with some modifications after testing different reaction times and enzyme concentrations. Using BSA as standard, protein concentrations were determined on Coomassie-stained SDS gels. 100 ng enzyme were used for each assay, which was performed at RT. Reaction time was adjusted to 20 min. Experiments were repeated several times, at least in duplicates. Results of the activity assays are summarized in Figure 22.

The enzymatic activity of wild-type NtPLC3 was investigated using different free Ca²⁺ concentrations (Ca²⁺/EGTA mixture; Owen 1976), ranging from 1 μM to 1000 μM. In seven independent experiments the activity of NtPLC3 increased starting with a minimum concentration of 1 μM free Ca²⁺, peaked at 500 μM and was low at 1000 μM (Figure 22A). All subsequent PI-PLC assays were performed at a free Ca²⁺ concentration of 10 μM, which roughly corresponds to the intracellular Ca²⁺ concentration at the tip of growing tobacco pollen tubes and which was the Ca²⁺ concentration used in published *in vitro* assays of plant PI-PLC activity (Staxén *et al.*, 1999; Kovar *et al.*, 2000). At this Ca²⁺ concentration, the activity of NtPLC3 was dependent on the amount of protein and showed

a linear increase (data not shown).

The NtPLC3 mutants, H¹²⁴A, D¹⁵⁶R and H¹²⁴A D¹⁵⁶R showed significantly reduced activity at the level of 5.38 %, of 9.73 % and of 8.53 % compared to wild-type activity, respectively (Figure 22B).

The specific PI-PLC inhibitor U-73122, 1-[6-((17b-3-Methoxyestra-1,3,5(10)-trien-17-yl)amino)hexyl]-1H-pyrrole-2,5-dione (Bleasdale *et al.*, 1990; Smith *et al.*, 1990), blocked PI-4,5-P₂ hydrolysis by recombinant NtPLC3 significantly in a dose-dependent manner with an IC₅₀ at 17.5 μM U-73122. Complete inhibition of NtPLC3 activity was observed at 80 μM U-73122 (Figure 22C). These results are consistent with data obtained for *Nicotiana rustica* PI-PLC, which was cloned from a guard-cell enriched cDNA library (Staxén *et al.*, 1999). 50 % inhibition of NrPLC was observed at 23 μM U-73122, whereas complete inhibition required 80 μM U-73122. The data are also in good agreement with values obtained for mammalian PI-PLC which showed an IC₅₀ at 10 μM U-73122 and complete inhibition at 50 μM U-73122 (Feißt *et al.*, 2005).

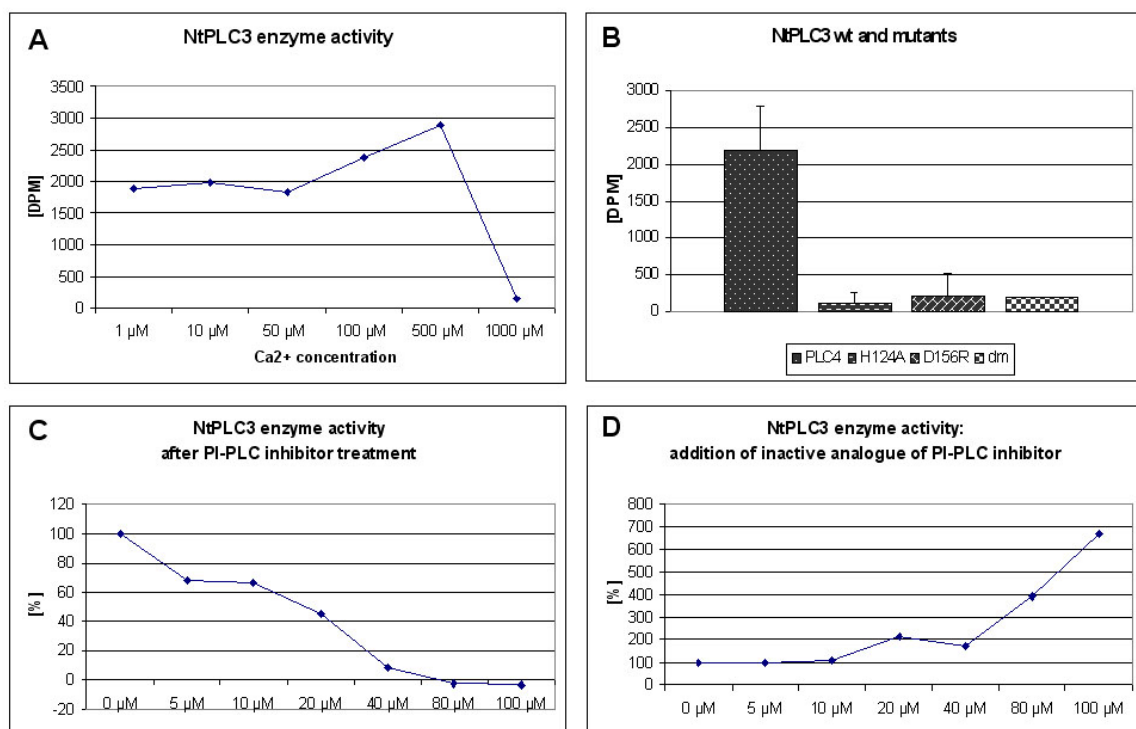


Figure 22: Enzyme activity of recombinant GST-NtPLC3 fusion proteins.

(A) *In vitro* PI-4,5-P₂ hydrolysis was Ca²⁺ dependent with a peak at 500 μM. Data presented are representative of one of seven independent experiments. (B) Point mutations in the active site significantly reduced NtPLC3's activity. Error bars indicate a confidence range of 95 %. (C) The amonisteroid U-73122 reduced PI-PLC activity in a concentration-dependent manner, whereas its inactive analogue U-73343 increased activity at 20 μM or higher (D). Data obtained with single representative experiments are shown in C and D. Experiments were repeated five times. Activity is expressed as a percentage of the activity obtained with PI-4,5-P₂ as substrate and 10 μM free Ca²⁺ in the absence of U-73122 or U-73343 (100 % = 0.749 nmol⁻¹ mg⁻¹ protein).

U-73343, 1-[6-((17 β -3-Methoxyestra-1,3,5(10)-trien-17-yl)amino)hexyl]-2,5-pyrrolidinedione, is an inactive analogue of U-73122, which contains a pyrrolidindione instead of a pyrroledione. Staxén *et al.* (1999) showed that U-73343 had no effect on the *in vitro* activity of NrPLC. Surprisingly and for reasons we cannot explain to date, we obtained different results. In our hands, U-73343 did not have an effect on NtPLC3 activity at concentrations of 5 and 10 μ M, but in five independent experiments this activity increased dramatically at concentrations of 20 μ M and higher (Figure 22D).

2.2.4 Effects of transient expression of NtPLC3 in pollen tubes of *Nicotiana tabacum*

2.2.4.1 Transient expression of wild-type and mutant NtPLC3

Particle bombardment is a suitable and widely used method of gene transfer into eukaryotic cells. In order to initiate the functional characterization of NtPLC3, wild-type and mutant versions of this protein, they were transiently over-expressed in tobacco pollen tubes after particle bombardment. Gene expression was driven by the strong pollen-specific promoter of the Lat52 gene. The lat52 promoter is known to be active in late stages of pollen development and specifically in pollen and anther tissue (Twell *et al.*, 1989). In order to visualize transfected pollen tubes, the yellow fluorescent protein (YFP) was co-transfected with NtPLC3 wild-type or mutants.

In these experiments, pollen tubes that expressed YFP along with the non-invasive marker protein β -glucuronidase (GUS) served as controls. These pollen tubes showed normal growth behaviour and morphology. Pollen tube length measurements were performed 6 h after particle bombardment using an epifluorescence microscope (Leica DM IRB) and ImageJ as the bioinformatic source.

Figure 23A to D show low magnification images of pollen tubes expressing wild-type and mutant NtPLC3. Control pollen tubes expressing YFP and GUS are depicted in Figure 23E. Obviously, over-expression of wild-type and mutant NtPLC3 even at high levels did not have an effect on pollen tube growth or morphology. Length measurements in Figure 23F support this observation. No significant difference in the length of pollen tubes expressing different proteins was detected after 6 h.

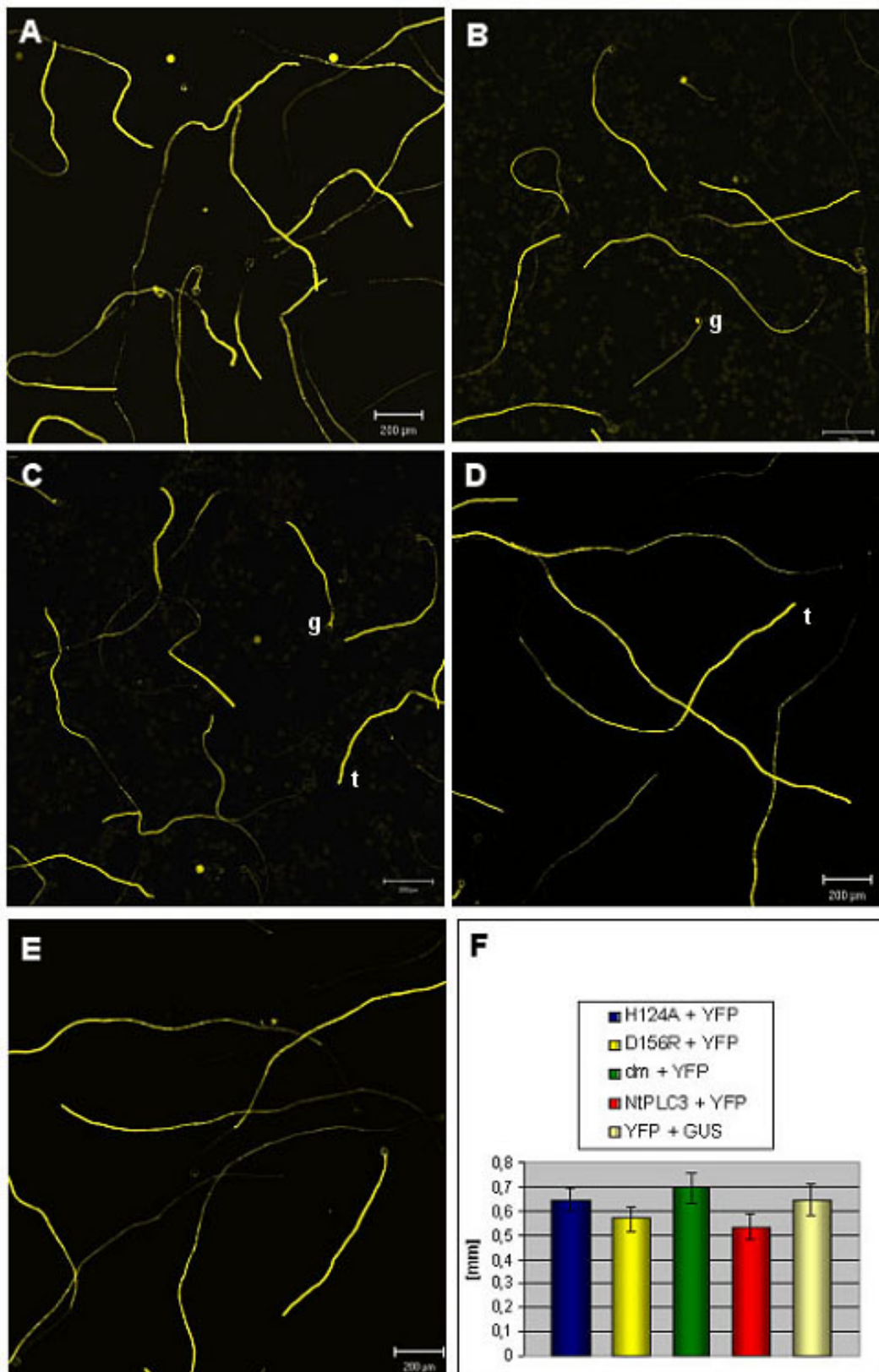


Figure 23: Transient over-expression of NtPLC3 wild-type and mutants in pollen tubes of *Nicotiana tabacum*. Low magnification (5 x) images are shown. Over-expression of NtPLC3 H¹²⁴A + YFP (A), of NtPLC3 D¹⁵⁶R + YFP (B), of NtPLC3 H¹²⁴A D¹⁵⁶R + YFP (C), of NtPLC3 wt + YFP (D) or YFP + GUS (E) under the control of the pollen-specific lat52 promoter. Pollen tube length measurements 6 h after particle bombardment are shown in (F). Error bars indicate a confidence range of 95 %. (g = pollen grain; t = pollen tube tip).

2.2.4.2 Subcellular localization of NtPLC3

Many plant PI-PLCs were described in the last few years, which all appeared to be membrane-associated enzymes, as indicated by biochemical experiments (Otterhag *et al.*, 2001; Mueller-Roeber and Pical, 2002). Only in one case membrane association of a plant PI-PLC isoform was demonstrated *in vivo*. Kim *et al.* (2004) expressed GFP fused to the NH₂-terminus of mung bean (*Vigna radiata* L.) Vr-PLC3 in *Arabidopsis* protoplasts and showed that the fusion protein co-localized with the plasma membrane marker H⁺-ATPase-RFP. A deletion mutant lacking the COOH-terminal C2 domain accumulated in the cytosol, pointing at a pivotal role of the C2 domain in membrane binding. However, these experiments were performed in a heterologous system and the images shown are not unambiguous.

To investigate the intracellular localization of NtPLC3, NH₂- and COOH-terminal YFP fusions under the control of the pollen-specific *lat52* promoter were generated.

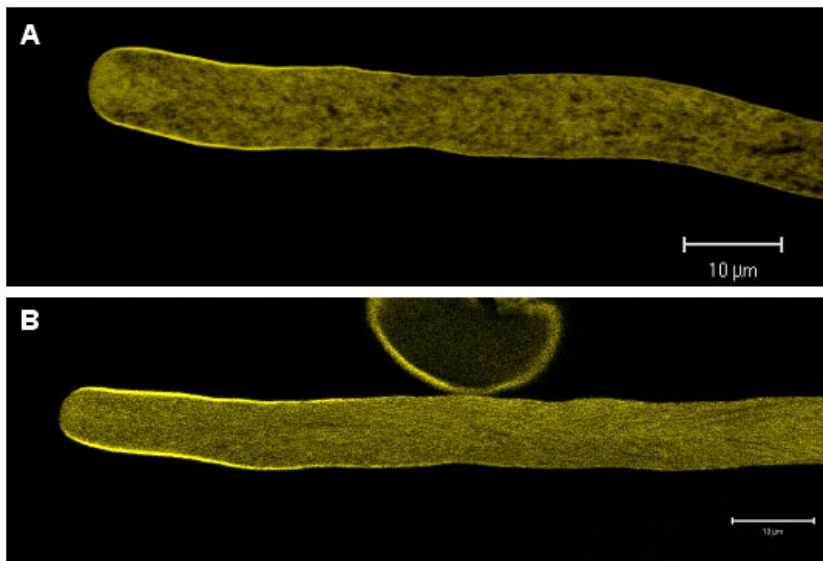


Figure 24: Transiently transfected pollen tubes of *Nicotiana tabacum*. Intracellular localization of YFP fused to the NH₂- or COOH-terminus of NtPLC3, respectively. Medial optical confocal sections 6 to 8 h after particle bombardment showing YFP-NtPLC3 (A) and NtPLC3-YFP (B).

Transiently expressed NtPLC3 fused to YFP clearly accumulated at the plasma membrane in the shank, but not at the tip of growing pollen tubes. The plasma membrane association of NtPLC3 was strong near the tip, fading away with increasing distance from this location. More significant membrane association was observed with YFP fused to the COOH-terminus of NtPLC3 (Figure 24B), as compared to the NH₂-terminal fusion.

Growth behaviour or morphology of most pollen tubes was normal (data summarized in Figure 27F). However, a small percentage of the pollen tubes (< 10 %) displayed reduced cytoplasmic streaming and growth. In such pollen tubes NtPLC3 YFP fusions were evenly distributed all over the plasma membrane and accumulated also at the tip (data not shown).

2.2.4.3 Subcellular localization of NtPLC3 domain-deletion mutants

The work of Kim *et al.* (2004) indicated an important function of the C2 domain of Vr-PLC3 in membrane association (see above). In addition, Otterhag *et al.* (2001) showed that the C2 domain of AtPLC2 is essential for lipid vesicle binding *in vitro*. Mueller-Roeber and Pical (2002) suggested additional hydrophobic moieties within the protein additionally to be involved in membrane binding. Nevertheless, it has not convincingly been shown whether the C2 domain of plant PI-PLCs is solely essential for membrane association of these enzymes or if not other regions contribute to this association.

To answer this question, six different truncated forms of NtPLC3 were fused to YFP. Based on the observation that full-length NtPLC3-YFP showed stronger plasma membrane association than YFP-NtPLC3, YFP was attached to the COOH-terminus of the different NtPLC3 truncations. In summary, the following fusions were generated (Figure 25): EF hand-YFP (aa 1 to 106), EF hand-X-Y-YFP (1 to 431), X-Y-YFP (111 to 431), X-Y-C2-YFP (111 to 588), C2-YFP (437 to 588) and EF-YFP-C2 (aa 1 to 106, aa 437 to 588).

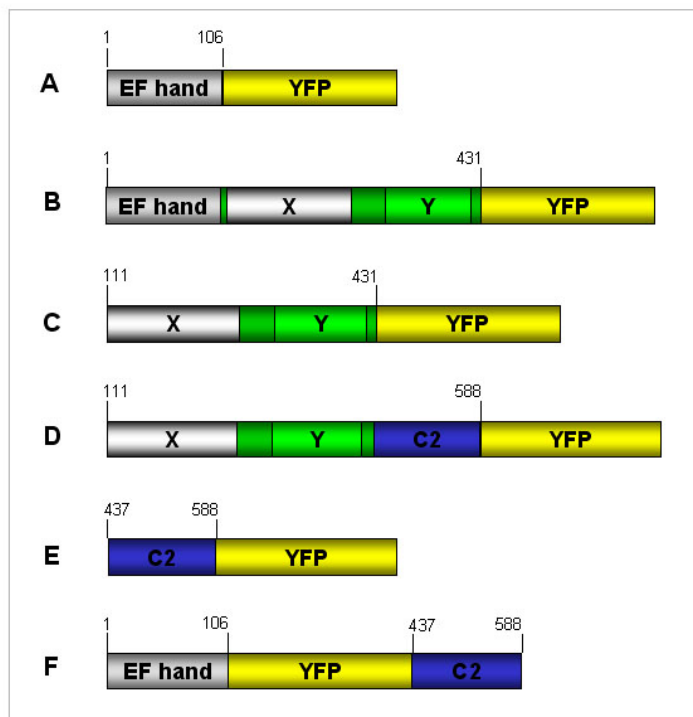


Figure 25: Schematic overview of NtPLC3 truncation constructs. A to F show deletion variants of NtPLC3, fused to YFP and generated for transfection and transient expression in pollen tubes. Numbers indicate the amino acid residues comprising the different domains.

The intracellular localization of all these fusion proteins upon transient expression in pollen tubes is shown in Figure 26. Confocal images taken 6 to 8 h after transfection demonstrated that single domains of NtPLC3 were not sufficient to target the PI-PLC to

the plasma membrane (Figure 26A to E). Only EF-YFP-C2 was localized at the plasma membrane of pollen tubes, both in the shank and in the tip (Figure 26F). From these observations we conclude that EF hand and C2 domain are both required for membrane binding of NtPLC3. Interestingly, in contrast to full-length NtPLC3, the EF-YFP-C2 fusion was associated with the plasma membrane also in the tip.

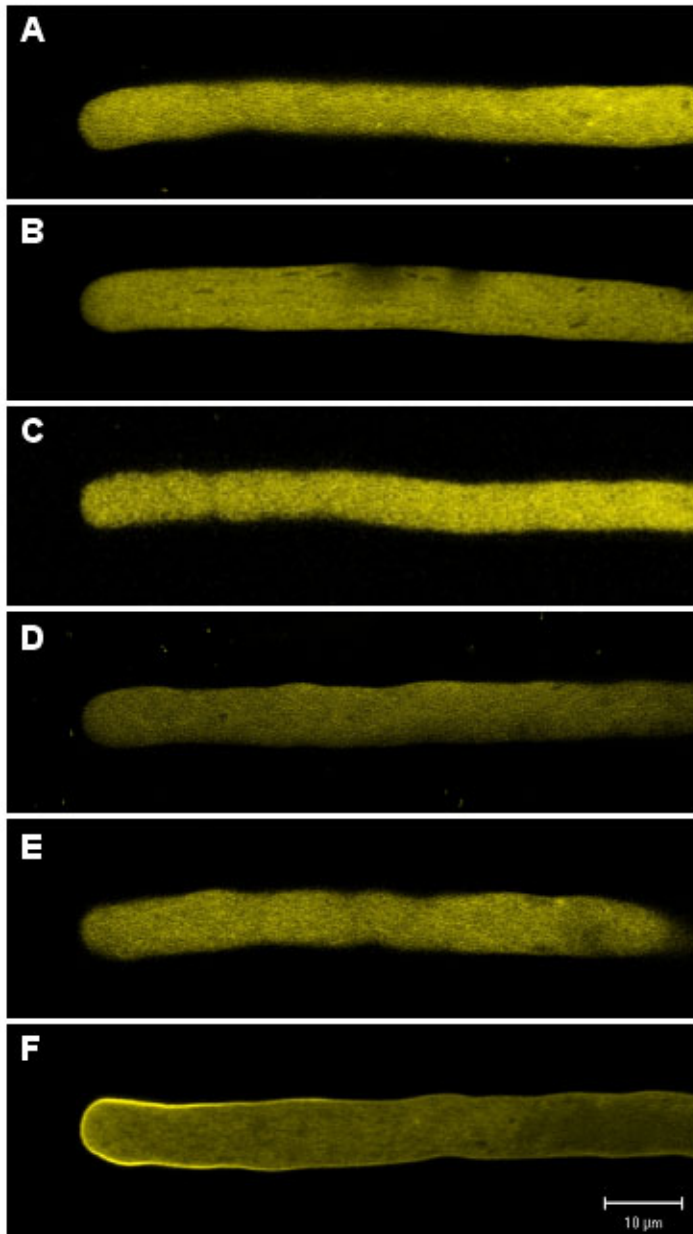


Figure 26 : Transient expression of domain-deletion mutants of NtPLC3 after particle bombardment. Medial optical confocal sections imaged 6 to 8 h after transfection. NtPLC3 EF hand-YFP (A), EF hand-X-Y-YFP (B), X-Y-YFP (C), X-Y-C2-YFP (D), C2-YFP (E) and EF hand-YFP-C2 (F).

A further control experiment was performed, in which YFP fused to the NH₂-terminus of the C2 domain also accumulated in the cytosol (data not shown), which supports the notion that indeed, both, the EF hand and the C2 domain are needed for membrane association of NtPLC3.

2.2.4.4 Determination of the specific function of NtPLC3's catalytic core in membrane association

Whereas full-length NtPLC3 fused to YFP was excluded from the plasma membrane at the pollen tube tip, the EF-YFP-C2 fusion protein associated with all areas of the pollen tube plasma membrane to the same extent (see previous chapter). This indicates that the catalytic core, which is missing in the EF-YFP-C2 fusion, has an essential function in excluding full-length PI-PLC from accumulating at the plasma membrane in the tip.

The pleckstrin homology domain (PH) of the mammalian PI-PLC δ_1 fused to YFP is known to bind specifically to PI-4,5-P₂ *in vivo* (Stauffer *et al.*, 1998; Lemmon *et al.*, 2002) and accumulates at the plasma membrane specifically at the tip of tobacco pollen tubes (Kost *et al.*, 1999). To further investigate the role of the X and Y domains in the localization of PI-PLCs, these domains (NtPLC3 aa 111 to 431) were attached in frame to the NH₂-terminus of a YFP-PLC- δ_1 -PH fusion that serves as a marker for PI-4,5-P₂. The resulting chimera XY-YFP-PLC- δ_1 -PH localized to the plasma membrane in the shanks, but not in the tip of pollen tubes (Figure 27E). This observation establishes a key function of the NtPLC3 X and Y domains in preventing the accumulation of this enzyme at the plasma membrane in the pollen tube tip.

Interestingly, all mutant versions of NtPLC3, which did not hydrolyze PI-4,5-P₂ *in vitro*, show the same intracellular localization as wild-type NtPLC3 in pollen tubes when transiently expressed as YFP fusion proteins (Figure 27C). Figure 27C serves as an example for all three mutants. This demonstrates that the enzymatic activity of the X and Y domains is not essential for the function of these domains in keeping NtPLC3 from the binding to the plasma membrane at the pollen tube tip.

Transient expression of truncated forms of NtPLC3 fused to YFP or of the XY-YFP-PI-PLC- δ_1 -PH fusion, did not dramatically affect pollen tube growth, although it slowed this process down in some cases (Figure 27F).

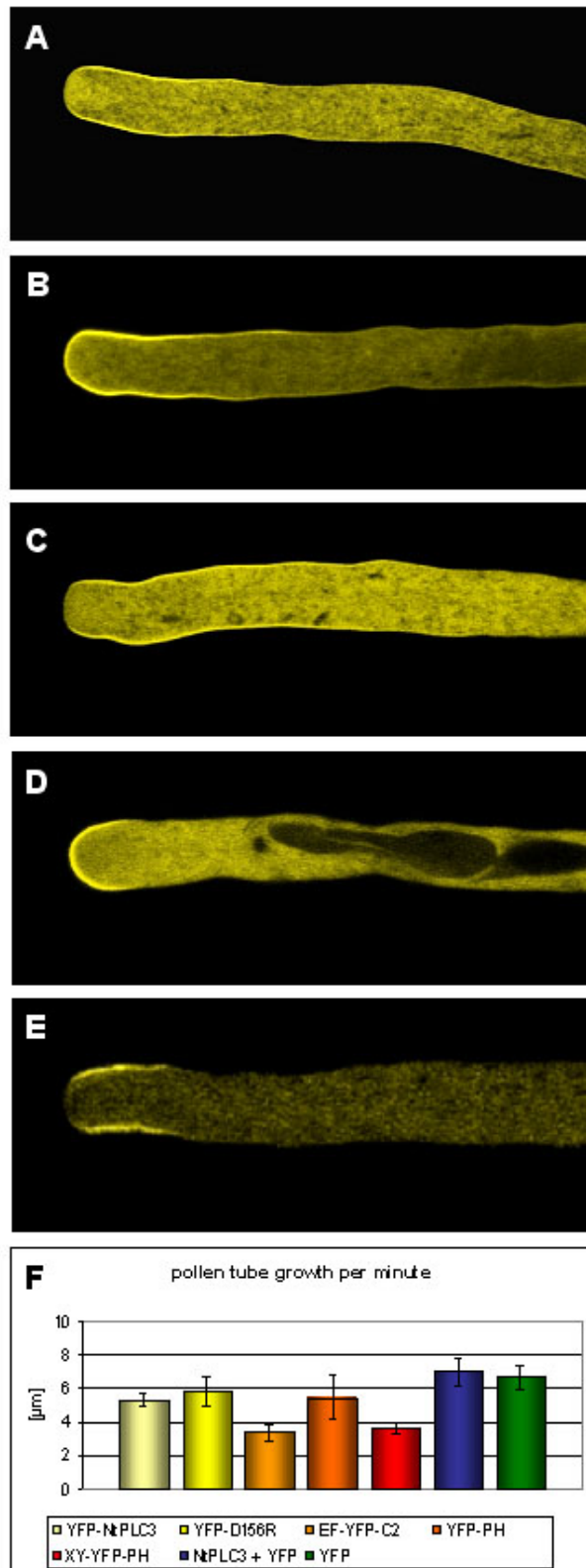


Figure 27: Tip-localization patterns achieved by distinct NtPLC3 fusion constructs 6 to 8 h after transient transfection. Medial optical confocal sections. (A) YFP-NtPLC3, (B) EF hand-YFP-C2, (C) YFP-NtPLC3 D¹⁵⁶R, representative for all three mutants, (D) YFP-PLC- δ_1 -PH or (E) NtPLC3 XY-YFP-PLC- δ_1 -PH. (F) Statistics of pollen tube growth rate per minute to ensure normal pollen tube growth of transfected cells. Error bars indicate a confidence range of 95 %.

2.2.5 Inhibition of PI-PLC activity by U-73122 treatment *in vivo*

The aminosteroid U-73122 has been used widely in animal cells as a specific inhibitor of PI-PLC activity (Bleasdale *et al.*, 1990; Smith *et al.*, 1990). However, the inhibitor has never been used to inhibit PI-PLCs in growing pollen tubes before. Therefore, it was necessary to perform dose-response experiments to determine the range of concentrations at which U-73122 affects pollen tube growth. Effects of 0.25 to 10 μM U-73122 on pollen germination and pollen tube growth were investigated. As controls served pollen tubes growing in growth medium or in medium supplemented with 0.25 % DMSO, in which stock solutions of both U-73122 and U-73343 were prepared. Tobacco pollen grains were suspended in liquid medium containing U-73122 or U-73343, an inactive analogue of this drug. Pollen germination and pollen tube growth was allowed to proceed for 5 h before taking low magnification (5 x) images using a transmission light microscope. Pollen tube length was measured in these pictures using the ImageJ software package.

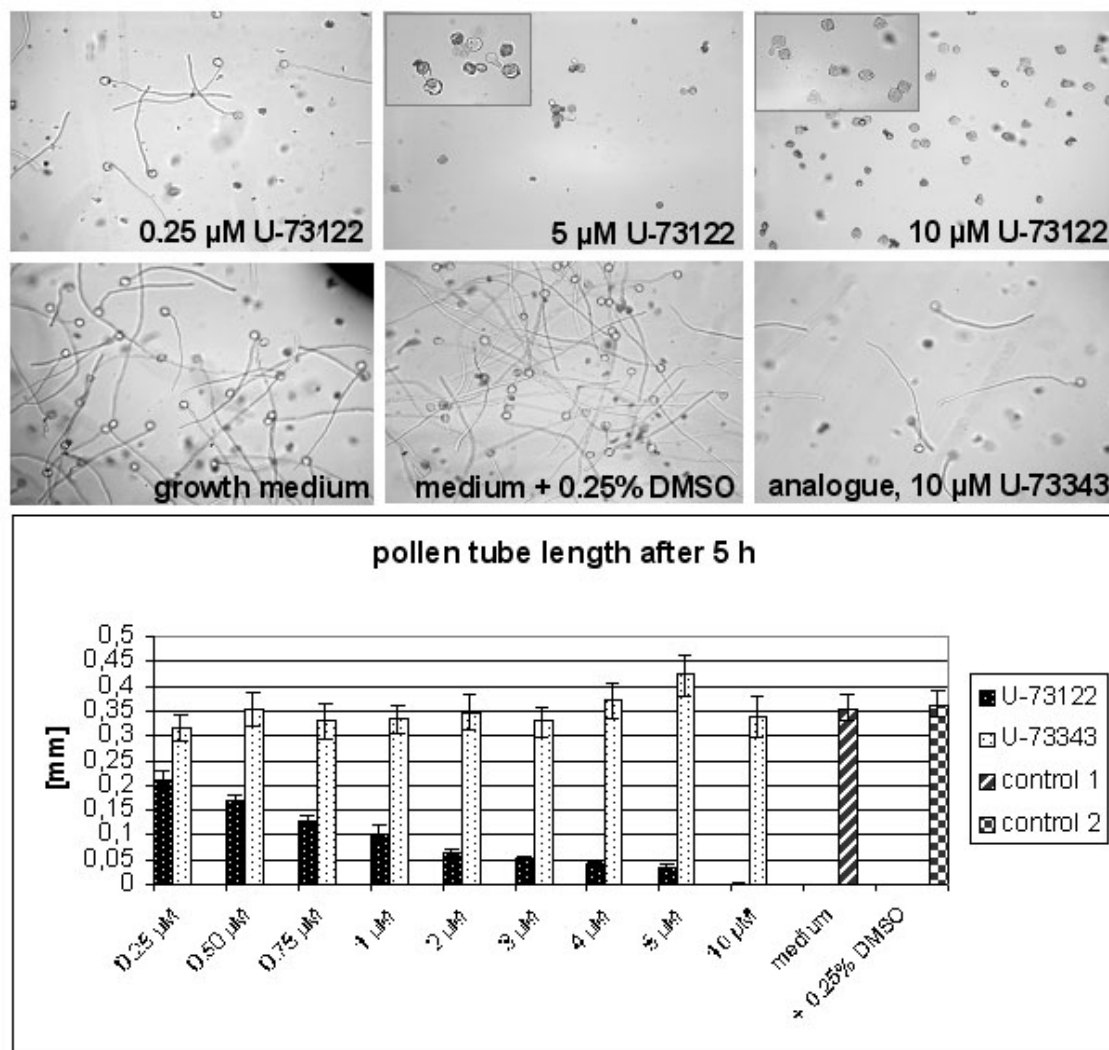


Figure 28: Dose-response experiment employing the PI-PLC inhibitor U-73122 and its inactive analogue U-73343.

At a concentration of 0.25 μM the PI-PLC inhibitor U-73122 did not show an effect on pollen tube morphology, although pollen tube length was slightly reduced compared to the controls. Pollen tube length was decreasing in a concentration-dependent manner. At 5 μM U-73122 pollen tube growth was depolarized resulting in the formation of balloons at the tip. The diameter of the balloons was comparable to that of pollen grains (see higher magnification in Figure 28). At 10 μM U-73122 the majority of the pollen grains did not germinate at all and only a few extremely short pollen tubes were visible. Figure 28 also shows that the inactive analogue U-73343 did not have an effect on pollen tube length or morphology.

Based on the dose-response experiment described above, a concentration of 5 μM U-73122 was employed in following *in vivo* experiments.

A dilution of the inhibitor with growth medium by a factor of 4 and a further incubation for 16 h did not result in normal growth or germination of pollen grains formerly treated with 5 μM and 10 μM U-73122, respectively. Thus, the inhibition of PI-PLCs by U-73122 was not reversible.

2.2.5.1 Complementation of PI-PLC inhibition by NtPLC3 over-expression *in vivo*

At 5 μM , U-73122 did not inhibit pollen germination, but depolarized pollen tube growth and resulted in the formation of short tubes with balloons at the tip. To demonstrate that these effects were due to specific inhibition of PI-PLC activity, we tested whether transient NtPLC3 over-expression counteracted U-73122 effects on pollen tube growth.

Pollen tubes transiently expressing NtPLC3 along with YFP 3 h after particle bombardment were treated for 2 h with 5 μM U-73122. Transformed and untransformed pollen tubes on the same plates were imaged with an epifluorescence microscope (Leica DM IRB) and length measurements performed with ImageJ. The length of transfected pollen tubes carrying the over-expression construct for NtPLC3 and not-transfected tubes on the same petri dish are compared in Figure 29.

NtPLC3 over-expression reduced the sensitivity of pollen tubes to U-73122, indicating that the effects of this drug on pollen tube growth are at least in part caused by the inhibition of PI-PLC activity.

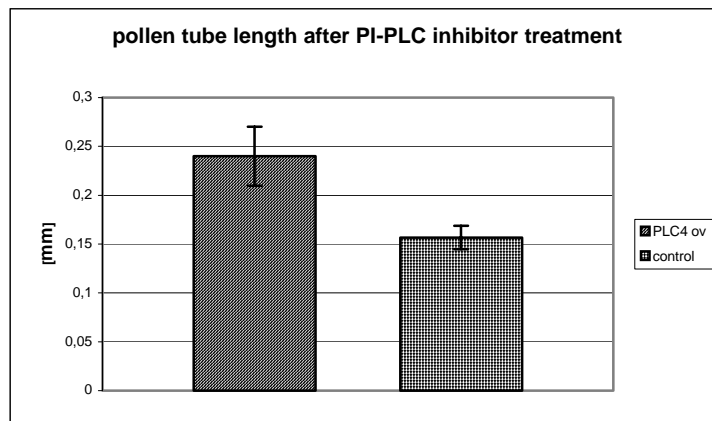


Figure 29: NtPLC3 complementation assay. Pollen tubes harbouring the NtPLC3 over-expression construct are significantly longer after PI-PLC inhibitor treatment than not-transfected pollen tubes growing on the same petri dish.

2.2.6 Visualization of PI-4,5-P₂ and its implication in pollen tube polarity

NtPLC3 hydrolyzes PI-4,5-P₂ *in vitro* and localizes to the pollen tube plasma membrane in the shank, but not in the tip. In contrast, PI-4,5-P₂ accumulates in the pollen tube plasma membrane specifically at the tip as demonstrated using the specific marker YFP-PLC- δ_1 -PH (Chapter 2.2.4.4). Interestingly, NtPLC3 and its substrate PI-4,5-P₂ appear to show a complementary distribution pattern in the pollen tube plasma membrane. This was confirmed by transient co-expression of YFP-PLC- δ_1 -PH and NtPLC3-RFP (Figure 30).

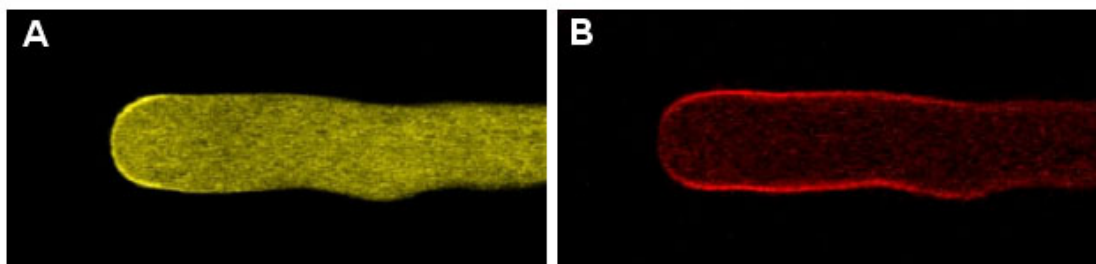


Figure 30: Medial optical confocal sections. Double labeling of YFP-PLC- δ_1 -PH (A) and NtPLC3-RFP (B) 6 h after particle bombardment. PI-4,5-P₂ and PI-PLC localize in a complementary pattern at the plasma membrane in the pollen tube tip.

PI-4,5-P₂ accumulates in the plasma membrane at the pollen tube tip as a consequence of the stimulation of a lipid kinase activity by Rac/Rop type small GTPases (see INTRODUCTION, Kost *et al.*, 1999). Over-activation of pollen tube Rac/Rop GTPases depolarizes pollen tube growth (Figure 3 and Kost *et al.*, 1999; Li *et al.*, 1999), as does the inhibition of NtPLC3 with U-73122 (see Figure 28). Together with the complementary pattern of PI-4,5-P₂ and PI-PLC accumulation, these observations are consistent with

NtPLC3 having a key function in preventing PI-4,5-P₂ from diffusing away from the tip, where it serves as an effector of pollen tube Rac/Rop GTPases. If this was true, NtPLC3 would play an important role in maintaining the polarity of pollen tube tip growth.

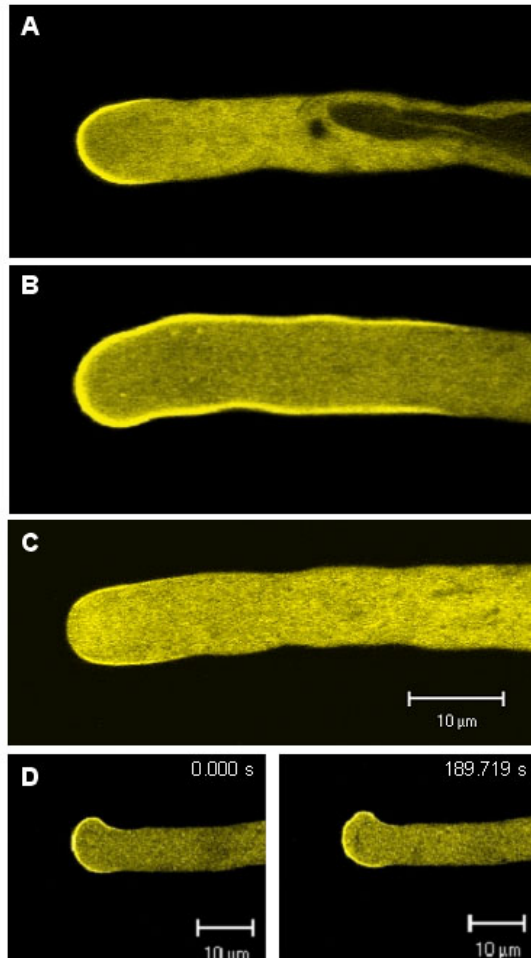


Figure 31: Medial optical confocal sections 6 h after particle bombardment. (A) YFP-PLC- δ_1 -PH, used as an *in vivo* marker for PI-4,5-P₂, labeled a restricted area at the plasma membrane in the pollen tube apex. (B) Shows the same pollen tube 30 min after addition of the PI-PLC inhibitor U-73122. PI-4,5-P₂ spread to a larger area of the plasma membrane at the pollen tube tip. (C) and (D) show that PI-4,5-P₂ did not spread to the flanks of pollen tubes when pollen tube growth was stopped using a drug that does not affect PI-PLC activity. (C) shows an untreated pollen tube expressing YFP-PLC- δ_1 -PH before addition of 50 nM Latrunculin B. This pollen tube was growing at a rate of 6.48 $\mu\text{m}\cdot\text{min}^{-1}$. (D) shows the same pollen tube 15 min after LatB treatment. The PI-4,5-P₂ labeling-pattern remained exactly the same as in the untreated tube, although Latrunculin B stopped growth.

To generate further evidence in support of this hypothesis the effect of U-73122 on PI-4,5-P₂ distribution in pollen tubes was visualized *in vivo*. Pollen tubes were transiently transfected with the PI-4,5-P₂ marker YFP-PLC- δ_1 -PH and imaged 6 h after particle bombardment (Figure 31A). PI-4,5-P₂ was localized in the plasma membrane at the pollen tube tip. Treatment with the PI-PLC inhibitor U-73122 caused PI-4,5-P₂ to spread to a larger area at the plasma membrane in the tip (Figure 31B). Because inhibition of PI-PLCs with U-73122 also resulted in a growth stop of the pollen tubes, it was necessary to perform a control experiment to ensure that the effect on PI-4,5-P₂ distribution was not due to the growth stop. Latrunculin B was used for that purpose, which is a widely used actin depolymerizing drug and known to inhibit pollen tube growth, but not cytoplasmic streaming at low concentrations (Vidali *et al.*, 2001). Figure 31C shows an untreated pollen

tube expressing YFP-PLC- δ_1 -PH, growing normally at a rate of $6.48 \mu\text{M} * \text{min}^{-1}$. Figure 31D shows the same pollen tube as in 30C 15 min after treatment with 50 nM Latrunculin B. Pollen tube growth was stopped, but the PI-4,5-P₂ localization remained the same as in the untreated pollen tube (31C).

In summary, these data show that NtPLC3 restricts PI-4,5-P₂ to a small area at the pollen tube tip and thereby ensures polarized pollen tube expansion.

2.2.7 Visualization of diacylglycerol and its dependence on PI-PLC activity

PI-PLCs hydrolyze PI-4,5-P₂ and thereby generate two second messengers. The water-soluble inositol 1,4,5-trisphosphate (InsP₃) and the membrane bound diacylglycerol (DAG). In this experiment, we have employed YFP-tagged Cys domains of Protein Kinase C- γ (Oancea *et al.*, 1998) to visualize DAG accumulation in tobacco pollen tubes.

In mammalian cells, the generation of DAG in the plasma membrane, by PI-4,5-P₂ hydrolysis, drives Protein Kinase C from the cytosol to the membrane. Protein Kinase C isozymes contain one or two globular C1 domains with a conserved Cys-rich motif, being a hallmark of C1 domains (Newton and Johnson, 1998). *In vitro* studies revealed that Cys1-domains from several Protein Kinase C (PKC) isoforms bind lipid membranes in the presence of diacylglycerol or phorbol esters. Cysteine-rich domains (Cys1-domains) are about 50-amino acid-long protein domains that complex two zinc ions and include a consensus sequence with six cysteine and two histidine residues (Newton and Johnson, 1998). YFP-tagged Cys1-domains, as fluorescent diacylglycerol indicators, have been used to visualize the localized production of DAG in individual cells and to provide insight into spatio-temporal differences of DAG signaling (Oancea *et al.*, 1998). Oancea *et al.* (1998) have fused the first Cys1-domain from Protein Kinase C- γ with the green fluorescent protein and transfected a cell line of the rat basophilic leukemia (RBL) model with this construct. We obtained the Cys1-GFP construct from Dr. Tobias Meyer (Stanford University, USA) and cloned it behind the lat52 promoter into a pollen-specific expression vector. Transiently expressed Cys1-YFP was localized at the plasma membrane in the pollen tube apex. The labeling pattern appeared in a tip-directed gradient, labeling was decreasing with increasing distance from the tip and was not detectable at the flanks of the pollen tube (Figure 32A). Simultaneous transient over-expression of Cys1-YFP and

NtPLC3, both under control of the *lat52* promoter, resulted in a spreading of the labeling to a larger area of the pollen tube tip, including to the flanks (Figure 32B). Especially when

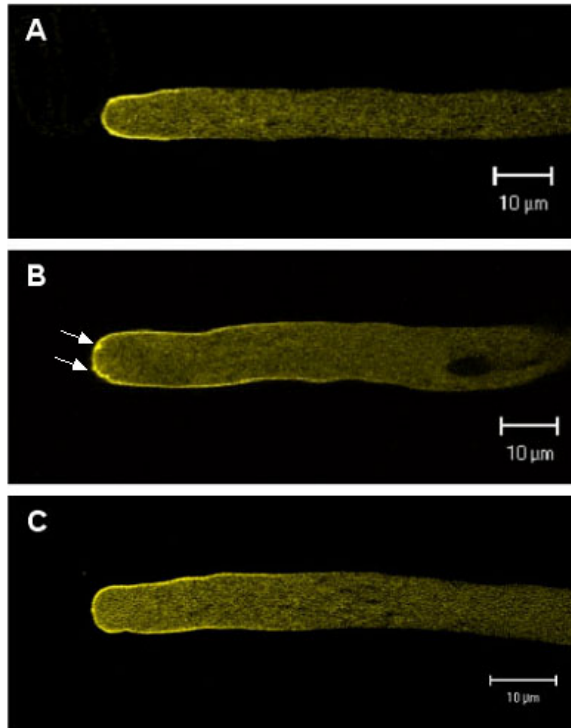


Figure 32: Medial optical confocal sections. (A) Tobacco pollen tube transiently expressing Cys1-YFP, used as a marker for DAG, 6 to 8 h after particle bombardment. Cys1-YFP is localized at the plasma membrane in the pollen tube tip. (B) Pollen tube expressing Cys1-YFP and NtPLC3. Cys1-YFP localization spreads to a larger area of the plasma membrane in the pollen tube tip and at the flanks. (C) Expression of Cys1-YFP and the inactive mutant NtPLC3 H¹²⁴A D¹⁵⁶R. Cys1-YFP localization is the same as in (B).

NtPLC3 was simultaneously over-expressed, small fluorescent vesicles became visible at the pollen tube tip (32B, arrows). These vesicles were moving fast from the flanks in direction to the tip. To test if the change in Cys1-YFP localization after NtPLC3 over-expression was due to over-expressed NtPLC3 activity, the inactive double mutant of NtPLC3, NtPLC3 H¹²⁴A D¹⁵⁶R, was co-transfected with Cys1-YFP. Figure 32C shows spreading of Cys1-YFP to the flanks of the pollen tube also after over-expression of the inactive NtPLC3 mutant. Interestingly, over-expression of NtPLC3 affects the accumulation of DAG, a product of the enzymatic activity of this protein, even when carrying a point mutation that disrupts activity. Furthermore, despite its effects on DAG accumulation, NtPLC3 over-expression does not affect pollen tube growth (see above). At this point we do not have a conclusion for these observations.

As DAG is the product of PI-4,5-P₂ hydrolysis by PI-PLCs it was interesting to study the accumulation of DAG in pollen tubes after PI-PLC inhibitor treatment. Pollen tubes transiently expressing the DAG marker Cys1-YFP showed a typical DAG accumulation pattern as well as normal growth before treated with U-73122 (Figure 33A, see also Figure

32A). After 15 min of inhibitor treatment the same pollen tube as shown in Figure 33A, displayed an altered labeling pattern and growth behaviour as observed by confocal microscopy. The YFP signal at the pollen tube apex had decreased, indicating that the amount of DAG at the tip was reduced and intracellular YFP-stained vesicles had appeared (Figure 33B). After 30 minutes of U-73122 treatment, membrane staining had completely disappeared and growth had stopped. YFP fluorescence was only detectable in the cytosol

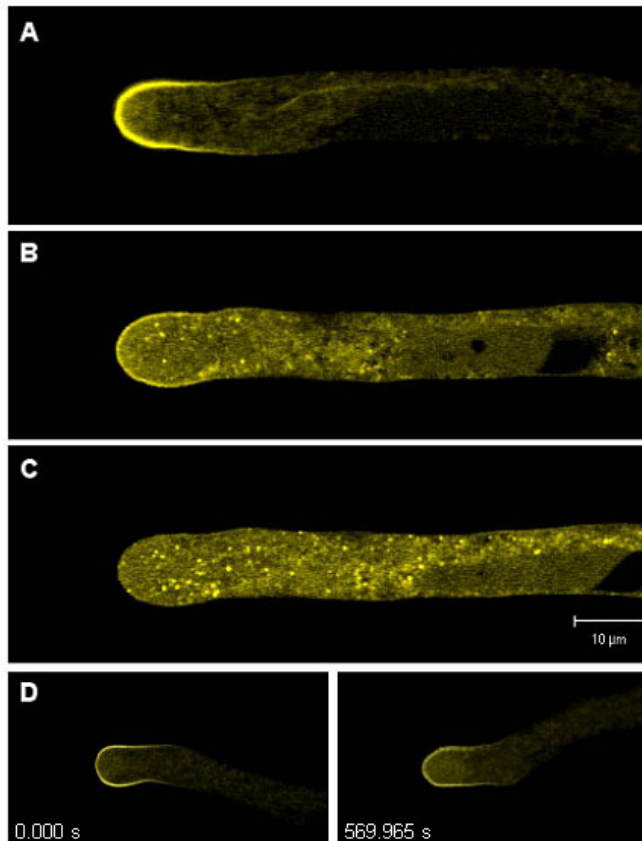


Figure 33: Medial optical confocal sections 6 to 8 h after particle bombardment. (A) Tobacco pollen tube expressing Cys1-YFP before inhibitor treatment. DAG is localized in the plasma membrane of the pollen tube tip. (B) Same pollen tube as in (A) 15 min after addition of PI-PLC inhibitor U-73122. Tip-labeling is slightly weaker, vesicles become visible in the pollen tube cytoplasm. (C) 30 min after inhibitor treatment. Tip-labeling has completely disappeared. Strong vesicle labeling. (D) Addition of Latrunculin B served as a control. 30 min after addition of Latrunculin B pollen tube growth was completely inhibited, DAG labeling remained the same as in untreated tubes, shown in a time series of almost 10 min in D (left and right).

and in numerous vesicles (Figure 33C). As described previously, it was necessary to perform a control in order to ensure that the membrane labeling disappeared because PI-PLC activity was inhibited and not because pollen tube growth was stopped. Figure 33D shows the first and the last image of a time series of almost 10 min recorded 30 min after the addition of 50 nM Latrunculin B to pollen tubes expressing Cys1-YFP. Pollen tube growth was stopped, but not cytoplasmic streaming by inhibitor treatment. The Cys1-YFP labeling pattern was not affected by Latrunculin B treatment.

In conclusion, Cys1-YFP appears to be a useful *in vivo* marker for DAG accumulation in tobacco pollen tubes. Interestingly, DAG accumulates not only in the plasma membrane at the flanks of the tip, where PI-4,5-P₂ and NtPLC3 overlap, but also at the extreme tip.

Inactivation of PI-PLC activity causes DAG to disappear from the plasma membrane within 30 minutes.

The nature of the Cys1-YFP labeled vesicles observed after U-73122 treatment is unclear. Based on their appearance, they might be endosomes. We have two different endosomal markers in our hands. The first is a CFP fusion to a FYVE domain. FYVE domains are widely used as markers for endosomal membranes. The FYVE domain represents a conserved adaptor domain whose primary function is to act as a membrane-attachment module that depends upon interaction with phosphatidylinositol 3-monophosphate, PI-3-P (Cullen *et al.*, 2001; Meijer and Munnik, 2003), which accumulates to high levels in the membrane of endosomes. The second marker is a YFP fusion to a *Nicotiana tabacum* Rab5 GTPase (generated by Stéphanie Cottier, unpublished). Rabenosyn-5 is a recently identified FYVE domain containing protein, required for homo- and heterotypic early endosome fusion.

Double-labeling experiments with Cys1-YFP and CFP-FYVE or Cys1-RFP and YFP-NtRab5 were not conclusive. Apparently, CFP-FYVE and YFP-NtRab5 expression prevented the formation of Cys1-YFP-labeled vesicles in U-73122 treated pollen tubes. The reason for this is unclear and need to be further investigated.

Although it has been suggested that DAG may be immediately phosphorylated to phosphatidic acid (PA) by a diacylglycerol kinase (DGK) and may not accumulate in plant cells (Meijer and Munnik, 2003), we visualized DAG in the plasma membrane of the pollen tube tips. Meijer and Munnik (2003) are of the opinion that in plants, a PI-PLC can be considered as ultimately generating PA and InsP₃.

However, our attempts to visualize PA in tobacco pollen tubes using a YFP fusion to the mammalian Raf1, which is known to directly interact with PA, were unsuccessful. Raf1 is a serine/threonine kinase and an essential component of the MAPK cascade. The PA-binding region of Raf1 is embedded in its kinase domain and contains three highly conserved cationic residues (Gosh *et al.*, 1996; Rizzo *et al.*, 2000). The GFP-PABR construct was a kind gift of Dr. Guillermo Romero (University of Pittsburgh, USA) and was cloned behind the lat52 promoter into a pollen-specific expression vector. The resulting construct comprised the amino acid residues 390 to 426 of mammalian Raf1 and was carrying the YFP-tag at its NH₂-terminus. Although recombinant Raf1 was shown to

bind PA *in vitro* (Gosh *et al.*, 1996) and to label endosomes in rat fibroblasts that over-expressed the human insulin receptor (HIRcB cells), it was not possible to visualize PA *in vivo* in pollen tubes of *Nicotiana tabacum*. The labeling remained always cytosolic (data not shown).

3 DISCUSSION

3.1 Identification of a novel pollen-specific protein that interacts with Nt-Rac5

Our intention in the present work was to identify a plant-specific guanine nucleotide exchange factor (GEF) in a yeast two-hybrid screen using a dominant negative mutant of the Rac/Rop GTPase Rac5 from *Nicotiana tabacum* as bait. When expressed in cells, dominant negative (DN) mutants of small GTPases are unable to interact with downstream targets of these proteins and are thought to bind specific GEFs in a “dead-end” complex, thereby preventing the activation of the endogenous Nt-Rac5 (see INTRODUCTION).

Based on the identification of dominant inhibitory mutant versions of mammalian and yeast Ras and Rac proteins, which contained single amino acid exchanges at RasS¹⁷N, RasS¹⁵A, RasD¹¹⁹N and Rac1T¹⁷N, respectively (Cool *et al.*, 1999; Feig, 1999; Debreceni *et al.*, 2004), we generated a corresponding DN mutant for the tobacco Nt-Rac5 by site-directed mutagenesis, Nt-Rac5 T²⁰N. The mutant is known to exhibit reduced Mg²⁺ binding capacity and therefore to remain in the GEF-GTPase intermediate conformation.

We identified a single protein that interacts with the DN-Nt-Rac5 mutant in a yeast two-hybrid screen. This protein comprises only 76 amino acid residues and does not show sequence similarity to characterized proteins. Nevertheless, homologies existed between hypothetical proteins from *Arabidopsis* and rice. Therefore, we termed the identified protein the tobacco hypothetical protein number 1 (Nt-Hypo1).

There are different types of mammalian Rho GEFs, which share only little or no sequence homology with each other and which were identified based on nucleotide exchange reactions *in vitro* or on over-expression studies *in vivo*. In order to biochemically verify whether Nt-Hypo1 is a plant-specific Rho GEF, we aimed at developing a protocol to assay the GTPase activity of Nt-Rac5 based on a method by Self and Hall (1995). However, it turned out to be difficult to determine the intrinsic GTPase activity of Nt-Rac5, because different experiments yielded variable results. Therefore, GEF assays have not been performed to date.

3.1.1 Transient over-expression of Nt-Hypo1 does not affect tobacco pollen tube growth or morphology

If Nt-Hypo1 had Rho GEF activity we would have expected an alteration of pollen tube morphology after transient expression of the protein in tobacco pollen tubes. As GEFs promote the GDP to GTP exchange at GTPases and lead to their activation, we would expect a constant activation of the Rac/Rop GTPases. Permanent activation as mimicked by the expression of constitutively active mutants of Rac/Rop GTPases, should lead to depolarized growth and to the formation of balloons at the pollen tube tip (compare Figure 3 e and Kost *et al.*, 1999; Li *et al.*, 1999).

Transient over-expression of Nt-Hypo1 in tobacco pollen tubes did not affect pollen tube growth or morphology. If Nt-Hypo1 may act in a multi-protein-complex, partner proteins were missing to ensure full activity of the complex. Possibly, Nt-Hypo1, which is a very small protein, does not function alone, but as part of a multi-protein complex, which may have Rho GEF activity.

3.1.2 Nt-Hypo1 accumulates in the cytosol of growing pollen tubes

Nt-Hypo1 was identified as an interactor of the DN mutant of the small GTPase Nt-Rac5, which associates with the plasma membrane at the pollen tube tip via its post-translationally prenylated COOH-terminus.

Transiently expressed YFP-Nt-Hypo1 fusion proteins in tobacco pollen tubes might have been expected to show a similar intracellular localization as Nt-Rac5. However, low expressing tobacco pollen tubes showed a diffuse cytoplasmic localization of YFP-Nt-Hypo1, whereas high expressing pollen tubes and pollen tubes ten to twelve hours after germination contained small fluorescent aggregates. The tendency of Nt-Hypo1 to form aggregates when over-expressed might indicate that at endogenous expression levels Nt-Hypo1 is part of a multi-protein or multi-enzyme complex.

3.1.3 Interaction of Nt-Hypo1 with Nt-Rac5 cannot be visualized *in vivo*

YFP fused to Nt-Hypo1 showed only cytoplasmic labeling, possibly because the amount of endogenous Nt-Rac5 was not sufficient to tether over-expressed Nt-Hypo1 to the membrane. Therefore, we transiently and simultaneously co-expressed YFP-Nt-Hypo1 with wild-type or CA and DN mutant forms of Nt-Rac5.

However, even under these conditions Nt-Hypo1 did not accumulate at the plasma membrane. Thus, we have been unable to show interaction of Nt-Hypo1 with Nt-Rac5 *in vivo*, possibly, because the two proteins bind to each other only relatively weakly.

3.1.4 Nt-Hypo1 interacts with Nt-Rac5 *in vitro*

The interaction of the two proteins Nt-Hypo1 and DN-Nt-Rac5 observed in yeast two-hybrid assays could not be verified *in vivo* by transient co-over-expression experiments. Therefore, it was important to demonstrate the protein-protein interaction *in vitro* by pull-down experiments. Recombinant Nt-Hypo1 as well as wild-type and mutant Nt-Rac5 were over-expressed in *E. coli* and tested for *in vitro* interaction. In these experiments, Nt-Hypo1 interacted with all three versions of Nt-Rac5, *i.e.* the wild-type, the constitutive active and the dominant negative mutant, although the stronger interaction was observed with the constitutively active form.

For reasons that are unclear at this time, these data are inconsistent with the result obtained in two-hybrid assays. Additional experiments are required to sort out the discrepancies between these two sets of data. *In vitro* interaction experiments should be performed using recombinant Nt-Rac5 that has been loaded with GDP or GTP, or that was treated with aluminum tetrafluoride, AlF_4^- , to lock it in the transitional GDP-bound conformation (Vincent *et al.*, 1998; Wu *et al.*, 2000). Such experiments would be more sensitive and should allow a more reliable characterization of the *in vitro* interaction between Nt-Hypo1 and DN-Nt-Rac5.

3.1.5 Effects of Nt-Hypo1 gene-knockdown

Inhibition of gene expression and specific gene-knockout has emerged as a powerful genetic tool in the past years. The identification and description of specific protein functions through loss-of-function mutants was employed extensively to elucidate various signaling pathways. The generation of loss-of-function mutant plants for Nt-Hypo1 was employed to gain information about its role in the tip-growing pollen tube as over-expression experiments were not informative (see above). Several strategies were employed to selectively inhibit Nt-Hypo1 gene expression.

First, we applied antisense oligodeoxynucleotides (ODNs), which were designed complementary to mRNA sequences encoding Nt-Hypo1 and other potentially pollen tube

proteins (*e.g.* Nt-Rac5). Antisense ODNs are thought to interfere with genetic information at various levels, such as transcription, mRNA stability in the cytoplasm and translation (Moutinho *et al.*, 2001). None of the antisense ODNs tested, had an effect on pollen tube growth or morphology, not even those targeted at Nt-Rac5 expression, which is essential for pollen tube elongation. Apparently, published protocols for ODN delivery into pollen tubes did not work in our hands or the ODNs used failed to down-regulate expression of the target gene.

Similar considerations are true for the *A. thaliana* line with a T-DNA insertion into the promoter region of a gene encoding an Nt-Hypo1 homologue. Pollen tube growth, morphology and fertilization were not affected in this T-DNA insertion line. However, we have not determined whether the expression of the Nt-Hypo1 homologue was in fact down-regulated in this line.

Effects of Nt-Hypo1 gene-knockout by RNA interference were studied more in detail, but still have to be considered as preliminary data. Tobacco plants were stably transformed with a construct encoding an intron-spliced hairpin RNA designed to specifically knock out the expression of Nt-Hypo1. Heterozygous F₁ pollen tube growth *in vitro* was subjected to histochemical GUS stainings to identify tubes containing the T-DNA insertion. Determination of the pollen tube length showed a significant growth reduction of transgenic pollen tubes in three of six tested lines. After selfing of heterozygous plants, all Nt-Hypo1 RNAi lines showed segregation of the T-DNA insertions insensitive at a 3:1 (resistant:sensitive for BASTA) ratio in the next generation. In a few cases, the ratio was even higher, which indicated the presence of multiple insertions in these lines. Only one transgenic tobacco line, 249-15-2, showed a segregation ratio of 1:2, which might indicate a defect in fertilization. Back-crossing of heterozygous RNAi plants as pollen donor to wild-type female plants were performed in one case (249-14-2) and resulted in 1:1 segregation in the next generation.

At this time we do not know if the expression of Nt-Hypo1 is down-regulated or completely abolished in the transgenic lines. Although, pollen tube growth was retarded in three of six tested primary lines *in vitro*, we can only state that pollen tube growth, morphology and fertilization were not affected *in vivo* based on results achieved after self progeny, but at this point we do not know if this might be true for plants in which Nt-Hypo1 is completely knocked-out.

3.1.6 Nt-Hypo1 interacts with several pollen tube proteins

Because of its specific interaction with DN-Nt-Rac5 in yeast two-hybrid assays, we considered it likely that Nt-Hypo1 might be a Rho GEF. However, the results obtained from over-expression of Nt-Hypo1 in pollen tubes and of the interaction studies *in vitro* did not support this hypothesis. It is possible, particularly considering the small size of the protein, that Nt-Hypo1 does not act alone, but as part of a larger complex.

Rho GEFs in other organisms were also described to be part of multi-protein complexes or to be only fully active when interacting with a second protein as in the case of DOCK180 and ELMO1 (see INTRODUCTION). In order to identify proteins that may be part of a GEF complex in pollen tubes, we performed a yeast two-hybrid screen using Nt-Hypo1 as bait.

The results of this screen will only be discussed very briefly here. It has to be considered that the information about identified proteins represents only preliminary data, *i.e.* all five identified proteins are truncated and we are dealing with single domains. Therefore, YFP fusions for subcellular localization studies are only performed with partial coding sequences and also further confirmations of protein-protein interactions by *e.g. in vitro* pull-down assays are still missing.

In the yeast two-hybrid screen Nt-Hypo1 was two times identified as an interactor with itself, which indicates that it might form homodimers. Five additive polypeptides were identified in the screen, which interact specifically with Nt-Hypo1, as confirmed in re-transformation assays (Chapter 2.1.6).

A truncated pectin esterase family protein, equivalent to pectin methylesterases (PMEs), was identified as a weak interactor of Nt-Hypo1. PMEs are ubiquitous cell wall enzymes and catalyze the demethylesterification of cell wall polygalacturonans and thereby modify the cell wall composition. PMEs consist of several domains and may encode so-called pre-proteins (Micheli, 2001). The identified clone 12-F comprises only a region of the mature protein, *i.e.* the pro-PME region, which is usually secreted to the apoplast. PMEs are shown to be localized in the apical pollen tube cell wall and to be mainly involved in enhancing pollen tube growth in the style and transmitting tract tissues (Wakeley *et al.*, 1998; Bosch *et al.*, 2005; Jiang *et al.*, 2005). However, it has to be considered that PMEs are expressed in abundance in pollen tubes and have already been identified in screens with other proteins (unpublished). Therefore, this result has to be considered with great caution as it may still be possible, that PMEs interact unspecifically with several proteins in the

cell.

Another positive interactor, which strongly binds to Nt-Hypo1 in yeast, shows sequence similarity to an *A. thaliana* phosphate translocator-related protein. This interaction is very peculiar, as phosphate translocator-related proteins are mostly described in mature chloroplasts (Fischer *et al.*, 1994; Knappe *et al.*, 2003). However, two classes of phosphate translocator-related proteins in vascular plants are described in the literature, which catalyze the uptake of phosphorus into living cells. Usually, the uptake occurs as a high-affinity Pi:H⁺ symport via a strict 1:1 counter exchange or as a low-affinity H⁺/Pi co-transport (Daram *et al.*, 1999). It has to be considered that these transports only have been described for roots and shoots and not for pollen tubes so far.

The third identified interactor with Nt-Hypo1 is another hypothetical protein with homologies to an *A. thaliana* hypothetical protein. In order to elucidate the function of Nt-Hypo1, the identification of further hypothetical proteins complicates the present work. Additionally, the *in vivo* subcellular localization of this hypothetical protein is also not convincing as it accumulated in the cytosol and the nucleus and this interactor therefore was of minor interest for the functional analysis of Nt-Hypo1.

The fourth interactor, instead, is a very interesting protein, as it shows sequence homology to a C2 domain-containing protein. The YFP fusion to the partial sequence of the protein after transient expression in pollen tubes resulted in a membrane association and surprisingly, it was not distributed all over the plasma membrane, but restricted to an area in close vicinity to the vegetative nucleus, several micrometers apart from the pollen tube apex. C2 domains are known as Ca²⁺/phospholipid-binding domains, which are present in several proteins. They were first described in protein kinase C, but are now also identified in PI-PLCs (see INTRODUCTION), PLDs or PI 3-kinase (Kopka *et al.*, 1998b). C2 domains mediate the Ca²⁺-dependent translocation of soluble proteins to membranes and the Ca²⁺- and phospholipid-dependent activation of enzymes (Essen *et al.*, 1996; Kopka *et al.*, 1998b). If Nt-Hypo1 and the identified C2 domain containing protein would also interact *in vivo*, it would be interesting if the C2 domain may mediate the membrane association of Nt-Hypo1. The reason for this spatially restricted membrane association still remains unclear. Compared to the membrane association of proteins involved in pollen tube tip growth, as *e.g.* the Rac/Rop GTPases or PH domain-containing proteins (Kost *et al.*, 1999), which are predominantly localized at the plasma membrane in the pollen tube apex, this protein was localized to an area of the pollen tube, which has not been further characterized.

The fifth and last interactor of Nt-Hypo1 identified in this screen is a pollen-specific protein, which shows highest similarity to already described pollen-specific proteins from tobacco, *A. thaliana* or *Brassica napus*. The tobacco pollen-specific protein was named Ntp303 and identified as a 69 kDa protein that belongs to the class of the late pollen-specific genes (Wittink *et al.*, 2000). Ntp303 is thought to function in the construction of membranes or the cell wall of pollen grains and pollen tubes, as well as in the polar organization of the cytoskeleton and in specific signaling events between the pollen tube and the pistil (Wittink *et al.*, 2000; de Groot *et al.*, 2004). GTP-binding sites as well as phosphorylation sites are predicted for Ntp303, additionally to the NH₂-terminal transit peptide, which might be related to its location at the cytoplasmic face of the membranes, where it might perform anchoring functions. Transgenic tobacco plants have already been generated, in which the Ntp303 gene is down-regulated. *In vitro* pollen tube growth was not affected by gene silencing, but the pollen tubes showed slower growth *in vivo* and arrested before they reached the ovary, so that fertilization failed (de Groot *et al.*, 2004).

The yeast two-hybrid screen verified that Nt-Hypo1 interacts with other proteins in the cell and supports the hypothesis that it may act in a multi-protein complex. Nevertheless, the five identified binding partners described above are proteins with very divergent functions and subcellular localizations. PME is thought to be restricted to the pollen tube apex, whereas the identified C2 domain containing protein exclusively localized to the pollen tube flanks and others were visualized in small aggregates in the pollen tube. Therefore, it has to be considered with great caution if most of these interactions might take place *in vivo*.

In addition, the interaction of Nt-Hypo1 with the pollen-specific protein Ntp303, which did also not show alterations in pollen tube growth or morphology *in vitro*, might be an interesting interactor and may suggest that Nt-Hypo1 might comprise similar functions in pollen tube growth in the style or in fertilization as Ntp303.

However, further experiments are required (*e.g.* co-over-expression experiments) to determine which, if any, of the proteins functionally interacts with Nt-Hypo1 in pollen tubes. This hypothesis has to be proved in further experiments and also through description of the previously mentioned Nt-Hypo1 RNAi plants. For this purpose, it is of major importance to identify full-length cDNAs encoding these proteins (*e.g.* by 5' RACE PCR) and to generate XFP fusion constructs as well as over-expression constructs for transient expression in tobacco pollen tubes, and to over-express the protein in bacteria followed by

in vitro pull-down assays. Another aspect would be to repeat the complete yeast two-hybrid screen and thereby on the one hand prove the interactions by obtaining the same protein interactors as before and on the other hand expand the screen to new binding partners.

3.1.7 Note added in proof

Nt-Hypol was shown to be a pollen-specific protein that interacted on the one hand with the low molecular weight GTPase Nt-Rac5, on the other hand with several divergent proteins. The putative loss-of-function in transgenic tobacco plants did not alter pollen tube growth or morphology, therefore, it might be concluded that Nt-Hypol may not be essential for polarized pollen tube growth *in vitro*. It may be involved in signal perception during *in vivo* pollen tube growth, guidance or fertilization. Although several different, independent experiments have been performed, its function could not be determined in the present work.

Furthermore, while I was preparing this thesis, a publication described the identification, cloning and functional analysis of plant-specific Rac/Rop GEFs (Berken *et al.*, 2005). Berken *et al.* (2005) performed a yeast two-hybrid screen with a dominant negative mutant (D¹²¹N) of Rop4 (= AtRac5), which was not able to bind nucleotides. Their intention was to identify plant-specific Rho GEFs and indeed, they identified proteins acting as plant-specific Rho GEFs in GTPase assays *in vitro*. However, no sequence homology could be detected to known Rho GEFs of the DH-PH type or DOCK180-related proteins (Berken *et al.*, 2005). Furthermore, in deletion mutant experiments they showed that the three conserved domains found in the newly identified plant proteins, the C1, C2 and C3 domains, also referred to as PRONE for plant-specific Rop nucleotide exchanger, are the minimal structural unit for the nucleotide exchange. PRONE was only active on Rop members of the family of small Rho GTPases and stimulated nucleotide dissociation from AtRop4 a thousand times and was shown to form a tight complex with nucleotide-free AtRop4 (Berken *et al.*, 2005).

Another publication described the identification of a protein, the Kinase partner protein (KPP), which is highly homologous to the plant-specific Rho GEFs identified by Berken *et*

al. (2005). Interestingly, the group was not aware of the fact that they were dealing with a guanine nucleotide exchange factor (GEF; Kaothien *et al.*, 2005). They obtained this protein as an interactor of two pollen-specific receptor kinases from tomato in a yeast two-hybrid screen and focused on the interaction of KPP with the pollen-specific receptor kinases and on its transient and stable expression in tobacco and tomato pollen tubes, respectively. Transient as well as stable over-expression of KPP in pollen tubes resulted in depolarized growth, showing the characteristic bulging of the pollen tube apex, which was not achieved by transiently over-expressing Nt-Hypo1 in pollen tubes. Stable transformation of tomato plants with KPP, additionally, resulted in reduced transmission of the gene in self-progeny caused by altered pollen tube growth and a subsequent reduced fertilization.

Both publications together give a very detailed and interesting overview about the plant-specific Rac/Rop GEF family. They performed a convincing *in vivo*, *in situ* and *in vitro* functional analysis of yeast two-hybrid interactors, which in turn resulted to be plant-specific GEFs. These two publications confirm that our attempt to identify a tobacco pollen-specific Rho GEF through a yeast two-hybrid screen using the DN-Nt-Rac5 as bait, was well thought. Although, we could not show Nt-Hypo1's GEF activity *in vitro* or *in vivo* to date, it might still be possible that it acts as a plant-specific Rho GEF in a multi-protein complex. Nevertheless, it may be advisable to perform another yeast two-hybrid screen and substitute the Nt-Rac5 T²⁰N, which interferes with Mg²⁺ binding, by the dominant negative mutant used in the screen performed by Berken *et al.* (2005), in which the nucleotide binding was completely abolished.

3.2 Identification of two novel phosphoinositide-specific phospholipases C from *Nicotiana tabacum*

Phospholipases constitute a diverse group of enzymes that are classified into different subfamilies, such as PLA₁, PLA₂, PLB, PLC or PLD, based on the site of hydrolysis on phospholipids (Figure 34). Each class is further divided into subfamilies based on sequence analyses, biochemical properties or a combination of both (Wang, 2001). Phospholipids do not only provide the backbone of biomembranes, but they serve at the same time as sources for signaling messengers. The activity of phospholipases does not only affect the stability of the membranes, but also regulates cellular functions. Thus, the activation of phospholipids is often an initial step in generating lipids and lipid-derived second messengers (Munnik *et al.*, 1998; Wang, 2001; Laxalt and Munnik, 2002).

The present work has focused on plant members of the subfamily of phosphoinositide-specific phospholipases C (PI-PLCs), which constitute a separate class of these enzymes and resembles most closely the mammalian δ and ζ PI-PLCs (Rhee and Bae, 1997; Saunders *et al.*, 2002).

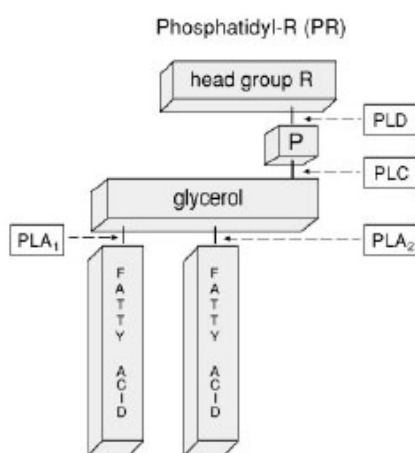


Figure 34: Structure, hydrolysis and names of the common phospholipids. General structure of a phospholipid: two fatty acyl chains esterified to a glycerol backbone, a phosphate, creating the phosphatidyl moiety, to which a variable headgroup (R) is attached. The positions that are subject to phospholipase activity are also indicated. (From Meijer and Munnik, 2003.)

Most of the function and/or regulation of PI-PLCs is known from investigations in the animal kingdom. PI-PLCs are known to hydrolyze the glycerophosphate ester linkage of phospholipids as a response to intra- or extracellular stimuli and thereby constituting the first step of a cellular signal transduction cascade. Hydrolysis of the phospholipid phosphatidylinositol 4,5-bisphosphate (PI-4,5-P₂) by a PI-PLC generates two second messengers, inositol 1,4,5-trisphosphate (InsP₃) and diacylglycerol (DAG). DAG remains associated with the plasma membrane and activates a protein kinase C in animal cells, whereas InsP₃ diffuses to the cytosol and releases Ca²⁺ from intracellular stores, such as the

vacuole or the endoplasmic reticulum: The control of cytoplasmic Ca^{2+} levels by the PI-PLC/InsP₃ pathway is a prominent signaling element known to regulate numerous important processes in eukaryotic cells (reviewed in Munnik *et al.*, 1998; Meijer and Munnik, 2003).

3.2.1 NtPLC3 and NtPLC4 are plant-specific PI-PLC isoforms from *N. tabacum*

Two full-length cDNAs encoding novel *N. tabacum* PI-PLC isoforms, NtPLC3 and NtPLC4, were identified by cDNA library colony hybridization using a homologous probe. Both isozymes are of the same length, they comprise 588 amino acid residues. They show significant sequence similarity to previously cloned plant PI-PLCs and contain invariant amino acid residues involved in catalysis or substrate recognition. These residues have been identified by Essen *et al.* (1996), who revealed the three-dimensional structure of a deletion variant of mammalian PI-PLC δ_1 (Δ 1 to 132). Ellis *et al.* (1998), instead, analyzed the activity of the same enzyme after introducing twenty different point mutations in the active site or hydrophobic ridge. The strict conservation of key residues in the active site of NtPLC3 and NtPLC4 suggests that these two enzymes use the same mechanism for substrate recognition and catalysis as other eukaryotic PI-PLCs.

3.2.2 NtPLC3 is a pollen-specific PI-PLC isoform

Numerous publications describe the tissue-specific expression of plant PI-PLCs. The *Arabidopsis thaliana* genome encodes nine putative PI-PLC genes, whose expression patterns have been studied by Hirayama *et al.* (1995 and 1997) and Hunt *et al.* (2004). AtPLC1S is organ-specifically expressed in vegetative tissue, *e.g.*, stems, leaves and roots, but hardly detectable in reproductive organs, such as siliques (Hirayama *et al.*, 1995). In contrast, AtPLC2 is expressed predominantly in the vascular tissue of all organs. These two isozymes differ from each other in the regulation of their expression pattern. AtPLC2 is constitutively expressed, whereas AtPLC1S is induced in response to environmental stresses, such as drought or salinity (Hirayama *et al.*, 1997).

Interestingly, all three identified *Solanum tuberosum* isoforms are constitutively expressed in all tissues, with the exception of StPLC1 which is absent from tubers (Kopka *et al.*, 1998a). Of the two known *Nicotiana rustica* PI-PLC isoforms, both are expressed in leaf

epidermal cells, but only one is expressed in guard cells (Pical *et al.*, 1997). Obviously, different plant PI-PLC isoforms are expressed in distinct cell types at various levels, which may indicate that they are functionally divergent.

In contrast to all other plant PI-PLCs investigated so far, which are all expressed in several different tissues, NtPLC3 is exclusively expressed in pollen and pollen tubes. Our initial attempts to clone new PI-PLC isoforms expressed in *N. tabacum* pollen tubes, based on PCR, have indicated that several isoforms must be present in these cells.

To initiate the functional characterization of the different PI-PLC isoforms in tobacco pollen tubes, we have investigated the role, which NtPLC3 plays during the polarized growth of these cells.

3.2.3 NtPLC3 hydrolyzes PI-4,5-P₂ *in vitro*

Before we addressed the question of the intracellular localization and *in vivo* function of NtPLC3 in pollen germination or pollen tube elongation, it was of major interest to ascertain that the cloned NtPLC3 cDNA encodes a functional enzyme.

Previous publications described an inactive PI-PLC isoform from pea, which failed to hydrolyze PI-4,5-P₂ *in vitro* (Venkataraman *et al.*, 2003). Also at least two *A. thaliana* genes have been indentified, which are thought to encode inactive PI-PLCs (AtPLC8 and AtPLC9). Their Y domains contain substitutions of several amino acids known to be essential for catalytic activity (Mueller-Roeber and Pical, 2002; Hunt *et al.*, 2004).

The capacity of recombinant NtPLC3 to hydrolyze [³H]PI-4,5-P₂ and to generate the second messenger InsP₃ was determined in a sodium cholate/PI-4,5-P₂ mixed micelle assay in the presence of different Ca²⁺ concentrations. The hydrolytic product of NtPLC3 was measured by liquid scintillation counting based on radio-labeled isotope release into the aqueous phase. Using this assay, it was shown that NtPLC3 hydrolyzed [³H]PI-4,5-P₂ in a Ca²⁺-dependent manner. NtPLC3 showed highest catalytic activity at a Ca²⁺ concentration of 500 μM free Ca²⁺ and much lower at 1000 μM Ca²⁺. Compared to the intracellular Ca²⁺ concentration in pollen tubes (0.1 to 10 μM) and to the Ca²⁺ dependence of other plant PI-PLCs, a requirement for 500 μM free Ca²⁺ for maximal activity is extraordinarily high. Most identified plant PI-PLCs reach their activity maximum at a concentration of 1 μM to 10 μM free Ca²⁺ (Kopka *et al.*, 1998a; Staxén *et al.*, 1999; Otterhag *et al.*, 2001; Coursol *et*

al., 2002). Only in one case, 100 μM Ca^{2+} was reported to be the optimal concentration for activity of a soybean PI-PLC (Shi *et al.*, 1995).

Clearly, NtPLC3 requires considerable higher levels of free Ca^{2+} for maximal activity than all other plant PI-PLCs characterized to date. So far we do not have an explanation for this observation. However, the optimal Ca^{2+} concentration for NtPLC3 activity is significantly lower than that of a class of non-membrane associated PI-PLCs, which has been described in the literature. These soluble PI-PLCs require Ca^{2+} concentrations in the millimolar range for maximal activity and preferentially hydrolyze PI (Mueller-Roeber and Pical, 2002).

NtPLC3 does not only differ from other plant PI-PLCs in its Ca^{2+} requirement, but also in its rate of PI-4,5- P_2 hydrolysis. It has been determined in several independent experiments that NtPLC3 hydrolyzes approximately 0.749 $\text{nmol} \cdot \text{min}^{-1}$ per mg protein at a Ca^{2+} concentration of 10 μM . This value is more than 300 times lower than the one detected for example for the *N. rustica* PI-PLC (Staxén *et al.*, 1999). Not only differences in the hydrolytic activity of various PI-PLCs, but also distinct assay protocols are likely to have contributed to these inconsistencies and make it even more difficult to compare one PI-PLC with the other. Staxén *et al.* (1999), *e.g.*, employ a different assay composition, which contains 1.5 mg MgCl_2 . MgCl_2 has been reported to increase the hydrolytic activity of PI-PLCs in wheat plasma membranes and of recombinant potato PI-PLCs in the presence of Ca^{2+} (Melin *et al.*, 1992; Pical *et al.*, 1992; Kopka *et al.*, 1998a), although it had no effect on a recombinant soybean PI-PLC (Shi *et al.*, 1995). In addition, Staxén *et al.* performed activity assays at 37°C, whereas we assayed the hydrolytic activity at 25°C. Interestingly, both groups were working with plant PI-PLCs and plant-specific enzymes are supposed to have a temperature optimum close to the environmental temperature. 37°C is an extremely high value, but might be closer to the temperature optimum of the *N. rustica* PI-PLC and thereby result in higher enzyme activity. In contrast to Staxén *et al.* (1999), we included the ionic detergent sodium deoxycholate in our assay mixture, a component, which was also reported to increase the hydrolytic activity of wheat plasma membrane PI-PLCs 4- to 5-fold at a concentration of 0.02 to 0.025 % (Pical *et al.*, 1992).

A direct comparison of the hydrolytic activity of different plant PI-PLCs based on the published results is difficult, because the protocols employed to assay the enzyme activities vary considerably from group to group. In any case, our results demonstrate that NtPLC3 hydrolyzes PI-4,5- P_2 *in vitro* in a Ca^{2+} -dependent manner, with an optimum at 500 μM free Ca^{2+} .

Although the Ca^{2+} -optimum of NtPLC3 was determined to be 500 μM , the enzyme activity of inhibitor treated or mutant NtPLC3 were assayed at 10 μM Ca^{2+} , which resembles more closely the intracellular concentration of the metal in pollen tubes and was chosen according to other published assay protocols (Drøbak *et al.*, 1994; Staxén *et al.*, 1999; Kovar *et al.*, 2000; Coursol *et al.*, 2002).

Two point mutations, H¹²⁴A and D¹⁵⁶R, individually and in combination, were introduced into the active site of NtPLC3. Both mutations affected residues predicted to be essential for enzyme activity (Essen *et al.*, 1996; Ellis *et al.*, 1998). Our results show that each of these mutations abolished the catalytic activity of NtPLC3. H¹²⁴A is thought to predominantly reduce the catalysis rate, whereas D¹⁵⁶R should result in a higher Ca^{2+} requirement for the catalysis of PI-4,5-P₂. Both single mutants and the double mutant showed a significantly reduced hydrolytic activity compared to the wild-type enzyme and were essentially inactive.

The PI-PLC antagonist U-73122 inhibited NtPLC3's activity in a concentration-dependent manner. U-73122 was identified in the mid to late 1980's as an aminosteroid, which selectively inhibited PI-PLC-dependent processes in human platelets and neutrophils (Bleasdale *et al.*, 1990; Smith *et al.*, 1990). It was subsequently employed in the evaluation of the role of PI-PLCs in cell activation and Ca^{2+} mobilization. Nevertheless, its mechanism of action or specific molecular target is still not clear to date.

Smith *et al.* (1990) found that significantly higher doses of the inhibitor were necessary to suppress PI-PLC activity *in vitro* than to inhibit Ca^{2+} mobilization under the same conditions, indicating that U-73122 might affect Ca^{2+} channels. Molecular targets of U-73122 others than PI-PLCs were also identified in some mammalian cell types, including a histamine H₁ receptor (Hughes *et al.*, 2000) and a 5-lipoxygenase (5-LO; Feißt *et al.*, 2005). 5-lipoxygenase is a key enzyme in the biosynthesis of leukotrienes in animal cells, which are important mediators of inflammatory and allergic reactions. *In vitro* experiments revealed that U-73122 potently inhibited 5-LO at concentrations much below those needed for PI-PLC inhibition ($\text{IC}_{50} = 1.8 \mu\text{M}$ U-73122; Feißt *et al.*, 2005).

Nevertheless, apart from putative other molecular targets, U-73122 was shown to inhibit PI-PLC activity in dose-response experiments *in vitro*, confirming that it is a direct PI-PLC inhibitor (Staxén *et al.*, 1999; Coursol *et al.*, 2002; Hou *et al.*, 2003; Feißt *et al.*, 2005).

Interestingly, significantly high concentrations of U-73122 are required to inhibit the activity of NtPLC3 *in vitro*, compared to lower concentrations sufficient to affect pollen tube growth *in vivo*. Whereas pollen germination is effectively blocked at 10 μM U-73122, a concentration of 80 μM is required to abolish the activity of NtPLC3 *in vitro*. Similar observations were made previously, whenever the sensitivity towards U-73122 of PI-PLC activity *in vitro* was described (Staxén *et al.*, 1999; Coursol *et al.*, 2002; Apone *et al.*, 2003).

The discrepancy noticed for NtPLC3 is not unique. It has been reported several times that enzyme specificities do not always correlate between *in vivo* and *in vitro* assays (Williams *et al.*, 2005). These observations have been explained by the fact that recombinant enzymes assayed *in vitro* may display different specificities when purified from heterologous expression systems and they might also lead to conflicting results in distinct assays (Mueller-Roeber and Pical, 2002; Ercetin and Gillaspay, 2004). Drøbak and Heras (2002) are of the opinion that the presentation of lipid substrates, in our case the PI-4,5-P₂, to the enzyme of interest, the NtPLC3, may differ substantially from the *in vivo* situation, which may contribute to a reduced sensitivity of recombinant enzymes towards inhibitors.

In our experiments, U-73122 was shown to inhibit PI-4,5-P₂ hydrolysis by NtPLC3 in a concentration-dependent manner, with an IC₅₀ = 17.5 μM and complete inhibition at 80 μM . These values are similar to those reported for other plant PI-PLCs (Staxén *et al.*, 1999; Coursol *et al.*, 2002), although most animal PI-PLCs are more sensitive to the drug (IC₅₀ ~ 6 μM ; Hou *et al.*, 2003).

A closely related inactive analogue of U-73122, U-73343, has widely been used as a negative control that fails to block agonist induced Ca²⁺ mobilization (Bleasdale *et al.*, 1990). Only a small modification, the substitution of the pyrrolidindione with pyrroledione, makes the difference and results in inefficient inhibition of PI-PLCs. PI-PLCs of *Nicotiana rustica* and *Digitaria sanguinalis* were shown to be insensitive to U-73343 (Staxén *et al.*, 1999; Coursol *et al.*, 2002). Interestingly, in our *in vitro* assays, U-73343 actually stimulated PI-4,5-P₂ hydrolysis by NtPLC3. In several independent experiments, at 10 μM Ca²⁺ and a concentration of 100 μM U-73343, we measured an increase of activity of about 700 % compared to untreated NtPLC3 under the same assay conditions. To date, we do not have an explanation for this result, in fact, it is most surprising, because U-73343 did not have a detectable effect on pollen tube growth or morphology *in vivo* (see Figure 28) and is not mentioned in any other publication to date.

U-73343 was not supposed to have any effect on PI-4,5-P₂ hydrolysis by NtPLC3, whereas the addition of a recently identified specific PI-PLC activator was. 2,4,6-trimethyl-*N*-(*meta*-3-trifluoromethylphenyl)-benzenesulfonamide (*m*-3M3FBS), at a concentration of 50 μM, did neither result in any alteration of the hydrolysis rate of NtPLC3 *in vitro*, nor on pollen tube growth or morphology *in vivo* (data not shown).

The activity of mammalian PI-PLCs, in addition to its Ca²⁺ sensitivity, is mainly controlled by two mechanisms, one involving heterotrimeric G-proteins and the other based on tyrosine kinases. Heterotrimeric G-proteins as well as small GTPases are well-documented in plant cells, and also reports of tyrosine kinases in plants exist, but none of them has been directly been implicated in PI-PLC activation to date (Munnik *et al.*, 1998). Therefore, the regulation of plant PI-PLCs has widely been studied, but to date the mechanism or molecules that are involved in this process are still under debate (Munnik *et al.*, 1998).

Addition of the G-protein activator mastoparan or its active analogue, Mas-7, to carrot cell cultures resulted in a decrease of PIP or PI-4,5-P₂ and a subsequent increase in InsP₂ or InsP₃ (Cho *et al.*, 1995). Mastoparan also activated PI-PLCs and increased the InsP₃ concentration in *Chlamydomonas* as well as in soybean culture cells (Legendre *et al.*, 1993). As a negative control, addition of mastoparan to purified PI-PLCs *in vitro* did not affect their activity, suggesting that the activation of these proteins by mastoparan requires additional cellular factors, which were lost during membrane isolation. Over-expression of an *A. thaliana* G-protein coupled receptor (GCR1) in tobacco BY-2 cells resulted in an increase of PI-PLC activity and in the InsP₃ concentration (Apone *et al.*, 2003). Nevertheless, no direct evidence exists that PI-PLCs are activated by G-proteins, their activators or by nucleotides (Melin *et al.*, 1987; Munnik *et al.*, 1998; Jones and Assmann, 2004).

Recently, it has been speculated on the involvement of a protein tyrosine kinase in downstream activation of a PI-PLC, resulting in InsP₃ production in the hypersensitive response of lemon seedlings (Ortega *et al.*, 2005), but convincing data are still missing.

Because of the fact that no direct modulator of PI-PLC activity had been identified, neither for mammals nor for plants, a screen in human neutrophils was performed to identify synthetic compounds, which stimulate PI-PLC activity in these cells. *M*-3M3FBS, identified in this screen, was shown to trigger a transient increase in the intracellular Ca²⁺ concentration in neutrophils (Bae *et al.*, 2003). Furthermore, the drug demonstrated to

specifically activate mammalian PI-PLCs β_2 , β_3 , γ_1 , γ_2 and δ_1 . *M*-3M3FBS was neither isoform specific, nor cell-type specific and was counteracting with the aminosteroid U-73122. *M*-3M3FBS's activation mechanism is still not clear, but it stimulated PI-PLCs either in the presence or in the absence of Ca^{2+} .

Nevertheless, *m*-3M3FBS did not activate NtPLC3 *in vitro* and did not alter tobacco pollen tube growth or morphology *in vivo* in our experiments (data not shown). This suggests that plant-specific PI-PLCs must employ a mechanism of activation different from its mammalian counterparts.

3.2.4 Transient expression of NtPLC3 in pollen tubes of *Nicotiana tabacum*

3.2.4.1 Transient over-expression of NtPLC3 wild-type and mutant versions does not affect pollen tube growth

PI-PLCs are known to be key enzymes in signal transduction processes and the activation of PI-PLCs is one of the earliest responses downstream of receptor stimulation in animal cells (Rhee and Bae, 1997). The signaling role for PI-PLCs was established in the 1980s, when PI-PLC-mediated hydrolysis of PI-4,5-P₂ was discovered, which in turn was found to regulate Ca^{2+} mobilization and protein phosphorylation in mammalian cells (reviewed in Martin, 1998).

In plant cells, PI-PLC functions have been described mostly in the context of biotic or abiotic stress response. PI-PLCs are involved in stomatal closure and in the response to drought, cold, salinity or pathogen attack (Hirayama *et al.*, 1995; DeWald *et al.*, 2001; Sánchez and Chua, 2001; Kim *et al.*, 2004; Zhai *et al.*, 2005).

An involvement of PI-PLCs in polarized pollen tube growth has not been directly shown to date. However, several publications have hinted at possible functions of substrates and products of these enzymes in the control of this process. Stress responses of plant cells including changes in PI-PLC activity have only been determined indirectly by measuring changes in the phosphoinositide levels. PI-4,5-P₂ turnover was measured, *e.g.*, in response to the phytohormone ABA in the stomata of *Vicia faba* or after osmotic stress applied to *A. thaliana* cell cultures (Lee *et al.*, 1996; Pical *et al.*, 1999; DeWald *et al.*, 2001; Hunt *et al.*, 2004). After 15 minutes of salt-stress, an increase in InsP₃ production, followed by an increase in the intracellular Ca^{2+} concentration was noticed in *A. thaliana* cell cultures (DeWald *et al.*, 2001). Additionally, PI-4,5-P₂ and InsP₃ have been shown to play crucial

roles in modulating the tip-focused Ca^{2+} gradient, membrane secretion and cytoskeletal organization in pollen tubes of *Papaver rhoeas* or *Agapanthus umbellatus* (Franklin-Tong *et al.*, 1996; Malhó, 1998; Monteiro *et al.*, 2005). Therefore, PI-4,5-P₂ and InsP₃ are thought to play a key role in the maintenance of pollen tube polarity. Also, Potocký *et al.* (2003) have shown that exogenously applied phosphatidic acid (PA) stimulated pollen germination and pollen tube elongation. In plants, PA is thought to be a product of diacylglycerol kinase (DGK) by phosphorylation of DAG, immediately after the generation of DAG by PI-4,5-P₂ hydrolysis. Phosphatidic acid, is emerging as another important second messenger in plant cells, which might play a role in the intracellular membrane traffic (Munnik *et al.*, 1998). It was shown to promote the formation of nascent secretory vesicles and to maintain the structural integrity of the Golgi apparatus by regulating the production of inositol phospholipids (Potocký *et al.*, 2003). Monteiro *et al.* (2005) also investigated the role of PA in growing pollen tubes and showed that a reduction in the intracellular PA level using butan-1-ol resulted in bulging of the pollen tube apex and in the formation of thick, non-directional actin microfilament bundles.

Because substrates and products of PI-PLCs were shown to play crucial roles in pollen tube growth, we were interested in the intracellular function of NtPLC3 in pollen tube growth. Interestingly, over-expression of full-length wild-type or mutant versions of NtPLC3 had no effect on pollen tube growth or morphology. The over-expression of one PI-PLC isoform in tobacco did not lead to major intracellular changes in PI-4,5-P₂ levels (Figure 23), which could possibly have resulted in an alteration of growth.

This observation is in accordance with results obtained from Sánchez and Chua (2001). They induced the expression of AtPLC1 in transgenic *A. thaliana* plants by dexamethasone treatment, but although detecting increases in AtPLC1 transcripts, no increase in InsP₃ levels has been detected, *i.e.* no stimulation of PI-PLC activity. In addition, the increase in AtPLC1 expression in the absence of ABA was not sufficient to induce the expression of ABA-responsive genes in vegetative tissues. Sánchez and Chua concluded that AtPLC1 may be a latent enzyme that requires a Ca^{2+} signal for activation *in vivo* and that the PI-PLC plays a role in secondary ABA responses.

PI-PLC activity in pollen tubes/plant cells appears to be tightly controlled by upstream regulators. Interestingly, these regulators are not titrated out by over-expressed inactive NtPLC3 mutants, as indicated by the fact that such mutants do not have dominant negative

effects on pollen tube growth. Conceivably, the stimulation of pollen tube PI-PLC activity by upstream regulators somehow depends on PI-PLC activity (positive feedback loop?).

3.2.4.2 NtPLC3 is a plasma membrane-associated enzyme

Plant PI-PLCs of class II are predominantly plasma membrane-associated enzymes (Shi *et al.*, 1995; Otterhag *et al.*, 2001; Mueller-Roeber and Pical, 2002; Kim *et al.*, 2003) as shown primarily using biochemical methods. Shi *et al.* (1995) isolated a cDNA encoding an active PI-PLC from soybean by screening an expression library with an antiserum raised against total proteins purified from plasma membranes. They furthermore showed that this protein in transgenic tobacco plants was mostly associated with membranes, although it was also detected in the cytosol. Otterhag *et al.* (2001), raised an antibody against a synthetic peptide specific for the COOH-terminus of *A. thaliana* AtPLC2, which cross-reacted with a polypeptide of approximately 66 kDa. This protein was predominantly enriched in the plasma membrane. In 2004, Kim *et al.*, showed that GFP fused to *Vigna radiata* PI-PLC3 accumulated at the plasma membrane of transiently transfected *A. thaliana* protoplasts. Co-localization with RFP fused to a plasma membrane H⁺-ATPase supported this finding. Further investigations showed that deletion of the COOH-terminal C2 domain resulted in loss of its membrane-binding capacity and a uniform accumulation of Vr-PLC3 in the cytosol.

In our experiments, transiently expressed full-length NtPLC3 fused at the COOH- or NH₂-terminus to YFP, was associated with the plasma membrane at the flanks of growing pollen tubes. Only weak cytoplasmic staining was detectable. From that observation we conclude that similar to related plant PI-PLCs, NtPLC3 is a plasma membrane-bound enzyme. Interestingly, NtPLC3 is exclusively localized to the flanks and not to the tip of pollen tubes. The functional implications of this localization pattern will be discussed below.

3.2.4.3 EF hand-like domain and C2 domain are essential for membrane association

PI-PLCs comprise several distinct domains. Mammals and plants share at least three of these domains, *i.e.*, the catalytic X and Y domains and the COOH-terminal calcium- and lipid binding domain, the C2 domain (Mueller-Roeber and Pical, 2002). The EF hand, which is present in all mammalian isoforms, is either incomplete or completely lacking in

plant PI-PLCs. A PH domain, which is found at the NH₂-terminus of most mammalian PI-PLCs, is also absent from plant isoforms. The PH domain has been shown to be essential for membrane association of mammalian PI-PLCs. Because plant PI-PLCs are missing a PH domain, their membrane binding mechanism must differ substantially from the one in animals. In plants, the C2 domain and other putative hydrophobic moieties are thought to facilitate membrane anchorage (Mueller-Roeber and Pical, 2002).

Several plant deletion mutants have been expressed so far. Kim *et al.* (2004) showed that the C2 domain in *Vigna radiata* PI-PLC3 is essential for membrane binding (see above). Otterhag *et al.* (2001) also showed that the C2 domain of *A. thaliana* AtPLC2 is essential for lipid vesicle binding *in vitro*.

For NtPLC3, we generated several single- or multiple-domain deletion mutants as YFP fusions to test in transient expression experiments, which domains are required for membrane association of the full-length protein. The only fusion protein showing membrane binding in this experiment was a combination of EF hand and C2 domain. In this fusion protein we replaced the catalytic core of NtPLC3 by YFP, which comprises almost the same size. We thereby demonstrated that both, the NH₂-terminal EF hand and the COOH-terminal C2 domain are essential for NtPLC3 to be targeted to the plasma membrane. It is nevertheless surprising that the EF hand-like domain is substantially involved in membrane association of NtPLC3. EF hands are known to consist of a conserved Ca²⁺-coordinating loop of twelve amino acid residues flanked on each side by short α -helical domains. This conserved motif is found in several other plant proteins that play key roles in signal transduction pathways (Kopka *et al.*, 1998b), but has not been implicated in membrane interactions to date. In contrast, the C2 domain is well known to be responsible for membrane association of numerous proteins from animals or yeast. C2 domains interact with phospholipids in a Ca²⁺-dependent manner and mediate Ca²⁺-dependent translocation of soluble proteins to membranes (Kopka *et al.*, 1998b). Many C2 domains are sufficient to mediate the membrane association. However, the C2 domain of NtPLC3 differs in its composition from other C2 domains. As described in chapter 2.2.1, several conserved amino acid residues are missing in the C2 domain of NtPLC3. Of the four conserved residues required for calcium binding and Ca²⁺-mediated membrane association of animal C2 domains (Essen *et al.*, 1996), only one is present in NtPLC3. This may explain why the C2 domain of NtPLC3 alone fails to mediate membrane association in pollen tubes.

3.2.4.4 The catalytic core is responsible for the absence of NtPLC3 from the pollen tube tip

In contrast to full-length NtPLC3 fused to YFP, the EF hand-YFP-C2 fusion protein accumulated at the pollen tube plasma membrane in the flanks of the apex, but also at the very tip. This observation raised the question, whether the X and Y domains, which are missing in the EF-YFP-C2 fusion protein, have a function in keeping full-length NtPLC3 from binding to the plasma membrane at the tip.

To provide further evidence for this hypothesis, we made use of the well-described PH domain of the rat PI-PLC δ_1 . This PH domain is essential for membrane anchorage of rat PI-PLC δ_1 and can be used as a biosensor for PI-4,5-P₂ when fused to GFP (Stauffer *et al.*, 1998; Kost *et al.*, 1999). Kost *et al.* (1999) have shown that GFP fused to this PH domain (GFP-PI-PLC δ_1 -PH) accumulated at the plasma membrane in the extreme pollen tube tip.

Here we showed that attaching the XY catalytic domain of NtPLC3 to the NH₂-terminus of the YFP-PI-PLC δ_1 -PH fusion prevented this fusion from associating with the pollen tube plasma membrane at the very tip. The chimera X-Y-YFP-PI-PLC δ_1 -PH accumulated at the plasma membrane in the flanks, but not at the tip of the pollen tube apex.

We therefore investigated the role of the X and Y domains in membrane association. From *in vitro* enzyme activity assays we know that three different NtPLC3 mutant versions are inactive and do not hydrolyze PI-4,5-P₂. The transient expression of YFP fusions of these mutants, nevertheless, showed that even if the enzyme is not active, it does not localize to the plasma membrane of the pollen tube apex.

From these observations we conclude that the catalytic core of NtPLC3, independent of its catalytic activity, is responsible for the absence of full-length NtPLC3 from the plasma membrane at the very tip of pollen tubes. Either a mechanism exists, which retains full-length NtPLC3 at the pollen tube flanks or on the other hand, another mechanism exists, a force acting on the catalytic core, which must be even strong enough that it also unspecifically eliminates the PH domain of PI-PLC δ_1 from the tip, when fused to NtPLC3 X and Y domains.

3.2.5 PI-PLCs maintain pollen tube polarity and restrict PI-4,5-P₂ to the tip

The membrane-permeable PI-PLC inhibitor U-73122 was shown to inhibit pollen tube growth *in vivo* (Chapter 2.2.5). Dose-response experiments have shown that the appropriate inhibitor concentration was 5 μ M U-73122. At a concentration of 5 μ M U-73122, pollen tube growth was significantly reduced and balloons were formed at the pollen tube tip. Below this concentration, pollen tubes germinated well, but showed reduced growth. At concentrations higher than 5 μ M the majority of the pollen tubes did not germinate at all. The inactive analogue, U-73343, did not alter pollen tube growth or morphology.

Massive ballooning at the tip is likely to result from a depolarization of growth. Kost *et al.* (1999) showed that the over-expression of a constitutively active mutant of the small GTPase Nt-Rac5 also resulted in the formation of large balloons at the tip, caused by depolarized pollen tube growth (compare Figure 3e). Our experiments indicate that the inhibition of PI-PLCs by U-73122 also resulted in depolarized growth.

On the basis of the light microscopic results, we investigated effects of U-73122 treatment on the distribution of PI-4,5-P₂ in growing pollen tubes. Again, we made use of the PH domain of the mammalian PI-PLC δ_1 , which interacts specifically and with high affinity with PI-4,5-P₂ (Lemmon *et al.*, 2002) and can be used as an *in vivo* marker for this lipid (Chapter 1.3.3.5.1; Stauffer *et al.*, 1998; Kost *et al.*, 1999). Treatment of pollen tubes showing normal PI-4,5-P₂ distribution with U-73122 resulted in spreading of the PI-4,5-P₂ labeling to a larger area of the plasma membrane at the pollen tube tip. Apparently, PI-PLC inhibition led to PI-4,5-P₂ over-production and spreading, which in turn depolarized pollen tube growth. Based on this, we conclude that pollen tube PI-PLC activity prevents spreading of PI-4,5-P₂, which accumulates in the plasma membrane at the tip in a Rac GTPase-dependent manner (Kost *et al.*, 1999) and thereby maintains the polarity of cell expansion.

PI-4,5-P₂ has a multifaceted role within the cell. It is known to modulate the activity of cytoskeleton-associated proteins, such as villin (Panebra *et al.*, 2001), ADF (Allwood *et al.*, 2002) or profilin (Drøbak *et al.*, 1994). It also regulates signaling proteins, such as PLD, ARF, ARF GTPase activating proteins and ARF GEFs (DeWald *et al.*, 2001) and vesicle-trafficking proteins. Additionally, it can be hydrolyzed to form the second messengers InsP₃ and DAG. PI-4,5-P₂ is a docking site for multiple proteins (Martin, 1998) and the over-production of PI-4,5-P₂ might therefore trigger effects by various enzymes for

cellular functions, which alter the normal signaling cascades and thereby alter pollen tube growth and morphology.

On the basis of our results after PI-PLC inhibition, we conclude, that PI-PLCs are mainly involved in the maintenance of polarized pollen tube growth. Figure 35 depicts the main molecules involved in this process and visualizes their spatially restricted localization within the cell.

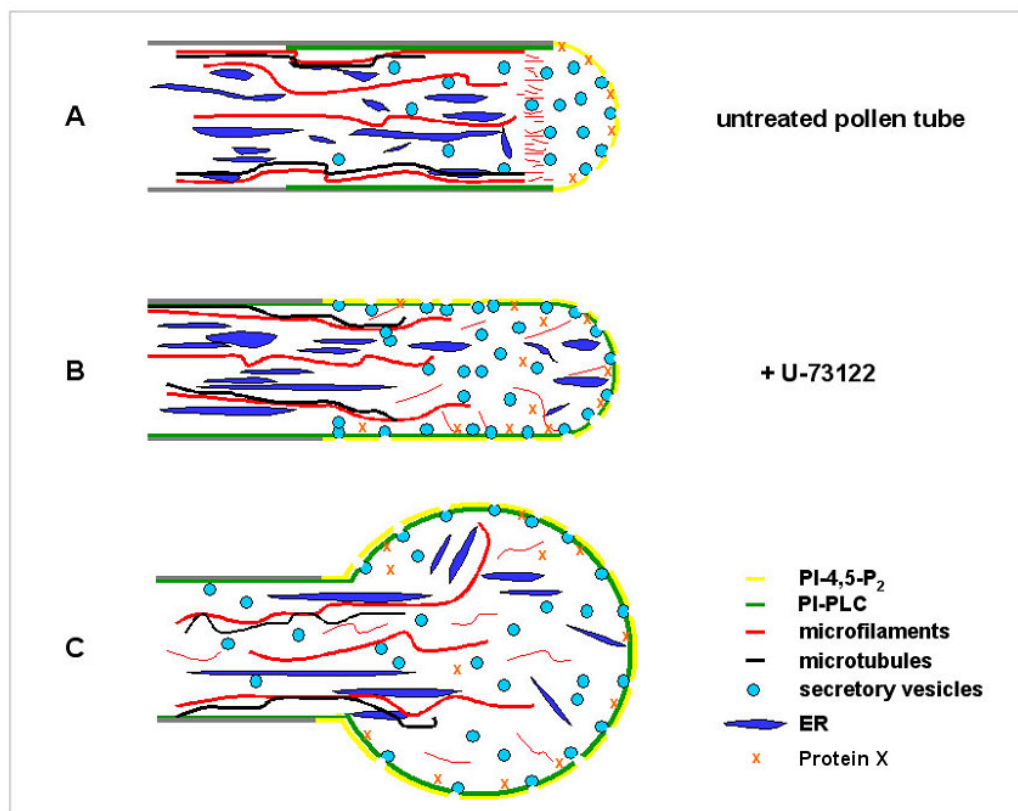


Figure 35: Model of the polar organization and distribution of molecules in pollen tubes.

(A) Untreated pollen tube. PI-4,5-P₂ is spatially restricted to the pollen tube tip. The PI-PLC is localized at the flanks of the pollen tube. Microfilaments are also organized in a polarized manner, thick actin bundles are found in the pollen tube shank and short filaments are organized in a subapical ring-structure. Microtubules are associated with thick actin bundles in the shank. The endoplasmic reticulum is also found in the shank. Vesicle fusion, instead, predominantly takes place with the plasma membrane in the tube apex. Proteins that mediate vesicle fusion or actin-binding proteins are as well thought to be localized in the tube apex, bound to PI-4,5-P₂ (Protein X). (B) After PI-PLC inhibitor treatment, PI-4,5-P₂ spreads to a larger area in the plasma membrane of the pollen tube flanks. It thereby facilitates vesicle fusion with a larger area of the plasma membrane and causes depolarized pollen tube growth. The polar organization of the pollen tube is abolished. The inhibited PI-PLC remains associated with the plasma membrane, but is now also localized in the plasma membrane of the tube apex. (C) After a longer incubation time in the PI-PLC inhibitor, PI-4,5-P₂'s distribution remains at the flanks and continued growth leads to the formation of a balloon at the pollen tube tip. Vesicle fusion continues all over the plasma membrane.

This hypothesis is consistent with the observation that NtPLC3 and PI-4,5-P₂, its substrate, accumulate at the plasma membrane in the pollen tube tip in a complementary pattern. Only a limited region of overlapping was detectable (Figure 29). We suppose that there must exist a mechanism, which prevents PI-4,5-P₂ in the tip region from being hydrolyzed by PI-PLCs. This might be facilitated through the association of proteins, such as actin-binding proteins, with PI-4,5-P₂.

It is known that plant homologues of the small GTPases of the Rac/Rop family and PI-4,5-P₂ act in a common pathway to regulate polarized pollen tube growth. Kost *et al.* (1999) showed that the small GTPase At-Rac2 associated with a PtdIns P-kinase, that specifically synthesized PI-4,5-P₂, indicating that the small GTPase Rac promoted accumulation of PI-4,5-P₂ in the plasma membrane specifically at the tip. Transient over-expression of constitutively active forms of At-Rac2 resulted in depolarized pollen tube growth and the formation of balloons at the tip (Figure 3e). This observation is consistent with the idea that activation of pollen tube Rac GTPases caused over-production of PI-4,5-P₂, which could not be hydrolyzed by endogenous PI-PLC activity. Subsequently, PI-4,5-P₂ spread to a larger area at the pollen tube flanks. We exactly mimicked the described situation by inhibiting the endogenous PI-PLCs with U-73122.

Inhibition of endogenous PI-PLC activity stopped PI-4,5-P₂ hydrolysis without affecting its synthesis. Therefore, PI-4,5-P₂ spread to a larger area in the plasma membrane of the flanks (Figure 30B). It is known that PI-4,5-P₂ facilitates vesicle fusion with the plasma membrane (Martin, 1998). If vesicles fused with a markedly enlarged area of the plasma membrane, the restricted incorporation of vesicles at the tip would be abolished and growth would take place all over the membrane, which in turn would result in bulging of the pollen tube apex.

It is unclear to this point, whether InsP₃ generated by PI-PLC-mediated hydrolysis of PI-4,5-P₂ plays a role in Ca²⁺ signaling in pollen tubes (see INTRODUCTION).

Apart from the restricted PI-4,5-P₂ distribution in the pollen tube, the complete polarized organization was disturbed (Figure 35B and C), as inhibition of PI-PLCs must also lead to a significant decrease in the tip-focused Ca²⁺ gradient (compare INTRODUCTION). Ca²⁺-dependent enzymes must at the same time be inhibited as well as downstream targets of the second messenger InsP₃ and pollen tube growth must stop sooner or later.

Profilin is a well-characterized actin-binding protein and might be a suitable candidate for PI-4,5-P₂ binding, among other proteins, in the pollen tube apex and may serve as an example here (referred to as Protein X in Fig. 35). It was shown to be a direct and specific interactor of polyphosphoinositides. These interactions dramatically affect the ability of plant PI-PLCs to bind PI-4,5-P₂ and to utilize it for second messenger production (Drøbak *et al.*, 1994; Kovar *et al.*, 2000). Drøbak *et al.* (1994) further demonstrated that one profilin molecule binds a minimum of ten PI-4,5-P₂ molecules and thereby potently inhibits its hydrolysis by PI-PLCs. They also showed that 1 μM profilin might lead to a 25 % reduction of the hydrolysis rate. Profilin could form a possible link between plant cell activation, second messenger production and the modulation of cytoskeletal dynamics (Hunt *et al.*, 2004). It might associate in unstimulated cells with PI-4,5-P₂ and prevent its hydrolysis *e.g.* at the pollen tube tip and at the same time be prevented itself from complex-formation with monomeric actin. As a response to cell activation, profilin would dissociate from the apical PI-4,5-P₂ resulting in an increase of PI turnover and would form complexes with unpolymerized actin (Drøbak *et al.*, 1994).

Another observation during these experiments was that transiently expressed NtPLC3-YFP was also localized in the plasma membrane of the pollen tip after inhibitor treatment (data not shown). When the pollen tube stopped its polarized growth, NtPLC3 localized to that area, which before was limited to the binding of other proteins to PI-4,5-P₂. In summary, an intracellular mechanism must exist, which actively eliminates NtPLC3 from the tip and retains it associated with the plasma membrane in the flanks. Whether this mechanism involves PI-4,5-P₂-binding by profilin (compare above) or another active mechanism remains to be investigated.

Nevertheless, it seems that the distribution of NtPLC3 in the pollen tube does not directly depend on the small GTPase Nt-Rac5. Over-expression experiments showed that the co-over-expression of NtPLC3 with Nt-Rac5 wild-type or CA-Nt-Rac5, respectively, did not alter the spatial localization of NtPLC3 (data not shown). NtPLC3 and Nt-Rac5 are both mainly involved in the regulation of polarized pollen tube growth, but they are only related to each other by the employment of putative co-factors, one of them being PI-4,5-P₂.

3.2.6 Diacylglycerol, a product of PI-PLC activity, accumulates at the plasma membrane in the pollen tube tip

PI-4,5-P₂ hydrolysis by PI-PLCs leads to the production of the second messengers diacylglycerol (DAG) and inositol 1,4,5-trisphosphate (InsP₃). DAG is a membrane-bound lipid and is known to activate protein kinase C (PKC) in animal cells. Interestingly, PKC homologues are missing from the *Arabidopsis* genome (Hirayama *et al.*, 1995). Munnik *et al.* (1998) have suggested that DAG does not accumulate in plant cells, but instead is immediately phosphorylated to phosphatidic acid (PA) by a diacylglycerol kinase (DGK). However, we have been able to detect an accumulation of DAG at the pollen tube tip. For this purpose we made use of the first cysteine-rich domain of the mammalian Protein Kinase C- γ .

Transient expression of Cys1-YFP in tobacco pollen tubes resulted in a strong labeling of the plasma membrane in the pollen tube apex. Further investigations strongly supported the notion that Cys1-YFP in tobacco pollen tubes serves as a specific marker for DAG, the product of PI-4,5-P₂ hydrolysis by PI-PLC activity. Upon treatment with the PI-PLC inhibitor U-73122, Cys1-YFP/DAG-labeling at the plasma membrane in the pollen tube tip decreased within 15 min and had completely disappeared after 30 min (Figure 33B and C). Interestingly, Cys1-YFP-labeled vesicles were visible in the pollen tube cytoplasm at this time.

Co-expression of NtPLC3, which does not affect pollen tube growth, led to spreading of the Cys1-YFP labeling from the apex to the flanks of pollen tubes. Under these conditions, we also observed Cys1-YFP-labeled vesicles, which moved rapidly from the flanks to the pollen tube tip. Surprisingly, co-expression of catalytically inactive NtPLC3 mutants (H¹²⁴A D¹⁵⁶R) had the same effect on Cys1-YFP labeling. Apparently, over-expression of NtPLC3 redistributes DAG to a larger area of the plasma membrane at the pollen tube tip, independent of its catalytic activity. It is not clear, whether NtPLC3's over-expression resulted in increased DAG levels or simply caused a redistribution of the lipid.

It is rather surprising that the substrate (PI-4,5-P₂) as well as the product (DAG) of the PI-PLCs are located in the pollen tube apex, whereas the PI-PLC is distributed to the flanks. Conceivably, accumulation of DAG at the pollen tube tip requires active transport. This hypothesis is supported by the appearance of vesicles, which move from the flanks to the tip and appear to fuse with the plasma membrane at the tip (compare Figure 32B).

Based on these observations, we hypothesize that DAG distribution in unstimulated cells or upon NtPLC3 over-expression, may be influenced by endocytotic membrane recycling from the flanks of the apex to the tip, which was proposed by Derksen *et al.* (1995) to have key functions in balancing membrane flow during pollen tube growth. According to this idea, during normal pollen tube growth DAG produced at the flanks of the pollen tube tip, where PI-4,5-P₂ and PI-PLC distribution patterns overlap, would be internalized and delivered to the tip incorporated into membrane or intra-cellular vesicles. These vesicles may only be visible in pollen tubes over-expressing NtPLC3 or treated with U-73122, because these cells contain increased levels of DAG or of free Cys1-YFP that is not membrane associated, respectively. In addition, the inhibition of pollen tube growth by U-73122 may block membrane recycling and cause an accumulation of DAG-transporting vesicles in the pollen tube cytoplasm.

Munnik *et al.* (1998) observed that not DAG accumulates after PI-PLC activation, but PA. We have tried to visualize phosphatidic acid (PA) in tobacco pollen tubes using YFP fused to the COOH-terminus of the serine/threonine kinase Raf1. Although this fusion protein has been shown to specifically visualize PA in MDCK cells (Gosh *et al.*, 1996) and in rat fibroblasts that over-expressed the human insulin receptor (HIRcB cells; Rizzo *et al.*, 2000), it was evenly distributed in the cytosol of tobacco pollen tubes with no membrane association or organelle labeling detectable. For unknown reasons, the Raf1-YFP fusion protein does not seem to be a suitable fluorescent marker for PA in tobacco pollen tubes.

However, PA appears to be an important second messenger in plant cells based on the work of Potocký *et al.* (2003) and Monteiro *et al.* (2005), who are investigating its role in plant signal transduction and in pollen tube growth. From animal cells PA is known to stimulate several activities such as protein kinases and small G-proteins. It also might amplify the PLC signaling cascade by activating PtdIns 4,5-kinase and PI-PLCs (Munnik *et al.*, 1998). PA was shown to stimulate pollen germination and pollen tube elongation (Potocký *et al.*, 2003). Monteiro *et al.* (2005) showed that a reduction of PA in pollen tubes resulted in bulging of the apex. It has to be noted, however, that PA is not only formed from DAG by DGK, it is thought to be mainly produced by PLD activity. The importance of the formation of PA via the PLC pathway remains, therefore, unclear.

The role of InsP₃, the second product of PI-PLC-mediated PI-4,5-P₂ hydrolysis, in pollen tubes is also uncertain. InsP₃ is an important Ca²⁺ regulator in animal cells, but the

identification of InsP₃ receptors in plant cells is still controversial. Although no orthologues of InsP₃-gated Ca²⁺-channels are found in the *Arabidopsis* genome, the presence of such channels in the tonoplast has been proposed (Munnik *et al.*, 1998 and references therein; deWald *et al.*, 2001). Munnik *et al.* (1998) are of the opinion that in plants InsP₃, similar to DAG may be rapidly metabolized and not act as a signaling molecule itself. They believe, InsP₃ may be quickly dephosphorylated to inositol, or phosphorylated to inositol hexakisphosphate (InsP₆) as in yeast cells (Meijer and Munnik, 2003). This has led to the suggestion that perhaps plants, fungi and slime molds have evolved a specific form of PI-PLC signaling that is different from the one in animal cells and that generates InsP₆ and PA as their second messengers instead of InsP₃ and DAG. This hypothesis would not only explain the absence of InsP₃-gated Ca²⁺-channels, but also the absence of protein kinases C from plant genomes.

To date no firm conclusion can be drawn concerning this issue. Further investigations are required to establish, which products of PI-4,5-P₂ hydrolysis have signaling functions in plants. Our results show that DAG accumulates in pollen tubes as a result of PI-PLC activity and are not consistent with the suggestion by Munnik *et al.* (1998) that this lipid is rapidly converted to PA in all plant cells. We consider this hypothesis postulated by Munnik *et al.* with great caution as it is exclusively supported by their own data (Munnik *et al.*, 1996; Laxalt and Munnik, 2002; de Jong *et al.*, 2004; Testerink *et al.*, 2004).

In conclusion, phospholipids and phosphoinositides might thus provide a link between signaling cascades and structural aspects of polarized pollen tube growth. It is known that PI-4,5-P₂ and small GTPases of the Rac/Rop family, are both located in the pollen tube apex (Kost *et al.*, 1999) and act in a common pathway to regulate tip growth. Ca²⁺ is known to be highly concentrated in the apex and to have essential functions in the control of pollen tube elongation (Pierson *et al.*, 1996). All three signaling modules have been implicated in the control of actin-cytoskeleton polymerization or depolymerization (Fu *et al.*, 2001). Extra- or intracellular signals might be transduced via the Rac/Rop GTPases - PI-4,5-P₂ pathway to the actin cytoskeleton to regulate cytoplasmic streaming, organelle or vesicle transport. PI-PLCs, in turn, act on PI-4,5-P₂ and restrict the distribution of this lipid to a limited area in the plasma membrane of the pollen tube tip. PI-PLCs are Ca²⁺ dependent enzymes, which need Ca²⁺ for their membrane association via the C2 domain and for catalysis. On the other hand, PI-PLCs can potentially increase intracellular Ca²⁺

concentrations through the generation of InsP_3 , which releases Ca^{2+} from internal stores. An increase in the intracellular Ca^{2+} concentration can activate various Ca^{2+} dependent enzymes including PI-PLCs. This positive feed-back loop can potentially stimulate a continued increase in Ca^{2+} and InsP_3 concentrations. On the other hand, PtdIns kinases and PtdIns P-kinases are inhibited by high Ca^{2+} concentrations, which results in decreased PI-4,5- P_2 production. Reduced availability of the PI-PLC substrate PI-4,5- P_2 will counteract InsP_3 production and Ca^{2+} release stimulated by the positive feed-back loop described above. Together, these mechanisms could be responsible for the oscillations at cytoplasmic Ca^{2+} levels that are observed at the tip of growing pollen tubes (Taylor and Hepler, 1997; Messerli *et al.*, 2000).

4 MATERIALS AND METHODS

4.1 Chemicals, kits, enzymes

Table 3: Chemicals, kits, enzymes – products and manufacturers

Product	Manufacturer
---------	--------------

Antibiotics

Acetosyringon (Hydroxy-dimethoxy-acetophenon)	Fluka; Neu-Ulm
Ammonium glufosinate (PESTANAL)	Riedel de Haen; Seelze
Ampicillin	Serva; Heidelberg
Carbenicillin	Sigma; Deisenhofen
Claforan (Cefotaxime)	Sigma; Deisenhofen
Kanamycin	Roth; Karlsruhe
Rifampicin	Serva; Heidelberg
Spectinomycin	Sigma; Deisenhofen
Ticarcillin	Sigma; Deisenhofen

Antibodies

anti DIG antibody	Roche Diagnostics; Mannheim
goat anti rabbit HRP	Santa Cruz Biotechnology; Santa Cruz, USA
goat anti rabbit IGG	Sigma Aldrich; Deisenhofen

DNA Polymerases

<i>Taq</i> DNA Polymerase	Genaxxon Bioscience; Stafflangen
<i>Pfu</i> DNA Polymerase	Promega; Madison, USA
Phusion High-Fidelity DNA Polymerase	Finnzymes; Espoo, Finland

DNA and Protein Standards

2-Log DNA Ladder (0.1-10.0 kb)	New England Biolabs; Bad Schwalbach
1 kb DNA Ladder	New England Biolabs; Bad Schwalbach
Prestained Protein Marker, Broad Range	New England Biolabs; Bad Schwalbach

Inhibitors and PI-PLC activator

U-73122: 1-[6-((17 β -3-Methoxyestra-1,3,5(10)-trien-17-yl)amino)hexyl]-1H-pyrrole-2,5-dione	Calbiochem; La Jolla, USA
U-73343 (inactive analogue of U-73122): 1-[6-((17 β -3-Methoxyestra-1,3,5(10)-trien-17-yl)amino)hexyl]-2,5-pyrrolidinedione	Calbiochem; La Jolla, USA
<i>m</i> -3M3FBS: 2,4,6-trimethyl- <i>N</i> -(<i>meta</i> -3-trifluoromethylphenyl)-benzenesulfonamide	Calbiochem; La Jolla, USA
Latrunculin B	Calbiochem; La Jolla, USA

Product	Manufacturer
---------	--------------

Kits

E.Z.N.A. Gel Extraction Kit	PeqLab; Erlangen
E.Z.N.A. Plasmid Purification Kit II	PeqLab; Erlangen
JetStar 2.0 (Maxi Prep)	Genomed; Löhne

Lipids

L- α -Phosphatidylinositol 4,5-diphosphate sodium salt	Fluka; Neu-Ulm
[³ H]Phosphatidylinositol 4,5-diphosphate (PI-4,5-P ₂), [Inositol-2- ³ H(N)]	Hartmann Analytic GmbH; Braunschweig

Modifying enzymes

Alkaline Phosphatase, Calf Intestinal (CIP)	New England Biolabs; Bad Schwalbach
Antarctic Phosphatase	New England Biolabs; Bad Schwalbach
Klenow Fragment (3'>5' exo-)	New England Biolabs; Bad Schwalbach
QuickChange™ Site-Directed Mutagenesis Kit	Stratagene; Amsterdam, The Netherlands
Quick Ligation Kit	New England Biolabs; Bad Schwalbach
Restriction Enzymes (all)	New England Biolabs; Bad Schwalbach
RNase A	Roth; Karlsruhe
RNaseOUT	Invitrogen; Karlsruhe
T4 DNA Ligase	New England Biolabs; Bad Schwalbach
T4 DNA Polymerase	New England Biolabs; Bad Schwalbach
T4 Polynucleotide Kinase	New England Biolabs; Bad Schwalbach

Northern Blot/RNA treatment

CDP-star	Roche Diagnostics; Mannheim
DIG blocking reagent	Roche Diagnostics; Mannheim
DIG PCR nucleotides	Roche Diagnostics; Mannheim
Duralon-UV Membranes 300 x 3cm	Stratagene; Amsterdam, The Netherlands
Morpholinopropane sulfonic acid (MOPS)	Serva; Heidelberg
Salmon sperm DNA	Sigma Aldrich; Deisenhofen
Trizol solution	Invitrogen; Karlsruhe

Nucleotides

Guanosine 5'-diphosphate (GDP)	Sigma Aldrich; Deisenhofen
Guanosine 5'-triphosphate (GTP)	Sigma Aldrich; Deisenhofen

Western Blot/protein treatment

Aminophthalhydrazine	Fluka; Neu-Ulm
BioTrace NT 30cm x 3MM, pure Nitrocellulose	Pall Corporation; Ann Arbor, USA
p-Coumaric acid	Fluka; Neu-Ulm
Non-fat dry milk powder	Roth; Karlsruhe

Product	Manufacturer
Yeast chemicals	
3-amino-1,2,4-triazole (3-AT)	Sigma Aldrich; Deisenhofen
CSM yeast medium -trp -leu -his	Qbiogene BIO-101 Systems; Heidelberg
Glassbeads 2.85-3.3 mm	Roth; Karlsruhe
Glasbeads 0.25-0.5 mm	Roth; Karlsruhe
Lithium acetate	Roth; Karlsruhe
Polyethyleneglycol (PEG) 6000	BDH (VWR International); Darmstadt
Polyethylenglycol (PEG) 3350	Sigma Aldrich; Deisenhofen
YPD medium	BD Biosciences Clontech; Bedford, USA
2 x YT medium	GibcoBRL; Karlsruhe
YNB yeast medium	Qbiogene BIO-101 Systems; Heidelberg

Others

Agar	Fluka; Neu-Ulm
	AppliChem; Darmstadt
Agar (Select)	Invitrogen; Karlsruhe
Agarose, Electrophoresis Grade	Invitrogen; Karlsruhe
Dimethylsulfoxide (DMSO)	Serva; Heidelberg
Lysozyme	Sigma Aldrich; Deisenhofen
Scintillation cocktail Optiphase "HiSafe" 3	Wallac Oy, Turku, Finland
Sodium deoxycholate	Sigma; Deisenhofen

All other chemicals, which have not been mentioned above, were from Amersham Pharmacia, Calbiochem, Difco, Fluka, GibcoBRL, New England Biolabs, Novagen, QIAGEN, Riedel deHaën, Roche Diagnostics, Roth, Sigma Aldrich, Stratagene or VWR International. Chemicals used in this study were of highest purity (*pro analysis; p.a.*). All solutions were prepared by using double distilled water.

In order to prepare sterile solutions and culture media heat-stable solutions and glass ware were autoclaved for 15 to 20 min at 121°C. Heat-sensitive solutions or antibiotics were prepared as concentrated stock solutions and sterile-filtered through a membrane filter (pore size: 0.2 µm; Millipore, Eschborn).

4.2 Apparatus

Table 4: List of apparatus used in the present work – Name and Manufacturer

Apparatus	Name	Company
Balances	Sartorius MC1, Laboratory LC 2200S	Sartorius; Göttingen
	Sartorius BL 150S (0.001-150g)	Sartorius; Göttingen
	Ohaus Scout II (0.1-1200g)	Ohaus Corporation; Pine Brook, USA
Blotting chamber (Western Blot)	Hofer TE 22	Amersham Pharmacia Biotech; Freiburg
Centrifuges	Biofuge <i>pico</i>	Heraeus (Kendro) GmbH; Hanau
	Biofuge <i>fresco</i>	Heraeus (Kendro) GmbH; Hanau
	Megafuge 1.0R	Heraeus (Kendro) GmbH; Hanau
	Sorvall J2-21	Beckman Coulter; Krefeld
Centrifuge Rotors	BS 4402/A	Heraeus (Kendro) GmbH; Hanau
	JA-14	Beckman Coulter; Krefeld
Electroporator	Gene Pulser II	BioRad; München
Electroporation Cuvettes	Electroporation cuvette (diameter 1mm)	Steinbrenner Laborsysteme; Wiesenbach
French Press	EmulsiFlex-C5	Avestin; Ottawa, Canada
Geldocumentation	BDA Digital TI 1	Biometra; Göttingen
Gel-electrophoresis chamber (agarose gels)	Hofer HE 33; mini horizontal submarine unit	Amersham Pharmacia Biotech; Freiburg
Glassware		Schott; Mainz / Simax; Czech Republic
Heatblock	QBT	Grant Instruments; Shepreth, UK
Hybridisation incubator	Techne Hybridiser HB-1D	Techne; Duxford, Cambridge, UK
Incubator (Shaker: 30°C and 37°C)	GFL 3005	Gesellschaft für Labortechnik mbH; Burgwedel
	GFL	Gesellschaft für Labortechnik mbH; Burgwedel
Incubator (30°C, Yeast)		Binder; Tuttlingen
Incubator (37°C, Bacteria)		Binder; Tuttlingen
Mixer	Variomag Mono	H+P Labortechnik AG; Oberschleißheim
	Variomag Monotherm	H+P Labortechnik AG; Oberschleißheim
pH Electrode	CyberScan 510 pH	Eutech Instruments; Ayer Rajah Crescent, Singapore
Plasticware		Greiner; Frickenhausen
Pipettes		Gilson; Middleton, USA
Power Supplies	EPS 601; EPS 2A200	Amersham Pharmacia Biotech; Freiburg
SDS Gel-electrophoresis Chamber	Hofer	Amersham Pharmacia Biotech; Freiburg
Sonication waterbath	Branson 3200 Ultrasonic Cleaner	Scientific Support; Hayward, USA
Scintillation Counter	Beckman LS6000SC	Beckman Coulter; Krefeld
Thermocycler	Biometra T gradient	Biometra; Göttingen
UV-Spectrophotometer	Ultraspec III	Pharmacia Biosystems; Freiburg
Vacuum pump	PK 2 DC	Ilmvac GmbH; Ilmenau
Vortex	Vortex Genie 2	VWR International, Darmstadt

4.3 Bacteria Strains

Table 5: Name of Organisms, resistance and reference

Organism	Genotype	Reference
<i>E. coli</i> XL1-Blue	<i>recA1 endA1 gyrA96 thi-1 hsdR17 supE44 relA1 lac [F- proAB lacIq Z.M15 Tn(Tetr)]c</i>	Stratagene; Amsterdam The Netherlands Studier and Moffat, 1986
<i>E. coli</i> BL21 (DE3)	F- <i>ompT hsdSB_(rB- mB-) galλ dcm</i> (DE3)	Stratagene; Amsterdam The Netherlands
<i>Agrobacterium tumefaciens</i> AGL1	rifampicine, carbenicillin resistant, cefotaxime/claforan, timentin sensitive	Lazo/Stein/Ludwig, 1991 Santa Cruz, USA

4.4 Yeast Strain

Table 6: Yeast strain, resistance and reference

Organism	Genotype	Reference
<i>Sacharomyces cerevisiae</i> HF7c	MATa, <i>ura3- 52, his3- 200, ade2- 101, lys2-801, trp1- 901, leu2- 3, 112, gal4-542, gal80-538, LYS2 :: GAL1UAS -GAL1TATA -HIS3, URA3 :: GAL4 17-mers(x3) -CYCITATA -lacZ</i>	Feilotter <i>et al.</i> , 1994 BD Biosciences Clontech Bedford, USA

4.5 Plant cultivation

4.5.1 *Nicotiana tabacum*

Pollen tubes for this study were exclusively collected from *Nicotiana tabacum*, Petit Havana SR1 plants. Sterile cultures of young plants were kept in a growth chamber under constant conditions: 17 h illumination per day at 25°C. Young tobacco plants already growing in soil were kept in a growth chamber under following conditions: 16 h illumination per day at 24°C during day and 18°C during night, with a relative humidity of 60 to 65 % during day and 70 to 75 % during night. When adult plants reached a height of more than 10 cm they were transferred to the green house, growing with varying conditions during the year, a minimum temperature of 18°C.

Growth media and soil:

Sterile tobacco plants were grown on 1 x MS medium, plus 30g/l sucrose and 1 % agar. Soil was mixed with sand in a ratio of 4:1. Two different types of soil were used, TKS1 and TKS 2 for further cultivation (both purchased from Floragard, Oldenburg).

4.5.2 *Arabidopsis thaliana*

All plants of *Arabidopsis thaliana*, ecotype Columbia, were grown in growth chambers under constant conditions: 16 h illumination per day; temperature: 24°C (day), 18°C (night); relative humidity: 60 to 65 % (day), 70 to 75 % (night).

4.5.2.1 Sterile cultures

Seeds of wild-type and T-DNA insertion lines of *Arabidopsis thaliana* were surface sterilized and sowed on agar plates containing ½ Murashige and Skoog medium with 1.5 % sucrose. Seeds were surface-sterilized for 10 min in 10 % sodium hypochloride plus 0.1 % Triton X-100, washed several times with sterile double distilled water and transferred to the plates by droplets from a sterile pipet tip and kept in the dark for two days at 4°C before transferring them to the growth chamber. Seedlings were grown on plates for 5 to 10 days before transferring them to soil.

½ MS: 2.1 g Murashige and Skoog medium plus 15 g/l sucrose and 1 % agar

4.5.2.2 Growth on Soil

Seedlings of *Arabidopsis thaliana* were transferred to and grown in a mixture of soil and sand in a ratio of 4:1 as explained above in the same chamber.

4.6 Methods related to the treatment of *Escherichia coli*

4.6.1 *E. coli* cultivation

For all cloning steps the *E. coli* strain XL1 Blue was used, the only exception is the over-expression of proteins, which is performed in *E. coli* strain BL21 (DE3). *E. coli* were grown either in liquid LB medium at 37°C shaking 200 rpm or on LB agar plates in a 37°C oven in the dark. The addition of antibiotics for specific selection of clones followed the autoclaving step, when the medium was cooled down to 60°C. Cell density in the liquid medium was measured at OD₆₀₀ using the Pharmacia LKB Ultraspec III photometer.

LB medium (Luria Bertani; Sambrook and Russel, 2001): 1 % Tryptone, 1 % NaCl, 0.5 % yeast extract; pH 7.0 (NaOH)

low salt LB: same as LB medium, NaCl reduced to 0.5 %

LB agar: LB liquid medium plus 1.5 % (w/v) bacto-agar

Antibiotic conc.: ampicillin 100 µg/ml; kanamycin 50 µg/ml; spectinomycin 100 µg/ml

4.6.2 Chemical transformation of competent *E. coli* cells (after Inoue *et al.*, 1990)

The preparation of competent cells was performed following a modified protocol of Inoue *et al.* (1990). A pre-culture of 20 ml LB was inoculated with a large single colony and grown for seven hours at 37°C. Aliquots of 1, 2 and 5 ml of the pre-culture were transferred to a final volume of 250 ml LB and grown ON at 20°C to an OD₆₀₀ of 0.55. Cells were kept on ice for 10 min before the centrifugation step (Beckman centrifuge J2-21: 3900 rpm, 10 min, 4°C). Supernatant was discarded and the pellet dissolved by swirling in 80 ml ice-cold Inoue buffer. After repeating the centrifugation step, the supernatant was removed and the pellet dissolved in 20 ml ice-cold Inoue buffer. 1.5 ml DMSO were added and the cells were kept on ice for another 10 min. Aliquots of 50 µl were prepared and immediately frozen in liquid nitrogen. Cells were stored at -80°C and thawed on ice immediately before use.

A maximum volume of 10 µl DNA was added to the cells, kept on ice for 20 to 30 min and heat-shocked for 45 sec at 42°C in a waterbath. Cells were placed on ice for another 5 min before adding 950 µl LB and incubating them for 1 h at 37°C in a shaker. 100 µl per aliquots were spread on selective agar plates (either ampicillin or kanamycin) and incubated at 37°C ON.

Inoue buffer: 55 mM MnCl₂; 15 mM CaCl₂; 250 mM KCl; 10 mM PIPES, pH 6.7

4.6.3 Transformation of *E. coli* via electroporation

A pre-culture of 20 ml LB was inoculated with a single colony of cells from a plate and grown at 20°C ON. One liter low salt LB was then inoculated with the ON culture and grown at 37°C to an OD₆₀₀ of 0.7. Cells were kept on ice for at least 5 min and harvested in 250 ml beakers by centrifugation (Beckman centrifuge J2-21: 4000 rpm, 15 min and 4°C). The supernatant was discarded and the pellet resuspended in ice-cold double distilled water (beakers filled completely). The centrifugation and wash steps were repeated. After the third centrifugation step, the supernatant was discarded and cells were resuspended in 20 ml ice-cold 10 % glycerol and finally combined. Cells were centrifuged again, the supernatant discarded and the pellet resuspended in 4 ml ice-cold 10 % glycerol. Cells were divided into several aliquots (50 µl cells each) and frozen in liquid nitrogen. Cells were stored at -80°C and thawed on ice directly before use.

For transformation 0.5 µl to 5 µl salt-free DNA (ligation assay or plasmids) per 50 µl cells were combined in an electroporation cuvette (inner diameter: 1mm) and cooled on ice. The GenePulserII (BioRad) served for electroporation and was used as indicated: 200 Ohm, 1.8 kV; 25 µF. Cells were electroporated for about 4.5 msec. The cuvette was washed with 900 µl LB and the whole assay transferred to a 15 ml plastic tube. Tubes were incubated for 1 h at 37°C. Variable amounts of transformed cells were spread on selective agar plates (ampicillin or kanamycin) and incubated upside down at 37°C ON in the dark.

4.6.4 Colony lift for cDNA library screen

A cDNA library screen (according to the protocol by Roche “DIG Application Manual for Filter Hybridization”) was performed in order to identify new PI-PLC isoforms in pollen tubes of *Nicotiana tabacum*. For this purpose a pollen tube cDNA library was used. The cDNA library consisted of 5.5 million clones, of which more than 90 % contained plasmids with cDNA inserts that were in roughly 1/3 of the cases larger than 1 kb. The cDNA library was restricted by EcoRI and XhoI and cloned into the MCS of pGAD-GH, a shuttle vector for use in *E. coli* and *Saccharomyces cerevisiae*.

The cDNA was transformed into *E. coli* XL1 Blue cells and plated on LB medium plus the appropriate antibiotic. After incubation ON at 37°C, the plate was transferred to 4°C. A plastic foil was placed on the laboratory bench and 1 ml drop of denaturing solution per membrane was placed on the foil. A membrane disc of a diameter of 82 mm (Millipore INYU 08250; Bedford, USA) was then placed for one min on the pre-cooled bacteria plate. When the membranes were lifted, they were turned around, so that the bacteria were on top. The membranes were placed onto a dry sheet of 3MM Whatman paper. The membranes were then placed on the drop of denaturing solution on the foil, making sure that the membranes were completely soaked in the liquid and incubated for 15 min. For neutralization, the membranes were lifted, briefly dried on new, dry, Whatman papers and placed on a new plastic foil containing a 1 ml drop of neutralization solution per membrane. An incubation for 15 min followed. The membranes were transferred to a 1 ml drop of 2 x SSC, followed by an incubation for 10 min. The transferred DNA was then crosslinked to the disc by UV-illumination (Stratalinker). The membranes were then washed twice for 5 min with wash buffer (1) at RT and once for 50 min at 65°C. Up to 20 membranes were placed in one hybridization tube, 15 ml of hybridization solution were added and incubated for 1 h at 42°C. A 745 bps fragment of the sequence of interest, (pWEN238-1; lat52::NtPLC3-1::NOS), was amplified by PCR using the primer pair wen77 – bot53, and DIG-labeled nucleotides. The PCR product was combined with 10 ml hybridization buffer, 200 µl of which were combined with 200 µl salmon sperm DNA and denatured at 95°C for 5 min. The probes were then added to the hybridization tube and hybridized ON. Membranes were washed once with 2 x SSC and 15 min at 55°C with wash buffer (2). Membranes were then rinsed with incubation buffer and blocked for 1 h with blocking buffer. 5 µl of the anti-DIG antibody were added to the blocking buffer and incubated for at least 1 h. Washing occurred three times for 15 min with wash buffer (2), membranes were rinsed with AP buffer and transferred to a film cassette, placed between two sheets of transparency paper. The chemiluminescence substrate (CDP-star) was diluted 1:100 with AP buffer, added to the membranes and incubated for 5 min. The film was exposed usually for 5, 15 and 30 min or ON.

Pre-hybridization solution: 50 % formamide, 4 x SSPE, 1 % SDS, 7.5 x Denhardt’s

Hybridization solution: 47 % formamide, 3 x SSPE, 1 % SDS, 6.5 x Denhardt’s

Denaturing solution: 0.5 M NaOH, 1.5 M NaCl

Neutralization solution: 1.5 M NaCl; 1.0 M Tris-Cl, pH 7.4

Wash buffer (1): 3 x SSC, 0.1 % SDS

Wash buffer (2): 100 mM maleic acid, 150 mM NaCl, 0.3 % Tween-20

AP buffer: 100 mM Tris-Cl, pH 9.5; 100 mM NaCl

Antibody: Anti DIG-AP-Fab-fragments

Chemiluminescence substrate: CDP-star (25 mM disodium 4-chloro-3-(3-methoxy-1,2-dioxetane-2,2'-(5'-chloro)tricyclo(3.3.1.1^{3,7})decan)-4-yl)-phenyl phosphate

4.7 Methods related to the treatment of *Agrobacterium tumefaciens*

4.7.1 Transformation of competent *A. tumefaciens*

For the preparation of electro-competent *Agrobacterium tumefaciens* an ON culture of 2 ml YEP was inoculated with one colony of agrobacteria and grown at 28°C, 200 rpm. The ON culture was then transferred into 200 ml YEP and grown at 28°C, 250 rpm, until the OD₆₀₀ reached 0.1 to 0.2 (about 3 to 4 h). Cells were harvested by centrifugation at 5.000 rpm at 4°C for 10 min. The supernatant was discarded and the pellet resuspended in 20 ml of 1 mM HEPES, pH 7.0, and then transferred to a 50 ml tube. The centrifugation and resuspension step was repeated twice. Then the pellet was resuspended in 20 ml 10 % glycerol and centrifugation repeated. Finally the pellet was resuspended in 2 ml 10 % glycerol and distributed to several pre-cooled tubes, frozen in liquid nitrogen and stored at -80°C until use. Competent *Agrobacterium tumefaciens* were combined with 1 µl of plasmid DNA in an electroporation cuvette (inner diameter: 1mm) and electroporated as explained earlier (see 4.6.3). The only few modifications: cells were grown in YEP medium for 2 h at 28°C in a shaker. After spreading cells to agar plates containing the appropriate antibiotics, cells were grown for 2 days at 28°C.

YEP: 10 g Bacto peptone, 10 g Bacto yeast extract, 5 g NaCl, ad 1 l

4.8 Methods related to the treatment of *Saccharomyces cerevisiae*

The identification of interaction partners between proteins was based on a yeast two-hybrid system, *i.e.*, the Matchmaker™ GAL4 system by BD Biosciences Clontech™ (Bedford, USA). As bait vector served the pGBKT7, which expressed proteins fused to the GAL4 DNA binding domain, and as prey, the pGAD-GH, expressing proteins fused to the GAL4 DNA activation domain (for details see 4.9.1).

4.8.1 *S. cerevisiae* cultivation

HF7c cells were either grown in liquid unselective YPAD or liquid selective SD medium at 30°C shaking 200 rpm or on SD agar plates at 30°C in the dark. Selection during growth in SD medium was achieved by either the addition or the absence of specific amino acids, such as leucine (L), tryptophane (T) or histidine (H). Cell density in the liquid medium was measured at OD₆₀₀ using the Pharmacia LKB Ultraspec III photometer.

YPAD medium: 10 g yeast extract, 20 g peptone, 20 g glucose, 40 mg adenine hemisulfate, pH 6.5 (HCl); ad 1 l. YPAD agar plates: 2 % (w/v) agar

SD medium: 1.7 g YNB, 5 g ammonium sulfate, 20 g glucose, 10 ml 1 % leucine, 5 ml 2 % tryptophane, 2 ml 1 % histidine, pH 5.8 (KOH), ad 1 l. 620 mg CMS-his-leu-trp, autoclave 15 min. Add 5 ml 1M 3-AT when medium cooled below 55°C for 5 mM 3-AT concentration.

SD agar plates: 2 % (w/v) agar

Table 7A:

Ingredients/stocks:			
YNB	yeast nitrogen base	100 x leu	L-Leucine (Serva 27690)
	defined medium: without ammonium sulfate, amino acids, glucose, agarose		2 g/200 ml (100 x)
	BIO 101; 4027-012 (227 g)		-20°C, unsterile
CMS-H-L-T	complete supplement mixture-H-L-T	200 x trp	L-Tryptophane (Serva 37422)
	BIO 101; 4530-122 (100 g)		2 g/100 ml (200 x)
3-AT	3-amino-1,2,3-triacole	500 x his	L-Histidine (Serva 24842)
	Sigma A-8056		0.5 g/50 ml (500 x)
	1 M in H ₂ O, filter sterilized, -20°C		-20°C, unsterile
10mg/ml sheared salmon sperm DNA	Stratagene 201190	1M lithium acetate	Roth 5447.1
	sonicated		13.2 g in 200 ml
			pH 7.5 (10 % acetic acid)
10 x TE	100 mM TrisCl/10mM EDTA	50% PEG 3350	filter sterilized
	autoclaved		Sigma P-3640
	pH 7.5		100 g in 200 ml
			filter sterilized

Table 7B:

Solutions (24 probes):	
1 x TE	10 ml 10 x TE, pH 7.5
	90 ml sterile H ₂ O
TE/LiAc	0.2 ml 10 x TE, pH 7.5
	0.2 ml 1M Lithium Acetate
	1.6 ml sterile H ₂ O
PEG/LiAc	1.5 ml 10 x TE, pH 7.5
	1.5 ml Lithium Acetate
	12 ml 50 % PEG 3350

Lysis buffer (10ml):	
2 ml	10 % Triton X-100
1 ml	10 % SDS
200 µl	5 M NaCl
100 µl	Tris-Cl, pH 8.0
20 µl	0.5 M EDTA
ad 10 ml	H ₂ O

4.8.2 Transformation of *S. cerevisiae* HF7c cells

4.8.2.1 Library scale

The library scale assay served to identify yeast two-hybrid protein-protein interactions of an already known protein, the bait, and its putative interactors. A pollen tube cDNA library (5.5 million clones, 95 % with insert, 30 % of the inserts >1 kb) was used as the prey in these experiments, representing genes expressed in tobacco pollen tubes three hours after germination.

A pre-culture of 100 ml SD -trp was inoculated with several colonies of HF7c cells containing the bait vector and grown at 30°C, 250 rpm for up to 48 h (OD₆₀₀ > 1.5). The

pre-culture was then transferred into 300 ml YPAD until it produced an OD₆₀₀ of 0.5 and further cultivated at 30°C, 250 rpm for approximately 6 h until the OD₆₀₀ reached 0.8. Cells were harvested by centrifugation (Beckman J2-21; 4.000 rpm; 5 min; RT), the supernatant discarded and the pellet resuspended and vortexed in 50 ml 1 x TE. Cells were pooled in one 50 ml-tube and centrifuged again (Heraeus Megafuge 1.0R; 3.500 rpm; 5 min; RT). The supernatant was discarded and the pellet resuspended in 1 ml TE/LiAc. The resuspended cells were combined with 200 µg of the tobacco pollen tube cDNA library in the prey vector and with 2 mg previously denatured (20 min, 95°C), sonicated salmon sperm DNA. Cells were vortexed and 6 ml PEG added and vortexed vigorously again. After an incubation of 30 min at 30°C at 250 rpm, 700 µl DMSO were added and cells were heat-shocked at 42°C for exactly 15 min. Then cells were immediately cooled down to RT on ice, centrifuged briefly, the supernatant carefully discarded and cells dissolved in 10 ml 1 x TE. 200 µl of transformed cells were plated on approximately 50 plates (diameter: 15 cm) lacking histidine to screen for two-hybrid interactions. Plating of a small amount of transformed cells on medium supplemented with histidine served as a control to identify the total number of co-transformants carrying the bait and the prey constructs screened. Plates were incubated upside down at 30°C for 3 to 14 days in the dark. Resulting colonies growing on histidine-lacking plates were purified, transformed into *E. coli* and tested in further plasmid scale experiments for true interaction with the bait.

4.8.2.2 Plasmid scale (re-transformation described for 24 probes)

The plasmid scale assay served as a tool to identify yeast two-hybrid protein-protein interactions of already known protein sequences and/or as a control to exclude false positive interactors identified in the library scale experiment. Bait and prey constructs were simultaneously co-transformed into HF7c cells using a small scale lithium acetate method following the manufacturer's instructions (manual PT3061-1; BD Biosciences-Clontech). As negative controls served co-transformed bait and prey constructs with empty pGBKT7 and pGAD-GH, respectively.

A pre-culture of 50 ml YPAD was inoculated with several colonies of HF7c cells and grown at 30°C, 250 rpm for 20 to 22 h, until OD₆₀₀ reached 1.5 or higher. At least 25 ml of the pre-culture were transferred to the main culture of 300 ml YPAD to produce an OD₆₀₀ of 0.5. Further cultivation occurred at 30°C, 250 rpm for 3.5 h until OD₆₀₀ reached 0.6 to 0.8. Cells were harvested by centrifugation (Beckman J2-21; 4.000 rpm; 5 min; RT), the supernatant discarded and the pellet resuspended and vortexed in 50 ml 1 x TE. Cells were pooled in one 50 ml-tube and centrifuged again (Heraeus Megafuge 1.0R; 3.500 rpm; 5 min; RT). The supernatant was discarded and the pellet resuspended in 1.5 ml TE/LiAc. 100 µl of competent cells were combined with 1 µg of plasmid DNA and 0.1 mg sonicated salmon sperm DNA, which had been denatured at 95°C for 20 min, in a 1.5 ml Eppendorf tube. Tubes were then vortexed and 0.6 ml PEG were added before vortexing vigorously again. Tubes were then placed in a shaker (300 rpm) at 30°C for 30 min. After the addition of 70 µl DMSO, cells were heat-shocked at 42°C for exactly 15 min and rapidly cooled down on ice for 2 min. Cells were again centrifuged (Biofuge *pico*; 13.000 rpm; 5 sec; RT) and the supernatant carefully discarded. Cells were finally dissolved in 0.4 ml 1 x TE and equal amounts of each assay of co-transformed cells were plated as fast as possible on histidine containing medium, to determine co-transformation efficiencies, and on histidine free medium supplemented with 0, 1 to 5 mM 3-AT to detect protein-protein interactions. Plates were incubated upside down at 30°C for 3 to 10 days in the dark. A successful transformation resulted in several hundred yeast colonies growing on histidine containing medium 3 days after transformation, specific yeast two-hybrid interactions were proved

by growth on histidine-lacking medium of HF7c cells transformed with bait and prey constructs and by the absence of growth on this medium of cells containing only bait or prey constructs along with empty pGAD-GH or pGBK-T7, respectively.

4.9 DNA-related techniques

4.9.1 Vectors

A list of commercial, modified and obtained vectors is presented at this point, because these vectors served as vehicles for further cloning and expression and form the basis for the plasmids generated in the present work.

The protein expression in *E. coli* was based on the pGEX vector system by Amersham Biosciences (Freiburg). The Glutathione S-transferase (GST) gene fusion system is an integrated system for the expression, purification and detection of fusion proteins produced in *E. coli*. The pGEX-4T-2 used in this study is controlled by the bacteriophage-related T7 tac promoter system, which can be induced by the lactose analog Isopropyl- β -D-thiogalaktosid (IPTG; Dubendorff & Studier, 1991) and results in high level expression of the protein. It contains additionally a thrombin or factor Xa protease recognition site for cleaving the protein of interest from the fusion product.

The Yeast Two-Hybrid interactions are all based on the MatchmakerTM system by BD Biosciences Clontech. The prey vector pGAD-GH expresses proteins fused to the GAL4 activation domain. Plasmid selection in *E. coli* is achieved with the ampicillin resistance gene, for selection in yeast the nutritional marker LEU2 is employed. The bait vector pGBKT7, in contrast, expresses proteins fused to the GAL4 DNA binding region, carries a kanamycin resistance for selection in *E. coli* and a TRP1 nutritional marker for selection in yeast.

The XFP fusion vectors as well as the over-expression vector are all based on the pUCAP vector (van Engelen *et al.*, 1995), which are modified in order to express genes in tobacco pollen tubes. The expression cassettes are all under the control of the pollen-specific *lat52* promoter (Twell *et al.*, 1989) and contain the multiple cloning site between promoter and *nos* polyA addition signal.

The pHANNIBAL vector is employed in this study in order to silence genes of interest in tobacco pollen tubes. Post-transcriptional gene silencing is achieved by expressing double stranded RNA in cells forming hairpin RNA resulting in severe reduction of the target mRNA. Hairpin constructs are constructed by using the generic vector pHANNIBAL (Wesley *et al.*, 2001), which is based on the Gateway[®] technology. The vector was a kind gift of Chris Helliwell; Canberra, Australia.

Table 8: List of vectors: commercials, modified vectors and obtained constructs**Table 8A: Commercials:**

Vector/Size	Description	Bac res	Reference
pBSK+ 2961 bps	CAP protein binding site - 938-901; mRNA (LacZ) starts at nt position 854; <i>lac</i> repressor binding site - 854-834	amp	Stratagene; La Jolla, USA
pGEX-4T-2 4970 bps	Proteins are expressed as fusion proteins with the 26 kDa glutathione S-transferase (GST)	amp	Amersham Pharmacia, Freiburg
pGAD-GH 8000 bps	GAL4(768–881) AD, LEU2, ampr	amp	Clontech; Bedford, USA van Aelst <i>et al.</i> , 1993
pGBKT7 7300 bps	GAL4(1–147) DNA-BD, TRP1, kanr, c-Myc epitope tag	kan	Clontech; Bedford, USA Louret <i>et al.</i> , 1997 Bartel <i>et al.</i> , 1993a
pHANNIBAL 5824 bps	derivative of cloning vector pART7 which was a derivative of pGEM-9Zf	amp	Helliwell and Waterhouse, 2003; Canberra, Australia
pTYB2 and 12 7474/7417 bps	<i>Sce</i> VMA intein/chitin binding domain, protein expression in <i>E. coli</i>	amp	New England Biolabs; Beverly, USA

Table 8B: Modified vectors:

Vector/Size	Description	Bac res	Reference
pWEN240 4291 bps	lat52::YFP::GA5::MCS::NOS	amp	based on pUCAP (van Engelen <i>et al.</i> , 1995)
pHD5 4294 bps	lat52::YFP::GA5::MCS::nos	amp	based on pWEN240
pHD27 3565 bps	Lat52::MCS-2::Nos	amp	based on pWEN240
pHD32 4365 bps	lat52::MCS-2::GA5::YFP::STOP::nos	amp	based on pWEN17 and pHD29
pHD135 13303 bps	prof::GUS::GFP--35S::BASTA—MCS, inverted-repeat cloning vector for binary expression in <i>Agrobacteria</i> and plants	spec	derivative of pHANNIBAL
pHD223 4311 bps	lat52::MCS-2::GA5::RFP::STOP::nos	amp	based on pHD32 plus RFPm1 (R. Tsien, 2000)

Table 8C: Obtained constructs:

Vector/Size	Description	Bac res	Reference
o29	mRFP1 in pRsetg	amp	Roger Tsien; San Diego, USA
o50	first Cys domain of PKC γ	kan/neo	Tobias Meyer; Stanford, USA, (Oancea <i>et al.</i> , 1998)
o51	cRaf1 (aa 390-426)	kan/neo	Guillermo Romero; Pittsburgh, USA (Rizzo <i>et al.</i> , 2000)
o52	cRaf1 R398A R401A	kan/neo	Guillermo Romero; Pittsburgh, USA (Rizzo <i>et al.</i> , 2000)

4.9.2 Plasmids

Table 9: Plasmids

Table 9A: Cloning information and name of constructs for Nt-Hypo1:

Name/ Size	Description	Cloning details	Bac res
pHD25 3218 bps	pBSK+ Nt-Hypo1	pBSK+ xSmaI plus PCR bot66-bot67	amp
pHD26 4498 bps	lat52::YFP-Nt-Hypo1::nos	pWEN240 xNgoMIV-SacI plus pHD25 fragment xNgoMIV-SacI	amp
pHD42 7543 bps	bait Nt-Hypo1 (full-length)	pHD36 xXmaI-SacI plus pHD25 xNgoMIV-SacI	kan
pHD60 3772 bps	Nt-Hypo1 over-expression	pHD27 xNgoMIV-SacI plus fragment pHD25 xNgoMIV-SacI	amp
pHD67 5207 bps	GST::Nt-Hypo1	pGEX-4T-2 xXmaI-XhoI plus fragment pHD25 xNgoMIV-XhoI	amp
pHD76 4584 bps	Nt-Hypo1::YFP	pHD32 xNgoMIV-SmaI plus fragment pHD25 xNgoMIV-MlyI	amp
pHD153 8223 bps	prey Nt-Hypo1 (full-length)	pHD37 xXmaI-SacI plus fragment pHD25 xNgoMIV-SacI	amp
pHD166 6094 bps	Y2H interactor Screen 12: clone F	pHD5 xSpeI-ApaI plus fragment Screen 12 clone F xSpeI-ApaI	amp
pHD167 5094 bps	Y2H interactor Screen 12: clone BBV	pHD5 xSpeI-ApaI plus fragment Screen 12 clone BBV xSpeI-ApaI	amp
pHD168 5094 bps	Y2H interactor Screen 12: clone BBX	pHD5 xSpeI-ApaI plus fragment Screen 12 clone BBX xSpeI-ApaI	amp
pHD170 4498 bps	CFP::Nt-Hypo1	pWEN242 xNgoMIV-SacI plus fragment pHD26 xNgoMIV-SacI	amp
pHD171 4584 bps	Nt-Hypo1::CFP	pHD54 xNgoMIV-XhoI plus fragment pHD76 xNgoMIV-XhoI	amp
pHD174 5494 bps	Y2H interactor Screen 12: clone BBT	pHD5 xSpeI-ApaI plus fragment Screen 12 clone BBT xSpeI-ApaI	amp
pHD248 7667 bps	Nt-Hypo1-Intein	pTYB2 xNdeI, blunt, xSmaI, CIP, plus pHD26 xNaeI-MlyI	amp
pHD249 16441 bps	Nt-Hypo1 construct for RNAi	pHD135 xAscI, CIP plus Hypo1 sense and antisense in pHANNIBAL xAscI	spec
pHD251 4844 bps	Y2H interactor Screen 12: clone BBQ	pHD5 xSpeI-ApaI plus fragment Screen 12 clone BBQ xSpeI-ApaI	amp
pHD252 5794 bps	Y2H interactor Screen 12: clone CG	pHD5 xSpeI-ApaI plus fragment Screen 12 clone CG xSpeI-ApaI	amp

Table 9B: Cloning information and name of constructs for NtPLC3 and 4:

Name/ Size	Description	Cloning details	Bac res
pHD73 6188 bps	YFP-NtPLC4 fusion	pWEN240 NgoMIV-ApaI plus fragment 3-8A1 xEcoRV-ApaI plus PCR fragment NtPLC4 in pBSK+ xNgoMIV-EcoRV	amp
pHD74 6259 bps	YFP-NtPLC3 fusion	pWEN240 NgoMIV-ApaI plus fragment 3-8B3 EcoRV-ApaI plus PCR fragment NtPLC3 in pBSK+ xNgoMIV-EcoRV	amp
pHD77 5462 bps	NtPLC4 over-expression	pHD27 xNgoMIV-ApaI plus fragment pHD73 xNgoMIV-ApaI	amp
pHD78 5533 bps	NtPLC3 over-expression	pHD27 xNgoMIV-ApaI plus fragment pHD74 xNgoMIV-ApaI	amp
pHD79 9984 bps	prey vector: NtPLC3 full-length	pHD37 xXmaI-ApaI plus fragment pHD74 xNgoMIV-ApaI	amp
pHD80 9882 bps	prey vector: NtPLC4 full-length	pHD37 XmaI-ApaI plus fragment HD73 xNgoMIV-ApaI	amp
pHD113 9230 bps	bait vector: NtPLC4 full-length	pHD36 xXmaI, CIP ,p HD73 xNgoMIV	kan
pHD114 9301 bps	bait vector: NtPLC3 full-length	pHD36 xXmaI plus pHD200 xNgoMIV-EcoRV plus pHD74 xEcoRV-XmaI	kan
pHD129 6188 bps	YFP::NtPLC4D156R	NtPLC4 Quickchange mutagenesis PCR with bot211/bot212 on pHD74	amp
pHD132 6158 bps	NtPLC3::YFP	pHD32 xNaeI-ApaI plus NtPLC3 without stop xSmaI-ApaI	amp
pHD133 6150 bps	NtPLC3::YFP	pHD32 xNgoMIV-XhoI plus PCR product NtPLC3 without stop xNgoMIV xXhoI	amp
pHD139 9763 bps	NtPLC4 cDNA without stop	PCR product wen77-bot207 without stop xSacI-XhoI plus cDNA 3-8A1 xSacI-XhoI	amp
pHD161 6920 bps	GST::NtPLC4	pGEX-4T-2 xXmaI-NotI plus fragment pHD113 xNgoMIV-NotI	amp
pHD162 6991 bps	GST::NtPLC3	pGEX-4T-2 xXmaI-NotI plus fragment pHD114 xNgoMIV-NotI	amp
pHD163 6158 bps	NtPLC4::CFP	pHD54 xNaeI-ApaI plus fragment pHD139 xSmaI-ApaI	amp
pHD164 5462 bps	NtPLC4 D156R over-expression	pHD27 xNgoMIV-ApaI plus fragment pHD129 xNgoMIV-ApaI	amp
pHD165 6261 bps	CFP::NtPLC3	pWEN242 xNgoMIV-ApaI plus fragment pHD78 xNgoMIV-ApaI	amp
pHD178 5620 bps	lat52::2xcMYC::GA5::NtPLC4::nos	pHD33 xNgoMIV-ApaI plus fragment pHD74 xNgoMIV-ApaI	amp
pHD199 5793 bps	NtPLC3-X-Y-C2::YFP	pHD32 xNgoMIV-SmaI plus PCR fragment NtPLC3 bot286-287 xNgoMIV-SmaI	amp
pHD200 5652 bps	NtPLC3-EF-X-Y::YFP	pHD32 xNgoMIV-SmaI plus PCR fragment NtPLC3 WEN74-bot288 xNgoMIV-SmaI	amp

Name/ Size	Description	Cloning details	Bac res
pHD201 4677 bps	NtPLC3-EF::YFP	pHD32 xNgoMIV-SmaI plus PCR fragment NtPLC3 WEN74-bot289 xNgoMIV-SmaI	amp
pHD202 4818 bps	NtPLC3-C2::YFP	pHD32 xNgoMIV-SmaI plus PCR fragment NtPLC3 bot290-287 xNgoMIV-SmaI	amp
pHD203 5441 bps	GST::NtPLC3-C2	pGEX-4T-2 xSmaI, CIP, plus PCR fragment NtPLC3 bot290-287 xNaeI-SmaI	amp
pHD204 6259 bps	YFP::NtPLC3 D156R	PCR Quickchange mutagenesis on pHD 74 xNgoMIV-EcoRV plus pHD74 xEcoRV-ApaI plus pWEN240 xNgoMIV-ApaI	amp
pHD206 5533 bps	NtPLC3 D156R over-expression	pHD27 xNgoMIV-ApaI plus fragment pHD204 xNgoMIV-ApaI	amp
pHD214 6416 bps	GST::NtPLC3-X-Y-C2	pGEX-4T-2 xSmaI, CIP, plus PCR fragment NtPLC3 bot286-287 xNaeI-SmaI	amp
pHD215 6275 bps	GST::NtPLC3-EF-X-Y	pGEX-4T-2 xSmaI, CIP, plus PCR fragment NtPLC3 wen74-bot288 xNaeI-SmaI	amp
pHD216 5300 bps	GST::NtPLC3-EF	pGEX-4T-2 xSmaI, CIP, plus PCR fragment NtPLC3 wen74-bot289 xNaeI-SmaI	amp
pHD217 6991 bps	GST::NtPLC3 D156R	pGEX-4T-2 xXmaI-NotI plus NtPLC3 D156R xNgoMIV-EcoRV plus pHD114 xEcoRV-NotI	amp
pHD218 6259 bps	YFP::NtPLC3 H124A D156R	pWEN240 xNgoMIV-ApaI plus PCR fragment NtPLC3 H124A on pHD204 xNgoMIV-EcoRV plus pHD74 xEcoRV-ApaI	amp
pHD224 6902 bps	GST::NtPLC4 D156R	pGEX-4T-2 xXmaI-NotI plus NtPLC4 D156R xNgoMIV-EcoRV plus pHD113 xEcoRV-NotI	amp
pHD225 6973 bps	GST::NtPLC3 H124A D156R	pGEX-4T-2 xXmaI-NotI plus pHD218 xNgoMIV-EcoRV plus pHD114 xEcoRV-NotI	amp
pHD226 5533 bps	NtPLC3 H124A D156R over-expr.	pHD27 xNgoMIV-ApaI plus fragment pHD218 xNgoMIV-ApaI	amp
pHD233 5181 bps	NtPLC3 EF::YFP::C2	pHD201 xPstI-NotI plus pWEN240 xPstI-NgoMIV plus PCR product bot290-bot323 on pHD74 xNgoMIV-NotI	amp
pHD234 5322 bps	NtPLC3 X-Y::YFP	pHD32 xXmaI-SmaI plus PCR fragment bot286-288 on pHD74 xNgoMIV-SmaI	amp
pHD235 5945 bps	GST::NtPLC3 X-Y	pGEX-4T-2 xSmaI, CIP, plus PCR fragment bot286-288 on pHD74 xNaeI-SmaI	amp
pHD240 8313 bps	NtPLC3 EF prey	pHD37 xXmaI, CIP, plus PCR fragment wen74-bot289 on pHD74 xNgoMIV-XmaI	amp
pHD241 9288 bps	NtPLC3 EF-X-Y prey	pHD37 xXmaI, CIP, plus PCR fragment wen74-bot289 on pHD74 xNgoMIV-XmaI	amp
pHD242 8958 bps	NtPLC3 X-Y prey	pHD37 xXmaI, CIP, plus PCR fragment bot286-bot288 on pHD74 xNgoMIV-XmaI	amp
pHD243 9429 bps	NtPLC3 X-Y-C2 prey	pHD37 xXmaI, CIP, plus pHD199 xNgoMIV-XmaI	amp

Name/ Size	Description	Cloning details	Bac res
pHD244 8454 bps	NtPLC3 C2 prey	pHD37 xXmaI, CIP, plus pHD200 xNgoMIV-XmaI	amp
pHD245 7797 bps	NtPLC3 EF-Intein	pTYB2 xEcoRI-SmaI plus pHD216 xEcoRI-SmaI	amp
pHD246 8442 bps	NtPLC3 X-Y-Intein	pTYB2 xEcoRI-SmaI plus pHD235 xEcoRI-SmaI	amp
pHD247 5533 bps	NtPLC3 H124A over-expression	pHD27 xNgoMIV-ApaI plus PCR fragment bot320-bot321 on pHD74 xNgoMIV-EcoRV plus pHD74 xEcoRV-ApaI	amp
pHD257 6259 bps	YFP::NtPLC3 H124A	pWEN240 xNgoMIV-ApaI plus PCR fragment NtPLC3 H124A xNgoMIV-EcoRV plus pHD74 xEcoRV-ApaI	amp
pHD258 6973 bps	GST::NtPLC3 H124A	pGEX-4T-2 xXmaI-NotI plus PCR fragment NtPLC3 H124 xNgoMIV-EcoRV plus pHD114 xEcoRV-NotI	amp
pHD273 6036 bps	NtPLC3::RFP	pHD133 xXbaI-XhoI plus PCR fragment bot324-bot329 on o29 xXbaI-XhoI	amp
pHD274 4548 bps	PKC γ (26-89) Cys1::YFP	pHD32 xSmaI-NcoI plus o50 xHindIII, blunt, xNcoI	amp
pHD275 4411 bps	YFP::HsRaf1 (390-426)	pWEN240 xHincII, CIP, plus o51 xBglII-EcoRI, blunt	amp
pHD276 4411 bps	YFP::Raf1 R398A R401A	pWEN240 xHincII, CIP, plus o52 xBglII-EcoRI, blunt	amp
pHD279 5876 bps	NtPLC3 X-Y::YFP::RnPLC- δ_1 -PH	pHD234 xXbaI, blunt, xBsrGI plus pWEN106 xSmaI-BsrGI	amp
pHD281 4809 bps	YFP::NtPLC3-C2	pWEN240 xXhoI-SacI plus fragment pHD233 xXhoI-SacI	amp
pHD282 4542 bps	PKC γ (26-89) Cys1::RFP	pHD223 xSmaI, CIP plus o50 xHindIII xNcoI, blunt	amp

Table 9C: Constructs used in this work, but generated by other lab members:

Name	Description	Bac res	Reference
pWEN105	lat52::RFP::PLC- δ_1 -PH::NOS	amp	Kost
pWEN106	lat52::YFP::PLC- δ_1 -PH::NOS	amp	Kost
pWEN208	lat52::Nt-Rac5::nos	amp	Kost
pWEN209	ADH1::Gal4DNAD::myc::Nt-Rac5::ADH	kan	Kost
pWEN210	lat52::Nt-Rac5-G15V::nos	amp	Kost
pWEN211	lat52::Nt-Rac5-T20N::nos	amp	Kost
pWEN220	lat52::ECFP::2xFYVE::NOS	amp	Kost
pWEN237	ADH1::Gal4DNAD::Nt-Rac5::T20N-C194S	kan	Kost
pWEN238-1	lat52::NtPLC3-1::NOS	amp	Kost
pWEN240	lat52::YFP::GA5::MCS::NOS	amp	Kost
pWEN242	lat52::CFP::GA5::MCS::NOS	amp	Kost
pHD5	lat52::YFP(no stop)::GA5::NgoMIV::SpeI::MCS::nos	amp	Kost
pHD23	YFP::Nt-Rac5	amp	Klahre
pHD32	lat52::MCS-2::GA5::YFP::STOP::nos	amp	Klahre
pHD33	lat52::2xcMYC::GA5::MCS-2::nos	amp	Klahre
pHD36	pGBKT7 with altered polylinker	kan	Klahre
pHD37	PGAD-GH with altered polylinker	amp	Klahre
pHD45	YFP::Nt-Rac5 T20N (DN)	amp	Klahre
pHD49	YFP::Nt-Rac5 G15V (CA)	amp	Klahre
pHD54	lat52::MCS-2::GA5::CFP::STOP::nos	amp	Klahre
pHD59	prey Nt-Rac5	amp	Klahre
pHD83	ADH1p::DB::Nt-Rac5 T20N::ADH1t	kan	Klahre
pHD85	YFP::Nt-Rab5	amp	Cottier
pHD115	GST::Nt-Rac5 (WT)	amp	Becker
pHD116	GST::Nt-Rac5 (CA)	amp	Becker
pHD117	GST::Nt-Rac5 (DN)	amp	Becker
pHD135	binary, RNAi; prof::GUS::GFP-35S::BASTA--MCS	spec	Bartels
pHD227	RFP::Nt-Rac5 (WT)	amp	Becker
pHD228	RFP::Nt-Rac5 (CA)	amp	Becker
pHD229	RFP::Nt-Rac5 (DN)	amp	Becker
pHD230	RFP::Nt-Rac5-R69A	amp	Becker
pHD254	RFP::Nt-Rac5Q64L	amp	Becker

4.9.3 Oligonucleotides

Oligonucleotides were exclusively purchased from MWG (Ebersberg) and delivered as lyophilized powder. Each oligonucleotide was dissolved in double distilled water and a DNA concentration of 100 pmol μl^{-1} was adjusted. Oligonucleotides were stored at -20°C and diluted to 20 pmol μl^{-1} before use in a sequencing reaction.

Table 10: Oligonucleotides

- i. Oligonucleotides are listed in 5' → 3' direction. Restriction sites are marked by bold letters.
- ii. Oligonucleotides used for site-directed mutagenesis are listed in 5' → 3' direction. Introduced point mutations are underlined.

Table 10A: Oligonucleotide primers for the amplification of Nt-Hyp01 sequences and antisense experiments

Name	Sequence	Restriction site(s)
Nt-Hyp01: probe for Northern Blot		
bot42	5'-GCACCAAGAGGCCGGAGG-3'	
bot43	5'-GAAATAAGACATTCAAAATAGGACAC-3'	
Nt-Hyp01: ATG and stop primers		
bot66	5'-TAGCCGGCGGAACAATGGGGAAGTACGTGGAG-3'	NgoMIV
bot67	5'-TAGAGCTCGAGTCGTTTCATCCAATTACAACG-3'	XhoI, SacI, MlyI
Nt-Hyp01: antisense primers		
bot157	5'-GCCAAAATCGCCAATAGA-3'	
bot158	5'-TTCCCCATCTCCCCTCCTC-3'	
bot159	5'-TCTATTGGCGATTTTGGC-3'	
bot160	5'-GACCGAATTCTATTGGCGA-3'	
bot161	5'-GCGTTGTTACAGAAAGCAC-3'	
bot162	5'-CATCATCAGCCTTGGAAAG-3'	
bot163	5'-GATCCTTGGTGTCCATTTC-3'	
NtHyp01: PCR primers for SALK line 531590 (At3g57450)		
bot176	5'-GGTTCCTTCCTTGTACTC-3'	
bot177	5'-GATCTCTAGCGTCATCATAC-3'	
Nt-Hyp01: pHANNIBAL primers		
bot245	5'-CGATGGATCCGGTACCGGAAGTACGTGGAGATGCTGGAT-3'	BamHI, KpnI
bot246	5'-CGATTCTAGACTCGAGGCCAGATGATGATCTCGTTAACAAACAC-3'	XbaI, XhoI

Table 10B: Oligonucleotide primers for the amplification of NtPLC sequences and introduction of restriction sites

Name	Sequence	Restriction site(s)
NtPLC: probe for Northern Blot (coding region)		
wen77	5'-CTGGGAATCAACTAAGTAGTG-3'	
bot53	5'-GTTCCGCTGAGTGAACCTG-3'	
NtPLC1 and NtPLC2 RT PCR		
wen74	5'-TTCTTCTCGAGGCCGGCGCAACAATGTGCGAGACAGACGTACAGAGTC-3'	NgoMIV, XhoI
wen75	5'-TTCTTCCGCGGTTAGACAAATTCGAAACGCATAAGAAGC-3'	SacII
wen76	5'-TTCTTCCGCGGCTAACCATGGTACCTGAAACTCGTG-3'	SacII

NtPLC: sequencing primers		
wen78	5'-CCCAGAATCTCTGAAAAGACG-3'	
wen79	5'-CAGATCTTCGATCCTGAAGC-3'	
wen80	5'-CATCTTTGGCGGAATTTGGC-3'	
wen81	5'-ATCATCTTCCACACCTGCTC-3'	
wen82	5'-TCCCCATAAATACGGTCAC-3'	
NtPLC: PCR primers		
wen83	5'-TTCTTACTAGTTATGTGCGAGACAGACGTACAGAGTC-3'	SpeI
wen84	5'-TTCTTCTCGAGTTAGACAAATTCGAAACGCATAAGAAGC-3'	XhoI
NtPLC3 and 4: 3' primers for COOH-terminal fusions (without stop codon)		
bot207	5'-CTGCCGGCCTCGAGAAGGACAAATTCGAAACGCATAAGAAGC-3'	XhoI, NgoMIV
bot208	5'-CTGCCGGCCTCGAGAAGGACATATTCGAAACGCATAAGAAGC-3'	XhoI, NgoMIV
NtPLC3 and 4: forward sequencing primer		
bot270	5'-CATGGAGCTCAAATGGTGGC-3'	
NtPLC: pHANNIBAL primers (for RNA interference)		
bot272	5'-ATGCGGATCCGAATTCCGTGTTCTGATATCAACTAAGC-3'	BamHI, EcoRI
bot273	5'-TAGCTCTAGACTCGAGACGCATAAGAAGCTTCACAGAGT-3'	XbaI, XhoI
NtPLC3: primers for truncation constructs		
bot286	5'-TTCTTCTCGAGGCCGGCGCAACAATGAATGAGCCTTTGTCTCATTAC-3'	NaeI, NgoMIV
bot287	5'-TCGAATCCCCGGGGACATATTCGAAACGCATAAGAAGCTTC-3'	SmaI
bot288	5'-TCGAATCCCCGGGTCCACAACCACCATTGGATCTGAAC-3'	SmaI
bot289	5'-TCGAATCCCCGGGCCACGTTTAGGATTAATAGGAGGAT-3'	SmaI
bot290	5'-TTCTTCTCGAGGCCGGCGCAACAATGGATATATTATTGAAAGCAGGTCC-3'	NaeI, NgoMIV
bot323	5'-ATGCGGCCGCATTAGACATATTCGAAACGCATAAG-3'	NotI
NtPLC3: probe for Northern Blot (3' UTR)		
bot342	5'-CTTTGTCAATATATGGGGTGAG-3'	
bot343	5'-TCACACATATTACCATAACATC-3'	
NtPLC3: primers for site-directed mutagenesis		
bot211	5'-GGTGTACGAGTAATTGAATTGCGTATATGGCCAAATTCC-3'	Asp 156 > Arg
bot212	5'-GGAATTTGGCCATATACGCAATTCAATTACTCGTACACC-3'	
bot320	5'-CATTACTTCATATACACAGGAGCTAATTCCTATCTAACTGG-3'	His 124 > Ala
bot321	5'-CCAGTTAGATAGGAATTAGCTCCTGTGTATATGAAGTAATG-3'	

4.9.4 Isolation of plasmid DNA

4.9.4.1 Plasmid DNA isolation from *E. coli*

4.9.4.1.1 TELT mini-preparation

The TELT miniprep method was an easy way of identifying positive clones after a ligation/transformation step. It has to be considered that the TELT miniprep is supposed to be a so-called “dirty” miniprep and that the DNA was neither used for further particle-bombardments nor cloning steps.

Single colonies were inoculated in 2 ml LB medium plus appropriate antibiotic, each in a 15 ml sterile plastic tube, and grown at 37°C, 200 rpm, for at least eight hours, preferentially ON. Approximately 1 ml of cells was transferred to 1.5 ml Eppendorf tubes and harvested by centrifugation in a Biofuge *pico*; 10.000 rpm, 2 min. The supernatant was discarded and the pellet dissolved in a TELT/lysozyme solution (see Table 11). After vortexing and incubation for 10 min, cells were heat-shocked for 3 min at 95°C and immediately cooled down on ice for 5 min. After spinning for 15 min at 13.000 rpm cell lysates were removed with a toothpick and 300 µl 96% ethanol were added to the tubes and incubated for 5 min at RT. The DNA was spun down at 13.000 rpm for 15 min, the supernatant was discarded and the pellet washed with 300 µl 70% ethanol. The pellet was dried upside down for about 15 min and dissolved in 50 µl 10 mM Tris-Cl, pH 8.0.

TELT solution: 50 mM Tris, 62.5 mM EDTA, 8 M LiCl, 10 % Triton-X 100

Table 11: Assay mixture for TELT mini-preparations

	12x + 1	24x + 2	36x + 5	48x + 6
Lysozyme	8.13 mg	16.25 mg	25.64 mg	33.77 mg
TELT sol.	1.625 ml	3.25 ml	5.1 ml	6.75 ml

4.9.4.1.2 Mini- and maxi-preparations

For DNA purifications, which served for particle bombardments and further cloning steps, also in order to gain larger amounts of DNA, the E.Z.N.A. plasmid purification kit (PeqLab, Erlangen) and the JetStar 2.0 maxi prep (Genomed, Löhne) were employed. Purifications were performed following the manufacturers' instructions.

4.9.4.2 *S. cerevisiae* HF7c glycerol stocks and plasmid preparation

Resulting colonies from a yeast two-hybrid screen were picked from the plate and transferred into 6 ml SD –leu –trp-liquid medium. Cells were grown at 30°C, 200 rpm for 48 h and then 750 µl of the culture were mixed with 750 µl of 50 % glycerol, vortexed and frozen at –80°C.

The rest of the cells was pelleted into a 2 ml Eppendorf tube and the supernatant discarded. The pellet was resuspended with 20 µl double distilled H₂O and 200 µl of lysis buffer, 200 µl phenol/chloroform (1:1; pH 8.0) and 200 mg glass beads (diameter: 425-600 µm) were added and the whole assay was vortexed for 2 min and centrifuged for 5 min at 1300 rpm. The upper, aqueous, phase was extracted and transferred to a new tube containing 200 µl chloroform. Tubes were centrifuged for another 5 min at max speed and the upper phase transferred to a new 2 ml-tube containing 20 µl 3 M NaAc and 400 µl EtOH. After mixing the tubes, an incubation of 1 h at –20°C in the freezer followed. Centrifugation at 4°C for 5 min at max speed pelleted the plasmid DNA. DNA was washed two times with 70 % EtOH and dried carefully upside down. The pellet was dissolved in 20

μ l double distilled H₂O and 2 μ l of DNA were dialysed for at least 15 min and transformed into XL1 Blue *E. coli* cells by electroporation. Transformation into *E. coli* served for a detailed characterization of the putative interactor. Larger amounts of DNA were gained by *E. coli* maxi preparations and served for restriction analyses and sequencing reactions as well as for yeast control experiments such as the plasmid scale transformation in order to confirm interactions between the proteins of interest.

4.9.5 Isolation of genomic DNA from plants

Two to five leaves were taken of each plant (*Arabidopsis* leaves' size), combined in a 1.5 ml Eppendorf tube and frozen in liquid nitrogen. Leaves were homogenized with a small plastic grinder until only a thin powder was visible. 800 μ l of CAPS buffer were added and leaves were macerated during 5 to 10 min. After centrifugation in a Biofuge *pico* at max speed for 5 min the supernatant was transferred into a new Eppendorf 1.5 ml tube and 750 μ l isopropanol were added and vortexed. Precipitation lasted from 30 min to 1 h at -20°C . A centrifugation step at max speed for 10 min pelleted the DNA, which was resuspended in 75 % EtOH with a pipet tip and pelleted. Washing was repeated twice. Finally the pellet was resuspended in 50 μ l sterile double distilled water by smooth vortexing. The insoluble part was briefly centrifuged and 1 to 2 μ l of the supernatant were used for PCR. The extracted DNA was stored at $+4^{\circ}\text{C}$.

CAPS buffer: 200 mM Tris-Cl, pH 7.5; 250 mM NaCl; 25 mM EDTA, pH 8.0; 0.5 % SDS

4.9.6 Determination of DNA concentration

Concentration and quality of a sample of DNA were measured with the UV spectrophotometer Pharmacia LKB Ultraspec III in quartz cuvettes ($d = 1$ cm). A solution containing 50 μ g per ml of double strand DNA has an absorbancy (optical density) of 1.0 at a wavelength of 260 nm. DNA quality measurement is based on the fact that OD at 260 nm is twice that at 280 nm if the solution contains pure DNA. Contaminants contribute to an additional OD which decreases the OD ratio between 260 and 280 nm. Clean DNA has an $\text{OD}_{260}/\text{OD}_{280}$ ratio of 1.86. DNA determination followed the formula: $\varepsilon = 20 \mu\text{l} \times \mu\text{g}^{-1} \times \text{cm}^{-1}$.

4.9.7 DNA restriction endonuclease analysis

The restriction endonucleases used in this study all belong to the type II of restriction endonucleases (Sambrook and Russel, 2001), which recognized a symmetric DNA sequence and cut in within this sequence. The only exception was Mly I, which was used to delete stop codons and produced blunt ends for COOH-terminal fusions. The volume of the added enzyme solution was maximal 10 % of the total volume of the restriction assay. Per μ g DNA 3 U of enzyme were used and the appropriate buffer added, following the manufacturer's advice (New England Biolabs; Bad Schwalbach). Incubation usually lasted from one to several hours at the optimal temperature for each enzyme. Restriction assays used to identify positive clones after a ligation/transformation reaction were performed with 1 μ g DNA, preparative assays for further cloning used 3 to 5 μ g DNA.

4.9.8 DNA dephosphorylation

In order to prevent a recircularization of single-cut vectors, the ends of the vector were dephosphorylated by CIP (Calf Intestinal Alkaline Phosphatase; New England Biolabs, Bad Schwalbach) and a circularization could only occur, when vector and insert were ligated by a phosphorylated linker-DNA. Per μg DNA 2 U of CIP were used and incubated at 37°C for 1 h in the restriction buffers 2, 3 or 4 supplied by New England Biolabs.

4.9.9 Ligation

For the ligation reaction 200 ng of vector and 3 times molar excess of the insert plus 2 U ligase were used in a total volume of 10 μl . Ligation buffer was supplied by the T4-DNA ligation kit (New England Biolabs) and the reaction was performed at 16°C preferentially ON. One to five μl of this assay were directly used for chemical transformations and/or electroporations.

4.9.10 cDNA synthesis

In order to synthesize cDNA from RNA, total RNA had to be extracted from plant tissue (see Trizol protocol 4.10.1). Then 2 μg RNA were transcribed by using the GeneRacer SuperScriptTM II RT Module by Invitrogen (Karlsruhe) employing an Oligo-dT primer and following the manufacturer's instructions. To prevent degradation of the RNA, RNaseOUTTM (Invitrogen) was added to the assay, and the cDNA was stored at -20°C .

4.9.11 PCR techniques

The polymerase chain reaction is a method to specifically and exponentially amplify DNA sequences in an automatic, cyclic, *in vitro* reaction by employing gene-specific oligonucleotides. A typical PCR-reaction consists of three temperature steps. First, the *template*, the double-stranded DNA, is denatured at 95°C in order to gain single-stranded DNA. Second, at lower temperature (68°C - 42°C) the specific oligonucleotides anneal to the single-stranded DNA (*annealing*). The third step, the *elongation*, serves for chain extension through a heat-stable DNA polymerase at 72°C . In the following cycles the products from the first reactions serve as well as templates. Apart from the *Taq* DNA polymerase, the *Pfu* and Phusion DNA polymerases were used in this study, which contain a $3' \rightarrow 5'$ exonuclease activity, a *proof-reading* function, in order to recognize and remove nucleotides incorporated by mistake to minimize mutational mistakes during the amplification reaction. For further cloning reactions *Pfu* and/or Phusion DNA polymerases were exclusively used and each PCR protocol was specifically adjusted. *Taq* DNA polymerase only served for control reactions to identify positive clones or correct orientations of inserts.

In a total volume of 50 or 100 μl per assay approximately 10 to 20 ng DNA template were used as well as 20 to 50 pmol oligonucleotide-primer, 20 nmol dNTPs and between 0.7 to 2.0 U DNA polymerase plus the appropriate buffer. The PCR was performed in a thermocycler Biometra T gradient (Biometra, Göttingen) and the temperature conditions were adjusted before each reaction. The annealing temperature was chosen considering the specific melting temperature, with respect to the length of each oligonucleotide.

Probes for Northern Blot analyses were produced in the same way with the exception of DIG-labeled nucleotides instead of unlabeled ones.

Table 12: Example reaction scheme for a *Taq* PCR

Example for a <i>Taq</i>-PCR:	initial denaturation	95°C	3 min	1 x
	denaturation	95°C	30 sec	20-30 x
	annealing	42-68°C	50 sec	
	elongation	72°C	1 min/kb	
	final elongation	72°C	3 - 5 min	1 x

4.9.11.1 Site-directed mutagenesis PCR

The site-directed mutagenesis is a method to introduce specific changes in a known DNA sequence. *In vitro* DNA mutations are introduced, which result in deletion, insertion or exchange of specific nucleotides. Structural and catalytic properties of proteins can easily be influenced by this method. In this study amino acids are substituted with gene-specific oligonucleotides against the NtPLC3 and NtPLC4 by site-directed mutagenesis based on the QuickChange™ site-directed mutagenesis kit by Stratagene (Amsterdam, The Netherlands) following the manufacturer's protocol.

4.9.12 Purification of PCR products

The purification of PCR products was done with the E.Z.N.A. Gel Extraction Kit from PeqLab (Erlangen).

4.9.13 Sequencing

Sequencing reactions were performed by the Sequence Laboratories Göttingen GmbH.

4.9.14 DNA agarose gel-electrophoresis

The separation of DNA fragments according to their length occurred in agarose gels with 0.7 to 1.5 % agarose in 1 x TAE buffer. Before loading DNA on the gel it was supplemented with 5 x loading buffer. After heating the appropriate amount of agarose in 1 x TAE buffer, the solution was cooled down to 60°C and the intercalating DNA-stain ethidium bromide was added to a final concentration of 0.5 µg ml⁻¹. Gels were run in horizontal electrophoresis chambers in 1 x TAE buffer at a constant current of 90 V for 1 h or longer. Finally the DNA was visible under UV illumination, images were taken or specific DNA bands were cut and further purified.

50x TAE buffer: 2 M Tris-base, 1 M Sodium acetate, 50 mM Na₂-EDTA, pH 7.2

5x loading buffer: 15 % (w/v) Ficoll, 0.05 % (w/v) Bromphenolblue, 0.4 % (w/v) SDS, 50 mM EDTA, pH 8.0 in TAE buffer

4.9.15 Purification of DNA fragments from agarose gels

The correct DNA band was separated from the rest of the agarose gel with a clean scalpel and purified with the E.Z.N.A. Gel Extraction Kit from PeqLab (Erlangen) according to the manufacturer's protocol.

4.10 RNA-related techniques

4.10.1 Isolation of total RNA

The RNA extraction for cDNA synthesis and Northern Blot analysis followed the so-called Trizol protocol following the manufacturer's recommendations (Invitrogen; Carlsbad, CA, USA). Plant tissue was frozen in liquid nitrogen and homogenized with a small plastic grinder until only a thin powder was visible. Approximately 200 mg of tissue was homogenized with Trizol (1 ml/100 mg) and incubated for 5 min at RT. 0.2 ml chloroform were added per 100 mg tissue, well shaken and further incubated for 2 to 3 min at RT. The tissue was centrifuged in a Biofuge *fresco* for 15 min at 12000 rpm and 4°C. The aqueous phase was transferred to a new tube and 0.5 ml per 100 mg tissue were added. After an incubation of 10 min, centrifugation in a Biofuge *fresco* for 10 min at 12000 rpm at 4°C followed. The pellet was washed with 75 % EtOH, vortexed and centrifuged again for 5 min at 7500 rpm at 4°C. The supernatant was discarded and the RNA dissolved in 20 µl double distilled water and stored at -20°C.

4.10.2 Determination of RNA concentration

Concentration and quality of a sample of RNA were measured in the same way as described for DNA with the UV spectrophotometer Pharmacia LKB Ultraspec III at an OD₂₆₀. RNA determination followed the formula: $\epsilon = 25 \mu\text{l} \times \mu\text{g}^{-1} \times \text{cm}^{-1}$.

4.10.3 Northern Blot analysis

The Northern Blot is a technique for detecting specific RNA, using a labeled DNA probe. It gives information about the expression level of RNAs and about their tissue specificity. In preparation for the blot 5 µg RNA per lane were adjusted to the same volume with water and the same volume of loading dye was added. Probes were then denatured for 5 min at 95°C and cooled down on ice before loading on the agarose gel. The gel usually contained 1.5 % agarose, 1 x MOPS and water. Formaldehyde was added after cooling down to about 55°C to a final concentration of 0.6 M. The gel was run in 1 x MOPS for usually 1.5 h and was soaked in 10 x SSC to remove the formaldehyd before taking a photograph of the gel with a ruler beside. The gel was then placed upside down on three 3MM Whatmann papers placed on a gel tray in a glass petri dish of 15 cm diameter. The Whatman paper at the bottom formed a bridge and contacted the 10 x SSC solution in the lower glass petri dish. A membrane (DuralonUV Membrane; Stratagene; Amsterdam, The Netherlands) was cut in exactly the same size as the gel and placed on the top, all air bubbles were removed. Three Whatman papers were placed on the membrane and an approximately 5 cm thick layer of tissues was placed on the top. Finally the second half of the glass petri dish was placed on the tissues, a weight was added and the blot lasted ON. The next morning the

membrane was removed and incubated for 5 min in 2 x SSC, dried to damp before UV-crosslinking (Stratalinker) the RNA with the membrane. In order to test the efficiency of the blotting another image of the membrane was taken with the UV-illuminator.

At the same time the sequence of interest was amplified by PCR and the nucleotides contain a certain amount of DIG-labeled nucleotides. 5 µl of the PCR product were loaded and confirmed by agarose gel-electrophoresis. The rest of the PCR product was added to 10 ml of hybridization buffer and mixed. 200 µl of the probe and 200 µl of salmon sperm DNA (10 mg ml⁻¹) were combined and denatured for 5 min at 90°C. Hybridization solution was heated to approximately 45°C and the blot was pre-hybridized for 30 min to 3 h in pre-hybridization buffer at 42°C before exchanging the buffer with hybridization buffer and adding the probe to the blot and hybridizing ON in the hybridization oven.

The washing stringency was adjusted for each probe according to the percentage of homology of probe to tissue RNA. Generally for a 100 % homology the blot was washed once with 2 x SSC at RT followed by three washing steps with 0.1 x SSC/0.1 % SDS at 55 °C for 15 minutes in the hybridization oven. The hybridization tube was drained off well and the membrane detached from the wall before returning to the hybridiser. The blot was rinsed once with incubation buffer before transferring it to a small plastic box and blocking for 1 h with blocking buffer at RT. Usually 1 µl of anti-DIG antibody (10 µl in 100 ml blocking buffer) was added to the blocking buffer and incubated for at least 1 h. After three washing steps for 15 min each with wash buffer, the blot was rinsed with AP buffer and transferred to a film cassette. Two layers of transparency sheet were cut and one placed in the cassette under the blot. The chemiluminescence substrate was diluted 1:100 with AP buffer, added to the blot and incubated for 5 min. The second transparency layer was placed on the blot and the film added. The film was exposed usually for 5, 15 and 30 min or ON.

Loading buffer (750µl): 100 µl 10 x MOPS, 135 µl 37 % formaldehyde, 50 µl 80 % glycerol, 1 µg bromophenol blue, 460 µl formamide, 5 µl H₂O

Pre-hybridization solution: 50 % formamide, 4 x SSPE, 1 % SDS, 7.5 x Denhardt's

Hybridization solution: 47 % formamide, 3 x SSPE, 1 % SDS, 6.5 x Denhardt's

Incubation buffer: 100 mM maleic acid, pH 7.5; 150 mM NaCl

Blocking buffer: 1 % blocking reagent (Roche Cat No. 1096176), 100 mM maleic acid, 150 mM NaCl

Wash buffer: 100 mM maleic acid, 150 mM NaCl, 0.3 % Tween-20

AP buffer: 100 mM Tris, pH 9.5; 100 mM NaCl

Antibody: Anti DIG-AP-Fab-fragments (Roche Cat No. 1 093 274)

Chemiluminescence substrate: CDP-star (25 mM disodium 4-chloro-3-(methoxyspiro)1,2-dioxetane-2,2'-(5'-chloro)tricyclo(3.3.1.1^{3,7})decan)-4-yl)-phenyl phosphate; Roche Cat No. 1 685 627)

4.11 Methods related to protein treatment

4.11.1 Discontinuous SDS polyacrylamide gel-electrophoresis (SDS PAGE; Laemmli 1970)

Proteins are denatured by sodium dodecylsulfate and negatively charged. Usually the ratio of SDS to amino acids is one molecule SDS to 1.4 amino acid residues. The charge of the protein is of minor importance compared to the negatively charged SDS-protein complex,

so that SDS-loaded proteins show an identical charge-mass-ratio. Thus, the separation is only based on the sieve effect of the polyacrylamide gel. Discontinuous SDS PAGE first focuses the proteins in the stacking gel to one line, whereas the separating gel divides the proteins according to their molecular mass.

Table 13A: Solutions and buffers used for SDS PAGE:

Solution/Buffer	Composition
PAA stock	Bisacrylamide 37.5:1; usually as 30 % solution
4 x Upper buffer	0.5 M Tris-Cl pH 6.8; 0.4 % (w/v) SDS
4 x Lower buffer	1.5 M Tris-Cl pH 8.8; 0.4 % (w/v) SDS
Loading buffer	0.2 M Tris-Cl pH 6.8; 8 % (w/v) SDS, 40 % (w/v) Glycerol, 400 mM DTT, 0.4 % BPB
Running buffer	5 mM Tris-Cl, pH 8.3; 14.4 g Glycine; 1 % SDS

Table 13B: Example assay for a discontinuous gel:

4 % stacking gel and 12 % separating gel

Solution/Buffer	stacking gel	seperating gel
PAA	375 μ l	2.00 ml
4x Upper buffer	625 μ l	-
4x Lower buffer	-	1.25 ml
H ₂ O	1.5 ml	1.75 ml
10 % APS	30 μ l	30 μ l
TEMED	7 μ l	7 μ l

Before loading proteins on the SDS PAGE, loading dye was added to the proteins and they were denatured at 95°C for 5 min. Gels were run at 90 V until proteins reached the separating gel and the current was then enhanced to 130 V and gels ran up to 2 h. Gels were removed from the apparatus and stained for 20 min in Coomassie-Brilliant-Blue. Destaining solution was afterwards added to the gels and constantly changed (3 to 4 times) until clear bands were visible. SDS PAGEs for Western Blot analyses were not stained, but immediately transferred to the Western Blot cassette.

Coomassie-Brilliant-Blue: 2.5 % (w/v) Coomassie-Brilliant-Blue R250, 10 % (v/v) glacial Acetic acid, 45 % (w/v) Methanol

Destaining solution: 7 % (v/v) glacial Acetic acid, 20 % (v/v) EtOH

4.11.2 Western Blot analysis

Sufficiently separated proteins in the SDS-PAGEs can be transferred to a nitrocellulose membrane for Western Blot analysis. For this procedure, an electric current is applied to the gel so that the separated proteins are transferred through the gel and onto the membrane in the same pattern as they separate on the SDS PAGEs.

When the SDS PAGE finished running the stacking gel was removed and the separating gel was placed in a Western-Blot cassette on a sponge and two layers of Whatman paper, pre-wetted in transfer buffer. A nitrocellulose (BioTracer®NT; PallCorporation; Ann Arbor, USA) was cut exactly in the size of the separating gel, pre-wetted and carefully placed on the gel, air bubbles were excluded. In the same way two layers of pre-wetted Whatman paper were also placed on the nitrocellulose, the sponge was added and the

cassette was closed and inserted into the transfer unit of the Western Blot chamber. The cassette was placed in that way that the current was flowing through the gel onto the nitrocellulose, *i.e.*, the gel in direction to the cathode and the nitrocellulose in direction to the anode. Transfer buffer was added to the chamber and the transfer occurred for four hours or ON with a setting of 20V / 40 mA. After four hours or the next morning the nitrocellulose was removed from the chamber. It could either be stored at 4°C until the immunostaining was started or directly be transferred to a plastic box or blocked with 5 % non-fat dry milk powder dissolved in PBS by gently shaking for at least 1 h in order to saturate unspecific binding. The polyclonal primary antibody, which binds specifically to the protein of interest, was added to the blocking buffer and incubated for at least 2 h at RT, preferentially ON. After removing the primary antibody the blot was washed three times with PBS for 15 min to remove unbound primary antibodies. The secondary antibody was also diluted in 5 % non-fat dry milk powder plus PBS and then added to the blot and incubated for another 2 h. The secondary antibody binds to the first antibody, coupled either with a horseradish peroxidase or an alkaline phosphatase. The blot was washed three more times with PBST for 15 min to remove unbound secondary antibodies. The whole procedure was then transferred to the dark room. Before, two transparency sheets were cut and one of them was placed into the film cassette, a luminol solution (A) and an oxidizing solution (B) were mixed in a 1:1 ratio in the dark room and distributed over the blot. After 1 min the excess liquid was drained off, the transparency sheet and the film added and the cassette was closed. Usually the exposure time lasted for 30 min according to the probes used. The principle of the HRP-enhanced chemiluminescence system (ECL) is that the peroxidase oxidizes luminol in presence of H₂O₂ and that the oxidation product then emits light which can be detected by the film.

Transfer buffer: 14.4 g/l Glycin, 3 g/l Tris-Cl, 0.05 % SDS

PBS: 137 mM NaCl, 2.7 mM KCl, 10 mM Na₂HPO₄, 2 mM KH₂PO₄

PBST: PBS + 0.3 % Tween-20

Solution A: 100 mM Tris-Cl, pH 8.5; 90 mM p-coumaric acid; 250 mM 3-aminophthalhydrazine

Solution B: 100 mM Tris-Cl, pH 8.5; 30 % H₂O₂

4.11.3 Protein over-expression and purification of GST fusion proteins from *E. coli*

Proteins encoded by a tobacco pollen tube cDNA library, identified by PCR or Yeast two-hybrid screens were expressed as recombinant glutathione S-transferase fusion proteins. Through the specific binding of GST to glutathione, which is further covalently bound to sepharose 4B through oxirangroups (binding capacity: > 8 mg GST ml⁻¹) it is possible to isolate fusion proteins from *E. coli* cell extracts in only one affinity-chromatographic step. The specific coding region of the proteins was cloned in frame into the multiple cloning site of the expression vector pGEX-4T-2 (Amersham Pharmacia, Freiburg), resulting in a NH₂-terminal GST fusion to the protein of interest. The respective plasmid was transformed by electroporation into *E. coli* strain BL21 (DE3; Stratagene; Amsterdam, The Netherlands). A pre-culture of *E. coli* transformants was grown in 2 ml LB medium at 37°C for several hours and 50 µl of the pre-culture transferred to a 1 l ON culture, which grew at RT to an OD₆₀₀ 0.6 to 0.9 and was then induced with 1 mM IPTG for 90 to 120 min. Cells were harvested by centrifugation in a Beckman centrifuge J2-21 for 5 min at 2800 x g and the pellet was dissolved in 20 ml lysis buffer plus proteinase inhibitors. Cells were then treated twice with french press EmulsiFlex-C5 (Avestin; Ottawa, Canada) at 13000 psi, centrifuged, the supernatant containing the protein was transferred to a new

tube and 300 μ l glutathione S-sepharose 4B (Amersham Pharmacia, Freiburg) were added to the supernatant and incubated for 30 min on ice. The fusion proteins produced were purified on a mini-column and eluted with 100 μ l glutathione elution buffer. For storage, proteins were stored on the beads in a storage buffer containing 50 % glycerol.

The purity of the affinity-chromatography-purified recombinant proteins were assessed by SDS PAGE and the amount of protein was determined on Coomassie-stained gels using BSA as standard.

Lysis buffer: 50 mM Tris-Cl, pH 7.5; 5 mM MgCl₂; 250 mM NaCl

Proteinase inhibitor mix: 100 mM Antipain-HCl, 10 mM Bestatin, 1 mM E-64, 10 mM Leupeptin, 1 mM Pepstatin A, 200 mM Phenantroline, 0.5M PMSF

Glutathione elution buffer: 10 mM glutathione (reduced); 50 mM Tris-Cl, pH 8.0

Storage buffer: 50 mM Tris-Cl, pH 7.5; 5 mM MgCl₂; 250 mM NaCl; 50 % glycerol

4.11.4 Antibody preparation

A NH₂-terminal GST fusion to the protein of interest was generated and treated the same way as described above. The protein was over-expressed and loaded onto a SDS PAGE. The gel was Coomassie-stained and a band at the expected size of the protein was separated from the rest. The whole gel slice was sent to Eurogentec (Seraing, Belgium) and one rabbit was immunized. The pre-immune serum, first and final bleed were tested by Western Blots (see protocol above).

4.11.5 *In vitro* interaction studies

Additionally to yeast two-hybrid interactions and *in vivo* interactions, *in vitro* pull-down assays were performed. GST fusion proteins of Nt-Hypo1 and Nt-Rac5 and its mutants were expressed in the pGEX-4T vector as described earlier. The pGEX-4T vector contains a thrombin-cleavage site to separate the protein of interest from its GST-tag. Wild-type Nt-Rac5, CA-Nt-Rac5 and DN-Nt-Rac5 were first cleaved off the GST by thrombin. After thawing the stored proteins on beads (-80°C) on ice and washing three times with PBS on a mini-column by centrifugation (Biofuge *fresco*: 3000 rpm, 1 min, 4°C), 500 μ l of thrombin (5000 U) were added and incubated for 3 h on ice by gently shaking. The flow-through was collected by centrifugation at 3000 rpm for 2 min at 4°C . 100 μ l of the cleaved-off protein were pre-incubated for 10 min in a proteinase inhibitor cocktail before the interaction reaction was started. Then an excess of the second protein, approximately 2.5 μ g, was added and adjusted with PBS to a total volume of 500 μ l. An incubation for 1 h on ice followed before washing the assay three times with 300 μ l PBS. Elution of the interaction products occurred through the addition of 100 μ l glutathione elution buffer, followed by a 15-min incubation on ice. As negative control served an excess of empty pGEX-4T vector added instead of the interactor to the fusion protein. Flow-through and elution products were separated on a 12 % SDS PAGE and tested by Western Blot analysis (see above).

Proteinase inhibitor cocktail: 100 mM Antipain-HCl, 1 mM E-64, 10 mM Leupeptin, 1 mM Pepstatin A, 0.5 M PMSF

4.12 Transient ballistic transformation of *Nicotiana tabacum* pollen grains

The transient transfection of *Nicotiana tabacum* pollen tubes with plasmids driven by the pollen-specific lat52 promoter was achieved by the use of the Biolistic PDS-1000/He system (Bio-Rad, München) according to the manufacturer's directions and described below.

4.12.1 Particle preparation

60 mg of gold particles of 1.6 μm diameter (BioRad, München) were washed with 1 ml EtOH by vortexing vigorously and centrifugation, two times with 1 ml sterile double distilled H₂O and finally dissolved in 1 ml 50 % sterile glycerol. For particle coating the gold suspension of 1.5 mg gold was constantly vortexed while 1 μg of plasmid and 25 μl of 2.5 M CaCl₂ and 10 μl 0.1 M spermidin were added. The assay was vortexed for further 3 min before spinning for 5 sec at < 4000 rpm. The supernatant was carefully removed and 125 μl 96 % EtOH were added by pipetting up and down and thereby dissolving the gold pellet. Tubes were centrifuged again, the supernatant discarded and the pellet dissolved in 18 μl 96 % EtOH. Tubes were again kept vortexing until they were distributed to two macrocarriers.

4.12.2 Pollen bombardment

Pollen grains were harvested immediately before use by vacuum filtration. One flower was used for one particle bombardment. Mature anthers were removed from the flower and vortexed in a volume of 5 ml 1 x PTNT, filtered and the liquid was removed through a nitrocellulose membrane (Millipore MF™ Membrane Filters, 0.45 μm). The nitrocellulose was pressed upside down on a small petri dish (diameter: 5.5 cm) coated with 1 x PTNT containing phytigel and thereby distributing the pollen equally on the plate.

When macrocarriers were covered with gold particles, the particles were delivered into the pollen tubes using 1100-pounds per square inch rupture discs under a vacuum of 25 inches of Hg. Transfection was achieved when the particle hit the nucleus of the pollen tube and expression was visible 4 to 6 h after bombardment. After bombardment, petri dishes with pollen tubes were sealed with parafilm and kept in the dark.

2 x PTNT: 10 % Sucrose, 0.6 % MES (15 mM), 0.06 % casein acid-hydrolase, 2 x salts, 20 mg/l rifampicin, 25 % PEG-6000; pH 5.9; filter sterilized and stored at 4 °C

10 x Salts: 10 mM CaCl₂, 10 mM KCl, 8 mM MgSO₄, 16 mM H₃BO₃, 300 μM CuSO₄

Phytigel: 0.5 % phytigel (Sigma P8169)

1 x PTNT plates (diameter: 5 cm): 50 % 2 x PTNT, 50 % 0.5 % phytigel (3 ml each plate)

4.13 Stable transformation of *Nicotiana tabacum* plants

The transformation of *Nicotiana tabacum* plants via “leaf-disc transformation” was performed by the use of *Agrobacterium tumefaciens*, strain AGL1 (rifampicin resistance; Lazo *et al.*, 1991).

4.13.1 Preparation of *A. tumefaciens* for transformation

A pre-culture of 5 ml YEP medium plus appropriate antibiotic was inoculated with a single colony of agrobacteria and incubated for two days at 28°C. 40 ml YEP-induction medium were inoculated with the pre-culture and shaken for four hours at 28°C. Cells were then harvested in a Heraeus Megafuge 1.0R at 5300 rpm for 5 min. The supernatant was discarded and the pellet resuspended in 40 ml MS-transformation medium.

4.13.2 Leaf-disc transformation

Sterily grown leaves of *Nicotiana tabacum* were cut into 1 cm² pieces and transferred into MS-transformation medium containing *Agrobacteria tumefaciens* and incubated for 30 min at RT. Leaf discs were then transferred to sterile petri dishes containing wet filter paper. Leaves were placed upside down on the filter paper, petri dishes sealed with parafilm and stored in the dark at RT. After two days the leaf discs were transferred to 40 ml MS-claforan liquid medium and slowly shaken for 20 min. This washing step was repeated once. Leaves were then transferred to selective MS-agar plates, containing ammonium glufosinate for tobacco selection, ticarcillin and claforan to inhibit further agrobacteria growth and carbenicillin in order to prevent growth of other microorganisms. Plates were kept at RT for several weeks under constant light in a growth chamber.

4.13.3 Shoot induction

Leaf discs were kept for several weeks until small calli were visible at their edges. Calli were isolated from the leaves and grown further on fresh selective MS-agar plates. After a few weeks, shoots were visible emerging from the calli and these shoots of about 2 to 3 cm height were then transferred to MS-solid selection medium.

4.13.4 From root induction to the flowering plant

Root formation was visible after another few weeks on MS-solid selection medium, containing ammonium glufosinate (2 mg l⁻¹) and ticarcillin (200 µg ml⁻¹). Small tobacco plants were transferred to soil when roots reached a length of about 3 to 4 cm. Then plants were cultivated in soil, first in the growth chamber, then, after reaching a certain size, in the green house until flowering occurred.

4.13.5 β-galactosidase assay

When plants were flowering, pollen grains were harvested from anthers and equally distributed on 1 x PTNT plates containing phytigel. Pollen tubes grew for 3 h in the dark at RT and were then submerged with 100 µl 5- Bromo-4-chloro-3-indolyl b-D-glucuronide

cyclohexylamine salt (X-Gluc) solution and incubated for a further 2 h. In transgenic pollen tubes the β -glucuronidase used X-Gluc as substrate and its product appeared in blue making the RNAi-pollen easily detectable.

4.13.6 Tobacco transformation media

Table 14: Tobacco transformation media

YEP liquid medium		Callus induction	
10 g	Bacto peptone	1 x	MS-salts
10 g	Bacto yeast extract	20 g/l	Sucrose
5 g	NaCl	0.8 % (w/v)	plant agar
ad 1l		adjust pH 5.8 with KOH	
YEP induction medium		400 mg/l	Glycine
	YEP liquid medium	100 mg/l	Nicotinic acid
10 mM	MES, pH 5.8	100 mg/l	Pyridoxin
20 μ M	Acetosyringon	10 mg/l	Thiamin
add appropriate antibiotic select for agrobacteria type and plasmid		100 mg/l	Myo-inositol
		1 mg/l	6-Benzylaminpurine (BAP)
		100 μ g/l	Naphtalenic acid (NAA)
		add appropriate antibiotic to control plant and agrobacteria growth	
MS transformation medium		Antibiotics	
1 x	MS-salts	Agrobacteria	
20 g/l	Sucrose	100 mg/l	Carbencillin or Rifaampicin
10 mM	MES	50 mg/l	Spectinomycin
200 μ M	Acetosyringon	50 mg/l	Kanamycin
adjust pH 5.8 with KOH		Tobacco	
MS claforan		200 mg/l	Claforan
1 x	MS-salts	200 mg/l	Ticarcillin
20 g/l	Sucrose	2 mg/l	Ammonium glufosinate
adjust pH 5.8 with KOH; autoclave and add		X-GLUC (GUS)	
200 μ M	Claforan	5 %	Mannitol
MS selection medium		0.1 M	Na-phosphate pH 7.0
1 g/l	MS powder	0.1 %	Triton X-100
20 g/l	Sucrose	5 mM	Potassium ferricyanide
0.8 % (w/v)	Agar	5 mM	Potassium ferrocyanide
add appropriate antibiotic to control plant and agrobacteria growth		0.2 % or 6 % DMF	X-Gluc
		ad 50 ml	

4.14 [³H] PI-4,5-P₂ activity assay

In this PI-PLC activity assay described earlier by Melin *et al.* (1992), the natural substrate of PI-PLCs, the L- α -Phosphatidylinositol 4,5-bisphosphate was used, ³H-labeled at the second position of the inositol ring. PI-PLCs are enzymes that hydrolyze [³H]-PI-4,5-P₂ into the lipid substrate diacylglycerol (DAG) and the water soluble [³H]-Inositol 1,4,5-trisphosphate ([³H]-InsP₃). The activity of the PI-PLC was determined by liquid scintillation counting of the radioactive water-soluble product [³H]-InsP₃.

4.14.1 Preparation of lipid stock solutions

[³H]-Phosphatidylinositol 4,5-bisphosphate from Hartmann Analytic GmbH (Braunschweig), with a specific activity of 240.5 GBq/mmol in a total volume of 500 μ l chloroform, was distributed to several 1.5 ml Eppendorf tubes to 0.74 kBq (20 reactions). The solvent evaporated under a stream of nitrogen for two hours, the tubes were closed in the presence of nitrogen and sealed with parafilm. Tubes were stored at -20°C and thawed immediately before use.

L- α -Phosphatidylinositol 4,5-bisphosphate disodium salt (Fluka, Neu-Ulm) was dissolved in chloroform to 1 mg/ml, distributed to several 1.5 ml Eppendorf tubes (10 μ l per tube, sufficient for ten reactions) and the solvent evaporated for several minutes under the hood. Tubes were closed, sealed with parafilm and stored at -20°C. The stock solution was prepared by dissolving the contents of a tube containing labeled and unlabeled PI-4,5-P₂ in a total volume of 100 μ l 0.1 % (w/v) sodium deoxycholate dissolved in 50 mM Tris-Cl (pH 6.0) and emulsified by sonification for 10 min to yield a solution of 0.2 mM PI-4,5-P₂ with a specific activity of 0.74 kBq.

4.14.2 Enzyme activity assay

Standard reaction mixture contained 50 mM Tris-maleate (pH 6.0), 1 to 1000 μ M free Ca²⁺ (Ca²⁺/EGTA buffer; Owen, 1976), a sonicated micellar suspension of 0.2 mM PI-4,5-P₂ spiked with 0.74 kBq [³H]-head group labeled PI-4,5-P₂ (see above), 0.02 % (w/v) sodium deoxycholate and 100 ng protein in a final volume of 50 μ l.

The reaction was started either by the addition of enzyme or of 10 μ l of PI-4,5-P₂ stock solutions in 0.1 % (w/v) sodium deoxycholate, as explained above.

The reaction was stopped after 20 min at 25°C by the addition of 1 ml chloroform/methanol (2:1, v/v) and incubation on ice for 5 min. Phase separation was achieved by the addition of 0.25 ml 1 N HCl. After vortexing vigorously and centrifugation for 5 min at 12 000 g in a table-top centrifuge, 0.45 ml of the top phase were transferred to a scintillation vial, supplemented with 3 ml scintillation cocktail Optiphase HiSafe3 (Wallac Oy, Finland) and radioactivity of the InsP₃ fraction was determined by liquid scintillation spectrometry. All data were corrected for background radiation.

Experiments with the PI-PLC inhibitor U-73122 and its inactive analogue U-73343 (Calbiochem; La Jolla, USA) were performed in the same way as described above. The inhibitor and its analogue were dissolved in chloroform and the solvent evaporated directly before addition of protein. The recombinant protein was preincubated in the presence of 1-100 μ M U-73122 or U-73343 for 15 min before adding the substrate lipids.

4.15 Microscopy

4.15.1 Light microscopy

Light microscopy images were used for pollen tube length measurements. For this purpose the inverse light microscope Leica DM IRB HC FLUO was used, employing the N Plan 5x/0.12 PH0, 10x/0.25 PH1 and 20x/0.40 CORR objective.

4.15.2 Epifluorescence microscopy

Epifluorescence images were recorded using the above mentioned Leica DM IRB microscope, equipped with a 50 W mercury lamp, a FITC filter block (excitation: 450 – 490 nm, dichroic: 510 nm; emission: 515 long pass) and a digital camera (ColorView12; Soft Imaging System, Münster, Germany). The same objectives were used as described above.

4.15.3 Confocal laser scanning microscopy

In order to achieve a better subcellular resolution of membrane or organelle labelings the confocal laser scanning microscopy was employed. The microscope used is a Zeiss LSM 510 Meta. Images were taken using the PLAN-Neofluar 5x/0.15 ∞ /0.17, the 10x/0.30, 25x/0.80 Imm Korr DIC ∞ /-, the 63x/1.2 W Korr ∞ /0.15-0.17, C-Apochromat and the PLAN Fluar 100x/1.45 Oil ∞ /0.17 objectives.

Wavelength and filter information:

YFP	excitation: 514 nm
	detection: BP 530-600 nm
	beam splitter: NFT 490

RFP	excitation: 543 nm
	detection: LP 560 nm
	beam splitter: NFT 490

CFP	excitation: 405 nm
	detection: BP 420-480 nm
	beam splitter: HFT 405/514

4.16 Bioinformatic methods

Images recorded by light and/or epifluorescence microscopy were processed with Adobe Photoshop. Digital confocal images were converted and processed with Zeiss LSM 5 Image Browser software. Pollen tube growth rates were measured with Zeiss LSM 5 Image Browser software, but pollen tube-length measurements on digital epi-fluorescence images were performed by using publicly available image analysis software, ImageJ (<http://rsb.info.nih.gov/ij/>). The statistics depending on these measurements were performed with MS Excel. Image presentations were done with MS Power Point 2000.

Software for molecular biology has diverse sources: Alignments, mappings and sequence translations etc. were done with HUSAR – Sequence Analysis Package, a Biocomputing Service at DKFZ (Heidelberg). BLASTs were provided by the National Center for Biotechnology Information (NCBI) at <http://www.ncbi.nlm.nih.gov/BLAST/Genome/>. Cloning preparations, vector designs and restriction enzyme selections were done with Sci Ed CloneManager5 software. Sequence analysis after sequencing was performed with Chromas, version 1.45 (McCarthy 1996-1998). Phylogenetic and molecular evolutionary analyses were conducted using MEGA version 3.0 (Kumar *et al.*, 2004).

5 ABBREVIATIONS AND LIST OF FIGURES AND TABLES

AB	Antibody
3-AT	3-amino-1,2,4-triazole
<i>A. thaliana</i> , At	<i>Arabidopsis thaliana</i>
<i>A. tumefaciens</i>	<i>Agrobacterium tumefaciens</i>
Ala	Alanine
Amp	Ampicillin
APS	Ammoniumperoxisulfate
Arg	Arginine
bp	Basepair
BLAST	Basic Local Alignment Search Tool
BPB	Bromophenol blue
Bq	Becquerel
BSA	Bovine serum albumine
°C	Degree centigrade
CA	constitutively active
Ca ²⁺	Calcium ion
cDNA	copy DNA
CFP	cyan fluorescent protein
Ci	Curie
Cl ⁻	Chloride salt
CLSM	Confocal laser scanning microscopy
cm	Centimeter
conc	Concentration
cpm	counts per minute
COOH-terminus	Carboxy-terminus
CRIB	Cdc42/Rac interactive binding motif
d	Days
da	Dalton
DAG	Diacylglycerol
DMSO	Dimethylsulfoxide
DN	dominant negative
DNA	Desoxyribonucleic acid
DNTP	2'-desoxynucleoside-5-triphosphate
dpm	disintegrations per minute
DTT	Dithiothreitol
<i>E. coli</i>	<i>Escherichia coli</i>
<i>e.g.</i>	<i>exempli gratia</i> (lat., for example)
EDTA	Ethylenediaminetetraacetic acid
EGTA	Ethylenglycol-bis(2-aminoethyl)-N,N,N',N'-tetra acetic acid
<i>et al.</i>	<i>et alii</i> (lat., and others)
EtOH	Ethanol
g	Gramme

g	gravitational acceleration
GAP	GTPase activating protein
GDI	Guanine nucleotide dissociation inhibitor
GDP	Guanosine-5'-diphosphate
GEF	Guanine nucleotide exchange factor
GFP	green fluorescent protein
GST	Glutathione-S-transferase
GTP	Guanosine-5'-triphosphate
GUS	β -glucuronidase (from <i>E. coli</i>)
h	Hour(s)
H ₂ O	water
Hg	Mercury
His	Histidine
³ H-PI-4,5-P ₂	Tritium-labeled phosphatidylinositol-4,5-bis-phosphate
<i>i.e.</i>	<i>id est</i> (lat., that is)
InsP ₃	Inositol-1,4,5-trisphosphate
IPTG	Isopropyl-b-D-thiogalactopyranoside
kan	Kanamycin
kb	Kilobase
kDa	kilo Dalton
kV	kilo Volt
l	Liter
LB	Luria Bertani (medium)
Leu	Leucine
μ g	Microgramme
μ l	Microliter
μ m	Micrometer
μ M	Micromolar
M	Molar
MCS	multiple cloning site
Mg ²⁺	Magnesium ion
min	Minute(s)
ml	Milliliter
mm	Millimeter
mM	Millimolar
mmol	Millimol
mRNA	messenger RNA
<i>N. tabacum</i> , Nt	<i>Nicotiana tabacum</i>
nm	Nanometer
nM	Nanomolar
nmol	Nanomol
NH ₂ -terminus	Amino-terminus

OD	Optical density
ON	over night
PAGE	Polyacrylamide gel-electrophoresis
PBS	Phosphate buffered saline
PCR	Polymerase chain reaction
PEG	Polyethyleneglycol
PI	Phosphatidyl inositol
PI-PLC	Phosphoinositide-specific phospholipase C
PI-4,5-P ₂	Phosphatidylinositol-4,5-bisphosphate
PIP-K	Phosphatidylinositol monophosphate kinase
pM	Picomolar
pmol	Picomol
PMSF	Phenylmethanesulfonylfluoride
psi	Pounds per square inch
RFP	red fluorescent protein
RIC	Rac interacting CRIB motif containing protein
RNA	Ribonucleic acid
RNAi	RNA interference
rpm	Revolutions per minute
RT	Room temperature
RT PCR	reverse transcription PCR
s	Second(s)
<i>S. cerevisiae</i>	<i>Saccharomyces cerevisiae</i>
SDS	Sodium dodecylsulfate
SSC	Standard saline citrat (buffer)
TAE	Tris-acetate-EDTA (buffer)
<i>Taq</i>	<i>Thermophilus aquaticus</i>
TEMED	N,N,N',N'-Tetramethylethylenediamine
Tm	Melting temperature
Tris	Tris(hydroxymethyl)aminomethanol
Trp	Tryptophane
U	Unit
UTR	untranslated region
UV	ultra violett
v/v	Volume per volume
Vol	Volume
WT	wild-type
w/v	Weight per volume
X-Gluc	5-Bromo-4-chloro-3-indolyl b-D-glucuronide cyclohexylamine salt
Y2H	Yeast Two-Hybrid
YFP	yellow fluorescent protein

One-letter code amino acid used in this work:

Alanine	A	Leucine	L
Arginine	R	Lysine	K
Asparagine	N	Methionine	M
Aspartic acid	D	Phenylalanine	F
Cysteine	C	Proline	P
Glutamine	Q	Serine	S
Glutamate	E	Threonine	T
Glycine	G	Tryptophan	W
Histidine	H	Tyrosine	Y
Isoleucine	I	Valine	V

For the presentation of nucleotides in nucleic acids the following symbols were employed:

Adenosine phosphate	A	Thymidine phosphate	T
Cytidine phosphate	C	Uridine phosphate	U
Guanosine phosphate	G		

Metric Units and other used units in this work are based on the international system of units, the Systéme Internationale d'Unités = SI.

<u>List of figures:</u>	Page
Fig. 1: Model of the polarized organization of pollen tubes	2
Fig. 2: The Rho GTPase cycle	8
Fig. 3: Transient over-expression of the <i>Arabidopsis thaliana</i> pollen tube Rac/Rop GTPase At-Rac2	11
Fig. 4: Phosphoinositide metabolism	19
Fig. 5: Schematic illustration of predicted domains from PI-PLC isoforms β , γ , δ , ϵ and ζ	20
Fig. 6: Molecular domain structure of animal PI-PLC δ and the plant PI-PLC isoform	23
Fig. 7: Yeast two-hybrid interaction of Nt-Hypo1 and Nt-Rac5 wild-type and mutant proteins	30
Fig. 8: CLUSTALW alignment of deduced amino acid sequences of Nt-Hypo1 with two unknown proteins from <i>A. thaliana</i> and <i>Oryza sativa</i>	31
Fig. 9: Northern Blot analysis of Nt-Hypo1	32
Fig. 10: Low magnification images of tobacco pollen tubes transiently expressing YFP and Nt-Hypo1	33
Fig. 11: Confocal sections of tobacco pollen tubes transiently expressing YFP-Nt-Hypo1	34
Fig. 12: Confocal sections of tobacco pollen tubes transiently expressing DN-Nt-Rac5 and YFP-Nt-Hypo1, respectively	36
Fig. 13: SDS PAGE showing recombinant GST-Nt-Hypo1 and GST-Nt-Rac5 (wild-type and mutants)	37
Fig. 14: Western Blot analysis of the <i>in vitro</i> interaction of Nt-Hypo1 with Nt-Rac5	38
Fig. 15: Low magnification images of transgenic tobacco pollen tubes expressing Nt-Hypo1 RNAi	42
Fig. 16: Yeast two-hybrid interaction of Nt-Hypo1 with five identified novel Interactors	44
Fig. 17: Confocal sections of five novel Nt-Hypo1 interactors	46
Fig. 18: Multiple sequence alignment of deduced amino acids of four plant PI-PLCs and two mammalian PI-PLCs	49
Fig. 19: Unrooted neighbour joining tree showing the relationship between 13 plant PI-PLC isoforms and two mammalian PI-PLCs	50
Fig. 20: Northern Blot analysis of NtPLC3	51
Fig. 21: SDS PAGES showing recombinant GST-NtPLC3 full-length and deletion mutants	54
Fig. 22: Results of the enzyme activity assays of recombinant NtPLC3 wild-type and mutants	55
Fig. 23: Transient over-expression of NtPLC3 wild-type and mutants in tobacco pollen tubes	57
Fig. 24: Confocal sections of tobacco pollen tubes transiently expressing YFP-NtPLC3 and NtPLC3-YFP, respectively	58
Fig. 25: Schematic overview of NtPLC3 truncation constructs	59
Fig. 26: Confocal sections of tobacco pollen tubes transiently expressing deletion mutants of NtPLC3	60
Fig. 27: Confocal sections of tobacco pollen tubes showing different tip-localization patterns achieved by distinct NtPLC3 fusion proteins	62

Fig. 28:	Dose-response experiment employing the PI-PLC specific inhibitor U-73122	63
Fig. 29:	Graphic showing the complementation of U-73122 treated pollen tubes with over-expressed	65
Fig. 30:	NtPLC3 Confocal sections of tobacco pollen tubes simultaneously expressing YFP-PLC- δ_1 -PH and NtPLC3-RFP	65
Fig. 31:	Visualization of PI-4,5-P ₂ in tobacco pollen tubes before and after PI-PLC inhibitor treatment	66
Fig. 32:	Visualization of DAG in tobacco pollen tubes	68
Fig. 33:	DAG localization after PI-PLC inhibitor treatment	69
Fig. 34:	Schematic model of structure, hydrolysis and names of the common Phospholipids	81
Fig. 35:	Pollen tube model showing the redistribution of PI-4,5-P ₂ after PI-PLC inhibitor treatment and the initiation of tip bulging	94

List of tables:

Table 1:	Segregation ratios of Nt-Hypo1 RNAi plants (F ₂ generation)	43
Table 2:	List of identified yeast two-hybrid interactors of Nt-Hypo1	45
Table 3:	Chemicals, kits, enzymes – products and manufacturers	101
Table 4:	List of apparatus used in the present work – name and Manufacturer	104
Table 5:	Names of bacteria strains, resistance and reference	105
Table 6:	Name of yeast strain, resistance and reference	105
Table 7:	List of ingredients, stocks and assay solutions for HF7c cell Transformation	110
Table 8:	List of vectors:	113
	A) Commercials	113
	B) Modified vectors	113
	C) Obtained constructs	113
Table 9:	Plasmids:	114
	A) Cloning information and name of constructs for Nt-Hypo1	114
	B) Cloning information and name of constructs for NtPLC3 and NtPLC4	115
	C) Constructs used in this work, but generated by other lab members	118
Table 10:	List of oligonucleotides:	119
	A) Oligonucleotide primers for the amplification of Nt-Hypo1 sequences and antisense experiments	119
	B) Oligonucleotide primers for the amplification of NtPLC sequences and introduction of restriction sites	119
Table 11:	Assay mixture for TELT mini-preparations	121
Table 12:	Example reaction scheme for a <i>Taq</i> PCR	124
Table 13:	Discontinuous SDS PAGE:	127
	A) Solutions and buffers	127
	B) Example assay	127
Table 14:	Tobacco transformation media	132

6 REFERENCES

- Altschul S.F., Madden T.L., Schäffer A.A., Zhang J., Zhang Z., Miller W., Lipman D.J.** (1997). Gapped BLAST and PSI-BLAST: A new generation of protein database search programs. *Nucleic Acids Research* **25**(17): 3389-3402.
- Apone, F., Alyeshmerni, N., Wiens, K., Chalmers, D., Chrispeels, M.J. and Colucci, G.** (2003). The G-Protein-Coupled Receptor CGR1 Regulates DNA Synthesis through Activation of Phosphatidylinositol-Specific Phospholipase C. *Plant Physiol* **133**: 571-579.
- Bae, Y.-S., Lee, T.G., Park, J.C., Hur, J.H., Kim, Y., Heo, K., Kwak, J.-Y., Suh, P.-G. and Ryu, S.H.** (2003). Identification of a Compound That Directly Stimulates Phospholipase C Activity. *Molecular Pharmacology* **63**: 1043-1050.
- Bedinger, P.** (1992). The Remarkable Biology of Pollen. *Plant Cell* **4**: 879-88.
- Bedinger, P.A., Hardeman, K.J. and Loukides, C.A.** (1994). Travelling in style: the cell biology of pollen. *Trends Cell Biol* **4**: 132-138.
- Berken, A., Thomas, C. and Wittinghofer, A.** (2005). A new family of RhoGEFs activates the Rop molecular switch in plants. *Nature* **436**: 1176-1180.
- Bertrand, J.-R., Pottier, M., Vekris, A., Opolon, P., Maksimenko, A. and Malvy, C.** (2002). Comparison of antisense oligonucleotides and siRNAs in cell culture and in vivo. *Biochemical and Biophysical Communications* **296**: 1000-1004.
- Bischoff, F., Vahlkamp, L., Molendijk, A. and Palme, K.** (2000). Localization of AtROP4 and AtROP6 and interaction with the guanine nucleotide dissociation inhibitor AtRhoGDI1 from Arabidopsis. *Plant Mol Biol* **42**: 515-530.
- Bishop, A.L. and Hall, A.** (2000). Rho GTPases and their effector proteins. *Biochemical J* **348**: 241-255.
- Bleasdale, J.E., McGuire, J.C. and Bala, G.A.** (1990). Measurement of phosphoinositide-specific phospholipase C activity. *Methods Enzymol* **187**: 226-37.
- Bosch, M., Cheung, A.Y. and Hepler, P.K.** (2005). Pectin Methyltransferase, a Regulator of Pollen Tube Growth. *Plant Physiol* **138**: 1334-1346.
- Brugnera, E., Haney, L., Grimsley, C., Lu, M., Walk, S.F., Tosello-Tramont, A.C., Macara, I.G., Madhani, H., Fink, G.R. and Ravichandran, K.S.** (2002). Unconventional Rac-GEF activity is mediated through the Dock180-ELMO complex. *Nat Cell Biol* **4**: 574-582.

- Chardin, P.** (1993). Structural conservation of Ras-related proteins and its functional implications. In: Handbook of experimental pharmacology: GTPases in biology. B. F. Dickey, and L. Birnbaumer, eds. (Berlin, Springer), pp. 159-176.
- Chen, C.Y., Cheung, A.Y. and Wu, H.M.** (2003). Actin-depolymerizing factor mediates Rac/Rop GTPase-regulated pollen tube growth. *Plant Cell* **15**: 237-249.
- Cherfils, J. and Chardin, P.** (1999). GEFs: structural basis for their activation of small GTP-binding proteins. *Trends Biochem Sci* **24**: 306-311.
- Cho, M.H., Tan, Z., Erneux, C., Shears, S.B. and Boss, W.F.** (1995). The Effects of Mastoparan on the Carrot Cell Plasma Membrane Phosphoinositide Phospholipase C. *Plant Physiol* **107**: 845-856.
- Christensen, H. E. M., Ramachandran, S., Tan, C.-T., Surana, U., Dong, C.-H. and Chua, N.-H.** (1996). Arabidopsis profilins are functionally similar to yeast profilins: identification of a vascular bundle-specific profilin and a pollen-specific profilin. *Plant J* **10**: 269-279.
- Cool, R.H., Schmidt, G., Lenzen, C.U., Prinz, H., Vogt, D. and Wittinghofer, A.** (1999). The Ras mutant D119N is both dominant negative and active. *Mol Cell Biol* **19**: 6297-6305.
- Côté, J.-F. and Vuori, K.** (2002). Identification of an evolutionary conserved superfamily of DOCK180-related proteins with guanine nucleotide exchange activity. *J Cell Sci* **115**: 4901-4913.
- Coursol, S., Pierre, J.-N., Vidal, J. and Grisvard, J.** (2002). Cloning and Characterization of a phospholipase C from the C₄ plant *Digitaria sanguinalis*. *J Exp Bot* **53**(373): 1521-1524.
- Cullen, P.J., Cozier, G.E., Banting, G. and Mellor, H.** (2001). Modular phosphoinositide-binding domains - their role in signalling and membrane trafficking. *Current Biology* **11**: R882-R893.
- Daram, P., Brunner, S., Rausch, C., Steiner, C., Amrhein, N. and Bucher, M.** (1999). Pht2;1 encodes a low-affinity phosphate transporter from Arabidopsis. *Plant Cell* **11**(11): 2153-66.
- Das, S., Hussain, A., Bock, C., Keller, W.A. and Georges, F.** (2005). Cloning of *Brassica napus* phospholipase C2 (BnPLC2), phosphatidylinositol 3-kinase (BnVPS34) and phosphatidylinositol synthase1 (BnPtINs S1) - comparative analysis of the effect of abiotic stresses on the expression of phosphatidylinositol signal transduction-related genes in *B. napus*. *Planta* **220**: 777-784.

- Debreceeni, B., Gao, Y., Guo, F., Zhu, K., Jia, B. and Zheng, Y.** (2004). Mechanisms of Guanine Nucleotide Exchange and Rac-mediated Signaling Revealed by a Dominant Negative Trio Mutant. *J Biol Chem* **279**(5): 3777-3786.
- de Groot, P., Weterings, K., de Been, M., Wittink, F., Hulzink, R., Custers, J., van Herpen, M. and Wullems, G.** (2004). Silencing of the pollen-specific gene NTP303 and its family members in tobacco affects *in vivo* pollen tube growth and results in male sterile plants. *Plant Mol Biol* **55**: 715-726.
- de Jong, C.F., Laxalt, A.M., Bargman, B.O.R., de Witt, P.J.G.M., Joosten, M.H.A.J. and Munnik, T.** (2004). Phosphatidic acid accumulation is an early response in the Cf-4/Avr4 interaction. *Plant J* **39**: 1-12.
- Derksen, J., Rutten, T., Lichtscheidl, I.K., de Win, A.H.N., Pierson, E.S. and Rongen, G.** (1995). Quantitative analysis of the distribution of organelles in tobacco pollen tubes: implications for exocytosis and endocytosis. *Protoplasma* **188**: 267-276.
- DeWald, D.B., Torabinejad, J., Jones, C.A., Shope, J.C., Cangelosi, A.R., Thompson, J.E., Prestwich, G.D. and Hama, H.** (2001). Rapid Accumulation of Phosphatidylinositol 4,5-Bisphosphate and Inositol 1,4,5-Trisphosphate Correlates with Calcium Mobilization in Salt-Stressed Arabidopsis. *Plant Physiol* **126**: 759-769.
- Drøbak, B.K. and Heras, B.** (2002). Nuclear phosphoinositides could bring FYVE alive. *Trends in Plant Science* **7**(3): 132-138.
- Drøbak, B.K., Watkins, P.A.C., Valenta, R., Dove, S.K., Lloyd, C.W. and Staiger C.J.** (1994). Inhibition of plant plasma membrane phosphoinositide phospholipase C by the actin-binding protein, profilin. *Plant J* **6**(3): 389-400.
- Ellis, M.V., James, S.R., Perisic, O., Downes, C.P., Williams, R.L. and Katan, M.** (1998). Catalytic Domain of Phosphoinositide-specific Phospholipase C (PLC). Mutational Analysis Of Residues Within The Active Site And Hydrophobic Ridge of PLC δ 1. *J Biol Chem* **273**(19): 11650-11659.
- Ercetin, M.E. and Gillaspay, G.E.** (2002). Molecular Characterization of an Arabidopsis Gene Encoding a Phospholipid-Specific Inositol Polyphosphate 5-Phosphatase. *Plant Physiol* **135**: 938-946.
- Essen, L.-O., Perisic, O., Cheung, R., Katan, M. and Williams, R.L.** (1996). Crystal structure of mammalian phosphoinositide-specific phospholipase C δ . *Nature* **380**: 595-602.

- Estruch, J.J., Kadwell, S., Merlin, E. and Crossland, L.** (1994). Cloning and characterization of a maize pollen-specific calcium-dependent calmodulin-independent protein kinase. *Proc Natl Acad Sci USA* **91**: 8837-8841.
- Etienne-Manneville, S.** (2004). Cdc42 - the centre of polarity. *J Cell Sci* **117**: 1291-1300.
- Etienne-Manneville, S. and Hall, A.** (2002). Rho GTPases in cell biology. *Nature* **420**: 629-635.
- Feig, L.A.** (1999). Tools of the trade: use of dominant-inhibitory mutants of Ras-family GTPases. *Nat Cell Biol* **1**: E25-27.
- Feijó, J.A.** (1999). The polar tube oscillator: towards a molecular mechanism of tip growth? in: *Fertilization in Higher Plants*. Cresti, M., Cai, G. and Moscatelli, A., eds. (Heidelberg/Berlin, Springer) pp.317-334.
- Feijó, J.A., Sainhas, J., Hackett, G.R., Kunkel, J.G. and Hepler, P.K.** (1999). Growing Pollen Tubes Possess a Constitutive Alkaline Band in the Clear Zone and a Growth-dependent Acidic Tip. *J Cell Biol* **144**(3): 483-496.
- Feijó, J.A., Sainhas, J., Holdaway-Clark, T., Cordero, M.S., Kunkel, J.G. and Hepler, P.K.** (2001). Cellular oscillations and the regulation of growth: the pollen tube paradigm. *BioEssays* **23**: 86-94.
- Feißt, C., Albert, D., Steinhilber, D. and Werz, O.** (2005). The Aminosteroid Phospholipase C Antagonist U-73122 (1-[6-[[[17-_-3-Methoxyestra-1,3,5(10)-trien-17-yl]amino]hexyl]-1*H*-pyrrole-2,5-dione) Potently Inhibits Human 5-Lipoxygenase in Vivo and in Vitro. *Molecular Pharmacology* **67**(5): 1751-1757.
- Fields, S. and Song, O.** (1989). A novel genetic system to detect protein-protein interactions. *Nature* **340**: 245-246.
- Fischer, K., Arbing, B., Kammerer, B., Busch, C., Brink, S., Wallmeier, H., Sauer, N., Eckerskorn, C. and Flügge, U.I.** (1994). Cloning and in vivo expression of functional triose phosphate/phosphate translocators from C3- and C4-plants: evidence for the putative participation of specific amino acid residues in the recognition of phosphoenolpyruvate. *Plant J* **5**(2): 215-26.
- Franklin-Tong, V.E., Dröbak, B.K., Allan, A.C., Watkins, P.A.C. and Trewavas, A.J.** (1996). Growth of Pollen Tubes of *Papaver rhoeas* Is regulated by a Slow-Moving Calcium Wave Propagated by Inositol 1,4,5-Trisphosphate. *Plant Cell* **8**: 1305-1321.
- Franklin-Tong, V.E. and Franklin, F.C.H.** (2003). The different mechanisms of *gametophytic* self-incompatibility. *Phil Trans R Soc London B* **358**: 1025-1032.

- Franklin-Tong, V.E., Ride, J.P., Read, N.D., Trewavas, A.J. and Franklin, C.H.F.** (1993). The self-incompatibility response in *Papaver rhoeas* is mediated by cytosolic free calcium. *Plant J* **4**(1): 163-177.
- Fu, Y., Wu, G. and Yang, Z.** (2001). Rop GTPase-dependent dynamics of tip-localized F-actin controls tip growth in pollen tubes. *J Cell Biol* **152**(5): 1019-1032.
- Geitmann, A. and Emons, A.M.** (2000). The cytoskeleton in plant and fungi cell tip growth. *J Microsc* **198**: 218-245.
- Geldner, N., Anders, N., Wolters, H., Keicher, J., Kornberger, W., Muller, P., Delbarre, A., Ueda, T., Nakano, A. and Jürgens, G.** (2003). The *Arabidopsis* GNOM ARF-GEF Mediates Endosomal Recycling, Auxin Transport, and Auxin-Dependent Plant Growth. *Cell* **112**: 219-230.
- Gosh, S., Strum, J.C., Sciorra, V.A., Daniel, L. and Bell, R.M.** (1996). Raf-1 Kinase Possesses Distinct Binding Domains for Phosphatidylserine and Phosphatidic Acid. *J Biol Chem* **271**(14): 8472-8480.
- Gu, Y., Wang, Z. and Yang, Z.** (2004). ROP/RAC GTPase: an old new master regulator for plant signaling. *Curr Opin Plant Biol* **7**: 527-536.
- Harada, A., Sakai, T. and Okada, K.** (2003). phot1 and phot2 mediate blue light-induced transient increases in cytosolic Ca^{2+} differently in *Arabidopsis* leaves. *Proc Natl Acad Sci* **100**(14): 8583-8588.
- Helliwell, C. and Waterhouse, P.** (2003). Constructs and methods for high-throughput gene silencing in plants. *Methods* **30**: 289-295.
- Hepler, P.K., Vidali, L. and Cheung, A.Y.** (2001). Polarized cell growth in higher plants. *Annu Rev Cell Dev Biol* **17**: 159-187.
- Heslop-Harrison, J., Heslop-Harrison, Y., Cresti, M., Tiezzi, A. and Moscatelli, A.** (1988). Cytoskeletal elements, cell shaping and movement in the angiosperm pollen tube. *J Cell Sci* **91**: 49-60.
- Higashiyama, T., Yabe, S., Sasaki, N., Nishimura, Y., Miyagishima, S.-Y., Kuroiwa, H. and Kuroiwa, T.** (2001). Pollen tube attraction by the synergid cell. *Science* **293**: 1480-1483.
- Hirayama, T., Ohto, C., Mizoguchi, T. and Shinozaki, K.** (1995). A gene encoding a phosphatidylinositol-specific phospholipase C is induced by dehydration and salt stress in *Arabidopsis thaliana*. *Proc Natl Acad Sci USA* **92**: 3903-3907.

- Hirayama, T., Mitsukawa, N., Shibata, D. and Shinozaki, K.** (1997). AtPLC2, a gene encoding phosphoinositide-specific phospholipase C, is constitutively expressed in vegetative and floral tissues in *Arabidopsis thaliana*. *Plant Mol Biol* **34**: 175-180.
- Holdaway-Clark, T.L., Feijó, J.A., Hacket, G.R., Kunkel, J.G. and Hepler, P.K.** (1997). Pollen Tube Growth and the Intracellular Cytosolic Calcium Gradient Oscillate in Phase while Extracellular Calcium Influx Is Delayed. *Plant Cell* **9**(11): 1999-2010.
- Homma, Y. and Emori, Y.** (1995). A dual functional signal mediator showing RhoGAP and phospholipase C- δ stimulating activities. *EMBO J* **14**: 286-291.
- Horsch, R., Fry, J., Hoffmann, N., Neidermeyer, J., Rogers, S. and Fraley, R.** (1988). In: *Plant Molecular Biology Manual*. Gelvin, S. and Schilperoort, R., eds. (Kluwer, Dordrecht, The Netherlands), Section A5: 23-50.
- Hunt, L., Mills, L.N., Pical, C., Leckie, C.P., Aitken, F.L., Kopka, J., Mueller-Roeber, B., McAinsh, M.R., Hetherington, A.M. and Gray, J.E.** (2003). Phospholipase C is required for the control of stomatal aperture by ABA. *Plant J* **34**: 47-55.
- Hunt, L., Otterhag, L., Lee, J.C., Lasheen, T., Hunt, J., Seki, M., Shinozaki, K., Sommarin, M., Gilmour, D.J., Pical, C. and Gray, J.E.** (2004). Gene-specific expression and calcium activation of *Arabidopsis thaliana* phospholipase C isoforms. *New Phytologist* **162**: 643-654.
- Hurley, J.H. and Meyer, T.** (2001): Subcellular targeting by membrane lipids. *Current Opinion Cell Biol* **13**: 146-152.
- Inoue, H., Nojima, H. and Okayama, H.** (1990). High efficiency transformation of *Escherichia coli* with plasmids. *Gene* **96**: 23-28.
- Jiang, L., Yang, S.L., Xie, L.F., Pua, C.S., Zhang, X.O., Yang, W.C., Sundaresan, V. and Ye, D.** (2005). VANGUARD1 Encodes a Pectin Methyltransferase That Enhances Pollen Tube Growth in the Arabidopsis Style and Transmitting Tract. *Plant Cell* **17**(2): 584-96.
- Jones, A.M. and Assmann, S.M.** (2004). Plants: the latest model system for G-protein research. *EMBO Reports* **5**(6): 572-578.
- Joos, U., van Aken, J. and Kristen, U.** (1994). Microtubules are involved in maintaining the cellular polarity in pollen tubes of *Nicotiana glauca*. *Protoplasma* **179**: 5-15.
- Kaothien, P., Ok, S.H., Shuai, B., Wengier, D., Cotter, R., Kelley, D., Kiriakopoulos, S., Muschietti, J. and McCormick, S.** (2005). Kinase partner protein interacts with

- the LePRK1 and LePRK2 receptor kinases and plays a role in polarized pollen tube growth. *Plant J* **42**(4): 492-503.
- Kieffer, F., Elmayan, T., Rubier, S., Simon-Plas, F., Dagher, M.C. and Blein, J.P.** (2000). Cloning of Rac and Rho-GDI from tobacco using an heterologous two-hybrid screen. *Biochimie* **82**: 1099-1105.
- Kim, Y.J., Kim, J.E., Lee, J.-H., Lee, M.H., Jung, H.W., Bahk, Y.Y., Hwang, B.K., Hwang, I. and Kim, W.T.** (2004). The Vr-PLC3 gene encodes a putative plasma membrane-localized phosphoinositide-specific phospholipase C whose expression is induced by abiotic stress in mung bean (*Vigna radiata* L.). *FEBS Letters* **556**: 127-136.
- Knappe, S., Flügge, U.-I. and Fischer, K.** (2003). Analysis of the Plastid *phosphate translocator* Gene Family in Arabidopsis and Identification of New *phosphate translocator*-Homologous Transporters, Classified by Their Putative Substrate-Binding Site. *Plant Physiol* **131**: 1178-1190.
- Kopka, J., Pical, C., Gray, J.E. and Mueller-Roeber, B.** (1998a). Molecular and Enzymatic Characterization of Three Phosphoinositide-specific phospholipase C Isoforms from Potato. *Plant Physiol* **116**: 239-250.
- Kopka, J., Pical, C., Hetherington, A.M. and Mueller-Roeber, B.** (1998b). Ca²⁺/phospholipid-binding (C2) domain in multiple plant proteins: novel components of the calcium-sensing apparatus. *Plant Mol Biol* **36**(5): 627-37.
- Kost, B., Spielhofer, P. and Chua, N.-H.** (1998). A GFP-mouse talin fusion protein labels plant actin filaments *in vivo* and visualizes the actin cytoskeleton in growing pollen tubes. *Plant J* **16**: 393-401.
- Kost, B., Lemichez, E., Spielhofer, P., Hong, Y., Tolia, K., Carpenter, C. and Chua, N.-H.** (1999). Rac homologues and compartmentalized phosphatidylinositol 4,5-bisphosphate act in a common pathway to regulate polar pollen tube growth. *J Cell Biol* **145**: 317-330.
- Kost, B., Mathur, J. and Chua, N.-H.** (1999b). Cytoskeleton in plant development. *Curr Opin Plant Biol* **2**: 462-470.
- Kovar, D.R., Drøbak, B.K. and Staiger, C.J.** (2000). Maize Profilin Isoforms Are Functionally Distinct. *Plant Cell* **12**: 583-598.
- Kumar, S., Tamura, K. and Nei, M.** (2004). MEGA3: Integrated software for Molecular Evolutionary Genetics Analysis and sequence alignment. *Briefings in Bioinformatics* **5**(2): 150-163.

- Laemmli U.K.** (1970). Cleavage of structural proteins during the assembly of the head of bacteriophage T4. *Nature* **227**: 680-685.
- Lancelle, S.A. and Hepler, P.K.** (1992). Ultrastructure of freeze-substituted pollen tubes of *Lilium longiflorum*. *Protoplasma* **167**: 215-230.
- Laxalt, A.M. and Munnik, T.** (2002). Phospholipid signalling in plant defence. *Current Opinion in Plant Biology* **5**: 1-7.
- Legendre, L., Yueh, Y.G., Crain, R., Haddock, N., Heinstein, P.F. and Low, P.S.** (1993). Phospholipase C Activation during Elicitation of the Oxidative Burst in Cultured Plant Cells. *J Biol Chem* **268**(33): 24559-24563.
- Lemmon, M.A.** (2003). Phosphoinositide Recognition Domains. *Traffic* **4**: 201-213.
- Lemmon, M.A., Ferguson, K.M. and Abrams, C.S.** (2002). Pleckstrin homology domains and the cytoskeleton. *FEBS Letters* **513**: 71-76.
- Lennon, K.A., Roy, S., Hepler, P.K. and Lord, E.M.** (1998). The structure of the transmitting tissue of *Arabidopsis thaliana* (L.) and the path of pollen tube growth. *Sex Plant Reprod* **11**: 49-59.
- Lewis, J.G., Lin, K.-Y., Kothavale, A., Flanagan, W.M., Matteucci, M.D., DePrince, R.B., Mook, R.A., Hendren, R.W. and Wagner, R.W.** (1996). A serum-resistant cytofectin for cellular delivery of antisense oligodeoxynucleotides and plasmid DNA. *Proc Natl Acad Sci USA* **93**: 3176-3181.
- Li, H., Lin, Y.K., Heath, R.M., Zhu, M.X. and Yang, Z.** (1999). Control of pollen tube tip growth by a rop GTPase-dependent pathway that leads to tip-localized calcium influx. *Plant Cell* **11**: 1731-1742.
- Li, S.-T., Huang, X.Y. and Sun, F.Z.** (2001). Flowering plant sperm contains a cytosolic soluble protein factor which can trigger calcium oscillations in mouse eggs. *Biochem Biophys Res Commun* **287**(1): 56-59.
- Lovy-Wheeler, A., Wilson, K.L., Baskin, T.I. and Hepler, P.K.** (2005) Enhanced fixation reveals the apical cortical fringe of actin filaments as a consistent feature of the pollen tube. *Planta* **221**: 95-104.
- Martin, T.F.J.** (1997). Phosphoinositides as spatial regulators of membrane traffic. *Curr Opin Neurobiol* **7**: 331-338.
- Martin, T.F.J.** (1998). Phosphoinositide Lipids As Signaling Molecules: Common Themes for Signal Transduction, Cytoskeletal Regulation, and Membrane Trafficking. *Annu Rev Cell Dev Biol* **14**: 231-264.

- Mascarenhas, J.P.** (1993). Molecular Mechanisms of Pollen Tube Growth and Differentiation. *Plant Cell* **5**: 1303-1314.
- Meijer, H.J.G. and Munnik, T.** (2003). Phospholipid-Based Signaling In Plants. *Annu Rev Plant Biol* **54**: 265-306.
- Melin, P.-M., Pical, C., Jergil, B. and Sommarin, M.** (1992). Polyphosphoinositide phospholipase C in wheat root plasma membranes. Partial purification and characterization. *Biochimica et Biophysica Acta* **1123**: 163-169.
- Messerli, M.A., Creton, R., Jaffe, L.F. and Robinson, K.R.** (2000). Periodic increases in elongation rate precede increases in cytosolic Ca^{2+} during pollen tube growth. *Dev Biol* **222**: 84-98.
- Micheli, F.** (2001). Pectin methylesterases: cell wall enzymes with important roles in plant physiology. *Trends Plant Sci* **6**(9): 414-419.
- Monteiro, D., Liu, Q., Lisboa, S., Scherer, G.E.F., Quader, H. and Malhó, R.** (2005). Phosphoinositides and phosphatidic acid regulate pollen tube growth and reorientation through modulation of $[Ca^{2+}]_c$ and membrane secretion. *J Exp Bot* **56**(416): 1665-1674.
- Moutinho, A., Hussey, P.J., Trewavas, A.J. and Malhó, R.** (2001). cAMP acts as a second messenger in pollen tube growth and reorientation. *Proc Natl Acad Sci U S A* **98**: 10481-10486.
- Mueller-Roeber, B. and Pical, C.** (2002). Inositol Phospholipid Metabolism in Arabidopsis. Characterized and Putative Isoforms of Inositol Phospholipid Kinase and Phosphoinositide-Specific Phospholipase C. *Plant Physiol* **130**: 22-46.
- Munnik, T., Irvine, R.F. and Musgrave, A.** (1998). Phospholipid signalling in plants. *Biochimica et Biophysica Acta* **1389**: 222-272.
- Munnik, T., de Vrije, T., Irvine, R.F. and Musgrave A.** (1996). Identification of Diacylglycerol Pyrophosphate as a Novel Metabolic Product of Phosphatidic Acid during G-protein Activation in Plants. *J Biol Chem* **271**(26): 15708-15715.
- Newton, A.C. and Johnson, J.E.** (1998). Protein Kinase C: a paradigm for regulation of protein function by two membrane-targeting modules. *Biochimica et Biophysica Acta* **1376**: 155-172.
- Nomikos, M., Blayney, L.M., Larman, M.G., Campbell, K., Rossbach, A., Saunders, C.M., Swann, K. and Lai, F.A.** (2005). Role of PLC-Zeta Domains in Ca^{2+} -Dependent PIP_2 Hydrolysis and Cytoplasmic Ca^{2+} Oscillations. *J Biol Chem* **280**(35): 31011-31018.

- Oancea, E., Teruel, M.N., Quest, A.F.G. and Meyer, T.** (1998). Green Fluorescent Protein (GFP)-tagged Cysteine-rich Domains from Protein Kinase C as Fluorescent Indicators for Diacylglycerol Signaling in Living Cells. *J Cell Biol* **140**(3): 485-498.
- Ortega, X., Velásquez, J.C. and Pérez, L.M.** (2005). IP₃ production in the hypersensitive response of lemon seedlings against *Alternaria alternata* involves active protein tyrosine kinases but not a G-protein. *Biol Res* **38**: 89-99.
- Otterhag, L., Sommarin, M. and Pical, C.** (2001). N-terminal EF-hand-like domain is required for phosphoinositide-specific phospholipase C activity in *Arabidopsis thaliana*. *FEBS Letters* **497**: 165-170.
- Owen, J.D.** (1976). The Determination Of The Stability Constant For Calcium-EGTA. *Biochimica et Biophysica Acta* **451**: 321-325.
- Palanivelu, R., Brass, L., Edlund, A.F. and Preuss, D.** (2003). Pollen tube growth and guidance is regulated by POP2, an Arabidopsis gene that controls GABA levels. *Cell* **114**: 47-59.
- Palanivelu, R. and Preuss, D.** (2000). Pollen tube targeting and axon guidance: Parallels in tip growth mechanisms. *Trends Cell Biol* **10**: 517-524.
- Pan, Y.-Y., Wang, X., Ma, L.-G. and Sun, D.-Y.** (2005). Characterization of phosphatidylinositol-specific Phospholipase C (PI-PLC) from *Lilium daviddi* Pollen. *Plant Cell Physiol* (in press).
- Perera, I.Y., Heilmann, I., Chang, S.C., Boss, W.F. and Kaufman, P.B.** (2001). A Role for Inositol 1,4,5-Trisphosphate in Gravitropic Signaling and the Retention of Cold-Perceived Gravistimulation of Oat Shoot Pulvini. *Plant Physiol* **125**: 1499-1507.
- Pical, C., Sandelius, A.S., Melin, P.-M. and Sommarin, M.** (1992). Polyphosphoinositide phospholipase C in Plasma Membranes of Wheat (*Triticum aestivum* L.). Orientation of Active Site and Activation by Ca²⁺ and Mg²⁺. *Plant Physiol* **100**: 1296-1303.
- Pical, C., Westergren, T., Dove, S.K., Larsson, C. and Sommarin, M.** (1999). Salinity and hyperosmotic stress induce rapid increases in phosphatidylinositol 4,5-bisphosphate, diacylglycerol pyrophosphate, and phosphatidylcholine in Arabidopsis thaliana cells. *J Biol Chem* **274**(53): 38232-40.
- Pierson, E.S., Miller, D.D., Callaham, D.A., van Aken, J., Hacket, G. and Hepler, P.K.** (1996). Tip-localized calcium entry fluctuates during pollen tube growth. *Dev Biol* **174**(1): 160-173.

-
- Pirone, D.M., Carter, D.E. and Burbelo, P.D.** (2001). Evolutionary expansion of CRIB-containing Cdc42 effector proteins. *Trends in Genetics* **17**: 370-373.
- Potocký, M., Eliáš, M., Profotová, B., Novotná, Z., Valentová, O. and Žárský, V.** (2003). Phosphatidic acid produced by phospholipase D is required for tobacco pollen tube growth. *Planta* **217**: 122-130.
- Qiu, J.L., Jilk, R., Marks, M.D. and Szymanski, D.B.** (2002). The Arabidopsis *SPIKE1* Gene is Required for Normal Cell Shape Control and Tissue Development. *Plant Cell* **14**: 101-118.
- Raftopoulou, M. and Hall, A.** (2004). Cell migration: Rho GTPases lead the way. *Dev Biol* **265**: 23-32.
- Read, P.W., Liu, X., Longenecker, K., Dipierro, C.G., Walker, L.A., Somlyo, A.V., Somlyo, A.P. and Nakamoto, R.K.** (2000). Human RhoA/RhoGDI complex expressed in yeast: GTP exchange is sufficient for translocation of RhoA to liposomes. *Protein Sci* **9**: 376-386.
- Rebecchi, M.J. and Pentylala, S.N.** (2000). Structure, Function, and Control of Phosphoinositide-specific phospholipase C. *Physiological Reviews* **80**(4): 1291-1335.
- Repp, A., Mikami, K., Mittmann, F. and Hartmann, E.** (2004). Phosphoinositide-specific phospholipase C is involved in cytokinin and gravity responses in the moss *Physcomitrella patens*. *Plant J* **40**: 250-259.
- Rhee, S.G. and Bae, Y.S.** (1997). Regulation of Phosphoinositide-specific phospholipase C Isozymes. *J Biol Chem* **272**(24): 15045-15048.
- Rizzo, M.A., Shome, K., Watkins, S.C. and Romero, G.** (2000). The Recruitment of Raf-1 to Membranes Is Mediated by Direct Interaction with Phosphatidic Acid and is Independent of Association with Ras. *J Biol Chem* **275**(31): 23911-23918.
- Rossmann, K.L., Worthylake, D.K., Snyder, J.T., Chen, L., Whitehead, I.P. and Sondek, J.** (2002). Functional Analysis of Cdc42 Residues Required for Guanine Nucleotide Exchange. *J Biol Chem* **277**(52): 50893-50898.
- Sambrook, J. and Russell, D.W.** (2001). *Molecular cloning: a laboratory manual*. (Cold Spring Harbor Laboratory Press).
- Sánchez, J.P. and Chua, N.-H.** (2001). Arabidopsis PLC1 is required for secondary responses to abscisic acid signals. *Plant Cell* **13**(5): 1143-54.
- Saunders, C.M., Larman, M.G., Parrington, J., Cox, L.J., Royse, J., Blayney, L.M., Swann, K. and Lai, F.A.** (2002). PLC ζ : a sperm-specific trigger of Ca²⁺ oscillations in eggs and embryo development. *Development* **129**: 3533-3544.

-
- Schmidt, A. and Hall, A.** (2002). Guanine nucleotide exchange factors for Rho GTPases: turning on the switch. *Genes Dev* **16**: 1587-1609.
- Self, A.J. and Hall, A.** (1995). Measurement of intrinsic nucleotide exchange and GTP hydrolysis rates. *Methods Enzymol* **256**: 67-76.
- Shi, J., Gonzales, R.A. and Bhattacharyya, M.K.** (1995). Characterization of a plasma membrane-associated phosphoinositide-specific phospholipase C from soybean. *Plant J* **8**(3): 381-390.
- Shigaki, T. and Bhattacharyya, M.K.** (2000). Decreased inositol 1,4,5-trisphosphate content in pathogen-challenged soybean cells. *Mol Plant Microbe Interact* **13**(5): 563-7.
- Smith, R.J., Sam, L.M., Justen, J.M., Bundy, G.L., Bala, G.A. and Bleasdale, J.E.** (1990). Receptor-Coupled Signal Transduction in Human Polymorphonuclear Neutrophils: Effects of a Novel Inhibitor of Phospholipase C-Dependent Processes on Cell Responsiveness. *J Pharmacology and Experimental Therapeutics* **253**(2): 688-697.
- Stauffer, T.P., Ahn, S. and Meyer, T.** (1998). Receptor-induced transient reduction in plasma membrane PtdIns(4,5)P₂ concentration monitored in living cells. *Current Biology* **8**: 343-346.
- Staxén, I., Pical, C., Montgomery, L.T., Gray, J.E., Hetherington, A.M. and McAinsh, M.R.** (1999). Abscisic acid induces oscillations in guard-cell cytosolic free calcium that involve phosphoinositide-specific phospholipase C. *Proc Natl Acad Sci USA* **96**: 1779-1784.
- Swann, K., Larman, M.G., Saunders, C.M. and Lai, F.A.** (2004). The cytosolic sperm factor that triggers Ca²⁺ oscillations and egg activation in mammals is a novel phospholipase C: PLCζ. *Reproduction* **127**: 431-439.
- Taylor, L.P. and Hepler, P.K.** (1997). Pollen germination and tube growth. *Annu Rev Plant Physiol* **48**: 461-491.
- Testerink, C., Dekker, H.L., Lim, Z.-Y., Johns, M.K., Holmes, A.B., de Koster, C.G., Ktistakis, N.T. and Munnik, T.** (2004). Isolation and identification of phosphatidic acid targets from plants. *Plant J* **39**: 527-536.
- Thompson, J.D., Higgins, D.G., Gibson, T.J.** (1994). CLUSTAL W: improving the sensitivity of progressive multiple sequence alignment through sequence weighting, position-specific gap penalties and weight matrix choice. *Nucleic Acids Res* **22**: 4673-4680.

- Twell, D., Wing R., Yamaguchi J. and McCormick, S. (1989).** Isolation and expression of an anther-specific gene from tomato. *Mol Gen Genet* **217**: 240–245.
- Twell, D., Yamaguchi, J., Wing, R.A., Ushiba, J. and McCormick, S. (1991).** Promoter analysis of genes that are coordinately expressed during pollen development reveals pollen-specific enhancer sequences and shared regulatory elements. *Genes Dev* **5**: 496-507.
- Valster, A.H., Hepler, P.K. and Chernoff, J. (2000).** Plant GTPases: the Rhos in bloom. *Trends Cell Biol.* **10**: 141-146.
- van Engelen, F.A., Molthoff, J.W., Conner, A.J., Nap, J.-P., Pereira, A. and Stiekema, W.J. (1995).** pBINPLUS: an improved plant transformation vector based on pBIN19. *Transgenic Res.* **4**: 288-290.
- Venkataraman, G., Goswami, M., Tuteja, N., Reddy, M.K. and Sopory, S.K. (2003).** Isolation and characterization of a phospholipase C delta isoform from pea that is regulated by light in a tissue specific manner. *Mol Gen Genomics* **270**: 378-386.
- Vernoud, V., Horton, A.C., Yang, Z. and Nielsen, E. (2003).** Analysis of the small GTPase gene superfamily of Arabidopsis. *Plant Physiol* **131**: 1191-1208.
- Vidali, L. and Hepler, P.K. (2001).** Actin and pollen tube growth. *Protoplasma* **215**:64–76.
- Vidali, L., McKenna, S.T. and Hepler, P.K. (2001).** Actin Polymerization Is Essential for Pollen Tube Growth. *Mol Biol Cell* **12**: 2534-2545.
- Vincent, S., Brouns, M., Hart, M.J. and Settleman, J. (1998).** Evidence of distinct mechanisms of transition state stabilization of GTPases by fluoride. *Proc Natl Acad Sci USA* **95**: 2210-2215.
- Wakeley, P.R., Rogers, H.J., Rozycka, M., Greenland, A.J. and Hussey, P.J. (1998).** A maize pectin methylesterase-like gene, ZmC5, specifically expressed in pollen. *Plant Mol Biol* **37**(1): 187-92.
- Wang, X. (2001).** Plant Phospholipases. *Annu Rev Plant Physiol Plant Mol Biol* **52**:211-231.
- Wesley, S.V., Helliwell, C.A., Smith, N.A., Wang, M., Rouse, D.T., Liu, Q., Gooding, P.S., Singh, S.P., Abbott, D., Stoutjesdijk, P.A., Robinson, S.P., Gleave, A.P., Green, A.G. and Waterhouse, P. (2001).** Construct design for efficient, effective and high-throughput gene silencing in plants. *Plant J* **27**(6): 581-590.
- Williams, M.E., Torabinejad, J., Cohick, E., Parker, K., Drake, E.J., Thompson, J.E., Hortter, M. and DeWald, D.B. (2005).** Mutations in the Arabidopsis

-
- Phosphoinositide Phosphatase Gene SAC9 Lead to Overaccumulation of PtdIns(4,4)P₂ and Constitutive Expression of the Stress-Response Pathway. *Plant Physiol* **138**: 686-700.
- Wittink, F.R.A., Knuiman, B., Derksen, J., Čapková, V., Twell, D., Schrauwen, J.A.M. and Wullems, G.J.** (2000). The pollen-specific gene *Ntp303* encodes a 69-kDa glycoprotein associated with the vegetative membranes and the cell wall. *Sex Plant Reprod* **12**: 276-284.
- Wu, G., Gu, Y., Li, S. and Yang, Z.** (2001). A genome-wide analysis of Arabidopsis ROP-interactive CRIB motif-containing proteins that act as ROP GTPase targets. *Plant Cell* **13**: 2841-2856.
- Wu, G., Li, H. and Yang, Z.** (2000). Arabidopsis RopGAPs are a novel family of Rho GTPase-activating proteins that require the Cdc42/Rac-interactive binding motif for Rop-specific GTPase stimulation. *Plant Physiol* **124**: 1625-1636.
- Yang, Z.** (2002). Small GTPases: Versatile Signaling Switches in Plants. *Plant Cell Supplement 2002*: S375-S388.
- Zhai, S., Sui, Z., Yang, A. and Zhang, J.** (2005). Characterization of a novel phosphoinositide-specific phospholipase C from *Zea mays* and its expression in *Escherichia coli*. *Biotech Lett* **27**: 799-804.
- Zheng, Z.L. and Yang, Z.** (2000). The Rop GTPase switch turns on polar growth in pollen. *Trends Plant Sci* **5**: 298-303.
- Zonia, L., Cordeiro, S., Tupy, J. and Feijó, J.A.** (2002). Oscillatory chloride efflux at the pollen tube apex has a role in growth and cell volume regulation and is targeted by inositol 3,4,5,6-tetrakisphosphate. *Plant Cell* **14**(9): 2233-2249.

7 APPENDIX

Nt-Hyp01

DEFINITION homology to a hypothetical protein from *A. thaliana*
SOURCE *Nicotiana tabacum* (common tobacco; ecotype Petit Havana SR1)
ORGANISM *Nicotiana tabacum*;
Eukaryota; Viridiplantae; Streptophyta; Embryophyta;
Tracheophyta; Spermatophyta; Magnoliophyta; eudicotyledons;
core eudicotyledons; asterids; lamiids; Solanales;
Solanaceae; *Nicotiana*..

(bases 1 to 625)

BASE COUNT 200 a 112 c 121 g 192 t

ORIGIN

```
1 GGAAACTTGC AAAATTTGGC ACCAAGAGGC CGGAGGAAGA AAGAGGAGGG GAGATGGGGA
61 AGTACGTGGA GATGCTGGAT GCCGGAGCCA AAATCGCCAA TAGAATTCGG TCCCATTATC
121 CCCAAACCTC CGGCTTGTAC TATCATCCGC CTAGCAACGA ACATCACGGT GCTTCTGTGA
181 ACAACGCCAT GGCAAATACA ACATCTCTGC TGGACCCATT TTCTTCCAAG GCTGATGATG
241 AAATGGACAC CAAGGATCTC ATTCTTTTCG TTGTAATTGG ATGAACGATA TATTTTTGTG
301 ACGGAAACCT TTTTCTTTAC CTTTATTTCT CTTGAGGCAA AGTCTATATT CTTGTAATTT
361 ATTACCTGTG TCCTATTTTG AATGTCTTAT TTCATATTTA ATGTTTAGAC TCAATACTTC
421 ACCAAACTTT TTTGTCACAT AAATATGTGT ATATGTAAAA AGAGAGAACG TCTAGTGTTT
481 GTTAACGAGA TCATCATCTG GCTATATATG TTACTTTTTG GGCTTTGATG ATATAACTGA
541 AAAAAGTACG GTGTCCTGAT AAATTCAGAA CACTTTCTAA TGATTGTTAC AATTTGAGCG
601 AAAAAAAAAA AAAAAAAAAA AAAAA
```

CDS

MGKYVEMLDAGAKIANRIRSHYPQTSGLYYHPPSNEHHGASVNNAMANTTSLLDPFSSKADDEMDTKDLILFV
VIG

Yeast two-hybrid interactors: Screen 12, bait: Nt-Hypo1**Clone 12-F**

DEFINITION homology to a pectin esterase family protein from *A. thaliana*

SOURCE *Nicotiana tabacum* (common tobacco; ecotype Petit Havana SR1)

ORGANISM *Nicotiana tabacum*; Eukaryota; Viridiplantae; Streptophyta;
Embryophyta; Tracheophyta; Spermatophyta; Magnoliophyta;
eudicotyledons; core eudicotyledons; asterids; lamiids;
Solanales; Solanaceae; *Nicotiana*.

(bases 1 to 635)

BASE COUNT 190 a 155 c 159 g 127 t

ORIGIN

```

1 CCTGATAATC TTATCAACAA CAGCACCAGC AGCGACAGCA ACTCACCTCA TCGCCGTCTC
61 CTTGAGGCGA ACAAGATCGA TCAGGACGGT TACCCTACAT GGTTCCCCGT TGCTGACCGT
121 AAGCTATTGG CAAAATCCGG AAAAGGGAAA GGAAAAGGAC ACGGTGGTGC TGCGGGAGGA
181 GCTGGGGTTG CTCCAGTACT TCCTCCAATC GGCCCCGGCC CAATTACTCC TCACGCAGTA
241 GTTGCCAAGG ATGGAAGCGG CAAATTTAAA ACCGTCACTG ATGCAGTCAG AGCGTACCCA
301 CCAAACCACC AAGGCAGATA CATTATCTAT ATCAAGGCCG GCGTTTATAA CGAGCAGGTC
361 CTTATCGATA AAAAACAAAC AAACGTGTTT ATGTATGGTG ATGGCGCAGG GAAATCTATC
421 ATCACTTGTG ACAAAAATGT TAAAATATTG AAATTCACCA CCTCCAAAAG TGCTACAGTC
481 GCTGTTGAGA GCGAGGGGTT CATAGCCAGA GGAATTACCT TCCGCAACAC AGCAGGTCCA
541 GAAGGGGAAC AAGCCGTGGC ACTTTANGAA TCAACGGGAG ATAGGGGCGG CGGGTATTTT
601 GACTNGCAGC ATGGGANGGG ATTTCAAGAA CACCN

```

ClustalW Alignment of 12-F with pectin esterase family protein from *Arabidopsis thaliana* (NP_182226; 588 aa)

```

      1                               50
PE  MIGKVVVSVS  SILLIVGVAI  GVVAFINKNG  DANLSPQMK  VQGICQSTSD
F  ~~~~~~
      51                               100
PE  KASCVKTLEP  VKSEDPNKLI  KAFMLATKDE  LTKSSNFTGQ  TEVNMGSSIS
F  ~~~~~~
     101                               150
PE  PNNKAULDYC  KRVMFYALED  LATIIEEMGE  DLSQIGSKID  QLKQWLIGVY
F  ~~~~~~
     151                               200
PE  NYQTDCLDDI  EEDDLRKAIG  EGIANSKILT  TNAIDIFHTV  VSAMAKINNK
F  ~~~~~~
     201                               250
PE  VDDLKNMTGG  IPTPGAPPVY  DESPVADPDG  FABLELED..  LDETIPITVV
F  ~~~~~~PDNLI  NNSTSLSNS  FHEELLEANK  ILCDIYETWF
     251                               300
PE  SGADRKLMAK  AGRGRRGGRG  .....  .....  SGARV  RINFVVARDG
F  PVVARKLMAK  SGRGKGRHG  GAAGGAGVAP  VLPPI  PGP  TPEAVVARDG
     301                               350
PE  SGQFKTVCLA  YD  C  F  E  N  R  G  F  C  L  I  Y  I  K  A  G  L  V  E  F  V  L  I  P  K  K  R  N  N  I  F  F  G  D  G
F  SGRFKTVCLA  YR  Y  P  R  H  G  F  Y  L  I  Y  I  K  A  G  V  E  F  E  O  N  L  I  D  R  K  R  T  V  F  F  V  G  D  G
     351                               400
PE  RRRTVLSYNR  S  A  L  S  G  T  T  L  L  A  T  V  Q  V  E  S  E  G  F  A  R  W  G  F  R  N  T  A  G  P  E  E  G
F  RGSITTCER  N  K  I  L  L  F  T  T  K  R  A  T  V  A  V  E  S  E  G  F  A  R  G  T  T  R  N  T  A  G  P  E  E  G
     401                               450
PE  AAARVNGDR  AV  I  N  C  R  F  D  F  Y  Q  D  T  L  Y  V  M  N  G  R  Q  F  Y  R  N  C  V  V  S  G  T  V  D  F  I  F  G  K  S
F  VALESTEDR  G  G  G  V  F  D  H  G  F  F  Q  H  ~~~~~~
     451                               500
PE  ATVIQNTLIV  VRKSGKQYN  TVTADGNELG  LGMKIGIVLQ  NCRIVPDRKL
F  ~~~~~~
     501                               550
PE  TPERLTVATY  LGRPWKFFST  TVIMSTEMGD  LIRPEGWKIW  DGEFHKSCR
F  ~~~~~~
     551                               600
PE  YVEYNRGP  AFANRRVNW  A  K  V  A  R  S  A  A  E  V  N  G  F  T  A  A  N  W  L  G  P  I  N  W  I  Q  E  A  N  V  P
F  ~~~~~~
     601
PE  VTIGL
F  ~~~~~~

```

Clone 12-BBT

DEFINITION homology to a phosphate translocator-related protein from
A. thaliana

SOURCE *Nicotiana tabacum* (common tobacco; ecotype Petit Havana SR1)

ORGANISM *Nicotiana tabacum*; Eukaryota; Viridiplantae; Streptophyta;
Embryophyta; Tracheophyta; Spermatophyta; Magnoliophyta;
eudicotyledons; core eudicotyledons; asterids; lamiids;
Solanales; Solanaceae; *Nicotiana*..

(bases 1 to 730)

BASE COUNT 218 a 156 c 138 g 217 t

ORIGIN

```

  1 TAACTATCTA TTCGATGATG AAGATACCCC ACCAAACCCA AAAAAAGAGA TCCTAGAACT
 61 AGTGGATCCC CCGGGCTGCA GGAATTCGGC ACGAGGGGAA GAAGAGGCAC AAATTAACAT
121 TGCTCTCTTT CTTCCACTTT CATAcATTCC CCACAAAAGT TCCCAAACAC ACACACACTC
181 ATCAAAGCAA AATAAAAAAA TCACCCTCCA AATTTTCAAG AAATAAATCT TGAAAACGTG
241 TGAGAATAGG GTCGTCGATT CAATCTATCT TGATGAGATT TTTCTAGCCG GGTTAATAAA
301 AAAAAAAAAA AAAAGGACTA GTAGTATCGA CAAGAGGGTA CATTCAAAAT CAAGAACCAA
361 TCATGTTGTC AGCACAATCA GAGAAACAGG CTTTTTTTCAT TGCCACACTT ATAACCTTTT
421 GGATTGCTAC TCTCAGCATT GTCTTTTGTG GGTCTGTTGT GGGTGGCAAT ATTTCTTTAA
481 GGTATCTGCC TGTTTCTTTT AACCAGGCTG TTGGTGCCAC AACCCCATTT TTCACTGCAT
541 TGTTTGCTTA TTTGATGACC CGGAAACAAG AAGCTTGGAT CACTTATGGT TGCCTTGTTT
601 CTGTTGTTAC TGGAGTTATA AATGCAAGTG GGGGCGAGCC AAGCTTCCAC CTTTATGGAT
661 TTCTAATGTG CATAGGTGCA ACTGCTGCTT AGAGCCTTTA AGTCTGTTCT TCANGGGGTC
721 CTTCTTTCTT

```

ClustalW Alignment of 12-BBT with phosphate translocator related protein from *Arabidopsis thaliana* (NP_187640.1; 355 aa)

```

      1                                     50
BBT ~~~~~~ NY LFDDEDTPPN
phosphate_tr_pep MSSHARGKEL IPLLFSHQK QPNLSISST TKMNKKNPQ KSDMSSSSSS

      51                                     100
BBT PKK..... .EILELVDPP G..... .. CRNFARG
phosphate_tr_pep PKKQTLFISS LIILWYTSNI SVLLLNKFL SNYGFKPPIF LTMCHMSACA

      101                                    150
BBT EE.EAQNIA LFLPLSYIPH KS..SCTHH SSKQNKITL QIFKKAIKT
phosphate_tr_pep ILSYVSTVEL KLVPLQYIKS RQFLKVAAL IIVFCASIVG GNISLRYIPV

      151                                    200
BBT VENVVDSIY LDEIFLAGLY KKKKRTSSI DKRVHKSRI NHVVTIRET
phosphate_tr_pep SFNCAVGAIT PFFTAFAIT MT.FKREAVY TYGALVPVVI GVVIAAGGEP

      201                                    250
BBT .....GFPH HTYNLLDCYS ..CHLLWVC C..... WQYFFKVSAC
phosphate_tr_pep GFHWFGSIM ISATAARAFK SVLGGILLSS EERLNSMNL MLYESPLAVI

      251                                    300
BBT FFAPGCWCHN FIFHCIVCLF DDPETRSLDH IWLPCSCC... WSFKCKW
phosphate_tr_pep ALLEVTFIME EDVMSVTLT GRQHKYMYIL LLVNSVMAIS ANLLNELVTK

      301                                    350
BBT GRAKLPPLWI SNVRCNCCL EPLSFFAGS FFL~~~~~
phosphate_tr_pep HTSALTQVI GAAGAVAVV ISILLERNPV TVHGIGGYSI TVLGVVAYGE

      351
BBT ~~~~~~
phosphate tr pep TKRRFR

```

Clone 12-BBV

DEFINITION homology to a hypothetical protein from *A. thaliana*
 SOURCE *Nicotiana tabacum* (common tobacco; ecotype Petit Havana SR1)
 ORGANISM *Nicotiana tabacum*;
 Eukaryota; Viridiplantae; Streptophyta; Embryophyta; Tracheophyta;
 Spermatophyta; Magnoliophyta; eudicotyledons; core
 eudicotyledons; asterids; lamiids; Solanales; Solanaceae;
Nicotiana..
 (bases 1 to 852)

BASE COUNT 263 a 199 c 199 g 191 t

ORIGIN

```

1 TTCAAAGCTG CAATGTTTCGT GTTGCGCCAT CGTACAAAAG GAAAGCAGAA AGCAGCTCAG
61 GTAGCTGTGT CATCCACCAA GGGAGATTGG AAGAAGCTGG TGGGGTCCAT GCGGCCTCTG
121 CATCTCCAGG ACAACAATAG CCAGGCGGCG TACGACTACT GTGCCACCAC ATCTTCACCC
181 TCAGCTTTGT CGTGTAGCGG AACCATGAGC CAGTACGCTT CGGCAAGCGA TCTCCAAGCA
241 ATGGATGTTC CTGCTGCTGG TGCACCCTCA ATTACTGACA GCATGAGCCA GTACGCTTCA
301 GCAAACGATC TCCAAGCACT GGAGGCCTCA ACTTCTTCTG GCACCATGAG CCAGTATGCT
361 TCCGCAAACA ATCTCCAAGA ACTCGATGAC GAGGAGGAAG AAGAGGATCC AGACCAGGTC
421 TTCGATGCTA TTGGCGCTGA CGACATGATC GATGCCAAGG CCGAGGAGTT CATCCTTCAG
481 TTTTACCAAC AGATGAGGCG TCAAAACATT GACTCAATGA GCGGCAATT CAATTAATTA
541 TTTAACTTAA TAAACACAAA GGGGAAAAAA AAAGAACAAG GTCAAGAATA AGTAAGGCTA
601 TACGTACGTG GAATTTTGTAG GCATGCACGC CCGCGGTTGG CTCATGATGA TCGACGTGCA
661 TGCATTTTAC ATAACATTTA TTAGTCCAAT TATACATGTT ATATGAAAGA GTTAGATCGA
721 AGAATGGACT AATAAACAAA GCATTCATCA TAAAAA AAAA AAAAAC TCGAGGGGGG
781 GCCCGGTACC CAATTGCCC TATAGTGAGT CGTATTACAA TTCACTGGCC GTCGTTTACA
841 ACGTCGGACT GG

```

ClustalW Alignment of 12-BBV with hypothetical protein from *Arabidopsis thaliana*

(CAB80709; 183 aa)

```

1 50
BBV FKAAMFVLRH RTKPKKAAQ VAVSSTKGDW KKLVSIRPL HLDNNRQ..
CAB80709 ~~~~~MEIQN QINIGEEIE NMKKKESRG FHVIVVLYL LRRRRRERPL

51 100
BBV .AANDYCATT SSPSALSCSG TMSQYASAD LQAMDVPAAG APSITDMSQ
CAB80709 NNGWRRVVE SFGQLKNDNV IVLPSEENIT ILPPSSPVT DEVPAEDDD

101 150
BBV YASANDLQAL EASTSAGTSS QVASANNLQF LDDEEEDDP LQ.VFDALGA
CAB80709 VSEMVVLLTA TSSSCSSGIE GYGSARSLRD NLCLDEDDDD LENVGNDG

151 188
BBV DDHIDAKAEI FIFLQFYQNR RQVIDSMSGQ FN~~~~~
CAB80709 DDHIDAKAEI FIFVRYEQNR MNQAYTERY KAKEMMV

```

Clone 12-BBX

DEFINITION homology to an unknown and a hypothetical/C2 domain-containing

protein from *A. thaliana*

SOURCE *Nicotiana tabacum* (common tobacco; ecotype Petit Havana SR1)

ORGANISM *Nicotiana tabacum*;

Eukaryota; Viridiplantae; Streptophyta; Embryophyta; Tracheophyta;

Spermatophyta; Magnoliophyta; eudicotyledons; core eudicotyledons;

asterids; lamiids; Solanales; Solanaceae; *Nicotiana*..

(bases 1 to 837)

BASE COUNT 260 a 156 c 225 g 195 t

ORIGIN

```

  1 TGATATTAAT GCTCAAGATC AAATGATCAA CGAGAACTTT CCAGAAGATG AAGAGAAATT
 61 GCAAATTAAC AATAAAATCC AGCTGTGGCA ATCGCAGAGT TTAGGCTATT CTGACGTCAA
121 CAACGGAGAA TTTCTAACC AGGCGGGCTC AATTTGTAAT GGGTCAATGG CGAACGGGTC
181 GGTAGTAAAC GGGTCGGAGC TGTGCTCCGA CATTGGGCCG TCGGCTTCCA TTGTGGCGGC
241 GGAGATAGCA AAGAAACTGC AACCTTTGCC GCCACCGCGG GTGCCGTCCA AAGAATTGAG
301 TAAAGAATAT TCCGGGGAAG GGGATGACGG AGAGAGCTCA ATATTGGAGG AGTTGACGGC
361 GGAGGAAGCG TACGCTAAAAG GGTTGGCGTT AAGTACGGAG GCAAGGAAGA AGGAGGCGGC
421 GGCACCGGAA AAATGTCAAA GGGGAAGCGG CGGACACCCA CGGCGGAACA CCCACGGTGG
481 ACTGTATTCT TGCTTTGGAA ATGCATATTG TTTCGAGTTC ACCATTGTTT GTGGGGCAAA
541 TAACAACAAC AATCAGGGGA ATCGTAGAGT TAATAGCAGT AATAAATACTG GCAAAGGCAG
601 AAAGAAGTGG TCTACTGATA AAAATTCAGC TTAATGTTGT ACGTATGTAC CCTTTTTGTA
661 TAGAAGTGTT TGTATTTAAC AACTTACCCA CACAGAGTAT TCCTACTGAT TTAATGAATG
721 CATTTGTATT TTATATATAA AAAAAAAAAA AAAAAACTCG AGGGGGGGCC CGGTACCCAA
781 TTCGCCCTAT AGTGAGTCGT ATTACAATTC ACTGGCCGTC GTTACAACGT CGGNCTG

```

ClustalW Alignment of 12-BBX with an unknown and a hypothetical protein from *Arabidopsis thaliana* (AAM67146; AAB80650; 391 aa and 602 aa, respectively)

```

301                                     350
AAM67146 .....TND YGVKTG.....
AAB80650 QSPNHNVLRP RSERQHEPDF IDQSPFFSMD RSRKTPRRST PMIEKPRPPR
BEX .....MINE NFPEDDEK...

351                                     400
AAM67146 .....VVTGN.. ...GGGGGG
AAB80650 DYDRTSSRAS PYLSRHGTPL RSNIVASTPI RSNIVSSSPM RSTVVGSTTR
BEX .....LQINNKI QLWQSCLGY SDVNNCEFPN

401                                     450
AAM67146 GGIIVGADSM VM.....SSLC
AAB80650 RSNILGSTPL RSNINGSTPI RSNYKATPMK SPMQFGTPMR SNLAGRPVLT
BEX QAGSICNGSM ANGSIVN...GSEL

451                                     500
AAM67146 SEDIQPSAEV VAAATACGLY NRKTAVKAA NKEDASILE GK.TEGIEYF
AAB80650 EDELQPSPE VAAQMAK..E RSCAYETESS ILSEWLDLDD SN.IEGIRSE
BEX CEDIQPSAST VAAETAK..E .LPLPPRV PSRELEKEYS GEGDDESSI

501                                     550
AAM67146 VTRWRAEKNG TVGAMGAAGS SIDSSG.... ..KGGGRRR RRRRKEKQC
AAB80650 LERWRTELPP LVDLSSHQS SDVSGAMVV ANVGGKSR KKTPAVKKKH
BEX LEELTAEAA .YAKLALS EARKKE.... ..A..AP EKCQRGGGH

551                                     600
AAM67146 GFRNGGEEK KGLFSCFGV FGCETISITC GGSGGGCDST KKRYNNKVV
AAB80650 NRRHTE..SG NGLFSCFSL CFWICTFVCG GGS..DQDGS KKGGSGLRP
BEX PERNTHS... .GLYSCFGA NCFEFTIVCG ANN..NNNQG NRRVNESQNT

601                                     614
AAM67146 NLSAVDETF S SAT
AAB80650 RLGSADLEY L----
BEX GRKRKKEVD KNSA

```

Clone 12-CG

DEFINITION homology to pollen-specific proteins from *N. tabacum*
 SOURCE *Nicotiana tabacum* (common tobacco; ecotype Petit Havana SR1)
 ORGANISM *Nicotiana tabacum*; Eukaryota; Viridiplantae; Streptophyta;
 Embryophyta; Tracheophyta; Spermatophyta; Magnoliophyta;
 eudicotyledons; core eudicotyledons; asterids; lamiids;
 Solanales; Solanaceae; *Nicotiana*..
 (bases 1 to 660)

BASE COUNT 176 a 166 c 162 g 155 t

ORIGIN

```

1 TTTGATACCC CTGAGGATGA TTTCATGGTC CTTGTGGCTG ATTGGTATAC CAAGAGCCAC
61 ACCGAATTGA AAAACTTGTT GGATAATGGG CGCGCTCTTG GACGGCCACA AGGTGTGATT
121 ATCAATGGAA AGAGCGGGAA AGGCGATGGT AAGGATGAGC CAATGTACAC TTTAACCCCT
181 GGAAAGACAT ACAGGTTTCAG GTTTTGCAAC GTTGGCATGA AGGATTCTAT TAATGTTAGA
241 TTCCAAGGCC ACACCATGAA ACTTGTGAA ATCGAAGGTT CTCACACGGT GCAAAACGTG
301 TACGAATCAC TAGACGTCCA CTTGGGACAA TGCATGTCTG TTCTGATAAC TGCTGATCAG
361 GATCCCAAGG ACTATTTCCCT CGTGGCCTCC ACGAGGTTCA CCAAGGAACC ACATGTTGCT
421 ACCGCCACAA TCCGTTATGC CAATGGCAAG GGACCCGCCT CGCCTGAATT GCCTAAGGCA
481 CCAGAAGGCT GGGCCTGGTC CCTGAANCAG TTCCGCTCCT TCCGTTGGAA TTTGACCGCA
541 AGCGCAGCTA GACCTAACCC CCAGGGATCT TACCATTATG GTCAGATCAA CATCACGCGC
601 ACCATCAAGC TAGTGACTTC GGCTGGGAAA CGTCGATGGC AAGCTTCGCT ATGCCATCAA

```

ClustalW Alignment with pollen-specific proteins from *Arabidopsis thaliana*, *Brassica napus* and *Nicotiana tabacum* (AAD10638; CAA45554; CAA43454; BAB01744; CAA47178)

```

151                                     200
AAD10638 IPVPYADPED DYTILINDWY TKSHTQLKKE LQSGRTIGRF DGILINGKSG
CAA45554 IPVPYADPED DYTVLIGDWY TKSHTQLKKE LQSGRTIGRF DGIVINGKSG
CAA43454 IPVPYADPED EYNVFVGDWY NKGHKILEKI LQSGRTIGRF DGILINGKSA
BAB01744 IPVPYADPED DYTVLIGDWY TKSHTQLKKE LQSGRTLGRF DGILINGKSG
CAA47178 IPVPYADPED DYTVLIGDWY TKSHTQVEKF LQSGRTIGRF DGIVINGKAG
CG ~~~~DTEED DMVLYADWY TKSHTLEKNL LQSGRALGRF GGVILINGKSG

201                                     250
AAD10638 ITDGSIDKPLF TLKPGKTYRW RICNVGLKAS LNFRIQNHKI KLVENEGSHV
CAA45554 KGDGSDAPLF TLKPGKTYRW RICNVGVKTE INFRIQNHKI KLVENEGSHV
CAA43454 NVGEAKKPLF TMEAGKTYNY RRCNLGRSE VNIREFGHPH KLVELEGSHY
BAB01744 KGDGSDAPLF TLKPGKTYRW RICNVGLKTE LNFRIQNHKI KLVENEGSHV
CAA47178 KGDGSDAPLF TLKPGKTYRW RICNVGIKTE LNFRIQNHKI KLVENEGSHV
CG KGDGKDEPMY TLTEGKTYRF RRCNVGKEDS LNVREFGHTM KLVELEGSHY

251                                     300
AAD10638 LQNDVDSLIV HVGQCFGVIV TADQEPKDYV HIASTRFLKE PLTTTGLLRY
CAA45554 LQNDVDSLIV HVGQCFGTIV TANQEPKDYV HVASSRFLDT VITTTGLLRY
CAA43454 VQNIINDSLDL HVGQCLSVLV TADQEPKDYV LVVSSRFLKQ ALSSVAIIRY
BAB01744 LQNDVDSLIV HVGQCYGTIL TANQEAADYV HVASSRFLKE VITTTGLLRY
CAA47178 LQNDVDSLIV HVGQCYGTIV SANQEPKDYV HVASSRFLKE VITTTGLLRY
CG VQNVVESLIV HLGQCM SVLI TADQEPKDYV LVASTRETKK PHVATATIRY

301                                     350
AAD10638 EGGKGPASSC LFAAF...V GMAWSLNCFR SFRWMLTASA ARPNPQGSYH
CAA45554 EGGKGPASSC LFAAF...V GMAWSLNCFR SFRWMLTASA ARPNPQGSYH
CAA43454 ANGKGPASPE LFAFP...PENTE GMAWSLNCFR SFRWMLTASA ARPNPQGSYH
BAB01744 EGGKGPASSC LFAFP...V GMAWSLNCFR SFRWMLTASA ARPNPQGSYH
CAA47178 EGGKGPASSC LFAAF...V GMAWSLNCFR SFRWMLTASA ARPNPQGSYH
CG ANGKGPASPE LFAAF...E GMAWSLNCFR SFRWMLTASA ARPNPQGSYH

351                                     400
AAD10638 YGRINITRTI KLVNTQGVVD GKRLRYALSGV SHTDPETPLK LAEYFGVADR
CAA45554 YGRINITRTI KLVNTQGVVD GKRLRFALNGV SHTEPETPLK LAEYFGISDK
CAA43454 YGRINITRTI KLFNMSQVG GKRLRYGLNGI SHTNGETPLK LVEYFGATNK
BAB01744 YGRINITRTI KLVNTQGVVD GKRLRYALNGV SHTDPETPLK LAEYFGVADR
CAA47178 YGRINITRTI KLVNTQGVVD GKRLRYALNGV SHTEPETPLK LAEYFGITDK
CG YGRINITRIK LNTSARFEMG ASLCHQ~~~~ ~~~~~~ ~~~~~~

```

Phosphoinositide-specific phospholipase C 3

DEFINITION *Nicotiana tabacum* phospholipase C 3 mRNA, complete coding sequence

SOURCE *Nicotiana tabacum* (common tobacco; ecotype Petit Havana SR1)

ORGANISM *Nicotiana tabacum*; Eukaryota; Viridiplantae; Streptophyta; Embryophyta; Tracheophyta; Spermatophyta; Magnoliophyta; eudicotyledons; core eudicotyledons; asterids; lamiids; Solanales; Solanaceae; *Nicotiana*..

(bases 1 to 1767)

BASE COUNT	541 a	324 c	408 g	494 t	
1	ATGTCGAGAC	AGACGTACAG	AGTCTGTTTC	TGTTTCCGGC	GGCGGTTCCG GGTAGTCGCC
61	GCTGAGGCTC	CGGCGGATGT	GAAGAATTTA	TTCAATAAAT	ATTCCGATAA CGGAGTGATG
121	AATGCAGAGA	ACCTTCAACG	ATTCTTAATT	GAGGTTTCAGA	AGGAGGAAAA TTCGAGTATA
181	GAGGATGCTC	AGGGTATTAT	GAATAATCTT	CATGACCTTA	AGATCCTTAA TATTTTTTCAT
241	CGGAGAGGTC	TTCATCTTGA	CGCATTTTTT	AAGTATCTTT	TTGCTGATAT TAATCCTCCT
301	ATTAATCCTA	AACGTGGGAT	TCACCATGAT	ATGAATGAGC	CTTTGTCTCA TTACTTCATA
361	TACACAGGAC	ATAATTCCTA	TCTAACTGGG	AATCAACTAA	GTAGTGATTG CAGTGATGTT
421	CCCATAATAC	AAGCCCTGCA	CCGAGGTGTA	CGAGTAATTG	AATTGGATAT ATGGCCAAAT
481	TCCGCCAAAAG	ATGATGTGGA	AGTTCGTCAT	GGAGGAACAT	TGACCACTCC GGTGCGCTC
541	ATCAAATGTC	TGAGGTCTAT	CAAGGAACAT	GCTTTTTTCTG	TATCTGAGTA TCCTGTTGTG
601	ATAACACTTG	AAGATCATTT	AACCCAGAT	CTTCAGGCAA	AAGTTGCGGA GATGATCACT
661	CAAACATTTG	GAGACATGCT	GTTTTCTCCC	GATTCATGTT	TGAAAACTT TCCCTCCCCA
721	GAATCTCTGA	AAAGACGTGT	TCTGATATCA	ACTAAGCCAC	CCAAAGAGTA CCTTCAGGCG
781	AAGGAAGTTA	AGGAAAAAGA	CTCGAAGAAA	GGAACGGAGT	CACCTGATAC AGAAGCTTGG
841	GGAAGGGAAG	TTTCAGACCT	TAAAGCCAGA	TACAATGATA	AGGATGATTC TGATGACGGA
901	GCAGGTGTGG	AAGATGATGA	AAGTGATGAA	GGAGATCCCA	ACTCGCAGCA AAATGTCGCA
961	CCAGAATACA	AGTGTTTAAT	TGCCATTTCAT	GCTGGAAAGG	GAAAAGGTGG ATTGTCAGAT
1021	TGGCTGAGGG	TTGATCCTGA	TAAAGTAAGA	CGACTTAGCT	TGAGTGAACA AGAACTTGGG
1081	AAGGCTGTAG	TTACTCATGG	AAAAGAAATT	ATCAGGTTCA	CTCAGCGGAA CTTGCTCAGA
1141	ATATACCCAA	AGGGCATAACG	TTTTGACTCA	TCCAATTACA	ATCCTTTTGT TGCATGGACG
1201	CATGGAGCTC	AAATGGTGGC	ATTCAATATG	CAGGGCTTTG	GAAGATCACT TTGGTTAATG
1261	CATGGTATGT	TCAGATCCAA	TGGTGGTTGT	GGATATGTTA	AGAAACCAGA TATATTATTG
1321	AAAGCAGGTC	CAAACAATCA	GATCTTCGAT	CCTGAAGCAA	ATTTGCCAGT CAAAACCTACA
1381	TTGAAGGTGA	CCGTATTTAT	GGGTGAAGGG	TGGTATTATG	ACTTCAATCA CACGCACTTT
1441	GATGCATACT	CGCCTCCAGA	TTTCTATGCA	AAGATAGGAA	TTGCCGGAGT TCCAGCTGAT
1501	AATGTAATGA	AGAAAAACAAG	GACTCTTGAG	GACAATTGGA	TACCAACTTG GGATGAAAAG
1561	TTTGAGTTCC	CATTAACAGT	TCCTGAGTTG	GCTCTACTTC	GCGTCGAAGT TCATGAGTAT
1621	GATATGTCTG	AAAAAGATGA	TTTTGCTGGC	CAAACCTGTT	TACCTGTTTC AGAACTAAGA
1681	CAAGGTATTTC	GAGCAGTTTC	ACTACACGAC	CGAAAGGGAG	AGAAATACAA CTCTGTGAAG
1741	CTTCTTATGC	GTTTCGAATA	TGTCTAA		

NtPLC3 coding sequence

1 MSRQTYRVCF CFRRRFRVVA AEAPADVKNL FNKYSDNGVM NAENLQRFLI
51 EVQKEENSSI EDAQGIMNNL HDLKILNIFH RRGLHLDAFF KYLFADINPP
101 INPKRGIHHD MNEPLSHYFI TGHNSYLTGN QLSSDCSDVP IIQALHRGVR
151 VIELDIWPNS AKDDVEVLHG GTLTTPVALI KCLRSIKEHA FSVSEYPVVI
201 TLEDHLTPDL QAKVAEMITQ TFGDMLFSPD SCLKNFPSPE SLKRRVLIST
251 KPPKEYLQAK EVKEKDSKKG TESPTEAWG REVSDLKARY NDKDSDDDGA
301 GVEDDESDEG DPNSQQNVAP EYKCLIAIHA GKKGGLSDW LRVPDKVRR
351 LSLSEQELGK AVVTHGKEII RFTQRNLLRI YPKGIRFDSS NYNPFVAWTH
401 GAQMVAFNMQ GFGRSLWLMH GMFRSNGGCG YVKKPDILLK AGPNNQIFDP
451 EANLPVKTTL KVTVMGEGW YYDFNHTHFD AYSPPDFYAK IGIAGVPADN
501 VMKKTRTLED NWIPTWDEKF EFPLTVPELA LLRVEVHEYD MSEKDDFAGQ
551 TCLPVSELRQ GIRAVSLHDR KGEKYNSVKL LMRFEYV

Phosphoinositide-specific phospholipase C 4

DEFINITION *Nicotiana tabacum* phospholipase C 4 mRNA, complete coding sequence

SOURCE *Nicotiana tabacum* (common tobacco; ecotype Petit Havana SR1)

ORGANISM *Nicotiana tabacum*; Eukaryota; Viridiplantae; Streptophyta; Embryophyta; Tracheophyta; Spermatophyta; Magnoliophyta; eudicotyledons; core eudicotyledons; asterids; lamiids; Solanales; Solanaceae; *Nicotiana*..
(bases 1 to 1767)

BASE COUNT	548 a	327 c	409 g	483 t				
1	ATGTCGAGAC	AGACGTACAG	AGTCTGTTTC	TGTTTCCGGC	GGCGGTTC	GGTAGTCGCC		
61	GCCGAGGCTC	CGGCGGATGT	AAAGAATTTA	TTCAATAGAT	ATTCCGATAA	CGGAGTAATG		
121	AATGCAGAGA	ACCTACAACG	ATTCTTAATT	GAGGTTTCAGA	AGGAGGAAAA	TGCGAGTTTA		
181	GAGGATGCTC	AGGGTATTAT	GAATAATCTT	CATGACCTTA	AGATCCTTAA	TATTTTTTCAT		
241	CGGAGAGGTC	TTCATCTTGA	CGCATTTTTT	AAGTATCTTT	TTGCTGATAT	TAATCCTCCT		
301	ATTAATCCTA	AACGCGGGAT	TCACCATGAT	ATGAATGAGC	CTTTGTCTCA	TTACTTCATA		
361	TACACAGGAC	ATAATTCTTA	TCTAACTGGG	AATCAACTAA	GTAGTGATTG	CAGTGATGTC		
421	CCCATAATAC	AAGCCCTGGG	CCGAGGTGTA	CGAGTAATTG	AATTGGATAT	ATGGCCAAAT		
481	TCCGCCAAAAG	ATGATGTGGA	AGTTCTGCAT	GGAGGAACAT	TGACCACCTCC	GGTTGCGCTC		
541	ATCAAATGTC	TGAGGTCTAT	AAAGGAACAT	GCTTTTACTG	TATCTGAGTA	TCCTGTTGTG		
601	ATAACACTTG	AAGATCATTT	AACCCAGAT	CTTCAGGCAA	AAGTTGCGGA	GATGATCACT		
661	CAAACATTTG	GAGACATGCT	GTTTTCTCCC	GATTCATGTT	TGAAAGACTT	TCCCTCCCCA		
721	GAATCTCTGA	AAAAACGTGT	TCTGATATCA	ACTAAGCCAC	CCAAAGAATA	CCTTCAGGCG		
781	AAGGAAGTTA	AGGAAAAAGA	CTCGAAGAAA	GGAACAGAGT	CGCCTGATAC	AGAAGCTTGG		
841	GGAAGGGAAG	TTTCAGACCT	TAAAGCCAGA	TACAATGATA	AGGATGATTC	TGATGAAGGA		
901	GCAGGTGAGG	AAGATGATGA	AAGTGACGAA	GGAGATCCCA	ACTCGCAGCA	AAATGTGCGA		
961	CCAGAATACA	AGCGTTTGAT	TGCCATTTCAT	GCTGGAAAGG	GAAAAGGTGG	ATTGTCAGAT		
1021	TGGCTGAGGG	TTGATCCTGA	TAAAGTAAGA	CGACTTAGCT	TGAGCGAGCA	AGAACTTGG		
1081	AAGGCTGTAA	TTACTCATGG	AAAAGAAAAT	ATCAGGTTCA	CTCAGCGGAA	CTTGCTCAGA		
1141	ATATACCCAA	AGGGCATAACG	TTTCGACTCA	TCCAATTATA	ATCCTTTTGT	TGCATGGACG		
1201	CATGGAGCTC	AAATGGTGGC	ATTCAATATG	CAGGGCTATG	GAAGATCACT	TTGGTTAATG		
1261	CATGGTATGT	TCAGATCCAA	TGGTGGTTGT	GGATATGTTA	AGAAACCAGA	TATACTATTG		
1321	AAAGCAGGTC	CTAACAATCA	GATCTTCGAT	CCTGAAGCAA	ATTTGCCAGT	CAAACTACA		
1381	TTGAAGGTGA	CCGTATTTAT	GGGGGAAGGA	TGGTATTATG	ATTTCAAACA	CACACACTTT		
1441	GATGCATACT	CGCCTCCAGA	TTTCTATGCA	AAGATAGGAA	TTGCCGGAGT	TCCGGCTGAT		
1501	AATGTAATGA	AGAAAACAAA	GACACTGGAG	GATAATTGGA	TACCAACTTG	GGATGAAAAG		
1561	TTTGAGTTCC	CATTAACAGT	TCCTGAATTG	GCTCTACTTC	GCGTCGAAGT	TCATGAGTAT		
1621	GATATGTCTG	AAAAAGATGA	TTTTGCTGGC	CAAACCTGTT	TACCTGTTTC	AGAACTAAGA		
1681	CAAGGTATCC	GAGCAGTTTC	ACTCCACGAC	CGAAAGGGAG	AGAAATACAA	CTCTGTGAAG		
1741	CTTCTTATGC	GTTTCGAATT	TGICTAA					

NtPLC4 coding sequence

1 MSRQTYRVCF CFRRRFRVVA AEAPADVKNL FNRYSDNGVM NAENLQRFLI
51 EVQKEENASL EDAQGIMNNL HDLKILNIFH RRGLHLDAFF KYLFADINPP
101 INPKRGIHHD MNEPLSHYFI YTGHN SYLTG NQLSSDCSDV PIIQALGRGV
151 RVIELDIWPN SAKDDVEVLH GGTLTTPVAL IKCLRSIKEH AFTVSEYPVV
201 ITLEDHLTPD LQAKVAEMIT QTFGDMLFSP DSCLKDFPSP ESLKKRVLIS
251 TKPPKEYLQA KEVKEKDSKK GTESPDTEAW GREVSDLKAR YNDKDDSDEG
301 AGEEDDESDE GDPNSQQNVA PEYKRLIAIH AGKGKGLSD WLRVDPDKVR
351 RLSLSEQELG KAVITHGKEI IRFTQRNLLR IYPKGIRFDS SNYNPFVAWT
401 HGAQMVAFNM QGYGRSLWLM HGMFRSNGGC GYVKKPDILL KAGPNNQIFD
451 PEANLPVKTT LKVTVMGEG WYDFKHTHF DAYSPPDFYA KIGIAGVPAD
501 NVMKKTKTLE DNWIPTWDEK FEFPLTVPEL ALLRVEVHEY DMSEKDDFAG
551 QTCLPVSELR QGIRAVSLHD RKGEKYNSVK LLMRFEFV

8 CURRICULUM VITAE

Name	Diana Helling
Date of birth	4 th of September, 1974
Place of birth	Bielefeld, Germany
Nationality	German
Marital status	Single

Education

08/1981 – 08/1985	“Vogelruthschule Brackwede”, Bielefeld
09/1985 – 08/19/91	“Brackweder Gymnasium”, Bielefeld
09/1991 – 06/1994	“Ratsgymnasium zu Bielefeld, Allgemeine Hochschulreife 06/1994”

International exchange

07/1994 – 07/1995	International Christian Youth Exchange (ICYE, Berlin), voluntary year of social service in Costa Rica, Central America
-------------------	---------------------------------------------------------------------------------------------------------------------------

University education

10/1995 – 09/1996	University of Paderborn Studies in English, Spanish, Pedagogics “Lehramt der Sekundarstufe I und II”
10/1996 – 05/2001	University of Bonn Studies in Biology, Spanish, Pedagogics “Lehramt der Sekundarstufe I und II”
05/2000 – 11/2000	“Staatsexamensarbeit”, Department of Plant Cell Biology, Faculty of Biological Sciences, University of Bonn Topic: “Über die Struktur und Dynamik des Endoplasmatischen Retikulums in <i>Arabidopsis thaliana</i> unter Stressbedingungen“. Supervisor: Prof. Dr. Diedrik Menzel
05/2001	“Erstes Staatsexamen für das Lehramt der Sekundarstufe I und II” Topics: Biology, Spanish and Pedagogics
06/2001 – 06/2003	Scientific assistant, Department of Plant Cell Biology, Botanical Institute, University of Bonn

since 07/2003

Scientific assistant, Laboratory of Developmental Biology,
Heidelberg Institute for Plant Sciences, University of Heidelberg,
Supervisor: Dr. Benedikt Kost

9 LIST OF PUBLICATIONS

COVERING PARTS OF THE DISSERTATION

Helling, D., Klahre, U. and Kost B. (2005).

“NtPLC3 is Involved in the Maintenance of Pollen Tube Polarity”. (Poster)
XVIIth International Botanical Congress, Vienna, Austria, July 17th to 23rd, 2005

Helling, D., Klahre, U. and Kost B. (2005).

NtPLC3 Maintains the Polarity of PI-4,5-P₂ Distribution and Cell Expansion in
Pollen Tubes of *Nicotiana tabacum*. (in preparation)

10 GENERAL STATEMENT

I declare that I am the sole author of this submitted dissertation and that I did not make use of any sources or help apart from those specifically referred to. Experimental data or material collected from or produced by other persons is made easily identifiable.

I also declare that I did not apply for permission to enter the examination procedure at another institution and that the dissertation is neither presented to any other faculty, nor used in its current or any other form in another examination.

(Diana Helling)

DANKSAGUNG

Meinen ausdrücklichen Dank möchte ich Herrn Prof. Dr. Thomas Rausch aussprechen, der unserer Nachwuchsgruppe “Entwicklungsbiologie” die Möglichkeit gegeben hat, uns im HIP zu etablieren und uns größte wissenschaftliche Freiheit gelassen hat. Weiterhin möchte ich ihm für die großzügige Bereitstellung der zahlreichen Geräte und Materialien danken.

Herrn Prof. Dr. David G. Robinson möchte ich für die Übernahme des Korreferats danken und dafür, dass er uns uneingeschränkten Zugang zum confocalen Laser Scanning Mikroskop ermöglicht hat, an dem ich den ein oder anderen Tag verbracht habe.

Herzlicher Dank gilt Herrn Dr. Benedikt Kost, meinem Doktorvater, der mich vor zwei-einhalb Jahren unter größten Schwierigkeiten in seine Arbeitsgruppe aufgenommen und mir die Möglichkeit gegeben hat, an neuen und spannenden Themen zu arbeiten. Überdies danke ich ihm für die fachliche Unterstützung und die zahlreichen wissenschaftlichen Diskussionen, sowie für die Sicherstellung der Finanzierung durch das Land Baden-Württemberg und die Deutsche Forschungsgemeinschaft.

Herrn Dr. Ueli Klahre gilt besonderer Dank zum einen für seine kompetente, fachliche und sprachliche Unterstützung, zum anderen für seine Ungeduld, mit der er mich immer weiter getrieben hat.

Frau Katja Piiper sei herzlich gedankt für ihre technische Unterstützung, das Gießen tausender Agarplatten und die hingebungsvolle Pflege und das Kreuzen meiner Pflanzen. Meinen beiden Kolleginnen, Stéphanie Cottier und Pridhee Kapoor, danke ich dafür, dass ich mich immer auf sie verlassen konnte und sie mich ab und zu aus dem tristen Alltag entführt und zu ihrer “Coke break” eingeladen haben.

Meinen Freunden danke ich, dass sie mich durch ihre Diskussionen, ihre Inspirationen und vor allem durch ihre Kritik dazu veranlasst haben, immer weiter zu machen und diese Arbeit fertigzustellen.

Mein allergrößter Dank gilt schließlich meinen Eltern für ihre Geduld, ihr Verständnis und ihre bedingungslose Unterstützung.